SGK AND DISRUPTED RENAL SODIUM HANDLING IN DIABETES

CLAIRE ELIZABETH HILLS

A THESIS SUBMITTED FOR THE DEGREE
OF DOCTOR OF PHILOSOPHY

THE DEPARTMENT OF BIOLOGICAL SCIENCES, THE UNIVERSITY OF WARWICK

SEPTEMBER 2006

MOLECULAR PHYSIOLOGY
DEPARTMENT OF BIOLOGICAL SCIENCES
UNIVERSITY OF WARWICK
GIBBET HILL ROAD
COVENTRY
WEST MIDLANDS
CV4 7AL

Contents

List of tables

List of Figures

Acknowledgements

I would like to thank my supervisors Dr Paul Squires and Dr Rosemary Bland for all their help and support during the past 4 years. Thank you for you continued encouragement, support and advice for which I am entirely grateful. I am particularly grateful to Dr Squires for all his help on the calcium imaging experiments and to Dr Bland for all her help with the Molecular Biology.

I would like to thank Jeanette Bennett for all her help and support in the lab over the past year and for making my working days at the bench so enjoyable.

Lastly I would like to thank all the members of Molecular Physiology, past and present for their support and unfailing friendship since being at Warwick, I shall miss you all.

Declaration

I hereby declare that the work submitted in this thesis was conducted by myself under the supervision of Dr Paul E Squires and Dr Rosemary Bland at the department of Biological Sciences, University of Warwick, with the exception of those instances where the contribution of others has been specifically acknowledged.

None of the information contained herein has been used in any previous application for a degree.

All sources of information have been specifically acknowledged by means of references.

Some of the work presented within this thesis has been published in:

Hills CE, Bland R, Wheelans DC, Bennett J, Ronco PM, Squires PE. (2006). Glucose-evoked alterations in connexin-43-mediated cell-to-cell communication in human collecting duct: a possible role in diabetic nephropathy. *Am J Physiol Renal Physiol.* **291**, F0000-F000.

Hills CE, Bland R, Wheelans DC, Bennett J, Ronco PM, Squires PE. (2006). High glucose upregulates ENaC and SGK1 expression in HCD cells. *Cell Physiol Biochem.* **18**, in press.

Which are contained within appendix I

Other studies I have carried out during this PhD which are not contained within this thesis are included in the following publications which are contained within appendix II:

Squires PE, Hills CE, Rogers GJ, Garland P, Farley SR, Morgan NG (2004) The putative imidazoline receptor agonist, harmane, promotes intracellular calcium mobilization in pancreatic β-cells. *Eur J Pharmacol.* **501**: 31-39, 2004.

Bland R, Markovic D, Hills CE, Hughes SV, Chan SLF, Squires PE, Hewison M. (2004) Expression of 25-hydroxyvitamin D3-1α-hydroxylase in pancreatic islets. *J Steroid Biochem Mol Biol.* **89-90**, 121-125.

Morgan NG, Cooper EJ, Squires PE, Hills CE, Parker CA, Hudson AL (2003) Comparative effects of efaroxan and β-carbolines on the secretory activity of rodent and human β-cells. *Annal NY Acad Sci.* **1009**, 167-174

Summary

Diabetic nephropathy is associated with secondary hypertension arising from aberrant sodium reabsorption in the kidney. This thesis characterises a novel human cell line derived from the human cortical collecting duct (HCD) to assess glucose-evoked changes in key elements, such as the serum and glucocorticoid inducible kinase (SGK1) and the epithelial sodium channel (ENaC), involved in the regulation of sodium transport. In addition I have also examined the effects of TGF-β1 and $[Ca^{2+}]_i$ on SGK1 and ENaC expression. RT-PCR, western blot analysis, immunocytochemistry and single cell imaging were employed to determine presence, localisation and function of these elements under various glycaemic conditions. Our data suggest that high glucose, TGF-β1 and $[Ca^{2+}]_i$ up-regulate both SGK1 and α-ENaC protein expression, which in turn stimulates Na^+ transport. In pathological conditions associated with aberrant Na^+ reabsorption, excessive levels of Na^+ may further exacerbate the state of hypertrophy, a common manifestation associated with diabetic nephropathy. Mechanical stress evoked TRPV4 mediated changes in $[Ca^{2+}]_i$. Propagation of this Ca^{2+} signal via the gap junction protein connexin 43 (Cx-43) was enhanced following glucose treatment, as was Cx-43 expression. Under pathophysiological conditions these changes and the increased expression levels of our key signaling elements, may lead to deranged Na^+ handling and inhibition of cell volume recovery mechanisms which together may further enhance the condition of diabetic nephropathy in Type II diabetes.

List of abbreviations

4α-PDD	4-α-phorbol 12,13-didecanoate
α	Alpha
AA	Arachidonic acid
Ab	Antibody
Ag	Antigen
AGEs	Advanced glycation end products
AMV-RT	Avian Myeloblastosis virus reverse transcriptase
AP-1	Activator protein-1
APES	3-aminopropyltriethoxysilane
APS	Ammonium persulfate
ADP	Adenosine di-phosphate
ADP-ribose	Adenosine diphosphoribose (ADP-ribose)
ASICS	Acid sensing ion channel
ATP	Adenosine tri-phosphate
β	Beta
BLINaC	Brain liver intestine sodium channel
BSA	Bovine serum albumin
Ca^{2+}	Calcium
$[Ca^{2+}]_I$	Intracellular calcium
CAMK	Calcium/calmodulin-dependent protein kinase
cAMP	Cyclic adenosine monophosphate
CRD	Cysteine rich domains
Cx	Connexin
Cx-26	Connexin 26
Cx-31	Connexin 31
Cx-31.1	Connexin 31.1
Cx-40	Connexin 40
Cx-43	Connexin 43
δ	Delta
DAG	Diacylglycerol
DEG	Degenerin
DMEM	Dulbeccos modified Eagles medium
DMSO	Dimethylsulfoxide
DNA	Deoxyribonucliec acid
dNTP	Deoxy nucleotide tri-phosphate
dsRNA	Double Stranded RNA
DTT	Dithithreitol
ECF	Extracellular fluid
ECL	Enhanced chemiluminescence
ECM	Extracellular matrix
EGTA	Ethyleneglycol bis (aminoethylether)-N,N,N',N-tetra-acetate
	linked immunoabsorbent assay
ENaC	Epithelial sodium channel
ER	Endoplasmic reticulum
ERK	Extracellular regulated kinases
EtBr	Ethidium bromide

FCS	Foetal calf serum
FaNaC	FMRFamide-gated sodium channel
Fura-2/AM	Fura-2 acetyoxymethylderivative
γ	Gamma
G protein	Guanine nucleotide-binding protein
GAPDH	Glyceraldehyde 3 phosphate dehyrdogenase
GLUT	Glucose transporter
GJIC	Gap junctional intercellular communication
HCl	Hydrochloric acid
HEPES	4-(2-Hydroxyethyl) piperazine-1-ethanesulfonic acid
hINaC	Human intestine sodium channel
HRP	Horseradish peroxidase
ICAM	Intercellular adhesion molecule
IDDM	Insulin dependent diabetes mellitus
Ig	Immunoglobulin
IGF	Insulin growth factor
IL	Interleukin
IP_3	Inositol triphosphate
IRS	Insulin receptor substrate
ITS	Insulin transferring sodium selenite
K^+	Potassium
K_{ATP}	ATP-sensitive potassium channel
KCl	Potassium chloride
kDA	Kilodalton
μg	Microgram
mg	Milligram
min	Minute
ml	Millilitre
μM	Micromolar
mM	Millimolar
MAPK	Mitogen activated protein kinase
MEK	Mitogen activated protein kinases/ERK kinase
MEKK	Mitogen activated protein kinases/ERK kinase kinase-1
MgCl	Magnesium chloride
MODY	Maturity onset diabetes of the young
mRNA	Messenger ribonucleic acid
MW	Molecular weight
n	Number
Na^+	Sodium
$[Na^+]_I$	Intracellular Sodium
Na^+/K^+ ATPase	Sodium Potassium ATPase
NaOH	Sodium hydroxide
Nedd4-2	Neural precursor cell-expressed developmentally downregulated gene 4
ng	Nanogram
P1 receptor	Purinergic receptor activated by adenosine
P2 receptor	Purinergic receptor activated by ATP and ADP
PAGE	Polyacrylamide gel electrophoresis
PBS	Phsophate buffered saline

PFA	Paraformaldehyde
PI3-K	Phosphatidylinositol-3-kinase
PDK1	Phosphatidylinositol-3,4,5-triphosphate (PIP3)-dependent kinase 1
PH	Pleckstrin homology
PIP2	Phosphatidylinositol-4,5-biphosphate
PKA	Protein kinase A
PKC	Protein kinase C
PLA_2	Phospholipase A_2
PLC	Phospholipase C
PMSF	Phenylmethylsulfonylfluoride
PPAR	Peroxisome proliferators activated receptor
PPARγ	Peroxisome proliferators activated receptor gamma
RNAi	RNA inhibition
RT-PCR	Reverse transcriptase polymerase chain reaction
RVD	Regulatory volume decrease
S.E.M	Standard error of the mean
SGK1	Serum and glucocorticoid inducible kinase
SDS	Sodium dodecyl sulphate
SERCA	Sarco(endo)plasmic reticulum Ca^{2+}-ATPases
siRNA	Short interfering RNA
sp1	Specificity protein 1
TBE	Tris-boric acid-EDTA
TEMED	N,N,N,N-tetramethylethylenediamine
Tg	Thapsigargin
TGF	Transforming growth factor
TGF-β	Transforming growth factor beta
Tris	Tris(hydroxymethyl)aminomethane
TRP	Transient receptor potential
TRPV4	Transient receptor potential vanilloid 4
Tween-20	Polyoxyethylene-sorbitan
v/v	Volume per volume
w/v	Weight per volume
WNK1	*with no lysine kinase 1*

Chapter 1

Introduction

1.1 Non insulin dependent Diabetes Mellitus

The maintenance of glucose homeostasis depends on a tightly regulated array of signalling cascades, all of which control the ability of the cells within the body to detect a significant change in blood glucose. Despite the varying demands of food and fasting, levels rarely stray outside the physiological range of 3.5-8 mM. Only when abnormalities arise is there inefficient uptake and subsequent metabolism of glucose. Consequently, our blood levels rise and we become hyperglycaemic. If left untreated, diabetes can result. A disease of multiple aetiology, diabetes has been classified into several subtypes that include Type I, Type II (otherwise known as non-insulin dependent diabetes (NIDDM)) and maturity onset diabetes of the young (MODY). Whilst Type I diabetes is an autoimmune disease in which destruction of β cells of the pancreas results in failure to secrete insulin, Type II diabetes is a complex heterogenous disorder encompassing a wide array of metabolic abnormalities associated with malfunctions in both insulin action and secretion; both of which are usually present at the time of diagnosis. (Nesher *et al.,* 1987)

According to the American Diabetes Association (ADA) (Expert committee 1997) Type II diabetes is defined as

"The most common form of diabetes, occurring with increasing frequency of age, usually associated with insulin resistance and always with either relative, or absolute insulin deficiency and not generally requiring insulin treatment for survival"

Typical risk factors that predispose an indivdual to Type II diabetes include age, race and background, a family history of diabetes, hypertension, high cholesterol, obesity and lifestyle factors; for example low physical activity, high-fat low-carbohydrate diet, alcohol and smoking

Untreated or poorly controlled Type II diabetes causes both hyperglycaemia and hyperlipidaemia which in turn can lead to the development of a range of secondary complications, macrovascular or microvascular, the latter of which includes retinopathy, nephropathy and neuropathy. The exact mechanisms of microvascular disease are still a matter of debate. The main sites to be affected are the retina, renal glomerulus, and the nerve sheath respectively (Wolf *et al.*, 2003).

1.2 Socioeconomic burden of Type II diabetes

In today's society, Type II diabetes is an enormous health problem. Increasing prevalence means that approximately 5-7% of the world's population is affected. However, this remains a rough approximation, since another 3% of the population remain undiagnosed (Bloomgarden 1996). The severity of the condition is dependent upon the degree of insulin insensitivity, a determining factor in the pathogenesis of the condition which is extremely variable from one individual to another. The prevalence of the condition varies considerably throughout the world. The World Health Organisation (WHO) estimates that 2% of the UK population are Diabetic, whilst the number is thought to be three to four times that in people of African and Caribbean ancestry (Gaillard TR *et al.*, 1997). Likewise, those of Hispanic American origin and in those from South Asia and Arabia living western lifestyles are far more at risk than white Europeans. Variability in both diet and lifestyle are thought to be the two main factors responsible for denoting the percentage population of a cohort affected. For example, a much higher prevalence of glucose intolerance and Type II diabetes has been observed in the Pima Indians living in the United States as compared with those living in Mexico (Bloomgarden 1996, Bennett *et al.*, 1976). This is thought a consequence of their sedentary lifestyle, coinciding with a high incidence of obesity as compared to their counterparts (Bloomgarden 1996)

There is no doubt that Type II diabetes is of increasing prevalence worldwide. The global increase is estimated to be 122% (from 135 million to 300 million people) between 1995 and 2025; 90% of these people will have Type II diabetes (King *et al.*, 1998). The developing world is predicted to suffer the most with an approximate 170% increase in incidence rate, affecting mainly the 45-64 year old age bracket

(King *et al.,* 1998). Whilst the disease is known to affect mainly older individuals, an increasing sedentary lifestyle in conjunction with a rise in the availability of so called fast food, is leading to a rise in the number of obese young adults in today's society. Consequently the identification of the disease in children and teenagers is far more frequent than in the past and since the number of obese young adults worldwide is on the rise, the resultant obesity epidemic looks set to cause a public health problem in years to come.

1.3 Insulin

1.3.1 Metabolic actions of insulin

Insulin, produced by the β cells of the pancreas, is a major anabolic hormone whose action is essential for growth, development and homeostasis of glucose, fat and protein metabolism (Virkamaki *et al.,* 1999, Le Roith 2001). Insulin stimulates the formation of metabolic storage compounds such as glycogen and triacyclglcyerols by facilitating the uptake of glucose into the cell via activation of a series of glucose transporters expressed in the cell membrane. Since cells are not permeable to glucose, a family of specialised glucose transporter (GLUT) proteins carry glucose into cells (Krusznynska, 2003). The principal stimulus for insulin secretion is a change in plasma glucose. In the liver, insulin promotes the metabolism of glucose via glycolysis and the Krebs cycle, whilst excess glucose is converted into the storage compound glycogen, thus insulin serves to regulate hepatic metabolism via control of the rate of catabolic reactions such as gluconeogenesis and β oxidation. Since the liver inactivates approximately 80% of insulin, the concentration of insulin in the systemic circulation is normally considerably lower than that found in the portal system. Even at these lower concentrations insulin can stimulate the synthesis of proteins in muscle cells through increased amino acid uptake and ribosomal protein synthesis. Of all the storage compounds, fat represents the most efficient means of storing energy, providing 9kcals per gram of stored substrate. Insulin promotes the formation of triglycerides in adipocytes through inhibition of intracellular lipolysis, hydrolysis of triglycerides from circulating lipoproteins and by increasing glucose transport into fat cells. The latter enables increased availability of

α-glycerol phosphate, used in the esterification of free fatty aids into triglycerides (Krusznynska, 2003).

1.3.2 Insulin-structure, secretion and mode of action

Human insulin is a peptide hormone produced by the β cells of the pancreatic islets. Structurally it is comprised of 51 amino acids and is structurally homologous to insulin like growth factors 1 and 2 and also to the ovarian hormone, relaxin (Kumar *et al.*, 2002). The gene for insulin codes for pre-proinsulin and is located on chromosome 11 (Kumar *et al.*, 2002). Pre-proinsulin is comprised of a signal sequence at the N-terminus (approximately 23 amino acids) that is cleaved following trafficking to the endoplasmic reticulum giving rise to proinsulin which is composed of an A chain, a joining C-peptide and a B chain. The C peptide is essential to the formation of disulfide bonds which form between cysteine residues allowing the A and B chains to adopt an appropriate conformation which will ensure efficient cleavage in the golgi apparatus. In the *trans*-golgi apparatus, pro-insulin is packaged into secretory granules where proteases begin to slowly cleave the proinsulin molecule at two spots resulting in release of the C-peptide. Cleavage of the C-peptide results in conversion of proinsulin into mature insulin comprised of 51 amino acids, 21 on the A chain and 30 on the B chain. The manufacture and release of insulin is illustrated in Figure 1.1 (Kumar *et al.*, 2002).

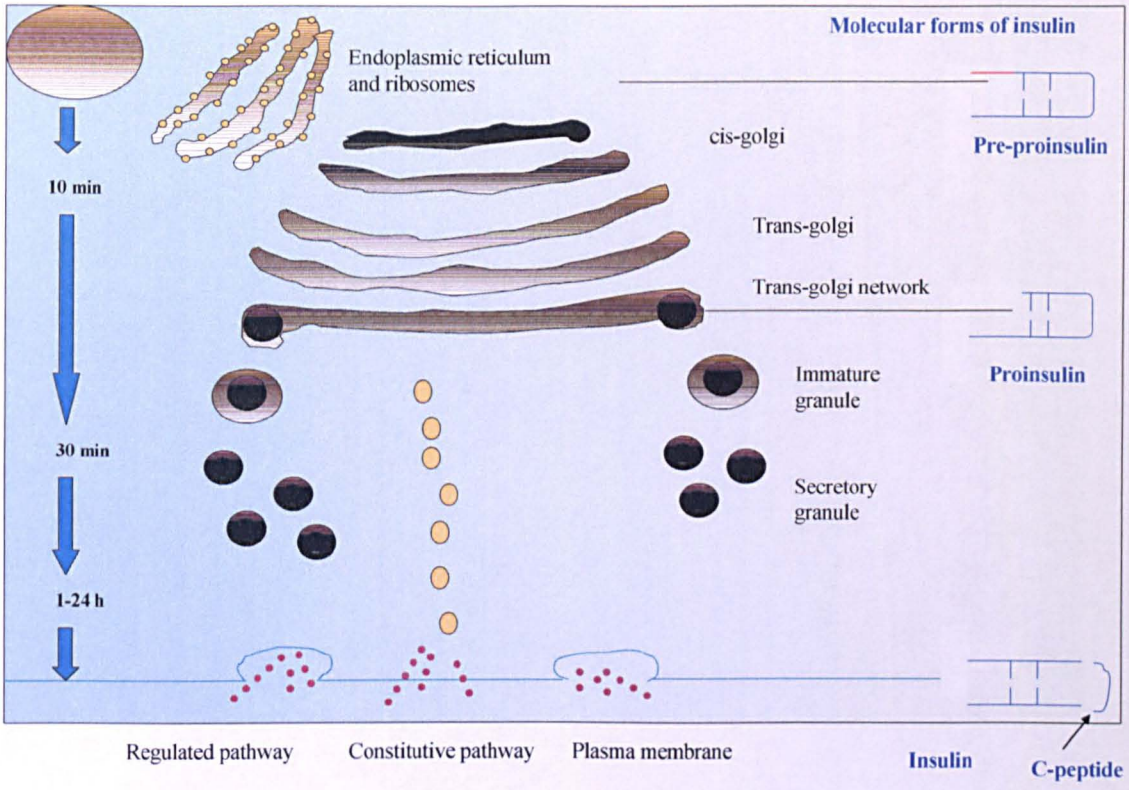

Figure 1.1 Insulin synthesis and secretion: The ribosomes manufacture pre-proinsulin from insulin mRNA. Cleavage of this pre region at the ER leaves pro-insulin at the golgi apparatus. At the golgi, proinsulin is parcelled into secretory granules. These mature and pass towards the cell membrane where they are stored before release. The C peptide splits off from proinsulin in the secretory process, leaving insulin as a complex of two linked peptide chains. A small amount of insulin is secreted by the β cell directly by the constitutive pathway which bypasses secretory granules (Kumar *et al.*, 2002).

Whilst there is still a degree of controversy as to whether C peptide exerts any functional biological role within the system, the fact that it is secreted in a 1:1 molar ratio with insulin makes it a useful marker for insulin secretion. When insulin is secreted, it enters the portal circulation and is carried to the liver where most of it is removed. However, C-peptide is not metabolised by the liver and thus whilst the concentration of insulin in systemic blood does not quantitatively mimic the secretion of insulin, measurements of C-peptide do.

Insulin is secreted in pulses every ten minutes or so in response to a variety of secretagogues. Whilst glucose is the best secretagogue, some amino acids and small ketoacids can also stimulate insulin secretion. The stages involved in secretion of

insulin have been proposed as follows and is illustrated in Figure 1.2 (Kumar *et al.*, 2002)

1. In humans, glucose enters the β-cell by the glucose transporter GLUT2.
2. Glucose is metabolised by glycolysis consequently raising $[ATP]_i$ by phsophorylating ADP.
3. The increased $[ATP]_i/[ADP]_i$ ratio closes the ATP-sensitive K^+ channel (K^+ATP) and results in depolarisation of the β cell (i.e the membrane potential is less negative).
4. This depolarisation results in an influx of calcium ions via calcium channels in the cell membrane through voltage-dependent Ca^{2+} channels.
5. The rise in calcium leads to the fusion of insulin containing granules with the cell membrane and exocytosis of the granule contents, ultimately leading to insulin release.

Secretion occurs in two main phases; the first phase represents the release of insulin stored in secretory granules, whilst the second phase, which is a longer sustained phase, may last up to several hours and is consequently reliant upon *de novo* synthesis of the hormone.

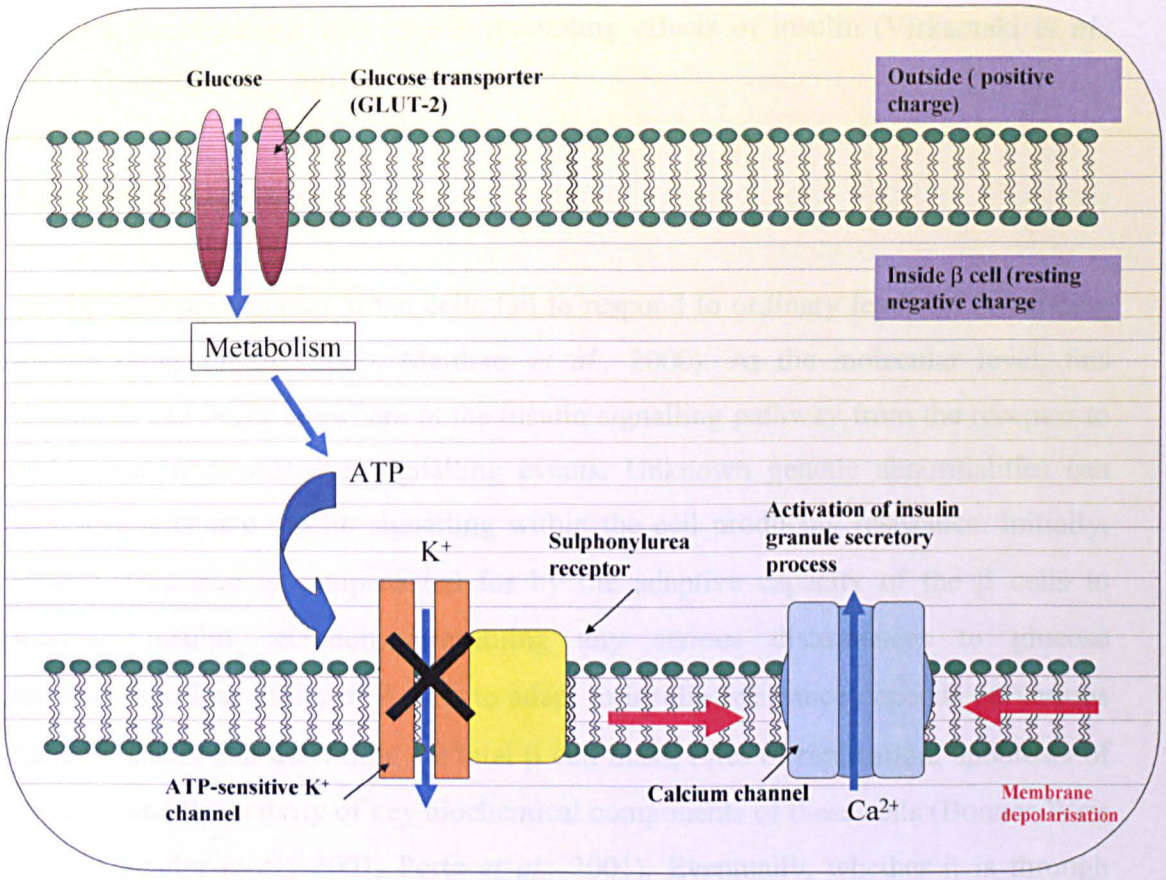

Figure 1.2 Local forces regulating insulin secretion from beta cells. Glucose enters the beta cell via the GLUT 2 transporter, which is closely associated with the glycolytic enzyme glucokinase. Metabolism of glucose within the beta cell generates ATP. ATP closes potassium channels in the cell membrane. If a sulfonylurea, binds to its receptor then this will close the K^+ channel and depolarise the membrane allowing calcium ions to enter via calcium channels in the cell membrane. The rise in intracellular calcium leads to fusion of the insulin containing granules with the cell membrane and exocytosis of the insulin rich granules contents (Kumar *et al.*, 2002)

Insulin mediates its effects through a heterodimeric receptor expressed in the cell membrane. This receptor is a tetramer with two α subunits, which comprise the insulin binding sites and two β subunits which traverse the cell membrane. When insulin binds to the α subunits, it induces a conformation change in the beta subunits stimulating the intrinsic tyrosine kinase activity. This results in phosphorylation of a number of target proteins including insulin receptor substrate (IRS) proteins which serve as docking sites for downstream effector molecules. This triggers two major signalling kinase cascades, the phosphoinositide 3-kinase (PI3-K) and the mitogen activated protein (MAP) kinase pathways. Together, these two signalling pathways

mediate the metabolic and growth promoting effects of insulin (Virkamaki *et al.*, 1999, LeRoith *et al.*, 2001)

1.3.3 Insulin resistance

Insulin resistance occurs when cells fail to respond to ordinary levels of circulating insulin (Kahn *et al.*, 2000, Matthaei *et al.*, 2000). At the molecular level, this resistance can occur anywhere in the insulin signalling pathway from the receptor to alterations in downstream signalling events. Unknown genetic abnormalities can therefore attenuate insulin signalling within the cell producing resistance. Initially, insulin resistance is compensated for by the adaptive capacity of the β cells to increase insulin secretion, preventing any serious disturbances to glucose homeostasis. The ability of β cells to adapt to insulin resistance depends on various genetic factors that determine the total β cell mass, rates of replication, apoptosis of the cells and the activity of key biochemical components of these cells (Bonner-Weir 2001, Chandra *et al.*, 2001, Porte *et al.*, 2001). Eventually, whether it is through increased insulin resistance or β cell burn out, the β cell is unable to compensate for the level of resistance and β cell failure can occur.

1.4 Anatomy of the mammalian kidney

Human adults produce on average a litre of urine (pH ~6) each day. Urine contains water and other by products of metabolism, such as urea as well as NaCl, KCl, phosphates and other substances present in excess of the body's requirements. The role of the kidney is to maintain, through elimination of these waste products, a homeostatic environment and therefore has 3 major functions:

1. Excretion, or the removal of waste products from body fluids

2. Homeostatic regulation of the volume and solute concentration of blood

The gross anatomy of the mammalian kidney is shown in Figure 1.3. Each individual has two kidneys one located each side against the dorsal inner surface of the lower

back. Despite their small size (150g), the kidneys receive a remarkably large blood flow, equivalent to about 20%-25% of the total cardiac output (Kumar *et al.*, 2002)

The kidney itself has two layers; an outer cortex and an inner medulla. The outer layer, the cortex is covered by a tough capsule of connective tissue, whilst the inner layer, the medulla consists of 6-18 distinct triangular structures called renal pyramids. The tips of these renal pyramids are referred to as papilla and project into the renal sinus. Adjacent pyramids are separated by bands of cortical tissue called renal columns which extend into the medulla. Collectively the renal pyramid, the overlying area of renal cortex and adjacent tissues of the renal columns are referred to as renal lobes. Urine production occurs in the renal lobes in microscopic structures called nephrons. Urine flows from these nephrons into the renal pelvis. The renal pelvis gives rise to the ureters which empty into the urinary bladder. Urine leaves the bladder via the urethra which leads to the end of the penis in males and into the vulva in females (Kumar *et al.*, 2002).

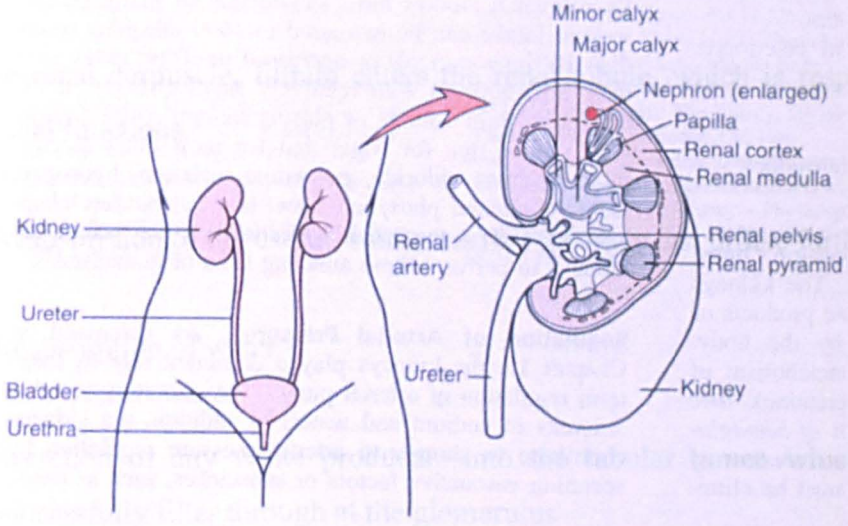

Figure 1.3 Gross anatomy of the mammalian kidney (Guyton *et al.*, 2005).

1.4.1 The nephron is the functional unit of the kidney

The functional unit of the mammalian kidney is the nephron (Figure 1.4A), an epithelial tube which may be, 50mm in length that is closed at the beginning but

open at its distal end. Each kidney contains roughly 1.25 million nephrons with a combined length of about 145 km (Kumar *et al.,* 2002). The beginning of the nephron starts with the renal corpuscle, a spherical structure enclosing the bowmans capsule, a cup shaped chamber approximately 200μm in diameter with a capillary network known as the glomerulus. The lumen of the capsule is continuous with the narrow lumen that extends through the renal tubule. Blood arrives at the bowmans capsule by way of an afferent arteriole and subsequently leaves via the efferent arteriole. From here blood flows into a network of capillaries that surround the renal tubule. These capillaries, in turn drain into small venules that return the blood to the venous system.

The glomerulus is the structure responsible for the first step in urine formation. Blood pressure forces water and dissolved solutes out of the glomerular capillaries and into the capsular space that is continuous with the lumen of the renal tubule. Filtration produces a protein-free solution referred to as the filtrate that resembles blood plasma.

From the renal corpuscle, filtrate enters the renal tubule, which is responsible for three crucial functions.

1. Reabsorption of the useful substrates that the body can utilise further

2. Reabsorption of water

3. Secretion of any waste products into the tubular lumen which failed to successfully filter through at the glomerulus

The nephron can be divided into three main regions (see Figure 1.4A), the proximal nephron, the Loop of Henle and the distal nephron. The proximal and distal nephron are convoluted tubules which lie in the kidney cortex, whilst the U shaped tube which separates these two tubes, commonly known as the Loop of Henle lies into the medulla. (Figure1.4B)

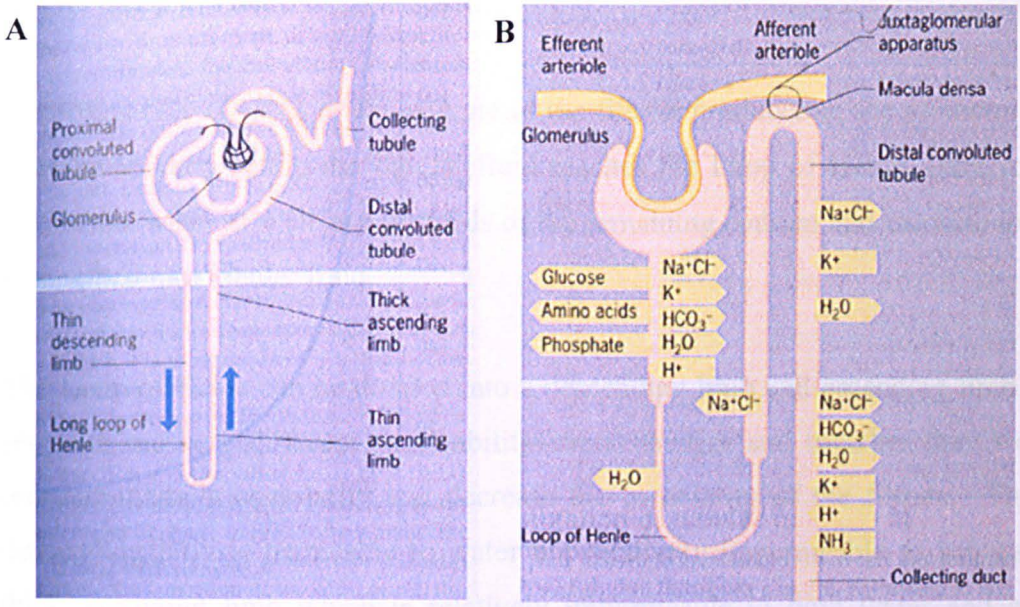

Figure 1 .4 Structure of the nephron (A) Main parts of the nephron (B) Sites of reabsorption or addition of substances into tubular fluid. (Kumar *et al.*, 2002)

1.4.1.1 The Proximal Convoluted Tubule

The Proximal Tubule is initially convoluted (PCT) and then straightens out as it leads down to the Loop of Henle. The cells lining the proximal tubule are tall, cuboidal epithelium covered in apical microvilli. In the proximal tubule many substances are reabsorbed including sodium (70%), potassium, calcium, phosphate glucose, amino acids and water. Solutes are initially reabsorbed into the peritubular fluid, the interstitial fluid which surrounds the renal tubule. The proximal tubule is highly permeable to water. Therefore as solutes are reabsorbed water will follow by osmosis, thus whilst the volume of the filtrate is reduced in the proximal convoluted tubule, the filtrate is not concentrated. The primary function of the PCT is reabsorption however cells can also secrete substances into the lumen that have bypassed filtration.

1.4.1.2 Loop of Henle

Approximately 60-70% of the volume of the filtrate produced at the glomerulus has been reabsorbed before the tubular fluid reaches the Loop of Henle. Here roughly half of the water as well as two thirds of the remaining sodium and chloride ions are reabsorbed into tubular fluid.

The Loop of Henle can be divided into a descending limb and ascending limb. Each segment has very different permeability characteristics and together they work to increase medulla osmolarity and decrease the osmolarity of the filtrate. The thin descending limb is permeable to water but relatively impermeable to solutes. The thick ascending limb which is relatively impermeable to both water and solutes contains active transport mechanisms that pump sodium and chloride ions from the tubular fluid into the peritubular fluid of the medulla. The exchange that occurs between these segments is called countercurrent multiplication. Countercurrent refers to the fact that the exchange occurs between fluids moving in opposite directions; Fluid in the descending limb travels towards the renal pelvis whilst that in the ascending limb travels towards the renal cortex. Multiplication refers to the fact that the effect of the exchange increases as movement of the fluid continues.

Countercurrent multiplication is a simple positive feedback loop and operates as follows

- Sodium and chloride are pumped out of the thick ascending limb and into the peritubular fluid.
- This pumping action elevates the osmotic concentration in the peritubular fluid around the thin descending limb.
- The result is an osmotic flow of water out of the thin descending limb into the peritubular fluid increasing the solute concentration in the thin descending limb.

- The arrival of a highly concentrated solution in the thick ascending limb accelerates the transport of sodium and chloride ions into the peritubular fluid of the medulla

Active transport at the apical surface of the ascending limb moves sodium, potassium and chloride ions out of the tubular fluid via a $Na^+/K^+/2Cl^-$ co-transporter. With each cycle of the pump, a sodium ion, potassium ion and two chloride ions are moved into the tubular cell. Potassium and chloride ions are pumped into the peritubular fluid by cotransport carriers. However potassium ions are removed from the peritubular fluid as the sodium-potassium exchange pump pumps sodium ions out of the tubular cell. The potassium ions then diffuse back into the lumen of the tubule through potassium leak channels. The net result is that Na^+ and Cl^- enter the peritubular fluid of the renal medulla. This removal of Na^+ and Cl^- ions from the tubular fluid in the ascending limb elevates the osmotic concentration of the peritubular fluid around the thin descending limb and subsequently draws water out of the thin descending limb by the process of osmosis. Solutes remain in the tubular fluid since the thin descending limb is impermeable to solutes, thus as the tubular fluid reaches the turn of the Loop of Henle, it has a higher osmotic concentration than it did as the start. (Figure 1.5)

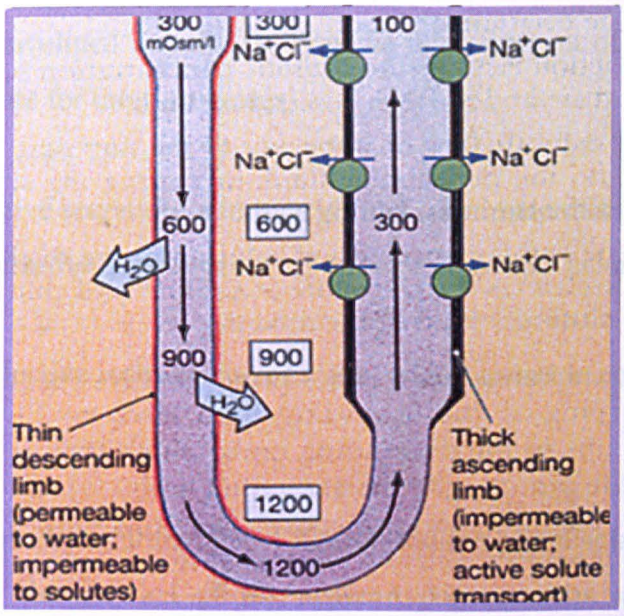

Figure 1.5: Counter-current multiplication and concentration of urine in the Loop of Henle. Active transport of NaCl along the ascending thick limb results in the movement of water from the descending limb (Martini F *et al.*, 2004)

Almost two thirds of the sodium and chloride ions that enter the thick ascending limb are pumped out of the tubular fluid. Since the thick ascending limb is not permeable to water; osmosis does not occur and thus the solute concentration in the tubular fluid is reduced. By the time the tubular fluid reaches the Distal Convoluted Tubule it has an osmotic concentration of only about 100mOsm/l, one third of the concentration of the peritubular fluid of the renal cortex. The rate of ion transport in the thick ascending limb is proportional to ion concentration in tubular fluid. As a result, more sodium and chloride ions are pumped into the medulla at the start of the thick ascending limb, where NaCl concentrations are highest than near the cortex. This determines the concentration gradient within the medulla. Sodium and chloride ions account for approximately two thirds of this gradient, the rest results from the presence of urea. Since the thick ascending limbs of the Loop of Henle, the DCT and the collecting ducts are impermeable to urea, therefore water reabsorption results in an increase in urea concentration. Urea reabsorption occurs in the papillary ducts where the epithelium is permeable.

1.4.1.3 The Distal Convoluted Tubule

The Distal Convoluted Tubule (DCT) is the third segment of the renal tubule and is an important site for three processes

1. The active secretion of ions, acids and other materials
2. The selective reabsorption of sodium ions and calcium ions from tubular fluid.
3. The selective reabsorption of water, which assists in concentrating the tubular fluid

The DCT reabsorbs a further 5% of filtered sodium establishing a negative charge in the lumen of this portion of the nephron consequently sodium reabsorption is accompanied by the movement of negatively charged chloride ions.

In the DCT, a group of specialised renin-secreting cells form a region called the macula densa. These cells are closely associated with smooth muscle fibres in the wall of the afferent arteriole. The fibres are referred to as juxtaglomerular cells and are situated on the afferent glomerular arteriole as it enters the glomerulus. Renin, converts angiotensinogen in the blood to angiotensin1 and is released in response to a drop in afferent arteriole pressure, a fall in tubular flow rate or a fall in sodium and chloride in the distal tubule via the macula densa. angiotensin 1 is converted by angiotensin converting enzyme (ACE) into Angiotensin II. Renin therefore promotes production of angiontensin II which acts via AII receptors to promote vasoconstriction of afferent and efferent arterioles. The dominant effect is on efferent arteriolar constriction so that glomerular filtration rate is increased.

1.4.1.4 The collecting system

As the hypotonic urine passes down the collecting ducts, both water and sodium are reabsorbed. Around 2-5% of filtered sodium is reabsorbed in the collecting ducts. Two characteristic cell types are involved in this process

Principal cells-These are involved in sodium reabsorption via the apically expressed epithelial sodium channel (ENaC) and the basolateral Na^+/K^+ ATPase (For further details see section 1.9).

Intercalated cells-These have no Na^+/K^+ ATPase but do have an H^+ ATPase responsible for establishing a hydrogen gradient. Energetic drive of the pump is derived from this H^+ gradient. As H^+ ions are removed from the cell, the net result is the secretion of bicarbonate coupled to the reabsorption of chloride. Intercalated cells are also involved in the reabsorption of potassium via an apical H^+/K^+ ATPase.

Water permeability is controlled in the collecting ducts by antidiuretic hormone (ADH) or vasopressin. Secreted by the pituitary in response to volume depletion, angiotensin II, pain, trauma and temperature, ADH binds to its corresponding V_2 receptors, stimulating adenyl cyclase and raising intracellular cAMP levels (Knepper *et al.,* 1993). This causes the fusion of intracellular vesicles containing the water channel aquaporin 2 (AQP2) with the apical cell membrane and the subsequent reabsorption of water (Brown, 2003) down an osmotic gradient established by the counter current multiplication of the Loop of Henle. If the permeability of the collecting ducts is low, there is no water reabsorption; yet sodium chloride is continually reabsorbed further diluting the urine. Contrary to this, if the permeability of the collecting ducts is high then water moves out of the hypotonic tubular fluid into the surrounding hypertonic interstitium. In the cortical collecting duct, tubular fluid equilibrates with the cortical interstitium which is at plasma osmolarity. In the deeper medullary collecting duct, tubular fluid then equilibrates with the high osmolality of the medullary interstitium producing concentrated urine.

1.5 Diabetic nephropathy

Of the complications associated with Type II diabetes, diabetic nephropathy is one of the most extensively studied conditions known to arise as a consequence of this hyperglycaemic state and is classically defined as:

"a progressive increase in urine albumin excretion, accompanied by rising blood pressure and a relentless decline in glomerular filtration, culminating eventually in end stage renal failure" (Grenfell 1997).

The condition refers to both structural and functional alterations that occur in the kidney of the diabetic patient (Reeves *et al.*, 2000). Whilst structural changes include renal hypertrophy, thickness of the glomerular basement membrane, and increased extracellular matrix accumulation in the glomeruli, functional disturbances include an increase in glomerular filtration rate, glomerular hypertension, proteinuria, systemic hypertension and finally renal failure. (Mason *et al.*, 2003)

The main pathological features of the diabetic kidney occur both in the glomerulus and in the tubule interstitium. In a normal subject, the glomerulus consists of a tuft of approximately 20-30 capillary loops, all of which arise from an afferent arteriole and subsequently drain into an efferent arteriole (Tisher 1981). These tufts are enclosed within the bowmans capsule. The mesangium and mesangial cells are composed of both cellular and matrix components involved in both production and degradation of extracellular matrix proteins, including Type I and Type IV collagen and fibronectin, providing structural support for the glomerulus (Kumar *et al.*, 2002). The capillaries within the glomerulus are surrounded by a basement membrane. Resting against this membrane, are a class of epithelial cells called Podocytes which extend into primary and secondary cytoplasmic processes branching into long projections called foot processes (Figure 1.6). These foot processes attach to the urinary side of the glomerular basement membrane where they interdigitate with adjacent cells forming filtration slits of ~2.5-5 nm. Across these slits, a highly organised network; of several glycoproteins form 'slit pores' responsible for filtration of water, solutes and macromolecules (Gnudi *et al.*, 2003).

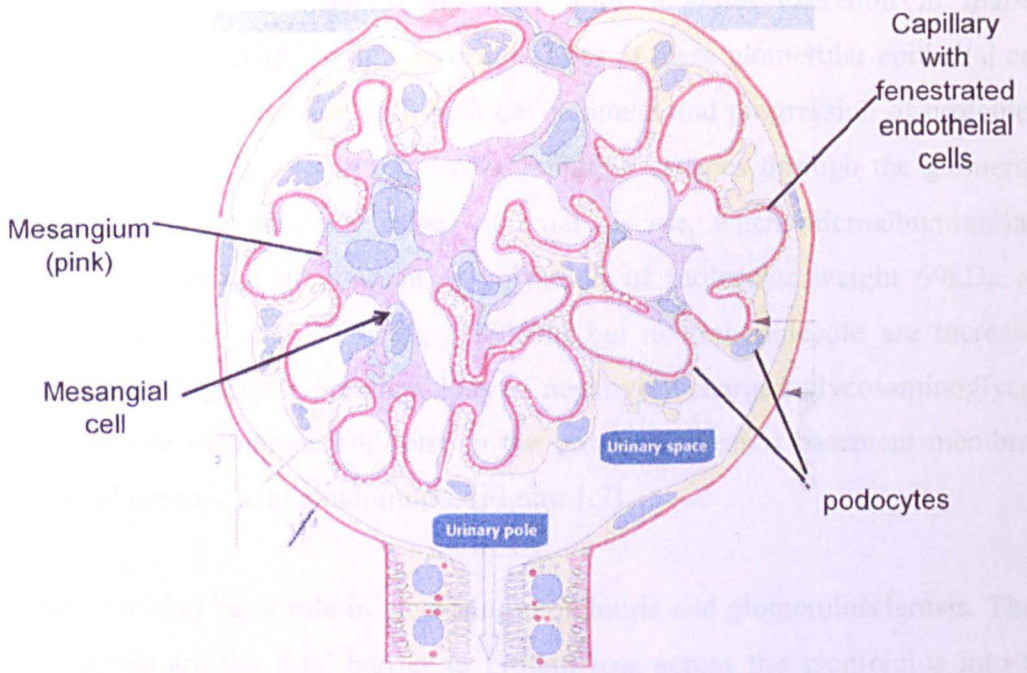

Figure 1.6 Schematic representation of a glomerular capillary tuft (Kierszenbaum *et al.*, 2002).

Together the fenestrated endothelium and the podocytes form the basement membrane. In patients with diabetes, both kidney and glomerular volume are increased (Mogensen *et al.*, 1979), the latter of which continues to enlarge with the disease (Osterby *et al.*, 1987). Glomerular enlargement is initially due to an increase in capillary surface area and subsequently to adaptive changes in the surviving glomeruli upon both thickening of the basement membrane and mesangial expansion (Mauer *et al.*, 1984)

In diabetes, mesangial expansion occurs when cells of the mesangium exhibit a reduction in their ability to successfully degrade matrix proteins. Mesangial expansion often manifests itself in the form of a diffuse lesion that develops into a more structured nodular appearance often occupying the central mesangial area (Morley *et al.*, 1988). This expansion occurs at the expense of the glomerular capillary lumen and filtration surface area. This reduction is glomerular filtation rate (GFR) correlates closely with the decline in renal function and the development of proteinuria (Mauer *et al.*, 1984).

It is widely accepted that the increased urine albumin excretion in diabetic nephropathy is mostly glomerular in origin. Loss of these glomerular epithelial cells has been reported to coincide with both development and progression of proteinuria in diabetic patients (Meyer *et al.,* 1999). Albumin escapes through the glomerular filtration barrier. In the early stages of renal disease, when microalbuminuria is present, the clearance of albumin, a polyanion of molecular weight 69kDa and immunoglobulin G (IgG), a larger (150kDa) but neutral molecule are increased. Increased intraglomerular pressure, loss of negatively charged glycosaminoglycans in the basement membrane and later in the process increased basement membrane pore size all contribute to albuminuria. (Figure 1.7)

The podocyte also has a role in increasing proteinuria and glomerulosclerosis. These foot processes are the final barrier to protein loss across the glomerulus into the urinary space. Like the basement membrane, podocytes are also covered in negatively charged proteins that repel anionic proteins such as albumin. This is essential as it prevents proteinuria through the aid of proteins such as nephrin which prevent escape of protein into bowmans capsule. Podocyte morphology is altered in diabetes where foot processes broaden and the effective pore size increases. Eventually the filtration barrier loses its selectivity and proteinuria ensues. With time damage results in complete loss of the podocyte (White *et al.,* 2002). Failure of these podocytes to regerenate means that this loss cannot be compensated for.

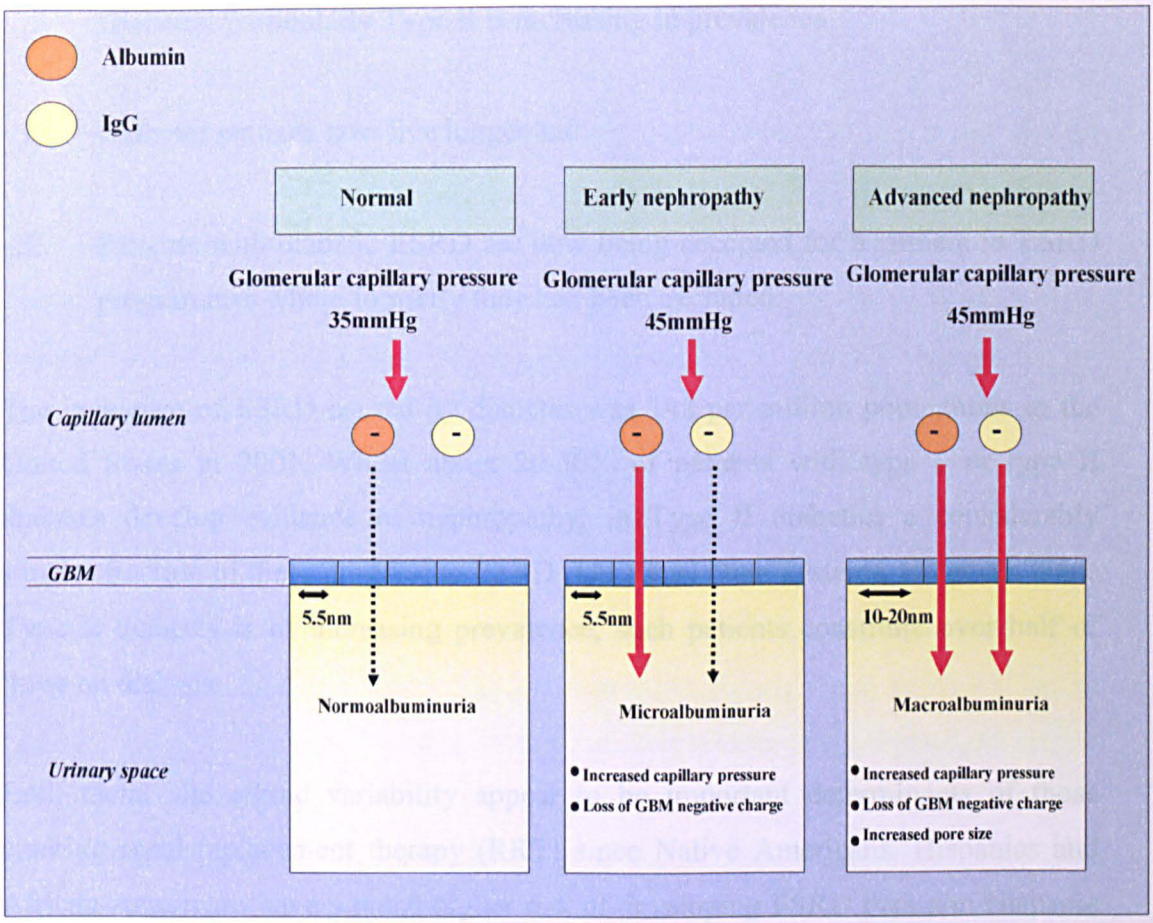

Figure 1.7 The evolution of proteinuria in diabetes. Filtration of plasma proteins such as albumin and the larger electrically neutral immunoglobulin (IgG) is normally restricted by the resting negative charge on the glomerular basement membrane (GBM) and by the size of the filtration pores. Increased glomerular capillary pressure and the loss of negative charge increase filtration of proteins including albumin in the early stage of microalbuminuria. With further loss of negative charge and enlargement of filtration pores in advanced nephropathy, albumin loss increases greatly and IgG is readily filtered (Gnudi *et al.*, 2003)

1.6 The socioeconomic burden of diabetic nephropathy

Worldwide, diabetic nephropathy is now the single commonest cause of entry into the renal replacement therapy programme (US Renal Data System) and has become the leading cause of end-stage renal disease (ESRD) in the US and Europe. This is due to the fact that:

i. Diabetes, particularly Type II is increasing in prevalence

ii. Diabetes patients now live longer and

iii. Patients with diabetic ESRD are now being accepted for treatment in ESRD programmes where formerly they had been excluded.

The incidence of ESRD caused by diabetes was 148 per million populations in the United States in 2001. Whilst about 20-30% of patients with type 1 or type II diabetes develop evidence of nephropathy, in Type II diabetics a considerably smaller fraction of these progress to ESRD (US Renal Data System). However, since Type II diabetes is of increasing prevalence, such patients constitute over half of those on dialysis.

Both racial and ethnic variability appear to be important determinants of those entering renal replacement therapy (RRT) since Native Americans, Hispanics and African-Americans have a much higher risk of developing ESRD than non-Hispanic Whites with Type II diabetes, thus the higher the proportion of individuals from ethnic minorities in one identified population, the higher the incidence of those entering RRT (American Diabetes Association., 2004). It is of no surprise therefore that the percentage entrance into the RRT varies widely geographically; from 54% in Brunei to 9.7% in Bulgaria (US Renal Data System)

1.7 Cell biology of diabetic kidney disease

Hyperglycaemia is one of the predominant factors in the development of Diabetic nephropathy. There is strong evidence that poor blood glucose control contributes towards the development of albuminuria, however and in those diabetic patients who undergo intensive therapy, the risk of transition from normo to microalbuminuria is only reduced by approximately 35% (Krolewski *et al.,* 1995). Some of the mechanisms that link hyperglycaemia to the functional/structural abnormalities of diabetic kidney disease have been elucidated.

A number of cellular events occur in the presence of high glucose that include increased flux of polyols and hexosamines, formation of reactive oxygen species (ROS), activation of PKC, transforming growth factor (TGF-β1), Smad-mitogen – activated protein kinase (MAPK) and G-protein signalling and altered expression of cyclin kinases, their inhibitors and of matrix proteins, matrix degrading enzymes and metallo proteinases (Gnudi *et al.,* 2003). These events are all thought to be interconnected and generally resulting in increased deposition of extracellular matrix (ECM), a hallmark of Diabetic nephropathy which contributes towards the development of renal disease (Mason *et al.,* 2003).

Sustained hyperglycaemia also leads to non-enzymatic protein glycation. This involves the covalent bonding of glucose to proteins in which a lysine amino terminal group is exposed. These glycated products undergo dehydration, oxidation and rearrangement to form toxic advanced glycation end products (AGEs) (Brownlee, 1995). AGEs can be either intracellular or extracellular depending upon how they are formed. Those acting intracellularly can activate PKC, MAPK and transcription factors eg NF-κB, whilst extracellular AGEs act via a receptor to modulate expression of various cytokines and ECM proteins. This interaction has been shown to induce the synthesis and release of various cytokines, including TGF-β1 and IGF, various ECM proteins and Type I and IV collagens (Sakurai *et al* 2003). In diabetic animals, AGE accumulation in the kidney is paralleled by the development of albuminuria, mesangial expansion, and glomerular basement thickening. These developments were found to be attenuated upon administration of Aminoguanidine (AGN), an AGE inhibitor (Edelstein *et al.,* 1992).

Kidney cells, as with cells at other sites of diabetic vascular complications, do not have an absolute requirement of insulin for glucose uptake, thus the intracellular glucose level more directly reflects its plasma concentration. Glucose entry into renal cells is facilitated by GLUT1 and GLUT4 (glucose transporters) as well as by both sodium co-transporters such as Sodium Glucose Transporter 1 (SGLT1) and Sodium Glucose Transporter 2 (SGLT2), which allow glucose into the cell for subsequent metabolism. GLUT 1 has been linked to the pathobiology of diabetic complications

following observations of excessive production of those proteins involved in enhanced ECM development under normal glucose ambience. Overexpression of GLUT 1 at a normal glucose concentration has been demonstrated to induce those phenotypic changes associated under conditions of hyperglycaemia (Heilig *et al.*, 1995). The administration of GLUT 1 antisense was found to diminish the production of fibronectin in mesangial cells, suggetsing that the regulation of these glucose transporters is critical since they appear to play a role in both extracellular and intracellular events (Heilig *et al.*, 2001)

Glucose metabolism feeds a number of related down-stream cascades (Figure 1.8) (Nelons *et al.*, 2000)

- Firstly glucose is phosphorylated by hexokinase and after several steps fructose 6-phosphate and glyceraldehyde 3 phosphate are produced leading to adenosine triphosphate (ATP), generating reactions with pyruvate and lactate as end products

- Secondly the glycerol phosphate is a precursor of Diacylglycerol (DAG). DAG is a powerful signalling molecule that modulates intracellular signalling events relevant to the pathogenesis of diabetic nephropathy (LeRoith *et al.*, 2004, Brownlee 2000) and stimulates activation of PKC. PKC has too emerged as a potential regulator of all aspects of the development and progression of diabetic nephropathy

- In conditions of high glucose, excessive sugar is shuttled into the hexosamine pathway in which fructose 6-phosphate is converted to glucose amine 6-phopshate by a rate limiting enzyme, glutamine fructose-6-phosphate–aminotransferase (GFAT). This leads to the production of UDP-N-acteylglucosamine, a precursor of proteoglycans, lycoproteins and glycolipids (Schleicher *et al.*, 2000) Inhibition of GFAT has been shown to inhibit promoter activities of certain molecules relevant to Diabetic nephropathy eg TGF-β1 and plasminogen activator protein (PAI)-1 by affecting phosphorylation of a number of transcription factors eg SP1 (Irvine *et al.*,

2005). Other transcription factors that bind to promoters of glucose responsive genes and other nuclear or cellular proteins are also believed to be affected by high glucose.

- As in the hexosamine pathway, intracellular glucose can be diverted into the polyol pathway. In this pathway, glucose is reduced to sorbitol, catalysed by an NADPH dependent enzyme aldose reductase. Sorbitol is then oxidised to fructose utilising NAD^+ as a cofactor (Chung *et al.*, 2003). This results in an increase in the ratio of reduced nicotinamide adenine dinucleotide (NAD) and associated metabolic changes including osmotic stress and an imbalance in the cellular redox. Aldose reductase inhibitors fail to prevent cellular and matrix changes in the kidney, suggesting that the polyol pathway may not be solely responsible for renal complications in diabetes mellitus (McAuliffe *et al.*, 1998)

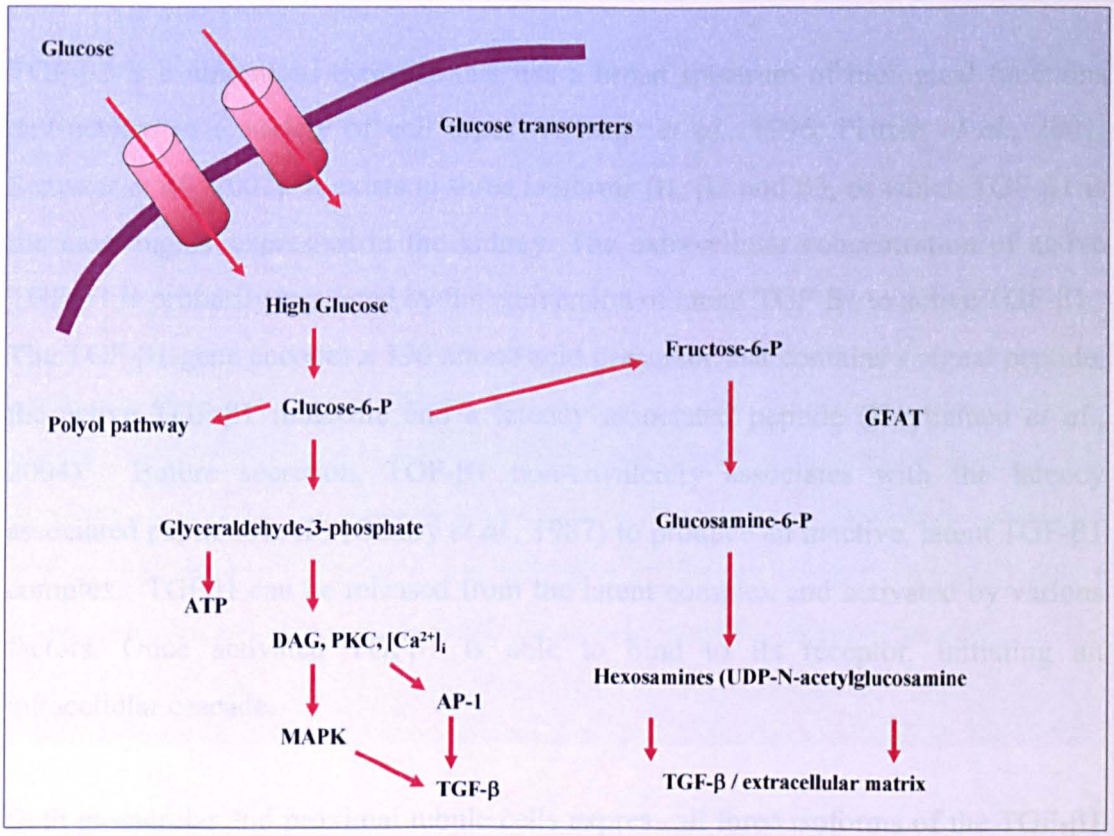

Figure 1.8: The metabolism of glucose in a cell and its possible involvement in the generation of TGF-β1.

1.8 Molecular mediators of Diabetic nephropathy

At the cellular level a number of key signalling molecules converge to bring about the pathogenesis associated with Diabetic nephropathy.

1.8.1 Transforming growth factor-β1

TGF-β1 is the founding member of the TGF-β superfamily that can be sub divided into 4 major families

The Mullerian inhibitory substance (MIS) family.
The inhibin/activin family
The bone morphogenetic protein (BMP) family and the
TGF-β family

TGF-β1 is a ubiquitous cytokine that has a broad spectrum of biological functions and actions in a variety of cell types (Arteaga *et al.,* 1996, Platten *et al.,* 2001, Schuster *et al.,* 2002). It exists in three isoforms β1, β2 and β3, of which TGF-β1 is the most highly expressed in the kidney. The extracellular concentration of active TGF-β1 is primarily regulated by the conversion of latent TGF-β1 to active TGF-β1. The TGF-β1 gene encodes a 390 amino acid precursor that contains a signal peptide, the active TGF-β1 molecule and a latency associated peptide (Hyytiainen *et al.,* 2004). Before secretion, TGF-β1 non-covalently associates with the latency associated peptide (LAP) (Gentry *et al.,* 1987) to produce an inactive, latent TGF-β1 complex. TGFβ1 can be released from the latent complex and activated by various factors. Once activated TGFβ1 is able to bind to its receptor, initiating an intracellular cascade.

Both glomerular and proximal tubule cells express all three isoforms of the TGF-β1 receptor (Border *et al.,* 1994). Following binding TGF-β1 activates a family of transcription factors known as Smads (Massague 2000), found in vertebrates, insects

and nematodes (Heldin *et al.*, 1997) Smad proteins consist of receptor regulated Smads, a common pathway Smad and inhibitory Smads.

- Receptor regulated (R) Smads are phosphorylated by TGF-β1 Type I receptor and include Smad 2 and Smad 3, 5 and 8 (Massague 2000).

- Smad 4 is a common pathway Smad that is not phosphorylated by the TGF-β1 Type I receptor (Massague 2000, Liu *et al.*, 1997).

- Inhibitory Smads include Smad 6 and Smad 7 which downregulate TGF-β1 signalling (Massague 2000).

- The Co-Smads form complexes with the R Smads. Although the Co-Smads are not required for the nuclear accumulation of R-Smad containing complexes, they are necessary for the formation of functional transcriptional complexes (Liu *et al.*, 1997)

TGF-β1 initiates its cellular response by binding to its distinct receptor, TGF-β receptor II (TβRII) which activates the TβRI kinase prior to phosphorylation of the receptor-regulated Smads (R-Smads). Activated R-Smads form oligomeric complexes with the common Smad (Co-Smad). These oligomeric complexes then translocate into the nucleus. In the nucleus, they may regulate the transcription of target genes by functioning as transcriptional activators and binding to DNA directly (Dennler *et al.*, 1998) or they may form associations with nuclear transcription factors such as AP-1. In many cell lines TGF-β1 is capable of positively regulating its own expression (Van Ibberghen-Schilling *et al.*, 1988,) Autoinduction of TGF-β1 transcription appears to be mediated through binding of an AP-1 complex to the TGF-β1 promoter. This autoinduction may be responsible for the pathologic induction of TGF-β1 that is associated with fibrosis of the kidney.

Abnormalities in TGF-β1 have been discovered in a wide variety of disorders, including autoimmune diseases, malignancies and chronic renal disease (Roberts *et al.*, 1998). Increased receptor expression has been described in experimental renal

disease models including membranous nephropathy, obstructive nephropathy and diabetic nephropathy (Chen S *et al.*, 2003)

The prosclerotic properties of TGF-β1 has suggested a role for TGF-β1 in diabetic glomerulopathy. TGF-β1 has emerged as having a key role in the development of renal hypertophy and accumulation of extracellular matrix in diabetes (Ziyadeh *et al* 1993) Renal fibrosis, characterised by increased accumulation of extracellular matrix (ECM) within renal tissue, represents the final common pathway for loss of renal function associated with primary disease states including diabetic nephropathy (Border *et al.*, 1995). Extensive studies have demonstrated that in both glomerular mesangial cells and tubular cells, the response to increased levels of TGF-β1 is an increase in synthesis of fibronectin, laminin and collagen (Ziyadeh *et al.*, 1993). In addition, TGF-β1 also inhibits the synthesis of metalloproteinases and activates the tissue inhibitor of metalloproteinases (Ma *et al.*, 1999). This results in a reduction in extracellular matrix degradation and further contributes to matrix accumulation.

In both human and experimental diabetes, TGF-β1 gene expression and protein secretion are increased in both the glomeruli and tubuli (Yamamoto *et al.*, 1993). The increased levels of TGF-β1 observed in hyperglycaemia arise from the activation of

1) UDP-N-Acteylglucosmine: Once transported into the cell, glucose is then shuttled into the glycolytic pathway for subsequent metabolism and the generation of ATP. However, under conditions of hyperglycaemia a vast amount of glucose is fed into the hexosamine pathway. Inhibition of this pathway has been linked to altered promoter activities of various molecules relevant to Diabetic nephropathy eg TGF-β1, through alteration to the phosphorylation status of transcription factors involved in binding to the TGF-β1 promoter (Kanwar YS *et al.*,2005)

2) PKC: Glucose is known to increase the de-novo synthesis of Diacylglycerol (Schena FP, *et al.*, 2005). Both DAG, and raised intracellular calcium $[Ca^{2+}]_i$ will activate the protein kinase PKC. PKC can activate the MAPK pathway. This will result in activation of the extracellular regulated kinase (ERK1/2)

which is able to induce phosphorylation of AP-1, a transcription factor complex composed of c-Jun and c-Fos. AP1 is thought to bind to the TGF-β1 promoter ultimately stimulating gene transcription

In addition, mechanical stretch, AGEs, lipids, angiotensin-2 and reactive oxygen species (ROS) have also been linked to the stimulation of TGF-β1 expression in renal cells (Ziyadeh *et al.*, 1994., Gruden *et al.*, 1999, Rocco *et al.*, 1992, Rumble *et al.*, 1997, Wolf *et al.*, 1995). Whilst glucose induced TGF-β1 is not considered the sole mediator in eliciting these deleterious effects associated with diabetic nephropathy, the administration of the TGF-β1 neutralising antibody decorin, a proteoglycan capable of binding and inactivating TGF-β1 (Border *et al.*, 1992) was found to effectively reverse the symptoms of diabetic nephropathy, indicating other mediators play a relatively small role compared to TGF-β1 (Ziyadeh *et al.*, 2000).

1.8.2 Protein kinase C

PKC, a family of serine/threonine kinases has at least eleven isoforms, many of which are upregulated in glomerular cells of hyperglycaemic rats (Whiteside *et al.*, 2002). PKC can be categorised into classical PKC, novel PKC, and atypical PKC on the basis of their common structural features.

- The classical PKC enzymes are comprised of two cysteine rich zinc finger like motifs (C_1 region), which are essential for interaction with phorbol ester and diacylglycerol (DAG), and a Ca^{2+} binding domain (C_2 region) in their regulatory region.

- The novel PKC enzymes do not require Ca^{2+} since the C_2 region is absent. The novel PKC enzymes are activated by phosphatidylserine and DG or phorbol esters.

- The atypical PKC enzymes, which lack the C2 region and one of the cysteine rich finger-like motifs in the C1 region are not activated by Ca^{2+}, DG phorbol

esters, but their activation depends on phosphatidylserine and cis-unsaturated fatty acids.

PKC activation regulates a number of cellular functions, including vascular permeability, contractility, cellular proliferation, basement membrane synthesis and signal transduction mechanisms (Koya *et al.*, 1998). PKC has emerged as a potential regulator of all aspects of the development and progression of diabetic nephropathy, with both DAG levels and subsequently PKC activation increased in a variety of tissues, including kidney glomeruli (Craven *et al.*, 1989).

PKC is a crucial downstream mediator of TGF-β1 and is thought to play a role in modulating TGF-β1 expression via regulation of transcription factors c-*fos* and c-*jun*, which form the activator protein (AP-1) transcription complex, which binds to and induces genes with AP-1 binding consensus sequences in their promoter regions (Ingram *et al.*, 1997). Genes encoding for TGF-β1, including fibronectin and laminin, all contain an AP-1 binding site in their promoter (Kim *et al.*, 1990).

Multiple cellular and functional abnormalities within the kidney have been attributed to the activation of PKC, since inhibition with various inhibitors has prevented the increase in ECM deposition, TGF-β1 upregulation and the development of albuminuria (Koya *et al.*, 2000).

1.8.3 P38 MAPK

Mitogen activated protein kinases (MAPKs) including the extracellular signal-related protein kinase 1/2 ERK, stress activated c-Jun N-amino terminal kinase (JNK) and p38 MAPK play a key role in the intracellular signal transduction cascade to integrate the transcription of genes for a variety of cellular responses (Cuschieri *et al.*, 2005). Activation of these serine/threonine kinases by phosphorylation, can lead to their translocation to the nucleus where they can then phosphorylate and activate transcription factors e.g. AP-1.

The classic MAPKs, ERK-1 and -2 are activated through Ras dependent transduction pathways and mediate cellular proliferation and differentiation by stimulating transcription factors that induce the expression of *c-fos* and other growth responsive genes (Bilato, 1995). In contrast, JNK and p38 MAPK lead to alterations in cell growth and other cellular dysfunctions and are strongly activated by ultraviolet light (han *et al.*, 1994), oxidants (Liu *et al.*, 1995), osmotic stress (Shapiro *et al.*, 1992), TNF-α (Beyaert *et al.*, 1996) to name but a few.

High glucose stimulates ERK and p38 MAPK in mesangial cells of diabetic animals (Haneda *et al.*, 1997, Igarashi, 1999). The PKC dependent increase in ERK activates TGF-β1 production via AP-1 (Haneda M *et al.*, 1997). TGF-β1 then augments p38 MAPK activation. Inhibition of MAPK prevents TGF-β1 induced fibronectin production and associated changes in Na^+ reabsorption. This ability of TGF-β1 to mediate its effects via p38 MAPK stems from a degree of cross-talk between MAPK and Smad pathways. TGF-β1 can directly activate ERK, p38 and JNK signalling pathways (Yue *et al.*, 1999), a result of a novel Mitogen Activated Protein kinase kinase kinase (MAPKKK) termed TGF-β activating kinase (TAK1) which participates in signal transduction of TGF-β1 enabling the activation of both the p38 and JNK pathway (Wang *et al.*, 1997). *c-Fos* and *c-Jun* regulated by ERK and JNK can bind directly to Smad 3, while the Smad 3-Smad 4 heterodimer can bind to the AP1 binding site of various promoters of the TGF-β1 target genes. This would suggest therefore that TGF-β1 signalling is central to the pathobiology of diabetic nephropathy.

1.9 The Epithelial Sodium Channel (ENaC)

1.9.1 DEG/ENaC ion channel family

The reabsorption of Na^+ into the bloodstream is of critical importance in maintaining blood volume homeostasis and is therefore central to blood pressure control and the prevention of secondary hypertension. At the molecular level, Na^+ is reabsorbed along the whole length of the nephron by a number of apically expressed transporters (Eaton *et al.*, 1995, Gamba *et al.*, 1999). Whilst it only accounts for a relatively small

proportion of the sodium reabsorbed (<5%), the concentration of both hormone receptors and other regulatory molecules that control Na^+ reabsporption in the distal nephron suggests that fine control of Na^+ reabsorption is most likely to be mediated in the distal nephron and the collecting duct. Key in this process is the epithelial sodium channel (ENaC), an apically expressed amiloride sensitive channel that moves Na^+ across absorptive epithelial in a wide variety of tissues including renal tubules, distal colon, skin and the lungs (Garty *et al.*, 1997).

The ENaC is a member of the ENaC/degenerin gene family which was first discovered at the beginning of the 1990s (Alvarez de la Rosa *et al.*, 2000). The name degenerin (DEG) is derived from the phenotype associated with mutation of the *deg-1* gene and other related genes that result in selective degeneration of sensory neurons involved in touch sensation (Mano *et al.*, 1999). In parallel to those studies in *C.elegans* which resulted in the identification of the DEG gene family, cloning studies in *Xenopus laevis* oocytes led to the isolation and sequencing of a cDNA encoding the α subunit of the ENaC (Cannessa *et al.*, 1993, Lingueglia *et al.*, 1993). Both ENaC and degenerins were found to have substantial sequence homology.

Identification of additional members formed a new subfamiliy of ion channels (Figure 1.9), all of which have wide tissue distribution and have been shown to function as receptors for taste, touch and acidic pH. Their role within the cell dictates their level of activity; with some constitutively active and others e.g. *C.elegans* degenerins requiring activating stimuli in the form of mechanical stimulation (Kellenberger *et al.*, 2002). Expressed only in animals with specialised organ functions for reproduction, digestion and coordination, the channels in vertebrates are subdivided into three main categories: ENaC, acid sensing ion channel (ASICS) and brain-liver-intestine sodium channel (BLINaC/human intestine sodium channel (hINaC). Aside from its role in Na^+ absorption, ENaC is expressed in both taste cells of the tongue and non epithelial cells including specialised sensory neurones (Kellenberger *et al.*, 2002). This latter observation has led to the supposition that ENaC like Degenerins may also be responsive to mechanical stimuli.

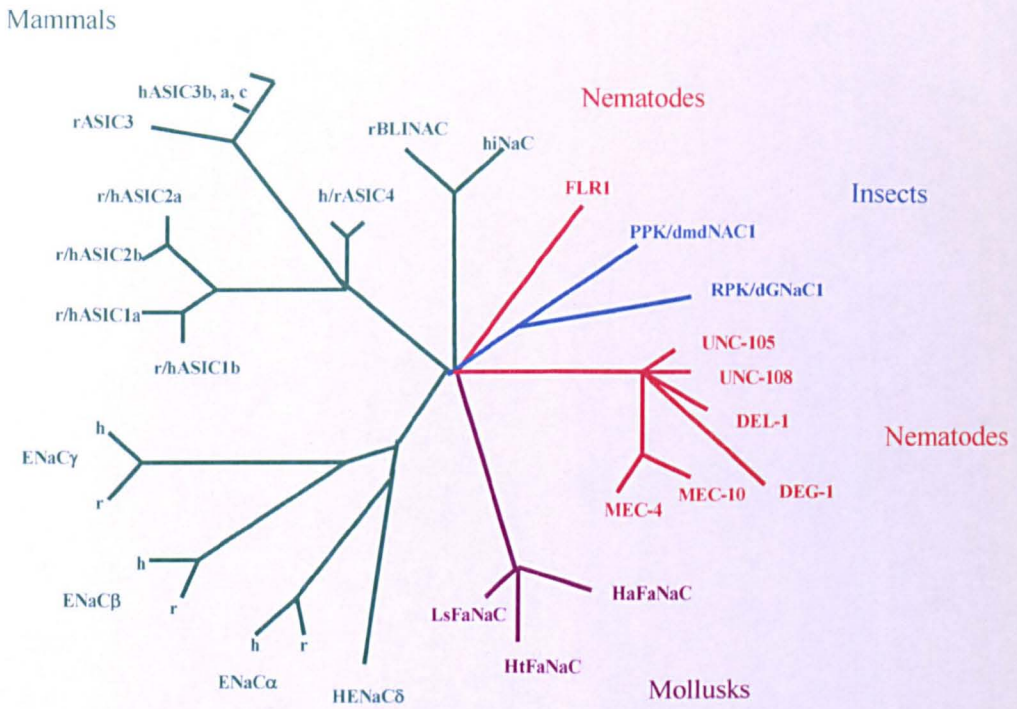

Figure 1.9: Phylogenetic tree of the epithelial sodium channel (ENaC)/degenerin (DEG) family showing the organisation into subfamilies of related sequences. The channels from vertebrates are divided into three groups: ENaC, acid sensing ion channels (ASICs) and brain liver intestine sodium channel (BLINaC)/human intestine sodium channel (hiNAC). ENaC/DEG proteins of invertebrates can be divided into four groups: 1) the degenerins from C*aenorrhabditis elegans*; 2) the *Drosophila* channels RPK/dGNaC1 and PPK/dmdNaCl; 3) FMRFamide-gated sodium channel (FaNaC), which is expressed in molluscs; and 4) FLR-1, which is the only characterised member of a group of *C.elegans* ENaC/DEG family members that are different from the degenerins (Kellenberger *et al.,* 2002).

1.9.2 ENaC at the molecular level

The ENaC is composed of three partly homologous subunits (α, β and γ) (Canessa *et al.,* 1993, Canessa *et al.,* 1994) inserted into the membrane with a proposed stoichiometry of one of two subunit compositions, a tetrameric structure comprising 2α:1β:1γ (Figure 1.10) Dijkink *et al.,* 2002, Firsov *et al.,* 1998, Kosari *et al.,* 1998) or an eight to nine subunit structure (Snyder PM *et al.,* 1998), the latter of which has

been reported to assemble prior to transport of the ENaC from the Golgi complex to the plasma membrane. To date however, the exact stoichiometry of the ENaC subunits when inserted into the plasma membrane remains to be resolved, with reports of both tetrameric and eight subunits structures reported in various cell types (Firsov D *et al.*, 1998, Staruschenko A *et al.*, 2005). This ability to assemble with different stoichiometries, in conjunction with variability in messenger RNA expression across tissue type raises the possibility that different stoichiometries may exert functional differences.

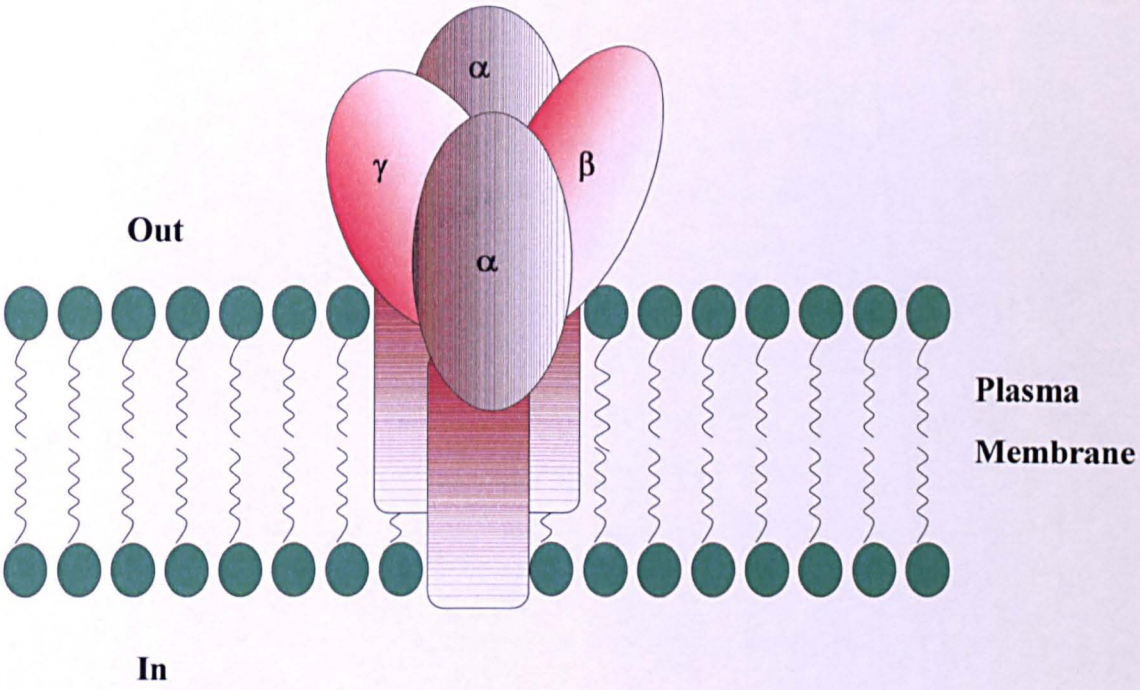

Figure 1.10: Model of the tetrameric assembly of an ENaC channel. The model shows the tetrameric assembly of ENaC subunits around the central pore and is based on functional analyses that demonstrate the three subunits to be inserted into the membrane as a tetramer.

The α subunit was first cloned by virtue of its ability to potentiate amiloride-sensitive Na^+ currents in *Xenopus* oocytes (Cannessa *et al.*, 1993, Lingueglia *et al.*, 1993), whilst neither expression of the β or γ subunit alone or in combination, is sufficient to generate a Na^+ current. However, when co-expressed with the α subunit, expression of all three subunits potentiates the Na^+ current suggesting that whilst all three subunits are required for formation of a fully functional channel, α subunit expression is a pre-requisite for Na^+ conductance (Canessa *et al.*, 1993).

Structurally, the ENaC subunits have two membrane spanning segments and a large glycosylated extracellular domain that contains both numerous potential N-linked glycosylation sites and two short NH_2 and COOH termini (Renard *et al.*, 1994, Canessa *et al.*, 1994). The C-terminal contains two proline rich regions the second of which is highly conserved and is referred to as the PY motif (xxPPxY) where x is any amino acid, P is proline and Y is tyrosine (Staub *et al.*,1996, Schild *et al.*, 1996) (Figure 1.11). Tyrosine residues present in the proline-rich motifs of β and γ subunits of ENaC are important in the regulation of ENaC activity, since recognition of the motif by endocytic machinery (Rotin D *et al.*, 2000) and its ability to form protein-to-protein interactions provides a possible link between tyrosine rich motifs and subsequent retrieval of the sodium channel from the membrane. The importance of these proline rich motifs in targeting the ENaC for degradation via a ubiquitin pathway is supported in those patients diagnosed with Liddle's syndrome, a hypertensive disorder in which a reduction in the rate of ENaC degradation leads to an increase in the number of functional complexes able to assemble at the apical membrane. In turn Na^+ reabsorption is increased and blood pressure rises (Shimkets *et al.*, 1994, Hansson *et al.*, 1995, Hansson *et al.*, 1995, Schild *et al.*, 1996, Firsov *et al.*, 1996). The extracellular domain represents more than half of the mass of the ENaC subunits and contains two conserved cysteine rich domains (CRD) II and III, reported to be involved in maintenance of the tertiary structure through disulfide bond formation.

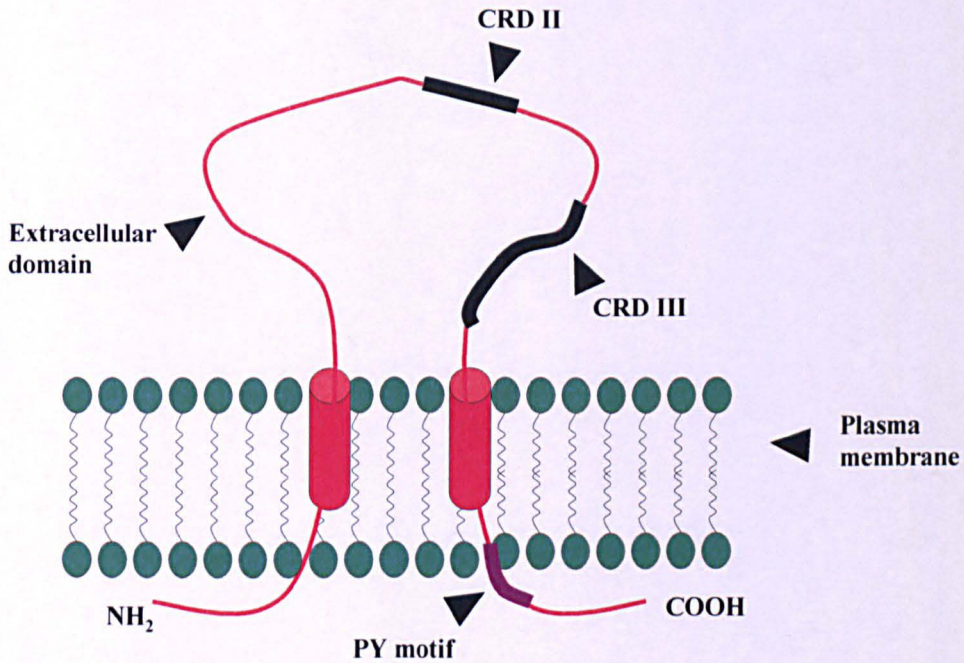

Figure 1.11: Membrane topology of the ENaC subunits. Each subunit has two membrane spanning segments, a large glycosylated extracellular domain comprising two cysteine rich domains (CRDII and III) and cytoplasmic N and C termini. The C termini, contains a proline rich motif, thought critical in enabling efficient regulation of ENaC activity (adapted from Snyder, 2002a).

1.9.3 ENaC in epithelial Na^+ transport

Regulation of ENaC mediated Na^+ transport is critical for a variety of processes. In the collecting duct of the kidney, ENaC is an integral component of the pathway for Na^+ reabsorption, serving to maintain salt homeostasis preventing increased blood pressure known to potentiate circulatory and renal system failure.

Located in epithelial cells of the connecting tubule (CNT), cortical collecting duct (CCD) and outer medullary (OMCD) collecting duct, (Duc *et al.*, 1994, Masilamani *et al.*, 1999, Schmitt *et al.*, 1999), ENaCs control fine regulation of Na^+ reabsorption. In hyponatraemia the natural response is to increase the rate of Na^+ reabsorption preventing further volume depletion. Contrary to this, in hypernatraemia Na^+ transport is decreased.

The transepithelial transport and reabsorption of Na^+ across an epithelial cell membrane is mediated via a two step transport process which is reliant upon the large electrochemical gradient for Na^+ that exists across the apical membrane. This electrochemical gradient provides the driving force for entry of Na^+ into the cell through the pore of the ENaC. The Na^+ transport process is completed by the Na^+/K^+ ATPase pump located in the basolateral membrane. This ATP driven pump couples the extrusion of three Na^+ and the uptake of two K^+ ions to the intracellular hydrolysis of one molecule of ATP, allowing for the reabsorption of Na^+ whilst maintaining throughout, a low $[Na^+]_i$ and high $[K^+]_i$ relative to our ECF (Taniguchi *et al.*, 2001) (Figure 1.12).

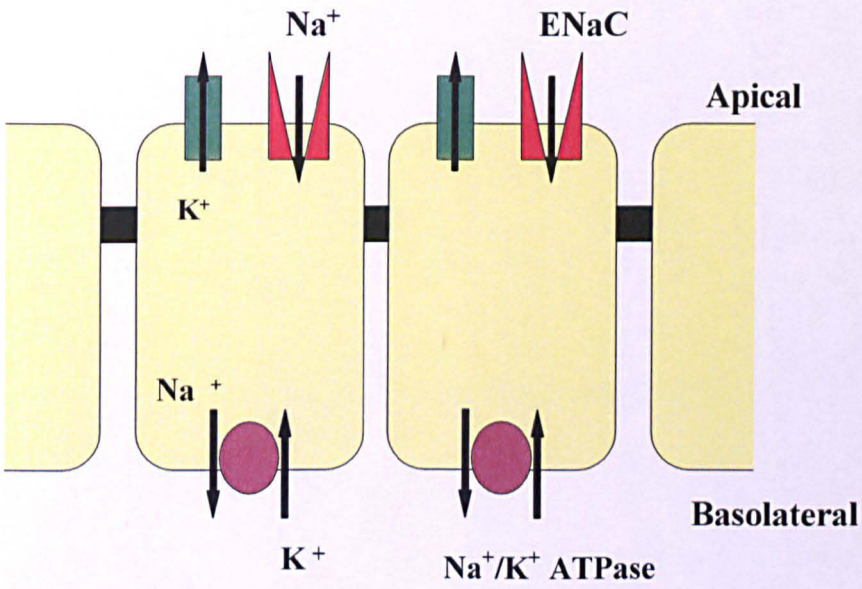

Figure 1.12: ENaC forms the pathway for epithelial Na^+ absorption. A model of renal epithelial cells. ENaC is expressed at the apical membrane, where it forms the pathway for Na^+ in the lumen to enter the cell. At the basolateral membrane, the extrusion of $3Na^+$ ions out of the cell by the Na^+/K^+ ATPase is accompanied by the influx of $2K^+$ ions into the cell, maintaining both low $[Na^+]_i$ and high $[K^+]_i$ concentration.

1.9.4 Hormonal regulation of ENaC

The regulation of ENaC is complex and depends upon a variety of hormonal signals. Whilst many of the mechanisms involved in ENaC regulation remain to be elucidated, a number of secondry messengers (cAMP), regulatory proteins (G proteins; kinases; proteases) and intra-and extracellular ions (Na^+, Ca^{2+}) have been associated with the regulation of this Na^+ channel (Garty *et al.,* 2001, Kellenberger *et al.*, 2002)

Na^+ transport via ENaC is regulated principally by two hormonal pathways:

1.9.4.1 Aldosterone

Tight regulation of the ENaC is critical in maintaining homeostatic $[Na^+]_i$ levels and is primarily mediated by the mineralocorticoid aldosterone, the principal hormone controlling salt and water balance in vertebrates. Increases in plasma aldosterone stimulate Na^+ reabsorption in the kidney collecting duct and distal colon, in part by increasing the rate of Na^+ entry through ENaC (Garty *et al.*, 1997). When aldosterone levels are low, ENaC is reportedly confined to an intracellular location in a vesicular pool (Snyder *et al.*, 2005). Aldosterone infusion or Na^+ restriction induces a dramatic redistribution of the ENaC to the apical surface (Masilamani *et al.*, 1999,), thereby enabling the channel to uptake Na^+. Therefore aldosterone acts by increasing the number of active ENaC channels at the cell surface, a process thought to be dependent on both transcription and translation (Alvarez de la Rosa *et al.*, 2002, Loffing *et al.*, 2001).

The effects of aldosterone are divided into three main phases: a lag period of 20-60 minutes, followed by an early phase over approximately 1-3 hours in which aldosterone induced regulatory proteins are able to act on pre-exisiting Na^+ transport machinery and a late phase initiated over a 6 -24 hour time period following hormone addition, during which a further increase in transport activity correlates with increased channel number and other elements of the transport machinery (Naray-Fejes-Toth *et al.*, 2004).

The increase in Na^+ reabsorption observed in the early phase of aldosterone action occurs prior to any significant increase in ENaC mRNA transcripts (Garty *et al.*, 1997). It has been proposed that aldosterone may induce the transcription of proteins which are able to directly modulate ENaC trafficking function. To date, two such gene products have been identified, K-Ras2 and serum and glucocorticoid inducible kinase (SGK1), both show increased message in response to increased aldosterone and increase aldosterone induced Na^+ current when overexpressed (Rotin D *et al.*, 2000). A role for K-Ras2 in mammalian epithelia however is yet to be established.

1.9.4.2 Vasopressin

Released by the pituitary in response to a decrease in ECF, vasopressin has been reported to stimulate Na^+ reabsorption in skin and urinary bladder epithelia of amphibians, in rat cortical collecting duct and in many *in vitro* and cultured epithelia possessing transport characteristics similar to the mammalian collecting duct (Tomita *et al.*, 1985, Reif *et al.*, 1986, Garty *et al.*, 1988, Schafer *et al.*, 1992, Schafer 1994, Garty *et al.*, 1997). However, whilst the channel responsible for this Na^+ reabsorption is ENaC, not all ENaC expressing epithelia respond to vasopressin driven Na^+ transport. Two mechanisms have been proposed explaining how vasopressin may mediate increased Na^+ reabsorption via ENaC. Firstly vasopressin is thought to increase the open probability and conductance of the channel (Prat *et al.*, 1993) or increase the number of channels in the membrane via a mechanism analogous to that observed upon vasopressin-stimulated insertion of AQP2 (Butterworth., 2001, Morris *et al.*, 2002). The binding of vasopressin to the V_2 receptor activates a G protein which leads to the downstream activation of adenylyl cyclase. This generates a rise in intracellular cyclic adenosine monophosphate levels (cAMP) which can activate protein kinase A (PKA), a protein kinase known for its ability to phosphorylate a number of downstream proteins which mediate the trafficking and fusion of intracellular vesicles containing AQP2. An increase in intracellular cAMP increases membrane trafficking of all three subunits, of which the α subunit has been reported to co-localise with the AQP2 channel (Harger *et al.*, 2001). Since neither one of these mechanisms is dependent on *de novo* protein synthesis, the increase in Na^+ transport in response to vasopressin is far greater than that observed following a rise in aldosterone.

1.9.5 Regulation of ENaC activity by Nedd4-2

Whilst aldosterone and vasopressin have been demonstrated as positive regulators of ENaC availability at the apical membrane, ubiquitination, a post-translational modification involving the covalent linkage of 76 amino acid long ubiquitin polypeptides on target proteins has been suggested to play a role in the regulation of ENaC through directing proteasomal mediated degradation of the channel thus preventing insertion into the apical membrane. Ubiquitination requires the sequential action of several enzymes. Firstly ubiquitin becomes activated in an ATP dependent manner by forming a thioester with a cysteine on the ubiquitin activating (or E1)

enzyme. It is then transferred on the cysteine of a ubiquitin conjugating (or E2) enzyme which will interact with a ubiquitin protein ligase (or E3 enzyme). These ubiquitin-protein ligases are thought to provide specificity by recognising and binding to specific target proteins, while attaching ubiquitin via an isopeptide bond between its COOH terminus and the ε-amino group of a lysine residue (Hershko *et al.*, 1998). Ubiquitination can be of two different types, mono and polyubiquitination (also referred to as multi). Whilst monoubiquitinated proteins are degraded in the lysosomes, polyubiquitinated proteins are recognised by and subsequently degraded by the 26s proteasome. The ubiquitin ligase neural precursor cell-expressed developmently downregulated protein (Nedd4-2) is an ENaC specific ubiquitin ligase that contains three or four WW domains (serving protein-protein interactions) that interact with the ENaC subunit PPxY domain (Staub *et al.*, 1996) and a calcium/lipid domain (CaLB/C2). Such ubiquitination would cause a decrease in ENaC at the cell surface. ENaC ubiquitination is followed by proteasomal degradation, interference of which negates the degradation of ubiquitinated proteins and ultimately depletes the available pool of free ubiquitin thus halting the ubiquitination reaction, allowing for accumulation of ENaC at the cell surface (Staub *et al.*, 1997).

1.9.6 Clinical conditions associated with aberrant ENaC mediated Na^+ reabsorption

Conditions linked to malfunction or mutations of the ENaC suggest it as a candidate gene for the control of blood pressure. Defects in the regulation of Na^+ transport underlie all of the known inherited forms of hypertension (Lifton *et al.*, 2002). Clinical disorders of the kidney due to malfunction of the ENaC complex are well described (Scheiman *et al.*, 1999) and include Liddle's syndrome, an autosomal dominant form of arterial hypertension characterised by severe hypertension, salt sensitivity, hypokalaemia, and low aldosterone and renin levels. Shimkets *et al.*, (1994) discovered that the genetic defect in the original Liddle's syndrome was a mutation in β-ENaC. Truncation of the β-ENaC gene resulted in a complete absence of carboxy terminus synthesis, expression of which is essential for recognition via endocytic machinery and subsequent channel retrieval from the apical membrane surface. Further truncations of both the β-ENaC and γ-ENaC C termini have

subsequently been reported. Thus, mutations of the cytoplasmic C-termini of the β and γ subunits in patients presenting with Liddle's syndrome inhibits degradation of the channel via the ubiquitin pathway (Staub *et al.,* 1996), consequently resulting in increased functional complexes at the apical membrane and increased Na^+ reabsorption. In contrast, loss of function mutations results in pseudohypoaldosteronism Type I (PHA-1), a condition associated with salt wasting, hyperkalaemia and metabolic acidosis that presents soon after birth (Grunder *et al.,* 1997, Chang *et al.,* 1996). Mutations in ENaC that have been identified in those patients with PHA-1 are recessive and produce physical disruption of the affected subunit causing loss of one or both membrane spanning domains. The end result is a defective ENaC which renders the individual unable to retain sodium and consequently leads to hypotension (Grunder *et al.,* 1997, Chang *et al.,* 1996).

1.10 The Serum and Glucocorticoid inducible kinase.

One of the key regulators involved in the Na^+ reabsorption in the nephron is the serum and glucocorticoid induced kinase (SGK1), an aldosterone regulated gene, which mediates Na^+ reabsorption via its actions on the ENaC. SGK1 is expressed in a variety of tissues including the kidney, eye, liver, heart, pancreas, skeletal muscle, and brain (Waldegger *et al.,* 1997) and is tightly regulated by numerous signalling cascades through control of its expression levels, intrinsic kinase activity and subcellular localisation. Thus SGK1 integrates into numerous pathways adapting to different roles within the cell, dependent upon the nature of the stimuli (Firestone *et al.,* 2003).

SGK1 was originally cloned as a glucocorticoid responsive gene from rat Con8 mammary tumour cells and was termed SGK1 to reflect its regulation at the transcriptional level by serum and glucocorticoids, with both glucocorticoids and serum capable of inducing SGK1 in both mammary epithelial cells and fibroblasts within 30 minutes (Webster *et al.,* 1993a, Webster *et al.,* 1993b).

The effects of aldosterone on SGK1 have been well documented in both *in vitro* and *in vivo* systems, including *Xenopus* A6 cells (Zecevic *et al.,* 2004), Primary rabbit CCD cells (Naray-Fejes Toth *et al.,* 1999), mouse M1 cells (Helms *et al.,* 2003) and

mouse and rat kidneys (Loffing *et al.*, 2001). This induction of SGK1 coincides with enhanced phosphorylation of an ubiquitin ligase involved in SGK1 degradation (see section 1.10.3), increased Na^+ reabsorption and decreased Na^+ secretion. The importance of aldosterone induced SGK1 is demonstrated under conditions of dietary Na^+ restriction where circulating levels of aldosterone increase, maintaining Na^+ homeostasis and ultimately preventing a fall in blood volume and therefore pressure (Farjah *et al.*, 2003).

The functional significance of SGK1 in regulation of transepithelial Na^+ transport is seen in a series of knockout experiments in *Xenopus laevis* in both A6 cells and M1 CCD cells. Transfection of these cells with SGK1 leads to an increase in transepithelial Na^+ transport whilst transfection of a dominant negative "kinase dead" SGK1 mutant or siRNA abolishes both dexamethasone and insulin dependent regulation of transepithelial Na^+ transport (Helms *et al.*, 2003, Alvarez de la Rosa *et al.*, 1999).

Interestingly, SGK1 knockout (KO) mice (SGK1 -/-) on a standard diet exhibit Na^+ reabsorption comparable to that of their wild-type littermates although circulating plasma aldosterone levels are significantly elevated. However, in SGK1 KO mice on a Na^+ restricted diet, activated compensatory mechanisms are no longer able to maintain Na^+ homeostasis. These data suggest that aldosterone dependent control of ENaC function does not rely solely on induction and activation of SGK1, a hypothesis further supported by reports of Nedd4-2 phosphorylation in mouse cortical collecting duct cells in the absence of any aldosterone and detectable SGK1 protein expression (Flores *et al.*, 2005).

1.10.1 SGK1 is a serine/threonine kinase

The SGK1 gene is located on chromosome 6q23 and contains several consensus sequences for transcription factors (Firestone *et al.*, 2003) and a functional glucocorticoid response element (GRE) located approximately 1000bp from the transcription start site that is highly homologous to the consensus GRE (Itani *et al.*, 2002). Additional regulatory transcription sites have also been identified and these

include p53 binding sites, a cAMP responsive element binding (CREB) protein site and a Sp1 responsive element (Firestone *et al.*, 2003, Lang *et al.*, 2001)

SGK1 has characteristic motifs of a serine/threonine kinase and is part of the family of AGC kinases. These include PKA, protein kinase G (PKG), PKC and protein kinase B/Akt/rac. Its catalytic domains shares 54% homology with those of Akt/PKB/ and rac kinases and 45% with that of PKA. Kinase activity of SGK1 has been demonstrated *in vitro* (Park *et al.*, 1999).

SGK1 is regulated by a variety of both hormonal and non hormonal stimuli and is involved in controlling a wide variety of cellular processes including apoptosis, ion transport and cellular differentiation, In contrast to most protein kinases an unusual property of SGK1 is its acute transcriptional control by different signal transduction pathways. In addition to serum and glucocorticoids, levels of expression have been shown to be acutely (30 minutes) regulated by aldosterone (Chen *et al.*, Naray-Fejes Toth), cell shrinkage (Waldegger S *et al.*, 1997), TGF-β1 (Waldegger s *et al.*, 1999, Lang *et al.*, 2000), follicle stimulating hormone (FSH) (Alliston *et al.*, 1997), osmotic stress and DNA damage (You *et al.*, 2004), p53 (Firestone *et al.*, 2003). This list is not exhaustive and many of these stimuli are highly cell specific (Table 1).

Stimuli	Cell or tissue type
Serum	Ubiquitous
Glucocorticoids	Ubiquitous
Aldosterone	Distal nephron
Cell shrinkage	HepG2, MDCK, neuroblastoma
Cell swelling	A6 cells
TGF-β1	U937, HepG2, intestine, fibroblasts, endothelial cells
Chronic viral hepatitis	Liver
Ischemic injury of brain	Brain
Neuronal excitotoxicity	Brain, glial cells
Memory consolidation	Brain, hippocampus
DNA damage	Fibroblasts
1α,25-dihydroxyvitamin D3	Squamous cell carcinoma
Psychophysiological stress	Brain, heart, Kidney
Iron	Intestine
Glucose	Endothelial cells
Endothelin-1	Endothelial cells
GM-CSF	Granulocytes
FGF	Mouse fibroblast cells
PDGF	Mouse fibroblast cells
Phorbolesters	Mouse fibroblast cells Rat ovarian granulosa cells
FSH	Rat ovarian granulosa cells
Sorbitol	mammary epithelial cells
UV raidation	mammary epithelial cells
Heat shock	mammary epithelial cells
Oxidative stress	mammary epithelial cells
PPARγ	Distal nephron
Protein kinase 53 (p53)	Mammary epithelial cells

Table 1.1 Stimuli that cause induction of SGK1 expression (reviewed in Loffing *et al.*, 2006)

1.10.2 Regulation of SGK1 by phosphorylation

Many AGC kinases possess phosphorylation sites in both their catalytic domain and C-terminal region. The motif in the catalytic domain is situated on the so called activation loop (A-loop) and was first identified in PKB/Akt, a kinase shown to be a target of phosphatidylinositol-3,4,5-triphosphate (PIP3)-dependent kinase 1 (PDK-1). PDK-1 is regulated by an upstream PI3K-dependent kinase (Kobayashi T *et al.*, 1999). Like PKB, SGK1 has also been shown to possess PDK1-phosphorylation sites. PDK1 phosphorylation of SGK1 occurs on Thr256 in the A-loop of the catalytic domain and Ser422 in a C terminal region termed the hydrophobic motif (H-motif) (Loffing *et al.*, 2006). However, unlike PKB, SGK1 does not possess Pleckstrin homology domains. In PKB and PDK-1, these PH domains allow for interaction with phosphoinositides and recruit both PKB and PDK1 to the membrane subsequently allowing for PDK1 mediated phosphorylation of PKB (Biondi *et al.*, 2001). Activation is very fast and occurs approximately two minutes after stimulation with either insulin or insulin-like growth factor. An absence of PH domains in SGK1 led to the discovery of an unknown PI3-K dependent kinase which phosphorylates Ser422 and has subsequently been denoted PDK-2 (Park *et al.*, 1999). This phosphorylation transforms SGK1 into a substrate for PDK-1 which is able to bind via its PDK-1 interacting fragment (PIF)-binding pocket to the H-motif of SGK1. This association promotes phosphorylation of Thr256 in the A-loop and renders SGK1 active. Activation of SGK1 and PKB is clearly very different since activation of SGK1 is not reliant on phosphoinositides or the PH domain in PDK1.

SGK1 has also been shown to contain consensus sites for phosphorylation by other intracellular signalling molecules, including cAMP dependent PKA (Perotti *et al.*, 2001). Activation of SGK1 by PKA could mediate the vasopressin driven increases in Na^+ reabsorption previously discussed in section 1.11.4 (Reif MC *et al.*, 1986). The exact mechanism behind this phosphorylation however requires further clarification. Other kinases capable of phosphorylating SGK1 include MAP kinases (ERK5 or p38), and WNK1 (*w*ith *n*o lysine *k*inase *1*). Whilst WNK1 is believed to play a role in Na^+ homeostasis, a direct phosphorylation remains to be confirmed (Xu *et al.*, 2005).

1.10.3 Regulation of SGK1 by ubiquitination

SGK1 protein has a half life of approximately 30 minutes (Webster *et al.*, 1993). Degradation of SGK1 is initiated upon ubiquitylation. Ubiquitinated SGK1 becomes associated with a membrane associated fraction of the cell prior to degradation by the 26s proteasome (Brickley *et al.*, 2002). The first 60 amino acids of the N-terminal region of SGK1 regulate its stability and SGK1-mutants that lack the first 60 amino acids of the N-terminal region results in a near loss in ubiquitin modification and proteasomal degradation (Brickley *et al.*, 2002). Controversy still surrounds how this N terminal is able to regulate the rate at which SGK1 is ubiquitinated it does however possess six lysines in its N terminus. Whilst lysines are known potential ubiquitylation sites, mutation of these residues to aspartates does not negate ubiquitinylation. In 2005, Snyder *et al.*, showed that Nedd4-2, a substrate of SGK1, increases SGK1 ubiquitination and degradation (Zhou *et al.*, 2005). SGK1 contains a PY motif, whilst Nedd4-2 comprises two consensus sites for phosphorylation by SGK1 (Park *et al.*, 1999). In *Xenopus* oocytes Debenoville *et al.*, 2001, demonstrated SGK1 induced phosphorylation of Nedd4-2 in a PY motif (P-P-X-Y where P is a proline, Y a tyrosine and X an amino acid) dependent manner. SGK1 phosphorylates at primarily Ser444, but can phosphorylate at Ser 338 (Debonneville *et al.*, 2001) of Nedd4-2 and ultimately induces the dissociation of the previously discussed Nedd4-2/ENaC complex in the cell, leading to increased apical targeting of the ENaC and increased Na^+ reabsorption (Snyder *et al.*, 2002)(see section 1.10.4 for further details).

1.10.4 Role of SGK1 in Na^+ reabsorption

In the kidney, the majority of studies have focussed on the regulation of SGK1 mRNA expression by aldosterone and glucocorticoids. Studies have shown that SGK1 appears to be expressed in the glomeruli and distal tubules, the medulla and with the highest abundance on the renal papilla (Chen *et al.*, 1999, Lang *et al.*, 2000, Bhargava *et al.*, 2001, Hou *et al.*, 2002). However, a predominant role for SGK1 in the kidney is in regulating and maintaining Na^+ homeostasis in principal cells of the collecting duct, where both ENaC and Na^+/K^+ ATPase expression is tightly regulated by aldosterone and SGK1. The effects of SGK1 on the Na^+/K^+ ATPase have been

shown to be independent of changes in protein expression or in abundance at the plasma membrane. This mode of regulation remains to be elucidated (Alvarez de la Rosa *et al.*, 2006).

Nedd4-2 is the negative regulator of ENaC cell surface expression (Kamynina *et al.*, 2002). In the absence of SGK1, the physical association between Nedd4-2 and ENaC results in ubiquitinylation of ENaC subunits inducing channel retrieval and proteasomal degradation. Consequently, blood Na^+, blood volume and thus blood pressure is reduced. Activation of ENaC by SGK1 serves to increase both the number of channels at the plasma membrane (Debonneville *et al.*, 2001) and increase activity of those already present in the membrane (Diakov *et al.*, 2004).

Activation of SGK1 is PI3-K dependent (Blazer-Yost *et al.*, 1999), phosphorylating at Ser 422 and Thr 256 via the two downstream kinases PDK2 and PDK1 respectively. Following its activation, SGK1 is able to bind to and inhibit Nedd4-2, an effect that appears to require a physical association between the PY motif of SGK1 and the WW domain of Nedd4-2. Through its PY motif, SGK1 phosphorylates the WW domain of Nedd4-2 itself (Debonneville *et al.*, 2001) impairing formation of the ENaC-Nedd4-2 complex. Dissociation of the ENaC-Nedd4-2 complex allows for increased apical ENaC surface expression and increased Na^+ reabsorption (Kamynina *et al.*, 2002, Snyder *et al.*, 2002).

SGK1 dependent inhibition of Nedd4-2 involves 14-3-3 proteins (Liang *et al.*, 2006). These proteins are found in all eukaryotes and regulate a wide range of biological processes. They interact directly with numerous target proteins altering their activity. This interaction is generally mediated by phosphorylation of specific binding sites (Toker *et al.*, 1990). SGK1 increases the binding of 14-3-3 to Nedd4-2 in a phosphorylation dependent manner, an interaction proven to be crucial for Nedd4-2 dependent ubiquitinylation of ENaC (Ichimura *et al.*, 2005).

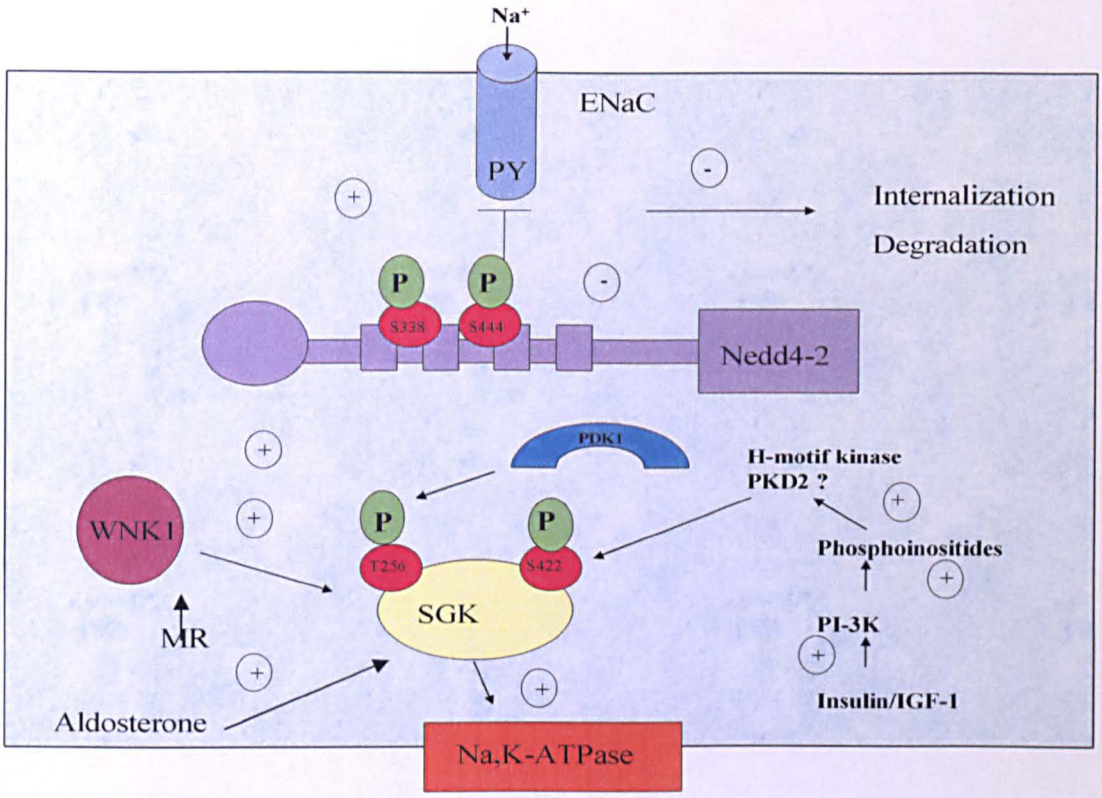

Figure 1.13: Regulation of epithelial Na^+ transport by SGK1: Aldosterone induces the expression of SGK1 by binding to the mineralocorticoid receptor (MR) and translocating into the nucleus. SGK1 is activated following phosphorylation on Ser422 by the first of two kinases. This unknown kinase, activated by a PI3-K dependent pathway (i.e insulin pathway) is referred to as 3-phosphoinositide-dependent protein kinase (PDK)-2 or hydrophobic motif (H-motif) kinase. Phosphorylation of Ser422 by PDK-2 allows PDK1 to subsequently bind at this residue, leading to phosphorylation at Thr256. Activation of SGK1 can also occur via WNK. SGK1 when activated is able to phosphorylate Nedd4-2 on Ser444 and Ser338. This phosphorylation allows binding of 14-3-3 on Ser444. This binding induces dissociation of the Nedd4-2/ENaC complex, enabling ENaC to translocate to the cell surface where it can then take part in Na^+ reabsorption (Adapted from Loffing *et al.*, 2005).

1.10.5 Pathophysiological role of SGK1

Whilst aldosterone is the main physiological regulator of epithelial Na^+ transport within the collecting duct, a variety of other hormonal and non-hormonal factors regulate the activity SGK1 which acts to integrate stimuli involved in regulating Na^+ transport. Recent evidence has led to the supposition that SGK1 may serve as a potential candidate in the development of diabetic secondary hypertension, because

SGK1 is also activated by insulin (Kageyama *et al.*, 1994) a process that might be of considerable relevance to the pathogenesis of hypertension associated with hyperinsulinaemia, hypertonicity (Waldegger *et al.*, 1997), glucose, increased intracellular calcium and the transforming growth factor TGF-β1 (Lang *et al.*, 2000) whose upregulation in Type II diabetes is thought to contribute towards those abnormalities which collectively manifest themselves as micro and macrovascular complications.

SGK1 has since been shown to be transcriptionally upregulated in both models and patients presenting with Diabetic nephropathy (Wang Q *et al.*, 2005, Lang *et al.*, 2000, Kumar *et al.*, 1999), a phenomenon that is thought to be mediated by the hyperglycaemia and high circulating insulin levels that precede the development of type II diabetes. Whilst the underlying mechanisms remain to be elucidated, further studies have identified a number of signalling molecules upstream of SGK1 which have been shown to be up-regulated in NIDDM. These molecules that include TGF-β1, PKC, DAG, $[Ca^{2+}]_i$ (Lang *et al.*, 2000) may trigger the induction and activation of SGK1.

1.10.6 SGK1 is regulated by cell volume

The loss of nephrons observed during the progression of renal disease is paralleled by a compensatory hypertrophy of the remaining nephrons of which is mediated via an increase in cell volume. Cell hypertrophy contributes to the onset and progression of diabetic nephropathy. Changes in sodium transport that either result in, or are the cause of hypertensive stresses, can instigate a number of downstream effector mechanisms that can influence both cell volume and integrity. Prolonged exposure of kidney epithelial cells to changes in osmolarity has thus led to a number of suggestions concerning the mechanisms involved in sensing changes in cell volume.

In addition to it's identification as a glucocorticoid responsive gene, SGK1 was also cloned in human liver cells as one of the principally volume-regulated protein kinases (Waldegger *et al.*, 1997) since it is markedly increased following hypertonic cell shrinkage. It is one of the principal volume-regulated protein kinases involved

in Na^+ transport in the kidney and contains a hyperosmotic stress regulated element of between 50 and 40bp that mediates the hyperosmotic induction of SGK1 transcription in response to the organic osmolyte 0.3M sorbitol (Bell *et al.*, 2000). Analysis of this promoter region identified a GC rich region that required binding of the transcription factor Sp1. Sp1 interacts with other transcription factors and may function as a target or a member of a multiprotein complex involved in hyperosmotic stress regulation of the SGK1 promoter. Activation of this pathway induces an increase in the production of an active SGK1 that maintains its dependence on the PI3-K pathway for its phosphorylation and activity.

The effect of hypertonic stress on SGK1 transcription has been demonstrated to be dependent on p38 MAPK (Waldegger *et al.*, 2000), with the phosphorylated form of p38 having been detected 1-2 hrs after hyperosmotic induction of SGK1. In further support of a role for p38 MAPK, application of pharmacological inhibitors of p38 MAPK was found to significantly reduce the induction of SGK1 expression in response to hypertonicity (Bell *et al* 2000).

P38 MAPK is phosphorylated and activated by the dual specificity MKK3/6 kinases in response to various forms of stress including hyperosmotic stress (see Figure 1.14). Transfection of cells with plasmids for either the wild type MKK3 kinase or the kinase dead form of MKK3 was found to either enhance or completely abolish the effect on SGK1 protein levels respectively, thus indicating that the hyperosmotic stress stimulation of SGK1 promoter activity requires the MKK3 mediated activation of p38 MAPK. As treatment with p38 inhibitors did not completely abolish the response to hyper-osmolarity, there is the possibility that MKK3 may have one or more as yet unidentified targets in addition to the p38-α or p38-β MAPK isoforms that are known to play a role in the hyperosmotic response (Bell *et al* 2000)..

Glycosuria exposes the renal epithelia to increased hypertonicity as the urine flows through the nephron and results in cell shrinkage at the apical side of the membrane. SGK1 may be involved in the hyperosmotic response to high glucose levels since p38 MAPK activity has been shown to be rapidly induced under hyperglycaemia (Igarashi *et al.*, 1999). Continuous exposure to increased osmolality may thereby see

constitutive expression/activation of SGK1 leading to the excessive and aberrant Na^+ reabsorption widely seen in diabetic nephropathy.

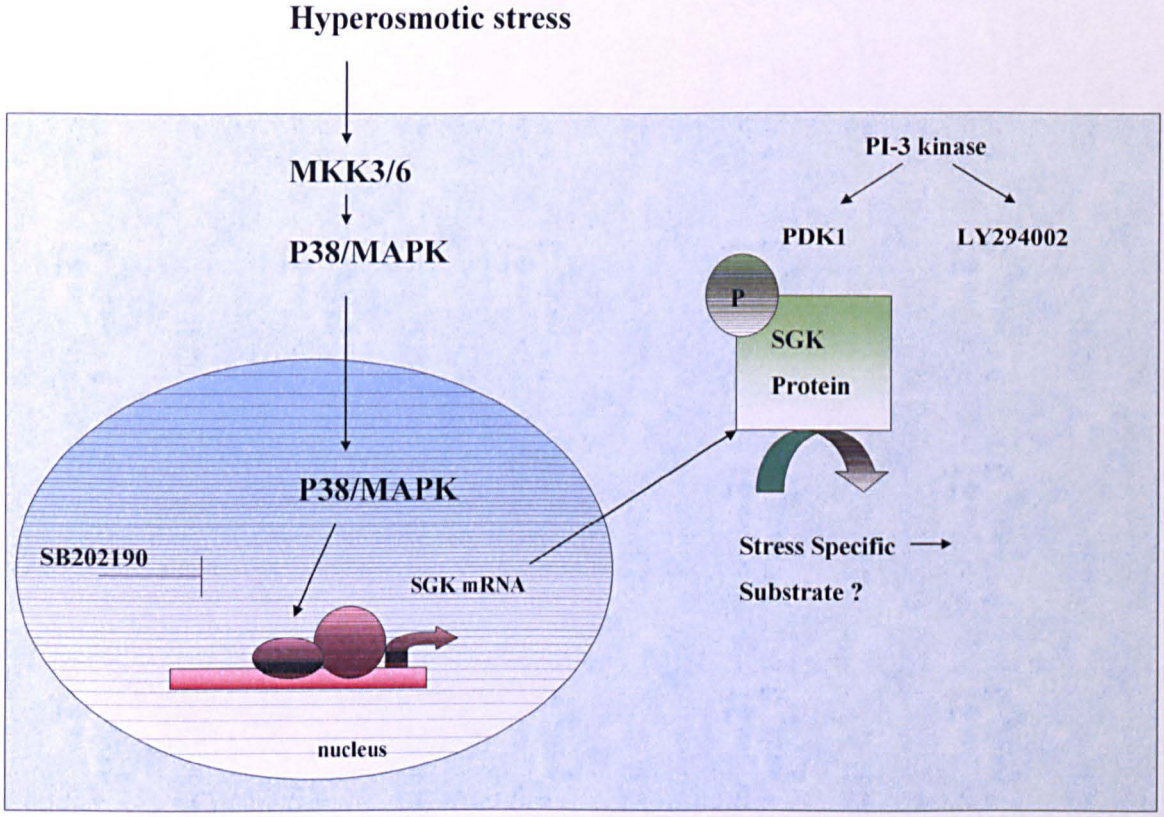

Figure 1.14 Regulation of SGK by hyperosmotic stress: The activation of SGK1 transcription in response to osmotic stress can be inhibited by the overexpression of a dominant negative kinase-dead form of MKK3 and by the p38 MAPK pharmacological inhibitors (SB202190). P38 MAPK when active targets a GC rich hypersomotic region located at -55 to -46 base pairs in the SGK1 promoter that includes the Sp1 transcription factor. Hyperosmostic stress leads to the production of a phosphorylated and enzymatically active SGK1 (adapted from Bell *et al.*, 2000)

1.10.7 TGF-β1 and the progression of renal disease via its actions on SGK1

Cell swelling will instigate a number of regulatory mechanisms aimed at restoring cell volume through a regulatory volume decrease (RVD). Any increase of cell volume mediated by SGK1 induced Na^+ entry, may further contribute to the progression of renal damage through impairment of matrix protein degradation. Vascular complications seen in diabetes are characterised by structural alterations of

extracellular matrix (ECM) components in glomeruli and large vessel walls (Yokoyama *et al.*, 1996).

The molecular and cellular events that occur during chronic renal failure also include the release of a number of different growth factors and cytokines. The multifunctional cytokine Transforming growth factor TGF-β1 has recently emerged as a key pathophysiological component in the cascade of events that contributes to the pathogenesis and progression of diabetic nephropathy (Fine *et al.*, 1985, Ling *et al.*, 1995, Sharma K *et al.*, 1996). Known to have powerful fibrogenic actions resulting from both stimulation of matrix synthesis and inhibition of matrix degradation, TGF-β1 has been implicated as the key mediator in the development of renal hypertrophy and increased matrix deposition (Chen *et al.*, 2001).

Previous studies have shown that under conditions of elevated levels of glucose TGF-β1 expression is markedly increased (Ziyadeh *et al.*, 1998, Hoffman *et al.*, 1998). A sequence of events has been proposed in which hyperglycaemia enhances production of both TGF-β1 and its receptors. Increased UDP-N-Acteylglucosamine (Kolm-Litty *et al.*, 1998), Diacylglycerol and protein kinase C (Fumo *et al.*, 1994, Kuya *et al.*, 1997) levels have all been related to the increased rate of glucose metabolism associated with Type II diabetes. Collectively with the aid of downstream signalling molecules, they enhance binding of specific transcription factors e.g. AP-1, SP-1 to the TGF-β1 promoter, thereby initating TGF-β1 transcription (Kim *et al.*, 1990, Liberati *et al.*, 1999) and raising TGF-β1 levels within the cell. Whilst the downstream targets of TGF-β1 mediating the pathophysiology of diabetic nephropathy remain largely elusive, the cell hypertrophy observed upon TGF-β1 upregulation may be in part be mediated by SGK1. A downstream target of TGF-β1, SGK1 has been shown to be transcriptionally up-regulated by TGF-β1 in various cell types (Lang *et al., 2000*). TGF-β1 also stimulates transcription, an effect reported to be mediated via p38 kinase (Bell *et al.*, 2000). TGF-β1 therefore utilises the same signalling pathway as for increased SGK1 transcription in response to osmotic stress. This ability to activate SGK1 via p38 MAPK is a consequence of cross talk between the TGF-β1 Smad signalling pathway and the MAPK signalling cascade. Studies in which SGK1 expression has been

studied following application of TGF-β1 have shown that SGK1 expression is enhanced, however in the presence of a p38 MAPK inhibitor, expression is blunted, thus indicating that the activation of SGK1 transcription via TGF-β1 is mediated via the p38 MAPK signalling pathway (Waerntges S *et al.*, 2002). Therefore TGF-β1 is implicated as a signalling component whose enhanced expression may exacerbate the cell hypertrophy in association with enhanced SGK1. Increased expression of TGF-β1 . mediates the renal actions of high ambient glucose promoting cellular hypertrophy, whilst stimulating extracellular matrix biosynthesis, two hallmarks of diabetic renal disease.

1.10.8 Other SGK isoforms

Recently two other isoforms of SGK1 were identified, SGK2 and SGK3. Like SGK1, SGK3 appears to be expressed in all tissues, whilst expression of SGK2 is restricted to the kidney, liver, pancreas and brain (Friedrich *et al.*, 2003). Both SGK2 and SGK3 share approximately 80% amino acid identity with SGK1 in their catalytic domains, whilst the N terminal exhibits most variability (Kobayashi *et al.*, 1999).

SGK2 and SGK3 have both been shown to possess the same phosphorylation consensus as SGK1 (and PKB/Akt) (Kobayashi *et al.*, 1999). However, functional differences between the isoforms exist and arise as a consequence of a number of different factors, including subcellular localisation and cofactors. However, since they share a degree of amino acid identity in their kinase domains, the potential exists for cross-talk between their signalling pathways. This is even further exemplified by their ability to activate identical pathways. SGK2 has been shown to stimulate the activity of numerous ion channels including the Na^+/K^+ ATPase pump (Henke *et al.*, 2002), ENaC (Friedrich *et al.*, 2003) and the Kv1.3 channel (Gamper N *et al.*, 2002), all of which are stimulated in the same cellular systems by SGK1 and SGK3.

SGK3 acts downstream of PI3-K; in parallel with PKB/AKT. It phosphorylates and inhibits Bad and FKHRL1, a proapoptotic protein and proapoptotic transcription factor respectively (Liu *et al.*, 2000). As with SGK2, SGK3 has also been implicated

in the regulation of numerous transporters and channels, including the Na^+/K^+ ATPase (Henke *et al.*, 2002), ENaC (Friedrich *et al.*, 2003), and the epithelial Ca^{2+} channel TRPV5 (Embark HM *et al.*, 2004).

1.11 TRP channels

The ability of living organisms to both sense and respond to alterations in their environment is critical to survival. Equipped with highly organised and developed sensory systems, we are able to detect alterations in light, taste, odour, sound and touch. Two of our five senses are based on mechanosensation and the ability to respond is reliant upon activation of mechanically gated ion channels coupled to our sensory system. These ion channels detect and subsequently transduce mechanically based stimuli into electrical signals. Whilst mechanosensors of both ear and hair cells permit hearing and balance (Hudspeth *et al.*, 1985), mechanoreceptors localized in sensory cells of the skin respond to touch (Garcia-Anoveros 1997). Despite the widespread utilisation of mechanosensation by many different cell types, little is known about the molecular components of these sensors.

With the availability of genetic screening, the recent identification of several vertebrate and invertebrate genes encoding a class of non selective cation channels has provided a number of clues as to the molecular make up of these receptors responsible for mechanotransduction.

Identification of the first transient receptor potential (TRP) protein came from studies examining *Drosophila* phototransduction (Wong *et al.*, 1989). Photoreceptor cells of *Drosophila* carrying *trp* gene mutations were found to exhibit sustained receptor potentials in response to continuous light exposure (Montell *et al.*, 1985, Cosens 1969), a consequence of calcium influx from the extracellular space. The *trp* gene was first cloned in 1989 and was subsequently shown to encode a calcium permeable cation channel (Wong *et al.*, 1989). To date, many channels bearing sequence homology to the drosophila *trp* have since been cloned from flies, worms and mammals. Collectively these channels form the TRP superfamily.

The TRP superfamily is an emerging group of channel proteins each of which have designated roles in different organ systems (Benham *et al.,* 2003, Clapham 2003). The commonly accepted nomenclature for TRP channels subdivides 28 channel subunit genes into 7 subfamilies: TRPP, TRPML, TRPA, TRPN, TRPC, TRPV and TRPM with evolutionary links from worms to mammals and sequence identity as low as 20%. With the exception of TRPN, each family contains at least one vertebrate representative (Clapham 2003, Montell *et al.,* 2005).

Whilst most ion channels are identified by their ligand function and ion selectivity, those members of the TRP superfamily are grouped based purely on homology alone since their functions are disparate and often unknown. Nonetheless, TRP channel activation is divided into three main categories.

Receptor activation. G protein coupled receptors and receptor tyrosine kinases capable of phospholipase C (PLC) activation are able to modulate TRP channel activity in at least 3 ways (a) hydrolysis of phosphatidylinositol (4,5) bisphosphate (PIP_2) (b) production of diacylglycerol (DAG) or (c) production of inositol (1,4,5) triphosphate (IP_3) with subsequent release of calcium from intracellular stores (Clapham *et al.*, 1995).

Ligand activation. Ligands that activate TRP channels can be broadly classified into small exogenous molecules e.g. capsaicin, endogenous lipids or products of lipid metabolism e.g. diacylglycerol, purine nucleotides and their metabolites e.g. adenosine diphosphoribose (ADP-ribose) and inorganic ions (Clapham *et al.*, 1995).

Direct activation. Direct stimuli capable of inducing TRP channel activation include mechanical stimuli, channel phosphorylation, a rise in temperature, a decrease in temperature and hypertonicity (Vriens *et al.,* 2004).

Ion channels within the TRP superfamily have diverse functions (table 2). The categorisation of these subfamilies based purely on amino acid sequence and structural similarity conveys no information regarding the function of channels within that subfamily. For example members of the TRPV subfamily are involved in both thermal sensing and calcium transport in epithelial tissues, whilst members of

the TRPM subfamily function as both mechanosensors and play a role in the regulation of cell growth control (reviewed in Ramsey *et al.*, 2006).

TRP subfamily	TRP Protein	Function
TRPC	TRPC 1-7	PLC dependent Ca2+ influx in CNS and peripheral tissues including kidney, TRPC1 can associate with TRPP2 (PDK2)
TRPV	1	Thermal receptor; noxious receptor
	2	Thermal receptor
	3	Thermal receptor
	4	Thermal receptor; noxious receptor; mechanoreceptor, osmoreceptor
	5	Epithelia Ca^{2+} transport
	6	Epithelia Ca^{2+} transport
TRPM	1	Cell growth control (a tumour suppressor)
	2	Contains an ADP-ribose and NAD binding domain; may be important in sensing oxidative stress and linking apoptosis to cellular NAD metabolism
	3	Possible mechanosensor
	4	Activated by high intracellular ca; may be important in regulation of membrane potential by intracellular Ca^{2+}
	5	Taste sensor
	6	Epithelial Mg^{2+} transport
	7	Involved in cellular uptake of divalent cations in every cell.
	8	Cold receptor, cell growth control
TRPP	1-5	PKD1 and PKD2 are important in ciliary mechanosensation; mutations of P1 and P2 cause polycystic kidney disease
TRPML	1	Sorting or transport of intracellular vesicles
	3	Mechanosensor
TRPA	1	Cold receptor

Table 1.2: Functions of mammalian TRP proteins (reviewed in Huang *et al.*, 2004)

1.11.1 Mammalian TRP channel structure

All TRP channels are putative six transmembrane polypeptide subunits with three to five ankyrin-repeat domains at the intracellular amino-terminal domain. These ankyrin repeats of 33 residues are considered a requirement in establishing a structural bridge between the channel and the cytoskeleton. These six transmembrane polypeptides are likely to assemble as tetramers to form cation-permeable pores. The pore region lies between transmembrane segment 5 and 6. Across the superfamily amino acid sequence identity is only ~20%, however within each subfamily amino acid similarity is much higher extending along the whole length of the peptide (Owsianik *et al.*, 2006). In addition all TRPs have multiple regulatory and protein interaction sites and multiple putative PKA and PKC phosphorylation sites.

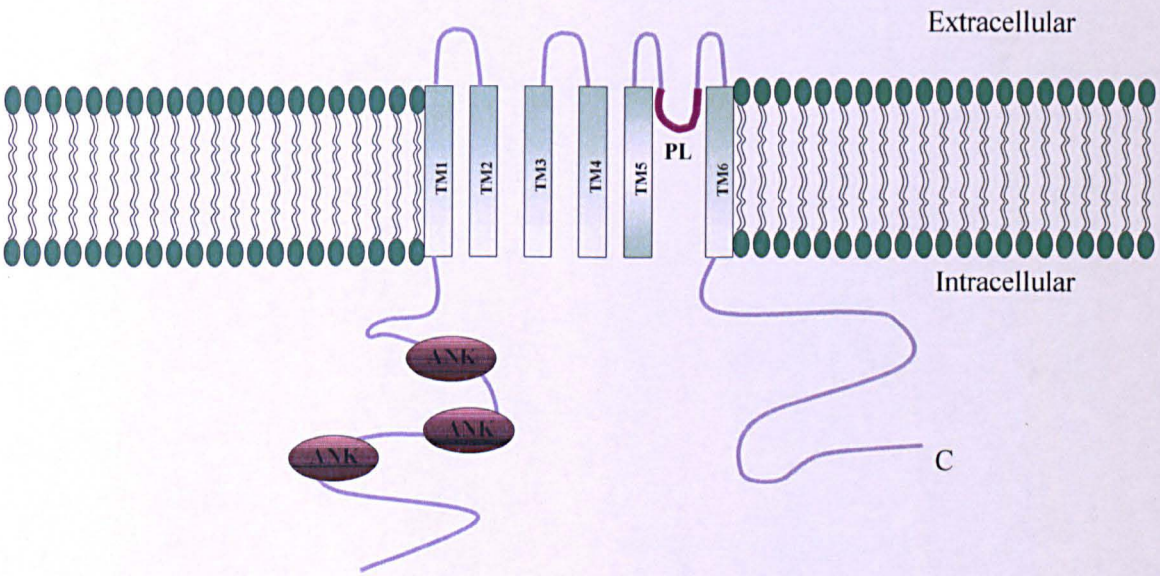

Figure 1.15: Membrane topology of TRP channels. The channel is characterised by six transmembrane segments (TM1-TM6), a pore loop segment (PL) between transmembrane segments 5 and 6, and from 3-5 ankyrin repeat domains in the N terminal segment (adapted from O'Neil *et al.*, 2005).

1.11.2 The TRPV subfamily

The founding members of the TRPV subfamily are OSM-9 in *C. elegans* and TRPV1 in mammals. OSM-9 was first identified following a genetic screen in *C.* elegans for those mutants lacking the ability to avoid steep osmotic gradients (Colbert *et al.*, 1997). OSM-9 mutants display additional insensitivity to "nose" touch and to certain odorants, suggesting the OSM-9 gene is responsible for the combined sensing of chemical, osmotic and touch stimuli. TRPV1, also known as the capsaicin receptor or vanilloid receptor 1, is the most thoroughly studied channel among the TRPV channels and was first identified in sensory neurons (Caterina *et al.*, 1997, Tominaga *et al.*, 1998). The TRPV channels can be sub-grouped into four branches by sequence homology, two are vertebrate branches and two invertebrate.

One branch includes four members of mammalian TRPVs, TRPV1 –V2,-V3, and V4, all of which respond to temperatures higher than 42, 52, 31 and 27°C respectively. The second mammalian branch comprises the calcium selective channels TRPV5 and TRPV6, both of which are thought to play a role in calcium uptake in the kidney and intestine (Hoenderop *et al.*, 2005). The last two branches of the TRPV subfamily include invertebrate TRP homologues. One invertebrate branch includes the mammalian TRPV4 homologue OSM-9 and *Drosophila* IAV (Gong *et al.*, 2004), whilst the other branch contains four *C. elegans* OCRs and *Drosophila* NAN (Kim *et al.*, 2003, Tobin *et al.*, 2002).

1.11.3 TRPV4 and cell volume regulation- a potential osmosensor?

The exposure of cells to a hypotonic environment will cause cell swelling. This is rapidly accompanied by the loss of both K^+ and Cl^- ions paralleled by the passive loss of water. This process is known as a regulatory volume decrease (RVD) and enables cell volume recovery in response to cell swelling. In several cell types, an RVD has been shown to be solely dependent on calcium influx. In these systems, volume regulation can be inhibited by either removing calcium from the extracellular

medium, or applying calcium channel blockers (Montroze-Rafizadeh *et al.*, 1991, Wong *et al.*, 1990 Shen *et al.*, 2001, Tinel *et al.*, 2002).

Prolonged exposure of kidney epithelial cells to changes in osmolality has led to a number of suggestions concerning the mechanisms involved in sensing these cell volume alterations. TRPV4 is rapidly activated under hypotonic conditions when expressed heterologously (Strotmann *et al.*, 2000). Subsequently TRPV4 activation has also been reported to be mediated by synthetic agonists including, the phorbol ester 4-α-phorbol 12, 13-didecanoate (4α-PDD) (Watanabe *et al.*, 2002), temperatures greater than 27°C (Guler *et al.*, 2002), acidic pH (Suzuki *et al.*, 2003), mechanical stress (Gao *et al.*, 2003) and endogenous ligands (Watanabe *et al.*, 2003b). Expressed in a wide variety of tissues including skin, lung epithelium and vascular endothelium (Wissenbach *et al.*, 2000, Strotmann *et al.*, 2000, Watanabe *et al.*, 2002), TRPV4 is highly expressed in the mammalian kidney (Liedteke *et al.*, 2000). RVD in renal tubule cells following exposure to hypoosmotic stress has been shown to be Ca^{2+} dependent. The hypotonic activation of TRPV4 with a concomitant rise in $[Ca^{2+}]_i$ and the reduced osmotic sensitivity of TRPV4 knockout mice has implicated TRPV4 as a possible candidate as a cellular osmosensor in the nephron (Liedtke *et al.*, 2000).

1.11.4 Activation of TRPV4 in response to hypotonicity

Conflicting data has emerged suggesting two potential mechanisms through which hypotonicity may influence TRPV4 function. In 2003, Xu *et al* reported that when HEK293 cells are exposed to a hypotonic environment, TRPV4 is rapidly (minutes) phosphorylated by Lyn Kinase at tyrosine residue Y253 in the first ankyrin binding repeat of the NH2 terminal domain. The response is specific to osmotic stress and is abolished in Y253F mutants (Xu *et al.*, 2003). Mutation of this site to any number of different residues blocked hypotonicity dependent calcium transients. However, these results are conflicting, since studies by the Nilius group failed to demonstrate any effect on the swelling induced activation of TRPV4 in the Y253 mutant (Vriens *et al.*, 2004). They proposed a mechanism consistent with previous findings that hypotonicity activates phospholipase A_2 dependent arachidonic acid release (Basavappa *et al.*, 1998), in which the activation of phoshpolipase A_2 (PLA_2) activates TRPV4 (Vriens *et al.*, 2004) as follows:

I. Swelling induced activation of phospholipase A (PLA_2)

II. PLA_2 dependent release of arachidonic acid (AA) from membrane phospholipids.

III. AA acts through the cytochrome P450 enabling cytochrome P450 mobilisation of AA to 5'6'-epoxyeicosatrienoic acid (5',6'EET)

IV. Activation of TRPV4 by the TRPV4 activating messenger 5'6' EET.

Contrary to the results by Xu *et al.*, 2003, this mechanism suggests that cell swelling activates TRPV4 by means of 5'6'EET and is not therefore, reliant on phosphorylation as a means of regulating channel activity.

Finally, the NH_2 ankyrin repeat domains of TRPV4 have also been suggested as fulfilling a role in TRPV4 activation, albeit a structural link between the channel and the cytoskeleton. Studies in which TRPV4 activation is delayed if these ankyrin repeats are lacking suggest a possible role for these domains in TRPV4 gating (Liedtke *et al.*, 2000).

1.11.5 Modulation of TRPV4 gating by calcium

Post translational modification of TRP channels and other cellular signalling mechanisms are thought to represent a mode by which constitutively active TRP channels can be regulated. Many protein kinases, including PKA, PKC and PKG have all been demonstrated to modulate TRP channel activity and, as discussed, TRP channels have been shown to possess multiple phosphorylation sites. Intracellular calcium is an important regulator of TRPV4 channels. Most calcium permeable channels are inhibited by large increases in intracellular calcium, a protective mechanism that minimises detrimental rises in $[Ca^{2+}]_i$. However, at lower concentrations depending upon the concentration, calcium can potentiate channel

activity. Numerous reports have demonstrated that an increase in $[Ca^{2+}]_i$ upon exposure to hypotonicity stimulates TRPV4 activity, a response which is abolished in the absence of extracellular calcium (Strotman *et al.*, 2003, Watanabe *et al.*, 2003a). This increase in TRPV4 activity has since been shown to be mediated by an intracellular binding site, evidence of which includes the ability of Ca^{2+} release from intracellular stores to restore TRPV4 activity in the absence of extracellular calcium, and the loss of TRPV4 currents following mutation of putative intracellular domains (Strotman *et al.*, 2003). The intracellular site responsible for regulating TRPV4 has since been identified as a calmodulin binding domain in the C terminus that binds calmodulin in a calcium dependent manner. This interaction is thought to induce a conformational change in TRPV4 thereby allowing increased channel activity (Strotmann R *et al.*, 2003).

The biphasic current observed upon TRPV4 mediated calcium entry would suggest that whilst small concentrations of calcium may potentiate TRPV4 a hypothesis supported by the fact that the Ca^{2+}-CAM interaction is mediated by submicromolar concentrations of calcium, a large increase in intracellular calcium inhibits any further activation (Strotmann R *et al.*, 2003). This dual regulation of TRPV4 by calcium will ultimately enable Ca^{2+} stimulus response whilst protecting from Ca^{2+} induced cellular damage.

1.12 Gap junctions

The ability of cells to co-ordinate their activities is a pre-requisite in maintaining the homeostatic environment within which they reside. The exposure of kidney epithelial cells to fluctuations in extracellular osmolarity necessitates not only mechanisms by which these cells are able to detect these osmotic changes, but mechanisms by which they are able to detect and subsequently convert these changes into transmittable signals. A widespread mechanism which ensures intercellular communication involves gap-junctions, plasma membrane channels which allow for the passive transfer of low molecular weight molecules such as Ca^{2+}, amino acids, water and nucleotides between coupled cells (Goodenough DA *et al.*, 1996). This exchange enables electrical and metabolic signals to spread widely among cell populations

including cells of the nephron, allowing surrounding cells to lock into a particular frequency of cellular activity. This ensures a simultaneous response across the epithelial layer in which efficient function and integrity of the overall nephron is maintained, enabling the maintenance of blood volume homeostasis.

The use of fluorescent dyes injected into cells has becomes a popular technique to establish whether cells are functionally coupled by gap junctions. Determining the biochemical nature of the messenger transmitted across these gap junctions however proves more difficult since the diversity of connexins has led to variation in channel permeability of a number of different signalling molecules. Among those signalling molecules thought to move across gap junctions are calcium and inositol tri phosphate (IP3).

Studies employing both calcium sensitive dyes and live cell imaging have confirmed that calcium itself, in response to a variety of stimuli, can propagate through gap junctions into neighbouring cells (Toyofuko *et al.,* 1998). Cells can also communicate via a local paracrine mechanism that may involve the release of ATP into the extracellular milieu. Extracellular ATP triggers calcium signalling by interacting with purinergic receptors on the plasma membrane (Bidet *et al.,* 2000). Since purinergic receptor mediated ATP release has been linked to both hemichannel activity and expression, it seems feasible that gap junctions not only communicate directly via the intercellular transfer of calcium, but also control calcium dependent cell signalling by regulating ATP release. Together the two pathways may coordinate with one another thereby enhancing both cell-to-cell communication and the overall performance of the cell.

Numerous reports have suggested a role for IP_3 as a gap junction secondary messenger (Sanderson *et al.*, 1990, Boitano *et al.*, 1992). IP_3 is able to stimulate the release of calcium from intracellular stores upon binding to its specific receptors located on the endoplasmic reticulum (Szlufcik *et al.*, 2006). Coupled to a calcium sensitive ion channel, receptor binding induces a conformational change which switches the ion channel into an open state. As a result calcium floods into the cytoplasm and intracellular calcium levels rise. The IP_3 induced calcium waves previously reported to arise as a consequence of gap junction mediated cell-to-cell

communication, have been reported in various cell types including pacemaker cells (Boitano *et al.,* 1992, Fry *et al.,* 2001). In these cells, the spread of IP_3 generates calcium waves allowing for increased synchronicity, thus enhancing coordination and allowing for amplification of the overall metabolic performance.

1.12.1 Connexins, connexons and gap junctions

To date, 21 human genes and 20 mouse genes for connexins have been identified (Sohl *et al.,* 2003). Connexins are commonly designated with numerical suffixes referring to the molecular weight of the deduced sequence in kilodaltons (e.g. connexin 26 or Cx-26). Each connexin shows tissue or cell type specific expression, whilst most organs and cells express more than one type of connexin. Examples include Cx-32 and Cx-43 both of which are expressed in numerous cell types including cardiac tissue, the kidney and hepatocytes, whilst other connexins, for example Cx-40 and Cx-62, are expressed only in retinal tissue. Not only do connexins show widespread variability in their tissue expression they also exhibit different patterns of expression during development e.g. increasing Cx-43 expression is the inverse of the Cx-40 expression pattern (Oyamada *et al.*, 2005).

All connexins share common features, they comprise four transmembrane helices; essential for enabling oligomerisation into hexameric connexon hemichannels, two extracellular loops rigidly held together by disulfide linkages critical for both docking and assembly of gap junction channels (John *et al.,* 1991) and three variable cytoplasmic domains: amino terminus, cytoplasmic loop and carboxy terminus (Kumar *et al.,* 1996) (Figure 1.16). The highly conserved amino terminal tail incorporates a putative calmodulin binding motif (Torok *et al.,* 1997) which is necessary for insertion of connexins into the membrane. High variation in amino acid sequences in the carboxy terminus ascribed functional differences (Martin *et al.,* 2000). The most intensively studied property of the carboxy tail is phosphorylation, a post-translational modification involving numerous protein kinases which through phosphorylation; control assembly, degradation and channel function.

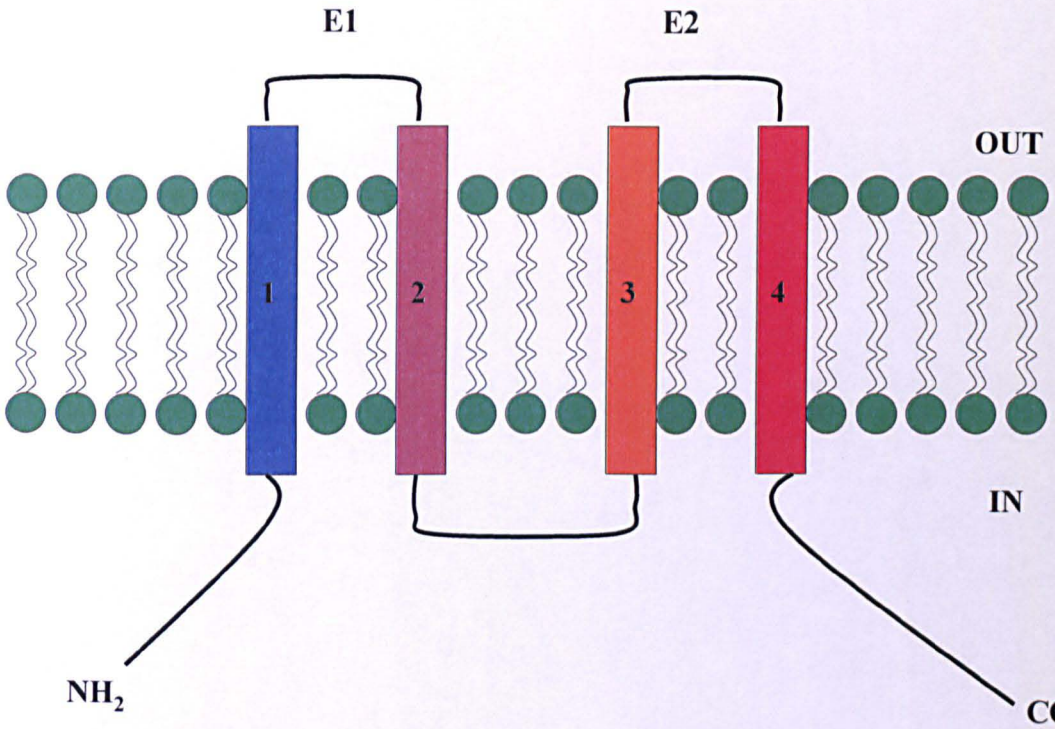

Figure 1.16: The transmembrane topology of a connexin. The connexion polypeptide is folded in the plasma membrane in the approximate shape of an M. The N and C termini project into the cytoplasm (IN) and the remaining segment traverses the membrane four times (1-4) with two short extracellular (EC) loops (E1 and E2). The third membrane spanning region is rich in hydrophobic acids and is believed to line the interior of the channel. The four membrane spanning regions and the extracellular loops are highly conserved between different connexins whereas the cytoplasmic regions vary (adapted from Li *et al.*, 2000).

Gap junctions consist of aggregates of transmembrane hemichannels or connexons. Each connexon is a six subunit structure formed when connexins oligomerise into a hexameric structure. The formation of gap junction channels stems from the extracellular interaction of two connexons or hemichannels, aligned between neighbouring cells. The interaction of two connexons creates a 2nm diameter aqueous pore that spans the two apposed plasma membranes creating a narrow pore through which both ions and molecules can transverse (Goodenough *et al.*, 1996, Evans *et al.*, 2002). Whether gap junctions assemble and membrane insertion is random or involves junctions being inserted into the centre or edge of pre-existing

clusters of gap junction plaques is unknown. There does however appear to be a requirement for extracellular matrix proteins, cadherins (Fujimito *et al.*, 1997) integrins and laminins (Lampe *et al.*, 1998) in facilitating their adhesion once inserted into the membrane.

Gap junction channels although typically formed between cells of the same type (homocellular gap junctions), have been reported to form between different cell types (heterocellular gap junctions) (Sandow *et al.*, 2003, Johnson *et al.*, 1973) (Figure 1.17). The channels themselves can adopt one of a variety of formations dependent upon the nature of the connexin involved and consequently are designated homotypic or heterotypic in nature. Two connexons each consisting of identical connexins can form a homotypic gap junction channel (Bittman *et al.*, 2002), in this case, the connexons are themselves referred to as homomeric. If the opposing connexons are not identical to each other yet homologous within themselves, the channel is termed heterotypic, whilst the connexins homomeric. Lastly, if the channel is heterotypic and each connexon is comprised of different connexin proteins, the connexon is referred to as heteromeric (Elenes *et al.*, 2001). Whilst both homomeric connexons and heteromeric connexons exist *in vitro* and *in vivo* (Valiunas *et al.*, 2001, Ahmad S *et al.*, 1999, Martinez *et al.*, 2002), it is the constituents of a gap junction channel ie the connexins involved and the formation that they adopt, which dictate both selectivity and permeability of the channel (Goldberg *et al.*, 1999).

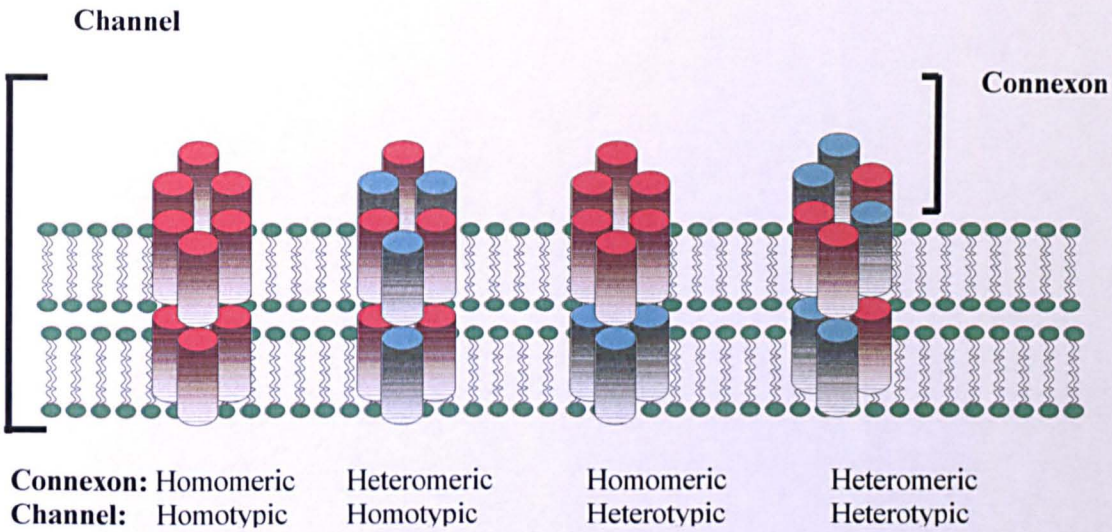

Figure 1.17: Possible arrangements of connexins in a gap junction channel unit. Gap junctions are comprised of opposing connexons. These connexons can adopt one of two comformations, homotypic or heterotypic, dependent upon the nature of the connexons involved in their formation. Since most cells express more than one connexin isoform, the hexameric connexon hemichannels can be homomeric or heteromeric depending upon the homology of the connexins involved in formation of the hexameric structure (Adapted from Evans *et al.*, 2002)

1.12.2 Gating mechanisms of connexin based hemichannels

Whilst functional gap junctions exist in an open state conformation, the ability to switch between an open or closed state is dependent upon a number of modulatory factors and is a necessity in pathophysiological conditions in which the ionic composition of the cell may alter. This ability to switch between an open and closed conformation uncouples neighbouring cells from one another, thereby serving as a protective mechanism through inhibition of a signal which may serve to cause overall tissue damage. The formation and degradation of gap junctions is a dynamic process, with reports of half lives of less than 2-5 hours in cultured cells and tissues (Evans *et al.*, 2002). The rapid synthesis and turnover of connexins is an indicator that gap junction number, composition and function are subject to tight regulation and are rapidly remodelled. Deficient or improper gap junction function has been

associated with a variety of diseases, including forms of neuropathy, cataracts, skin disease, heart disease, and hypertension (Pal *et al.*, 2000, Kelsell *et al.*, 2001, Dasgupta *et al.*, 2001, Haefliger J-A *et al.*, 2001), regulation therefore is critical.

In most hemichannels studied to date, opening is enhanced at positive membrane potentials or when extracellular calcium is below 1mM (Stout C *et al.*, 2003, Verselis VK *et al.*, 2000). The open probability of gap junctions therefore is reported to decrease in conditions in which calcium concentrations may become dangerously high. In the kidney, changes in cell volume have been reported to be accompanied by a rise in intracellular calcium (Montrose-Rafizdeh *et al.*, 1991). This increase in calcium has been shown, in both kidney and numerous other cell types, to evoke instigation of cell volume recovery mechanisms ultimately enabling volume restoration throughout. However, under conditions in which the concentration of calcium becomes dangerously high, this rise may trigger communication of specific Ca^{2+} mediated signals to neighbouring cells. Calcium may also induce closure of gap junction channels which will ultimately serve as a potential safety mechanism; isolating healthy cells from dying or injured cells. In conjunction with alterations in intracellular calcium levels, hemichannels are also sensitive to intracellular acidification with exposure to either a low or high pH solution inducing channel closure (reviewed in Peracchia *et al.*, 1997).

Activity of gap junctions can also be influenced by post translational modification of the connexin subunits. With the exception of Cx-26 and Cx-36, all connexins are phosphoproteins (Saez *et al.*, 1998.) Kinases known to be involved in modulating gating behaviour through phosphorylation include PKC, mitogen activated protein kinase (MAPK) and the cAMP dependent protein kinase (PKA). Whilst both PKC and MAPK have been implicated as negative regulators of hemichannel gating, PKA via its effects on intracellular cAMP, has been shown to oppose the effects of both PKC and MAPK modulating hemichannel gating in a positive manner. Either way, phosphoamino acid analysis confirms the majority of these phosphorylation events to occur on serine residues located within the cytoplasmic loop region. An exception to this rule is Cx-56, since this can be phosphorylated both in the cytoplasmic loop region and at its C terminal domain (Berthoud *et al.*, 1997).

PKC has received considerable attention regarding it ability to act as a regulator of gap junction gating since it has been shown to increase Cx-43 phosphorylation and subsequently decrease gap junction communication. In mammalian cell lines, the opening of Cx43 hemichannels induced by low extracellular calcium is blocked following the activation of PKC (Li H *et al.*, 1996, Liu *et al.*, 1997). A similar response observed in *Xenopus* oocytes expressing Cx-46 (Ngezahayo *et al.*, 1998), supporting the notion that PKC mediated phosphorylation is critical in regulating the gating behaviour of hemichannels. Furthermore, mutation of the PKC phosphorylation site Ser368 in Cx-43 to an alanine, results in a constituitively open hemichannel (Bao *et al.*, 2004). Since both phorbol esters and PKC activating reagents are also capable of inhibiting gap junction intercellular communication these compounds are often used extensively in the lab to modulate and study gap junction function. Contrary to the effects of PKC, increased intracellular cAMP levels have been shown to increase both Cx-43 phosphorylation and Cx-43 mediated intercellular communication (Atkinson *et al.*, 1995, Burghardt *et al.*, 1995).

The availability of multiple serine/threonine kinases within a cell allows for stringent control of intercellular communication via phosphorylation of pre-exisitng hemichannels. Ultimately the nature of the phosphorylation will determine the conformation adopted by the hemichannel, its gating properties and consequently the rate of gap junctional intercellular communication.

1.13 Aims

Diabetic nephropathy is the leading cause of end stage renal disease in patients with type II diabetes and is associated with aberrant sodium reabsorption in the kidney that can result in secondary hypertension. Whilst numerous animal studies have reported deranged transcriptional regulation of signalling elements in sodium handling, unlimited availability of cells of the human cortical collecting duct would facilitate the identification of key signalling elements that may serve as a potential therapeutic target for the prevention of secondary hypertension. The overarching aim of this thesis was to determine those mechanisms involved in the regulation of both SGK1 and ENaC under glycaemic conditions comparable to those observed in a type II diabetic in order to determine the implications that this may have for $[Na^+]_i$ levels and ultimately blood volume homeostasis. Specific hypothesis to be tested include:

1. Does the human cortical collecting duct (HCD) cell line represent a useful model for the study of sodium transport in renal epithelia?

- To confirm expression of all key recognition elements involved in sodium transport in the collecting duct e.g.. SGK1, α, β and γ ENaC, thus confirming the Human Cortical Collecting Duct (HCD) cell line a suitable model for the study of renal Na^+ rebasoption

2. Are changes in SGK1 and ENaC associated with glucose evoked changes in Na^+ handling in HCD cells?

- Assess the influences of variable concentrations of glucose on SGK1 and α-ENaC expression and localisation

- Elucidate a role for other key signalling components e.g. TGF-β1 and $[Ca^{2+}]_i$ associated with hyperglycaemia in the expression of SGK1 and α-ENaC.

- Determine the effects of high glucose on intracellular Na^+ levels.

3. Are mechanoreceptors involved in resolving physical changes to the cell membrane?

- Identify and confirm the nature of the receptor involved in detection and transduction of cell volume changes.

- Confirm a role for $[Ca^{2+}]_i$ in the response to alterations in extracellular osmolarity in HCD cells

4. Is cell-to-cell communication essential for efficient Na^+ reabsorption in the HCD cell?

- Determine the mechanism by which cells of the cortical collecting duct communicate upon exposure to a surrogate form of osmotic stress.

- Identify the means by which signal transmission is mediated from a discrete point of physical contact.

- Assess the influence of gap junction uncouplers and purinergic receptor antagonists on signal transmission.

5. Is cell-to-cell communication compromised in a pathophysiological state? Are the key recognition elements involved in signal transduction subject to alterations in expression under glycaemic conditions?

- Confirm the effects of elevated glucose, TGF-β1, and $[Ca^{2+}]_i$ on those signalling molecules involved in cell-to-cell communication .

- Assess the effects of elevated glucose levels on cell-to-cell communication.

Chapter 2 Materials and Methods

2.1 Materials

Sigma Aldrich Company, Poole, U.K. rabbit serum, goat serum, dithiothreitol (DTT), phenylmethylsulfonylfluoride (PMSF), bromophenol blue, bovine serum albumin, (BSA), polyoxyethylene-sorbitan (Tween-20), ethidium bromide, 3-(N-morpholino), sodium dodecyl sulphate (SDS), triton-X 100, hydrochloric acid (HCl), dimethylsulfoxide (DMSO), 4-(2-Hydroxyethyl)piperazine-1-ethanesulfonic acid (HEPES), ammonium persulfate (APS), N,N,N',N'-Tetramethylethylenediamine(TEMED), β-mercaptoethanol, fura-2 am, Pluronic F-127, 3 aminopropyltriethoxysilan (APES), lucifer yellow, ouabain, amiloride, dexamethasone, insulin transferrin selenate (ITS), fetal calf serum, ionomycin, thapisgargin, SBF-1/AM. Transforming growth factor beta (TGF-β1), Trypsin, Acetone, TRITC conjugated phalloidin, RNA miniprep kit, paraformaldehyde (PFA), 4',6-diamidino-2-phenylindole (DAPI), Igepal-CA-630, GenElute mammalian total RNA miniprep kit

Affinity Bioreagents, New Jersey, U.S. Primary antibodies (see table 2.1)

Bioline, London, U.K. Hyperladder.

Biogenesis, Poole, UK. Glyceraldehyde-3-phosphate dehydrogenase (GAPDH)

Gibco, Paisley, UK. Dulbecco modified eagle medium (low glucose) (DMEM), HAMS F-12, Dulbecco modified eagle medium: HAMS nutrient mixture F-12, 1:1 mix (DMEM F-12)

Promega, Southamptom, U.K. Random primers, avian myeloblastosis virus reverse transcriptase (AMV), rRNAsin ribonuclease, deoxynucleotide triphosphates (dNTP)

Invitrogen, Paisley, U.K. Lipofectamine, all primers (see table for details), Taq DNA polymerase, TRPV4 siRNA, magnesium chloride buffer ($MgCl_2$)

Amersham Biosciences U.K Limited, Little Chalfont, U.K. enhanced chemiluminescence (ECL), rainbow protein markers, Anti-mouse immunoglobulin horseradish peroxidase

Eppendorf, U.S. Water, molecular biology grade

Biorad, Hertfordshire, U.K. Protein assay reagent

Millipore U.K, Ltd, Watford, U.K. Whatman:p81 phosphocellulose 3mm filter paper

Fisher Scientific, Leicestershire, UK. Glycine, Tris (hydroxymethyl) methylamine, sodium chloride, HPLC grade methanol, Acetic acid.

Santa Cruz, California, U.S. Cx-43 siRNA, primary antibodies (see table 2.2)

The Binding site, Birmingham, UK. Primary antibodies (see table 2.2), Anti-sheep/goat immunoglobulin horseradish peroxidase, Anti-rabbit immunoglobulin horseradish peroxidase

Molecular probes, Netherlands. Alexa 488 goat anti-rabbit, Alexa 488 goat anti-sheep.

2.2 Tissue culture

2.2.1 Maintenance of HCD cells

HCD cells were derived and supplied by Professor P.M Ronco. Cells were obtained from normal human kidney cortex and immortalized with SV-40 virus. Clones were selected using the monoclonal antibody, Ab272, which specifically recognizes collecting duct principal cells (1). HCD cells (passages 18-30) were maintained in DMEM/Hams F-12 medium supplemented with 2% fetal calf serum (FCS), glutamine (2mM), 15mM HEPES, transferrin (5μg/ml), Na_2SeO_3 (5ng/ml), insulin (5μg/ml) and dexamethasone ($5x10^{-8}$ M). Cells were grown at 37°C in a humidified atmosphere of 5% CO_2 in air in vented flasks.

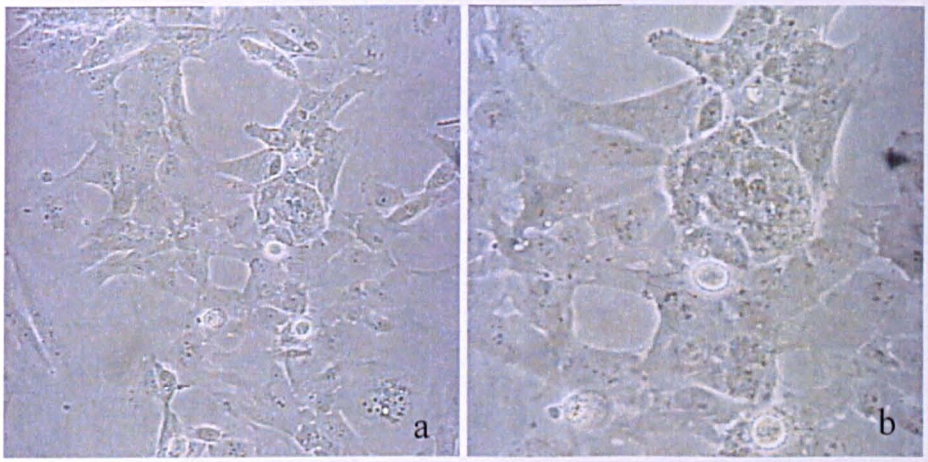

Figure 2.1 Light micrograph of HCD cells after maintenance in tissue culture: The human collecting duct (HCD) cell line is a polarised epithelial cell line expressing characteristics of the principal cells of the kidney. Panels a, and b show phase morphology of HCD cells in culture at x20 and x40 magnification respectively.

2.2.2 Subculturing

Cells were allowed to reach 80-90% confluence and then detached by incubation with 3ml of phosphate buffered saline (PBS) containing 0.3mM EDTA and 0.08% (w/v) trypsin for 3-4 minutes at room temperature. Trypsin was inactivated by the addition of 15ml of medium containing 5% FCS. Cells were then collected in a universal and centrifuged at 260g for 5 minutes. Resuspension of the cell pellet in media allowed for cells to be distributed as required.

2.2.3 Freezing and thawing of cells

Stocks of cells were maintained in liquid nitrogen. Cells were trypsinised and pelleted by spinning at 260g Cell pellets were resuspended in 3ml FCS containing 10% dimethyl sulfoxide (DMSO) 1.5ml aliquots were used to fill 2ml cryovials. To reduce ice crystal formation cells were stored at -80°C overnight and then transferred to liquid nitrogen the following day for future storage. To revive cells, an ampoule was thawed rapidly at 37°C. The contents of this ampoule were then transferred to a universal containing 20mls media and cells were pelleted at 260g for five minutes. Cells were resuspended in 32ml fresh media and transferred into two 75cm^2 flasks.

2.3 Reverse transcriptase polymerase chain reaction (RT-PCR)

Polymerase chain reaction (PCR) is a simple yet powerful technique which allows for the logarithmic amplification of any known DNA sequences within a double stranded DNA molecule. The technique employs a pair of primers that hybridize and flank to sequences on opposing strands of the target. These primers are extended by a DNA polymerase so that a copy is made of the designated sequence. After making this copy, the same primers can be used again, not only to make another copy of the input DNA strand but also of the short copy made in the first round of synthesis, hence amplification becomes logarithmic. PCR consists of three general steps.

i. **Denaturation:** The reaction mixture is heated to 95°C for a short time period in order to denature the target DNA into single strands enabling them to act as template strands for DNA synthesis. Since it is necessary to raise the temperature to separate the two strands, a thermo stable DNA polymerase is required to prevent the need for new polymerase every cycle. Taq polymerase is a thermo-stable DNA polymerase that was first isolated from Thermus aquaticum, a bacterium that grows in hot pools and can thus withstand high temperatures.

ii. **Primer annealing:** Following denaturation of the strands, the mixture is rapidly cooled to allow for primer binding to occur. Calculation of this annealing temperature is dependent on a number of factors including both primer length and GC content, and is calculated carefully to ensure that the primers bind only to the desired DNA sequences. The two parental strands do not re-anneal with each other since the primers are in large excess over the parental DNA.

iii. **Elongation:** The temperature of the mixture is raised to approximately 72^0C and kept at this temperature for a pre-set period of time. This ensures that the DNA polymerase binds to and elongates each primer, ultimately copying the single strand templates. At the end of the incubation both parental strands have been made partially double stranded.

2.3.1 RNA preparation

RNA was prepared from 80% confluent HCD cells by acid-guanidinium extraction (Chomczynski *et al.*, 1987) using a genelute mammalian total RNA miniprep kit (Sigma) following the manufacture's instructions. RNA was stored at -80°C

2.3.2 Reverse transcriptase polymerase chain reaction (RT-PCR)

Complementary DNA was synthesized by reverse transcription using a Promega Reverse Transcription System following an adapted method. 1μg of total RNA and 0.5μg of random hexamers, in a final volume of 11μl, were incubated at 70°C for 5

minutes, and then allowed to cool slowly to 25°C to allow for primer annealing. Primer extension was then performed at 37°C for 60 minutes following the addition of 1x (final concentration) reaction buffer (50mM Tris-HCl (pH 8.3), 50mM KCl, 10mM $MgCl_2$, 10mM dithiothreitol and 0.5mM spermidine), 1mM (final concentration) of each deoxynucleotide triphosphates (dNTP), 40U of rRNAsin ribonuclease inhibitor and 15U of Avian Myeloblastosis Virus (AMV) reverse transcriptase in a final volume of 20µl. The RT mixture was heated to 95°C for 5 minutes, then 4°C for 5 minutes. An aliquot of 4µl cDNA was used in subsequent PCR reactions. cDNA was stored at -20°C

2.3.3 PCR amplification of cDNAs

Amplification of specific cDNAs was carried out using primers specific for the gene of interest. PCR reactions (20µl) were set up containing 1.5mM $MgCl_2$, 1 x NH_4 buffer (50mM KCl, 10mM Tris HCl pH 9, 0.1% Triton x-100), 0.2mM of each dNTP, 0.5µM of each primer and 1U of Taq DNA polymerase. Amplification of samples was performed using an initial denaturation step of 95°C (5minutes) followed by between 30-35 cycles consisting of one minute of denaturing at 95°C, one minute of annealing at the optimised temperature (50-60°C) and a one minute extension at 72°C. A final elongation step of 72°C for seven minutes was included in all PCR amplifications (see table 1 for primer details). As a negative control, template cDNA was replaced with RNase free water. Following amplification, PCR products (10µl) were mixed with 4µl loading buffer (1mM EDTA pH 8, bromophenol blue 0.25% w/v, xylene cyanol 0.25% w/v, and 50% v/v glycerol) and run on 1% (w/v) agarose gels containing ethidium bromide at 80 volts. PCR products were visualized on a Genegenius Bioimaging system UV transilluminator (Syngene Cambridge U.K).

Target	Primers (5'→ 3')	Direction	Annealing temp	Product size (*bp*)	Origin
SGK1	AGGGCAGTTTTGGAAAGGTT	F	51	699	Primer 3
	GCAGAAGGACAGGACAAAGC	R			
α-ENaC	GGCATCTTCATCAGGACCTACT	F	50	601	Rauz *et al.*, 2003
	ACATGATCCGTAACTGCAACT	R			
β-ENaC	GTGCCAATCAGGAACATCTAA	F	50	1000	Rauz *et al.*, 2003
	CACTTTCAACTCTGCTTTGCAC	R			
γ-ENaC	GGGACTATCCACCTGCAAGA	F	50	696	Rauz *et al.*, 2003
	CACGTGCTGCTCCACTTTTA	R			
TGF-β1	AGAGGTCGCTTGGGAATTTT	F	58	341	Primer 3
	TTTGGAAACCATGTCAAGCA	R			
Cx-26	ACCTTGCTGTGCCTCAGTTT	F	55	309	Primer 3
	TATACCAGCACCCGGAAGAC	R			
Cx-31	TTCGGGTGACCTCATCTTTC	F	55	307	Primer 3
	CCCGCATGTGTGTTCTTCTA	R			
Cx-31.1	TTGCAACCTTTCCTTCTGCT	F	55	392	Primer 3
	TTCCACAAGGGGAATCTGAG	R			
Cx-40	ATGAGCAGTCTGCCTTTCGT	F	55	338	Primer 3
	GGTCGCTCTTTCCCTTAACC	R			
Cx-43	CCCGTGAGAACACCAAGTTT	F	58	597	Primer 3
	TCACTCCAGGGCATTTCTTC	R			
TRPV4	CCCGTGAGAACACCAAGTTT	F	59	618	Primer 3
	TCACTCCAGGGCATTTCTTC	R			

Table 2.1 PCR primers used in this study. F= forward primer, R= reverse primer. All primers were supplied by invitrogen Paisley, UK.

2.4 SDS gel electrophoresis

Electrophoresis is a widely available technique used for the separation of charged macromolecules, e.g. proteins in an electric field. The electrophoretic mobility of a charged particle depends on a number of factors including the overall charge of the molecule, its molecular weight and shape. Since the overall charge of a given molecule is dependent on the number of amino acid side chains available for ionisation at a given pH. Those molecules with a greater charge will migrate towards the opposing electrode faster than those molecules with a lesser charge providing they are of a similar molecular weight.

Polyacrylamide gel electrophoresis (PAGE) can also be performed under denaturing conditions, typically in the presence of the ionic detergent Sodium Dodecyl Sulfate (SDS-PAGE) or under reducing and denaturing conditions (SDS-PAGE in the presence of a reducing agent such as dithiothreitol (DTT) or beta mercaptoethanol which break disulfide bonds). Prior to resolving the sample by SDS-PAGE, the protein sample is heated to 95^0C. By disrupting non-covalent intra- and intermolecular bonds, the protein is effectively rendered devoid of secondary and tertiary structure. Consequently, the denatured protein molecules become coated with the negatively charged SDS at a concentration of approximately 1.2 g SDS per gram of protein, thus giving the protein molecules a net unit negative charge per unit mass. As a result, the molecular weight of these proteins becomes the only determinant in their separation.

Proteins are loaded onto a polyacrylamide gel and exposed to an electric field. The formation of polyacrylamide from its acrylamide monomers produces a gel with a sieve like effect in which proteins migrate and separate according to their size only. The pore sizes in the gel can be controlled by choosing appropriate concentrations of acrylamide and the cross linking reagent methylene bisacrylamide. The higher the concentration of acrylamide used the smaller the pore size in the final gel. Whilst small proteins will migrate fastest through the gel, larger proteins are held back by the cross linking in the gel and migrate at a slower rate.

2.4.1 Cell lysate protein preparation

HCD cells were allowed to reach approximately 70-80% confluency. Medium was removed and cells were washed with sterile PBS. Using a cell scraper, cells were scraped into 3-4ml of a mixture of PBS and the protease inhibitor Phenylmethylsulphonylfluoride (PMSF) (0.5mM). Cells were pelleted at 180g for 5 minutes. Total cell lysates were then prepared by two different methods, dependent upon which antibody was to be used to probe that sample.

1. Cells were lysed open with 250µl lysis buffer (0.25M Tris pH 7.8, 0.5% v/v NP40, 1mM PMSF, 5mM DTT) at 4°C disrupting the cell membrane and releasing both membrane and cell contents. Cells were then vortexed and gently agitated at 4°C for a period of 30 minutes. Cells were then spun at 76g for 5 minutes to pellet cell debris and the supernatant aliquoted and stored at -80°C

2. Cell pellets were resuspended into 200-300µl of PBS+PMSF (0.5mM). These preparations were then vortexed briefly and subjected to three cycles of freeze-thaw therefore disrupting cell integrity Samples were centrifuged at 76g to pellet cell debris and the supernatant collected. Samples were then aliquoted and stored at -80°C.

2.4.2 Protein concentration determination

Protein concentrations were determined using the Bio Rad protein Assay. This assay is a dye-binding assay which relies on a change of colour of the dye in response to various concentrations of protein. The absorbance maximum for an acidic solution of Coomassie® Brilliant Blue G-250 dye shifts from 465 nm to 595 nm when binding to protein occurs. A standard curve was prepared using BSA (0-20µg protein). Protein samples (10µl) were mixed with water (790µl) and dye concentrate (200µl). This mixture was then left for five minutes. Samples were read on a spectrophotometer at 595nm and protein concentrations calculated using the standard curve.

2.4.3 Sample preparation

5µg of protein was diluted to 10µl with dH_2O and mixed with 20µl of sample buffer (125mM Tris pH 6.8, 6.4mM DTT, 20% (v/v) glycerol, 0.025% (v/v) bromophenol blue, 10% (v/v) water). Samples were then heated to 95°C for 5 minutes.

2.4.4 Preparation and running of gel

Gel equipment (Biorad) was assembled. The resolving gel was poured between the two glass plates and allowed to polymerise for 30-40 minutes (see table 2.2 for details of gel reagents). As oxygen interferes with polymerisation, a layer of water was gently pipetted onto the top of the gel to form an airtight seal. When polymerisation of the gel was complete, the stacking gel was prepared and poured on top of the resolving gel. A well-forming comb was inserted and the stacking gel left to polymerise for 15 minutes. When polymerisation of the stacking gel was complete, the combs were removed and the wells were washed thoroughly with water. Samples were then loaded into the wells of the gel and separated by sodium dodecyl sulphate (SDS) polyacrylamide gel electrophoresis (4.5% stacking gel, 7.5% or 10% resolving gel) at 200 volts for 50 minutes in electrophoresis buffer (25mM Tris, 192mM glycine and 0.1% (w/v) SDS).

Reagent	**Stacking gel 4.5%**	**Resolving gel (7.5%)**	**Resolving gel (10%)**
Acrylamide (33%)	1.5ml	3ml	4ml
1.5M Tris pH 6.8	2.5ml	-	
1.5M Tris pH 8.8	-	1.5ml	3ml
10% SDS	100µl	120µl	120µl
Ammonium persulfate (10% w/v)	40µl	100µl	100µl
TEMED	10µl	10µl	10µl
dH_20	5.8ml	5.84ml	4.84ml

Table 2.2 Reagents required for stacking gel and resolving gel preparation

2.5 Western blotting

Western blotting is the term given to the technique by which proteins are transferred from the polyacrylamide gel to a more accessible medium ultimately enabling the detection of proteins via specific antibodies (Figure 2.2). In this procedure, a sandwich of gel and solid support membrane (Nitrocellulose or Polyvinylidene Fluoride (PVDF) is compressed in a cassette and immersed in buffer between two parallel electrodes. A current is passed at right angles to the gel ultimately inducing the separated proteins to electrophorese out of the gel and onto the solid support membrane. Once the proteins have been transferred to the solid support membrane, the membrane is referred to as a "blot". Electroblotting preserves the resolution of electrophoretic transfer and allows for further analysis using specific antibodies raised against proteins of interest. The western blot is then incubated with a primary antibody, visualised by enhanced chemiluminescence (ECL) using a secondary antibody conjugated to horseradish peroxidase (HRP). The chemiluminescent reaction occurs as a consequence of the ability of HRP to oxidise a peracid salt, raising the oxidation state of the haem group central to HRP. Reducing this to the ground state forms a luminol radical, which releases light. In enhanced chemiluminescence, enhancer molecules react with the haem group in place of luminol leading to the formation of enhancer radicals. These radicals in turn produce luminol radicals, the decay of which emits light in a reaction which is sustained for a far greater time period than in the absence of these enhancer molecules (Whitehead *et al.*, 1979).

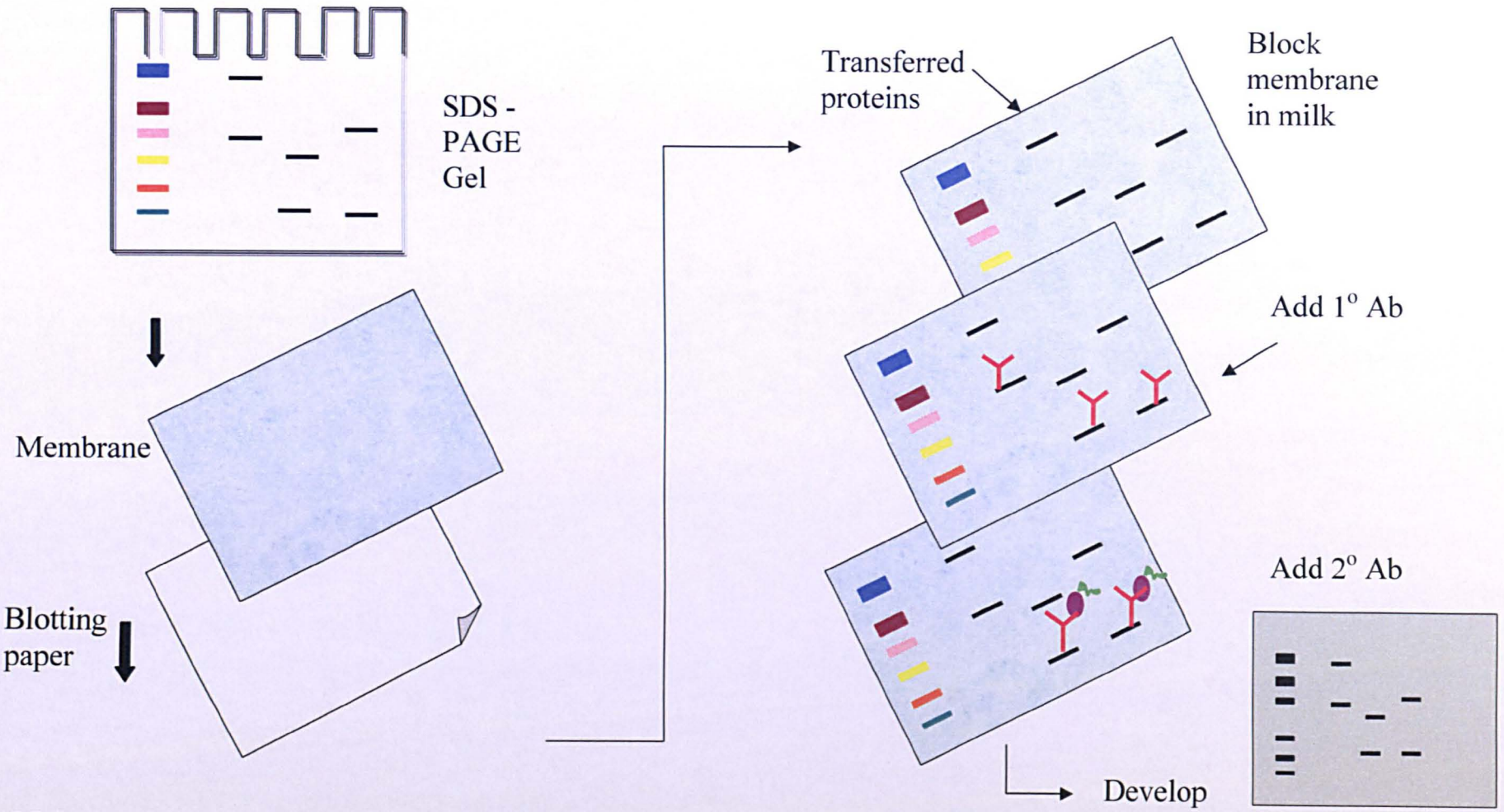

Figure 2.2 Schematic diagram to illustrate western blotting

2.5.1 Electrophoretic transfer

Immobilin P membrane (Millipore) was cut to size and soaked in methanol for 3 seconds. The membrane was then placed into water for 2 minutes and then equilibrated in transfer buffer (25mM Tris, 400mM Glycine, 20% (v/v) Methanol, 2l water) for 10-15 minutes. Two sheets of chromatography paper and fibre pads were also incubated in transfer buffer for 15 minutes. After electrophoresis gels were also soaked in transfer buffer for 10 minutes. The gels and membrane were then assembled in a transfer cassette as follows

Fibre pad
Chromatography paper
Gel
Immobilin membrane
Chromatography paper
Fibre pad

Proteins were transferred 1 hour at 100 volts; 4°C.

2.5.2 Immunodetection

To prevent non specific binding and reduce background, membranes were incubated in 20% non fat milk (marvel) w/v in PBS-Tween ((PBS-T) 0.1% v/v) for 1 hour at 25°C. The membrane was incubated overnight at 4°C in primary antibody made up in PBS-T (0.05% v/v). After three 10 minute washes in PBS-T (0.1%), the membranes were incubated with the secondary antibody (horseradish peroxidase- conjugated) in PBS-T (0.05%) for 60 minutes at 25°C followed by three 10 minute washes in PBS-T (0.01%) Specific proteins were detected using ECL detection reagent chemiluminescence system (Amersham Biosciences) and were visualised after exposure of membranes to X-ray film for 1-10 minutes

2.5.3 Antibody optimization and confirmation of specificity

All primary and secondary antibodies were optimized to ensure an efficient combination of protein staining with minimal background noise. Optimization was achieved by testing a range of dilutions of both primary and secondary antibody (see table 1.3 for optimal conditions)

Ab	Species raised in	1° dilution	2° dilution	Company
α-ENaC	Rabbit	1:600	1:2000	Affinity Bioreagents
γ-ENaC	Rabbit	1:600	1:2000	Affinity Bioreagents
SGK1	Sheep	1:3000	1:30,000	The Binding Site
TGF-β1	Rabbit	1:500	1:40,000	Santa Cruz
GAPDH	Mouse	1:20,000	1:20,000	Biogenesis
Cx-43	Rabbit	1:200	1:3000	Santa Cruz
TRPV4	Sheep	1:1000	1:30,000	The Binding site

Table 2.3 Optimized antibody dilutions used for western blotting. Conditions were optimised for both primary and secondary antibodies to achieve optimal binding and minimal background noise. Primary antibodies were obtained from Santa Cruz, Affinity Bioreagents and The Binding Site. Secondary antibodies were obtained from The Binding site. (section 2.1 for further details).

To confirm specificity of our secondary antibodies, western blots were incubated with both primary and secondary anti-sheep (The Binding Site) (figure 2.3 panel A1) or anti-rabbit (The Binding site) (figure 2.3 panel; B1). In parallel to this a second western in which the membrane was incubated with secondary antibody alone (figure 2.3 panel A2 and B2) was performed. Specificity was confirmed when a band on only the blot probed with both primary and secondary antibody was visualised by ECL detection.

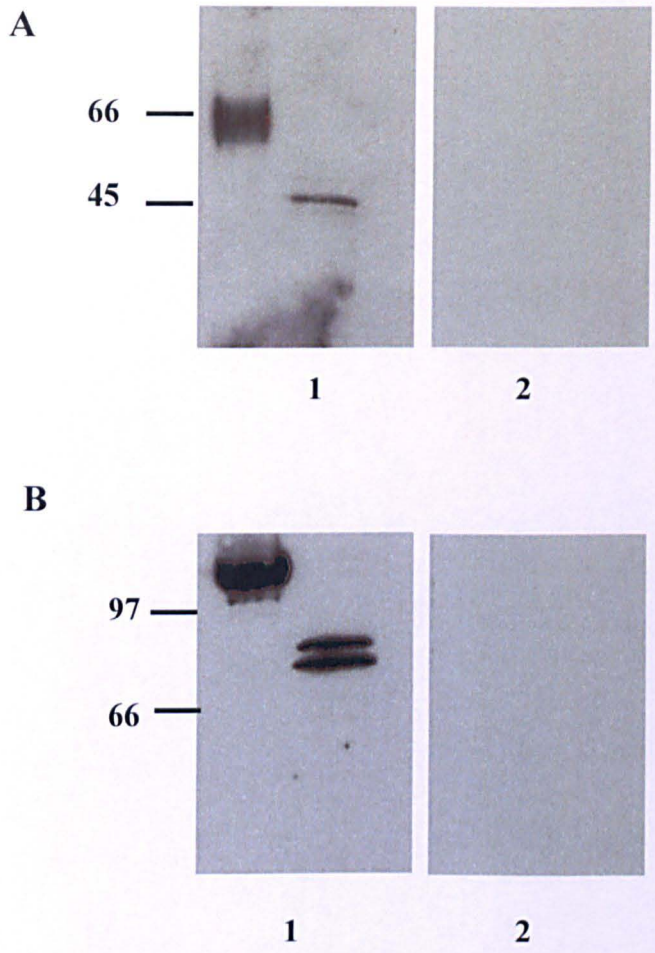

Figure 2.3 Confirmation of specificity of anti-sheep and anti-rabbit secondary antibodies. Membranes were incubated with a specific primary antibody and either anti-sheep (A1) or anti-rabbit (B1) secondary. In parallel, membranes from which the primary antibody was omitted from the overnight incubation and blots were probed with either anti-sheep (Panel A2) or anti-rabbit (Panel B2) secondary.

2.6 Immunocytochemistry

The immunocytochemical localisation of an antigen involves fixing and stabilizing the antigen, saturating non-specific binding sites, binding the primary antibody and lastly visualising the primary antibody. Following fixation of the cells, any non specific binding is eliminated by addition of a blocking agent. Addition of the primary antibody results in detection of the antigen of interest. The application of a fluorescent conjugated Alexa 488 secondary antibody allows for visualisation of our protein of interest (figure 2.4).

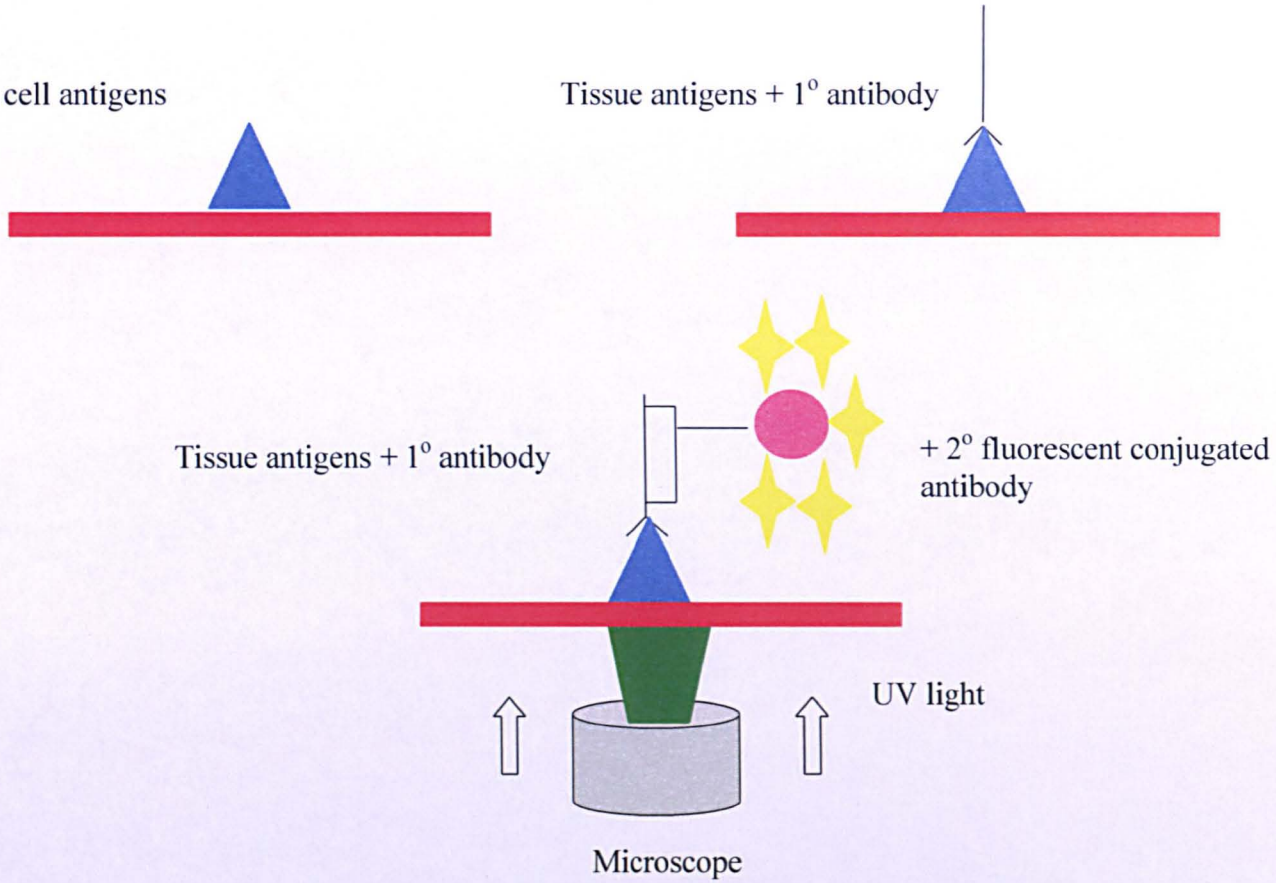

Figure 2.4 Localisation of an antigen using immunocytochemical staining. Non-specific protein binding is blocked with an appropriate blocking agent. Primary antibody is added to the fixed cells allowing for an interaction to form between our antigen of interest and primary antibody. After washing, a secondary fluorescent conjugated antibody raised against the animal in which our primary antibody is raised is added and viewed under a fluorescence microscope.

2.6.1 Preparation of APES treated coverslips

Coverslips were cleaned in acetic acid for a period of 30 minutes and left to soak. Coverslips were then washed with copious quantities of distilled water. To remove any final traces of acetic acid coverslips were placed in 70% ethanol for 30 minutes followed by further washing with distilled water. Coverslips were then placed into a solution of 10 ml acetone mixed with 200µl 3-aminopropyltriethoxysilane (APES) and left for 5 minutes. After 3x10 minute washes, coverslips were air dried before being placed in 6 well plates. Finally, all plates were exposed to UV radiation for 20 minutes to sterilise coverslips prior to plating with cells.

2.6.2 Cell fixation

Fixatives work by several means: formation of cross-linkages (e.g., aldehydes such as glutaraldehyde or formalin); protein denaturation by coagulation (e.g., acetone and methanol); or a combination of the above.

Cells were grown to 80% confluence on APES treated coverslips in culture media. Media was removed and cells incubated at room temperature for 30 minutes with 4% paraformaldehyde (PFA). PFA was removed and cells were washed with PBS for 3x10 minute washes. Cells were stored for future use at 4°C in PBS and sodium azide to prevent any bacterial growth and contamination.

2.6.3 Antibody staining procedure

Cells were removed from the fridge and warmed to room temperature for approximately 1 hour. Any residual traces of sodium azide were removed by washing with PBS (3 x 10 mins). To prevent any non-specific binding, cells were incubated for 1hr at 25°C in a blocking solution comprised of PBS-Triton (0.01%) (v/v), containing 10% (v/v) goat serum. The blocking solution was removed. Following 3 x10 minute washes with PBS, the nuclear stain DAPI (4',6-diamidino-2-phenylindole, dihydrochloride; 1µM) was added to each coverslip for 3minutes. After washing with PBS (3x5 minutes), cells were incubated with the cytoskeletal stain TRITC-conjugated-phalloidin diluted at 1:100 in PBS-Triton (0.01%) for 1

hour at 25°C. Following further washing (3x5 minutes), cells were incubated overnight at 4°C with primary antibody (1:100) diluted in PBS-Triton (0.01%). Following antibody incubation, cells were washed with PBS and then incubated in Alexa 488 conjugated secondary antibody for 1 hour at 25°C in the dark. Secondary antibodies were diluted (1:400) in PBS-Triton (0.01%). Cells were washed (3x10minutes) and coverslips mounted in anti-fade citifluor (glycerol/PBS solution: Agar Scientific) on glass slides.

2.6.4 Antibody specificity

As with the western blots, appropriate controls were performed in which primary antibody was omitted from the staining process to test for the specificity of the secondary antibodies. Controls were performed for both secondary Alexa-conjugated anti-rabbit (figure 2.5/1d) and secondary anti-sheep (figure 2.5/2d) and specificity confirmed when only those cells stained with both primary and secondary antibody fluoresced under UV light (figure 2.5/1b and 2.5/2b)

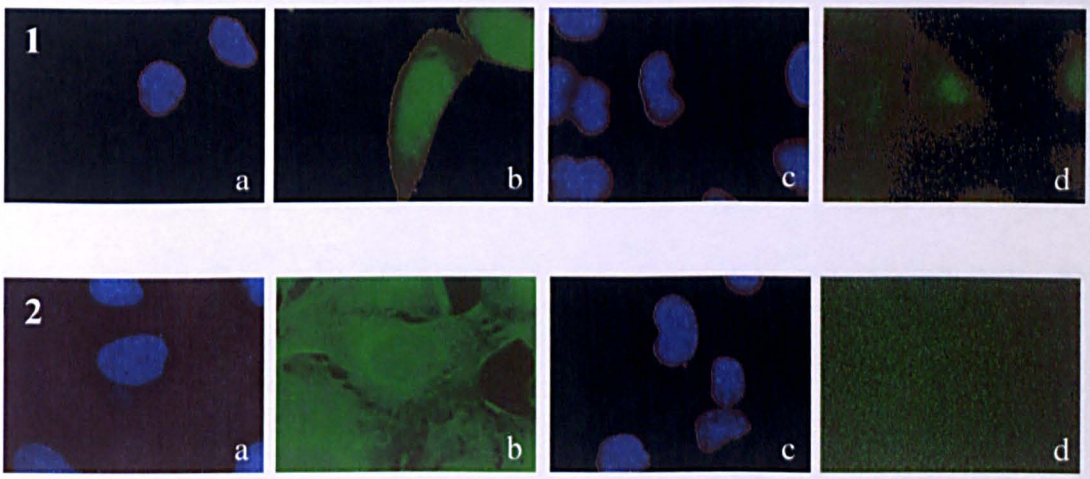

Figure 2.5 Confirmation of specificity of secondary antibodies used in immunocytochemical staining. HCD cells were stained with the nuclear stain DAPI and a primary antibody. Staining was then visualized by addition of either a fluorescent conjugated secondary anti-sheep (1/b) or anti-rabbit (2/b) antibody. Panels 1/d and 2/d represent staining of cells in which primary antibody was omitted. These images confirm specificity of our secondary antibodies.

2.7 RNA interference

RNA interference (RNAi) is a phenomenon in which double-stranded RNA (dsRNA) suppresses expression of a target protein by stimulating the specific degradation of the target mRNA. RNAi is utilised by most eukaryotes *in vivo* for anti-viral defense, or gene regulation and has become an important research tool for gene silencing.

Preliminary attempts to use RNAi in mammalian systems employed long dsRNAs as triggers, but led to the induction of a non-specific Type I interferon response rather than sequence-specific silencing. This interferon response resulted in widespread changes in protein expression, masking any sequence-specific effects and eventually leading to apoptosis. This suppression has been attributed to an antiviral response, which takes place through one of two pathways. In one pathway, long dsRNAs activate a protein kinase, PKR. Activated PKR, in turn phosphorylates and inactivates the translation initiation factor eIF2a, leading to repression of translation. In the other pathway, long dsRNAs activate RNase L, which leads to non specific RNA degradation.

Following uptake into the cell, the dsRNAs enter a cellular pathway known as the RNA interference (RNAi) pathway (figure 2.6). The dsRNAs are then subject to processing by Dicer, an RNase III polymerase that cleaves the dsRNAs resulting in the generation of small interfering RNAs (siRNAs), short RNA duplexes of 19-21 nucleotides with two nucleotide 3' overhangs. These siRNAs are then incorporated into endoribonuclease containing complexes known as RNA-induced silencing complexes (RISCs), unwinding in the process. Activated RISCs bind to complementary transcripts by base pairing interactions between the siRNA anti-sense strand and complementary mRNA. The bound mRNA is then cleaved and sequence specific degradation of mRNA results in gene silencing.

Whilst the introduction of long dsRNA into mammalian cells initiates a potent anti-viral response, this response can be bypassed by the introduction of siRNAs. These siRNas are then incorporated into the endoribonuclease containing complex (RISCs) as described above.

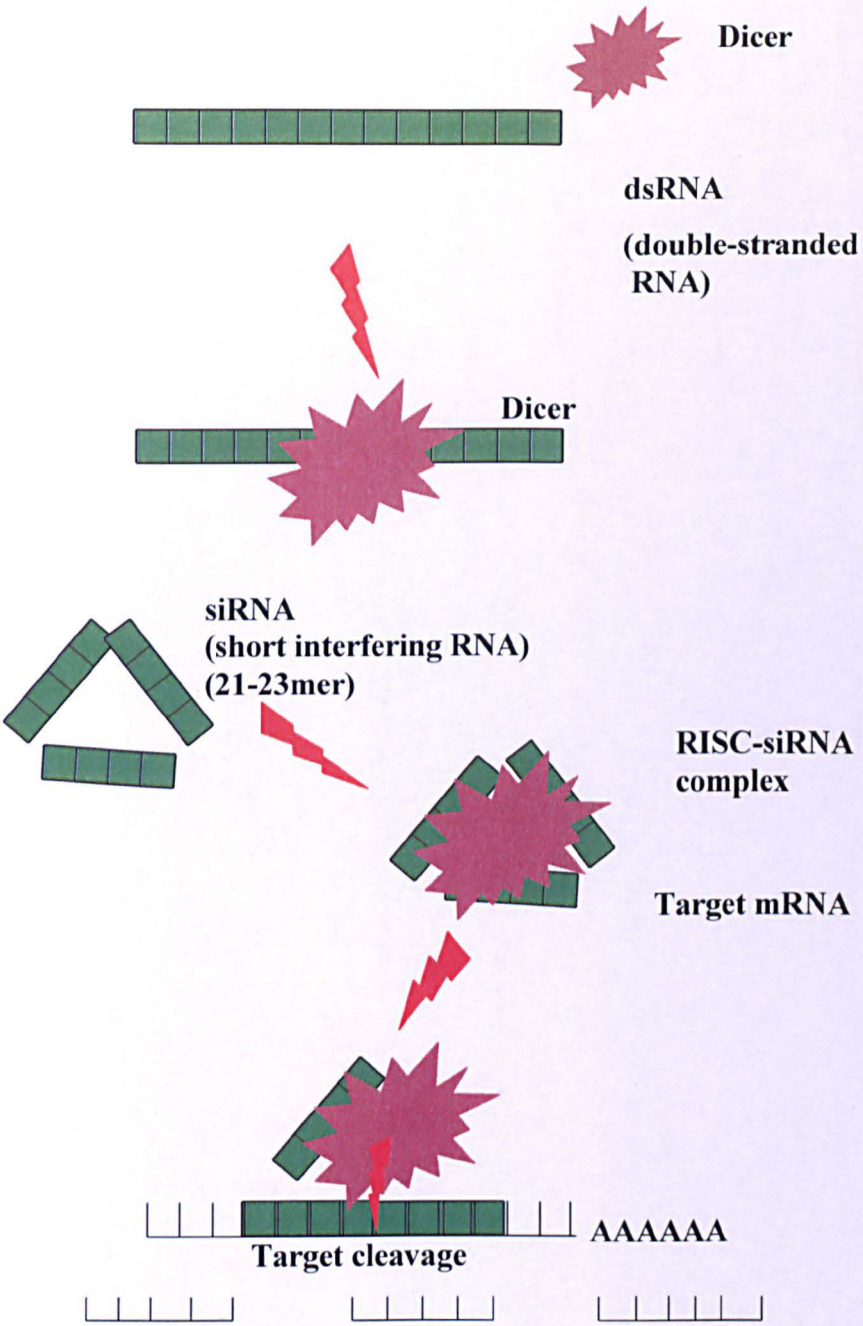

Figure 2.6 Simplified schematic diagram of the proposed RNA interference mechanism. dsRNA is introduced into a cell and becomes processed by the dicer enzyme to form siRNA, The siRNA forms a multicomponent nuclease complex, the RNA induced silencing complex (RISC). The target mRNA recognised by RISC is cleaved in the centre of the region complementary to the siRNA and degraded.

2.7.1 Transfection of HCD cells with Cx-43 siRNA

HCD cells were, seeded at a density of 1 x 10^5 on 6 well plates and allowed to adhere overnight. Cells were also seeded on to APES treated coverslips in 6 well plates at the same density.

The knockdown of Cx-43 was achieved by two different siRNA protocols.

1. Transfection of cells with a pool of four Cx-43 specific siRNA duplexes (Santa Cruz). Transfection of siRNAs (4μg) was conducted using lipofectamine (4μl) (Invitrogen) following manufacturers instructions. Briefly lipofectamine and siRNAs were diluted into optiMEM medium (invitrogen). Diluted lipofectamine lipids were mixed with diluted siRNAs and the mixture was incubated for 30 minutes at room temperature to allow for complex formation. Mixtures were further diluted in optiMEM and added to each well such that the final concentration of siRNA was 80nM. Cells were then incubated in this transfection mix for 14 hours overnight. This transfection mix was then replaced with the desired tissue culture media and cells harvested 24, 48, 72 and 96 hours after transfection. Negative controls included untransfected cells, lipid alone, 2 scrambled siRNAs, one of which was fluorescein conjugated (Santa Cruz).

2. The siLentGene U6 cassette RNA interference System (Promega). Specific Cx-43 and scrambled sequences were selected using the Promega design tool. U6 expression cassettes were constructed following the manufacturers instructions. Transfection of the U6 DNA expression cassettes were performed using silentGene transfection reagent (Promega) such that the final concentration of cassettes was 160ng/ml. In order to localise transfected cells, cells were co-transfected with RFP (0.5μg pDsRed2-C1). Cells were harvested and assayed 72 hours after transfection. Negative controls included untransfected cells, lipid alone, RFP alone and a scrambled siRNA. (These studies were performed by Dr Dianne Wheelans).

2.7.2 Transfection of HCD cells with TRPV4 siRNA

Cells were allowed to grow to 40% confluence in 6 well plates or APES treated coverslips. Lipofectamine and TRPV4 specific siRNA (invitrogen) were diluted into OptiMEM medium (Invitrogen). Diluted lipofectamine lipids were mixed with diluted siRNAs (8μg) and the mixture was incubated for 30 minutes at room temperature for complex formation. Mixtures were further diluted in OptiMEM and added to each well such that the final concentration of siRNAs was 80nM. Cells were then incubated in this transfection mix for 14 hours overnight. This transfection mix was then replaced with the desired tissue culture media and cells harvested 24, 48, 72 and 96 hours after transfection. Negative controls included untransfected cells, lipid alone, 2 scrambled siRNAs, one of which was fluorescein conjugated (Santa Cruz).

2.8 Microfluorimetry studies

2.8.1 Determination of intracellular calcium concentration $[Ca^{2+}]_i$

Changes in $[Ca^{2+}]_i$ were measured by single cell dual excitation microfluorimetry using the fluorescent dye Fura-2/AM (Grynkiewicz *et al.*, 1985). Fura-2/AM is a widely used uv-excitable fluorescent calcium indicator. Upon calcium binding, the fluorescent excitation maximum of the indicator undergoes a shift from 380 nm (Ca^{2+}-free) to 340 nm (Ca^{2+}-saturated), while the fluorescence emission maximum is relatively unchanged at ~510 nm. The indicator is typically excited at 340 nm and 380 nm respectively and the ratio of the fluorescent intensities corresponding to the two excitations gives a ratiometric indication of cytosolic $[Ca^{2+}]_i$. Measurement of calcium concentration using this ratiometric method avoids interference due to uneven dye distribution and photobleaching The biochemical mechanism underlying acetoxymethyl (AM) ester loading of Fura 2/AM into cells is that the AM ester form is membrane permeant and therefore able to enter cells. Hydrolysis by esterases within the cell releases the fluorescent probe which is not membrane permeant and ultimately the probe becomes trapped within the cell.

HCD cells were seeded and grown overnight on APES-coated coverslips at a density of $5x10^4$. Cells were loaded for 30 minutes at 37°C with 2.5μM of Fura-2/AM (Sigma, UK). Coverslips were washed and placed in a steel chamber, the volume of which was approximately 500μl. A single 22mm coverslip formed the base of the chamber, which was mounted into a heating platform on the stage of an Axiovert 200 Research Inverted microscope (figure 2.7).

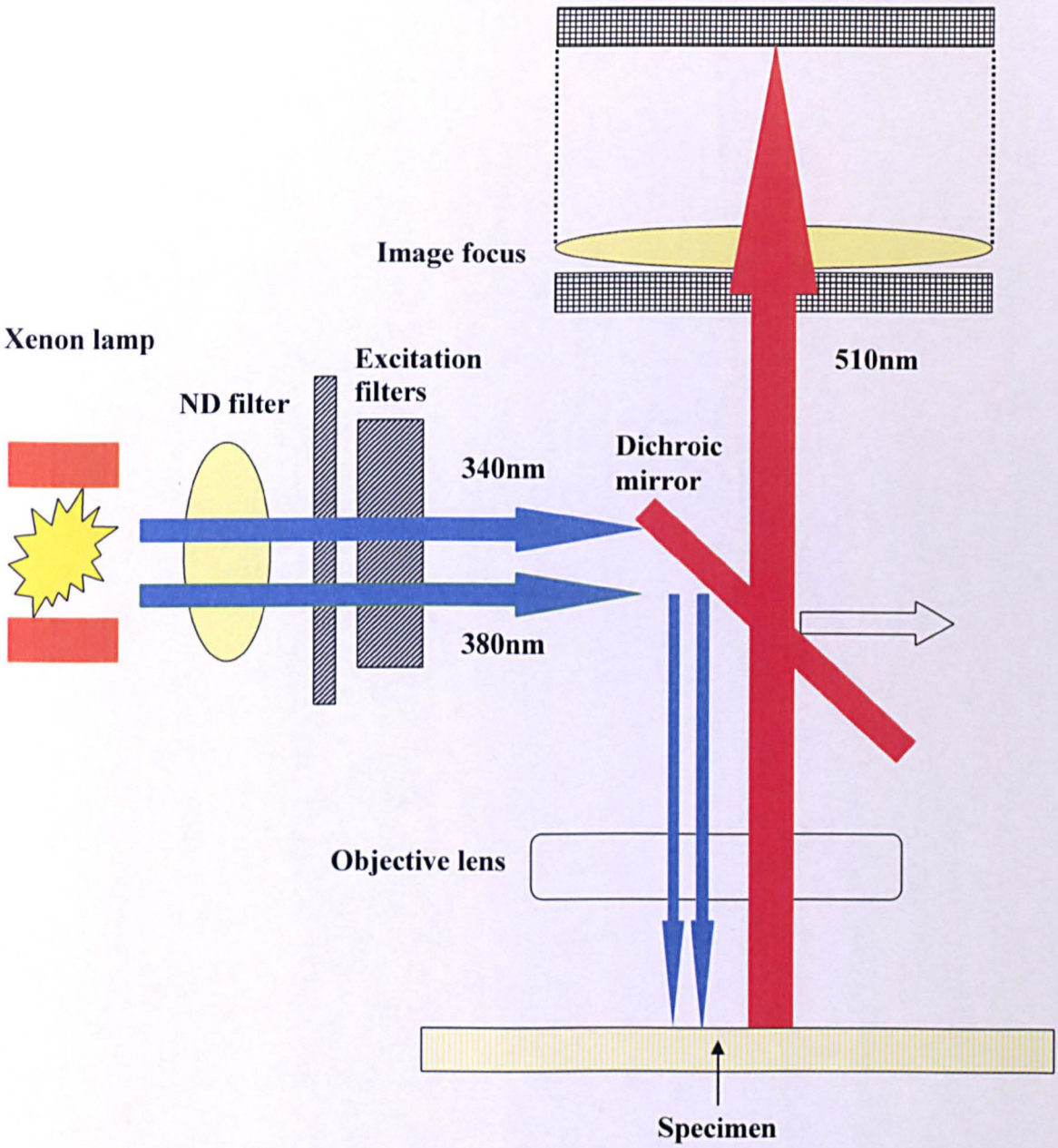

Figure 2.7 Hardware schematic for dual excitation single emission epi-fluorescent microscopy. Groups of cells loaded with a ratiometric dye (e.g. Fura-2/AM) are firmly attached to coverglass of limited thickness to allow the epi-fluorescent objectives to record changes in fluorescence intensity. The CCD amplifies the photon signal and allows on-line digitised recording of fluorescence changes.

Using a Metafluor imaging workbench (Universal Imaging) fluorescent images of the cells within a field of view were obtained and multiple regions of interest were monitored (figure 2.8)

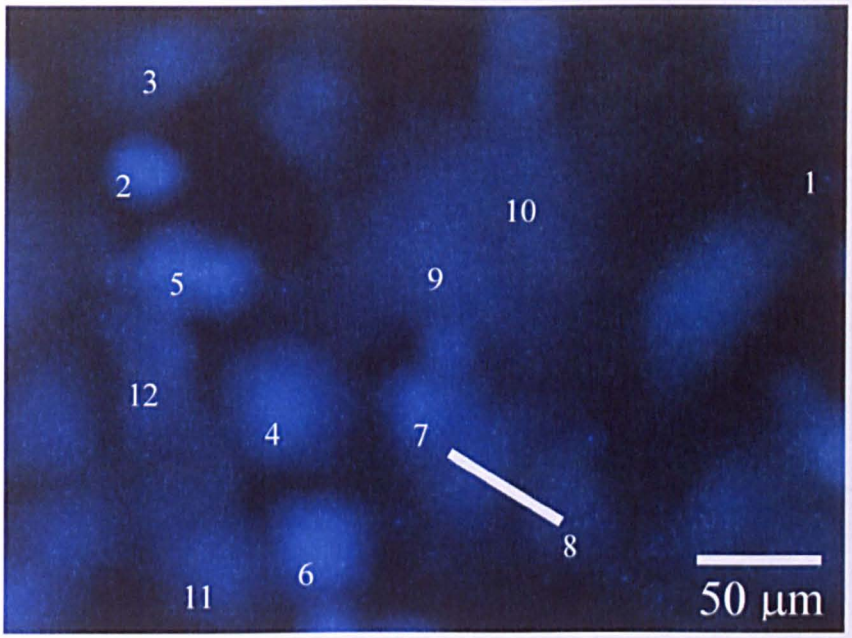

Figure 2.8 HCD cells loaded with Fura-2/AM. HCD cells were loaded with the Ca^{2+} fluorophore Fura-2/AM (2.5µM) for 30 minutes at 37°C. Cells were then placed into a chamber bathed in tissue culture media and placed on a UV microscope. Using metafluor imaging software multiple regions of interest were recorded within a single field of view, and subsequently numbered. This allows us to monitor elevations in $[Ca^{2+}]_i$ in adjacent cells.

Cells were illuminated alternatively at 340nm and 380nm. Emitted light was filtered using a 510nm long-pass barrier filter and detected using a Cool Snap HQ CCD charge coupled device (Roper Scientific). Changes in the emission intensity of Fura-2/AM expressed as a ratio of dual excitation were used as an indicator of changes in $[Ca^{2+}]_i$ using established procedures. Data was collected at 3 second intervals for multiple regions of interest in any one field of view. All records have been corrected for background fluorescence (determined from cell-free coverslip). All experiments were carried out at 37°C using unsupplemented DMEM/Hams F-12 as the standard extracellular medium.

2.8.2 Determination of intracellular sodium concentration $[Na^+]_i$

Changes in $[Na^+]_i$ were measured by single cell dual excitation microfluorimetry using the fluorescent dye SBF-1/AM . SBF-1/AM is a dual excitation single emission dye with spectral properties similar to Fura-2/AM. SBF-1/AM is comprised of benzofuranyl fluorophores linked to a crown ether chelator. The cavity size of this crown ether confers selectivity for Na^+ and when a Na^+ ion binds to SBF-1/AM the indicators fluorescence quantum yield increases causing a significant change in the ratio of fluorescent intensities excited at 340/380 nm (bound/unbound modes of the dye). Poor efficiency of dye uptake necessitates the use of a dispersal agent. Pluronic F-127 is a non ionic surfactant polyol that has been found to facilitate the solubilisation of water insoluble dyes and other materials in physiological media. As figure 2.9 clearly shows, the efficiency of SBF-1/AM dye uptake into HCD cells appeared to be far greater when the dye was loaded in conjunction with pluronic F-127 as compared to loading of the dye alone.

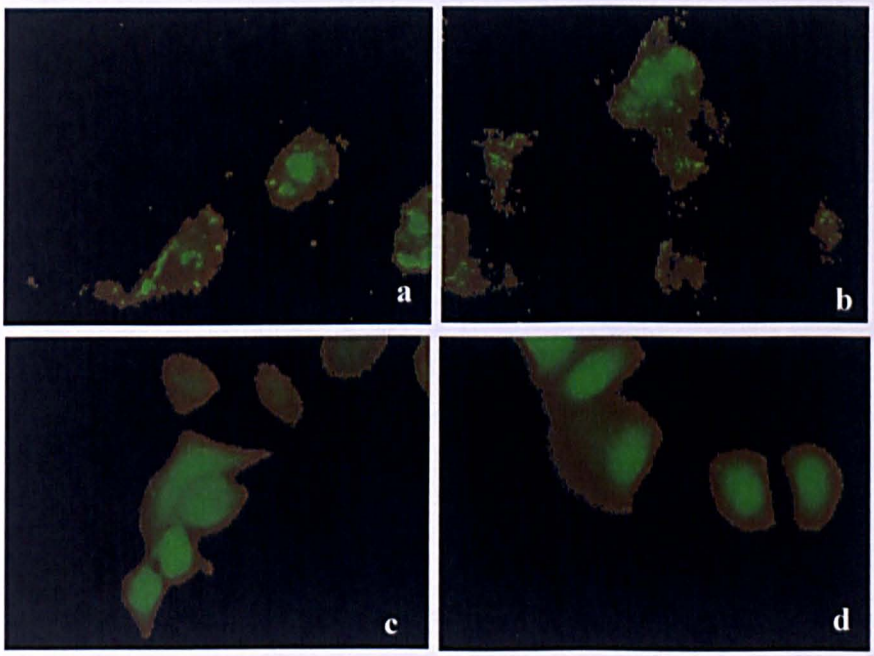

Figure 2.9 HCD cells loaded with the Na^+ fluorophore SBF-1/AM in the absence and presence of pluronic F-127. Initial studies confirmed that when incubated with SBF-1 alone, an insufficient loading efficiency of the dye was achieved (panels a and b) However, when loaded with the detergent pluronic acid, the level of fluorescence obtained when cells were illuminated was found to be far greater (panels c and d).

HCD cells seeded and grown overnight on APES-coated coverslips were loaded with 20 µl SBF/Pluronic acid (20% v/v). Cells were incubated for 90 minutes in a humidified atmosphere (5% CO_2) at 37°C. As previously stated HCDs are a polarized, epithelial cell model, which compensate Na^+ influx via apical epithelial sodium channels with Na^+ efflux at the basolateral pole via a Na^+/K^+ ATPase. Therefore in order to resolve small changes in cytosolic Na^+ concentration it was necessary to inhibit extrusion mechanisms in both control and experimental conditions. Cells were incubated with the Na^+/K^+ ATPase pump inhibitor ouabain for the last 30 minutes of the incubation period. Inhibition of this Na^+ pump and any increased sodium channel activity in the apical membrane will be reflected via increased fluorescence levels indicative of increased $[Na^+]$ as ions accumulate within the cell (figure 2.10).

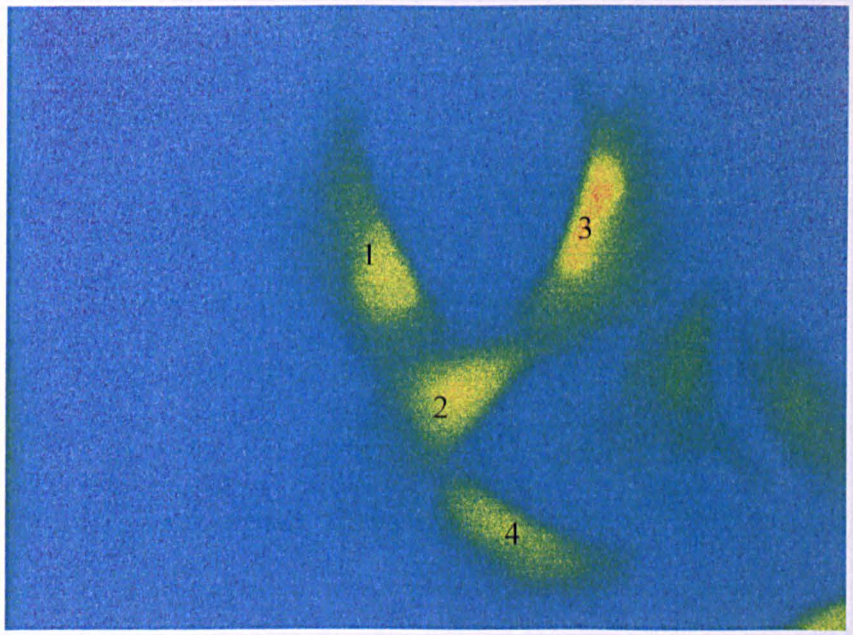

Figure 2.10 HCD cells loaded with the Na^+ fluorophore SBF-1. HCD cells were loaded with SBF-1 (5µM)/pluronic acid for 1 1/2 hours. Cells were then placed into a chamber bathed in tissue culture media and placed on a UV microscope. Using metafluor imaging software multiple regions of interest were recorded within a single field of view, and subsequently numbered. This allows us to monitor elevations in $[Na^+]_i$ in adjacent cells.

Changes in the emission intensity of SBF-1/AM expressed as a ratio of dual excitation (see section 2.7.1) were used as an indicator of changes in $[Na^+]_i$ using established procedures (Ref). Data was collected at 3 second intervals for multiple

regions of interest in any one field of view. All records have been corrected for background fluorescence (determined from cell-free coverslip). All experiments were carried out at 37°C using unsupplemented DMEM/Hams F-12 as the standard extracellular medium.

2.8.3 Mechanical stimulation experiments

Cells were allowed to adhere on APES treated coverslips overnight. Prior to stimulation cells were loaded with Fura-2/AM (section 2.7.1). Coverslips were the washed and placed in a steel chamber (constructed in house, Kings College London) and mounted into a heating platform on the stage of an Axiovert 200 Research Inverted microscope. Individual cells within a cluster (6-12 cells/cluster) were stimulated via touch using a femtotip electrode delivery system (Eppendorf, Hamburg, Germany). A microelectrode was connected to the micromanipulator using an electrode holder and the x40 objective was used to position the over the cell to be stimulated. Following stimulation $[Ca^{2+}]_i$ was measured. Maintained Fura-2 fluorescence, confirmed cytosolic loading and therefore membrane integrity.

2.8.4 Lucifer yellow studies

Lucifer yellow is a membrane impermeant fluorescent tracer with a low molecular weight of 457.3, making it a powerful tool to evaluate the strength of cell-to-cell communication via gap junctions. An individual cell within a cell cluster was microinjected with lucifer yellow dilithium salt (dissolved in 150mM LiCl/10mM Hepes (pH 7.2). Cells were injected using femtotips (internal diameter 0.5±0.2μm) and the Injectman/Femtojet 5247 delivery system. The fluorescent tracer was allowed to fill the injected cell and to propagate into the neighbouring cells by diffusion. The duration for injections was set at 3sec at an injection pressure of 2 PSI and a compensation pressure of 0.7 PSI. Dye transfer was recorded over a subsequent 10minute period using Metamorph acquisition software and a Cool Snap HQ CCD camera. After dye transfer the electrode was removed and dye coupling evaluated by counting the number of fluorescent cells. An absence of dye leakage into the surrounding media confirmed that membrane integrity had remained intact.

2.9 Data Analysis

Autoradiographs were quantified by densitometry (TotalLab 2003). Statistical analysis of data was performed using one-way ANOVA test with a Tukey's Multiple Comparison post-test. Data are expressed as arithmetic mean ± SEM and *n* denotes the number of experiments. Significance was taken as * $P<0.05$, ** $P<0.01$, *** $P<0.001$.

Chapter 3

Characterisation of the HCD cell line

3.1 Introduction

Diabetes induced increases in SGK1-mediated activation of Na^+ reabsorption via ENaC may, in part, be contributory to the development of secondary hypertension observed in NIDDM. Understanding how SGK1 is regulated and in turn, how SGK1 regulates ENaC mediated Na^+ reabsorption may help identify novel therapeutic targets in the future treatment of secondary hypertension. Understanding the homeostatic mechanisms involved in regulating renal Na^+ retrieval necessitates the use of readily accessible and physiologically appropriate model systems. One way to ensure a continuous source of material would be to immortalise renal cells of a defined origin and use these for experimentation. This would enable generation of a homogeous population; thus negating the problem of variation within culture.

The human collecting duct (HCD) cell line (Ronco *et al.*, 1995) was originally established in 1995 from a kidney that had been removed for a localized adenoma. Cells from the non tumorous part of the kidney were removed and digested with collagenase prior to culture in a defined medium at 37°C. Cells were then transfected with a recombinant plasmid harbouring a complete SV40 genome and cultured over a 4-5 week period checking for expression of SV40 antigens at each stage. The transformed cell population was then regularly cultured at 37°C in defined media plus 2% FCS. Confirmation of tubular origin was supported by immunological studies in which principal cells of the collecting duct were identified following incubation with the principal cell specific antibody mAb 272. Whilst previous reports have suggested this cell line to represent a suitable culture system in which to study the cell biology of water reabsorption (Ronco *et al.*, 1995), little is known about the expression of those key signalling elements involved in Na^+ reabsorption, including their modes of regulation.

In this chapter, I have confirmed both expression and cellular localisation of those key signalling elements involved in the regulation and maintenance of blood volume homeostasis and have demonstrated that this novel human cortical collecting duct

(HCD) cell line is a suitable model for the study of Na^+ reabsorption in the principal cells of the human collecting duct. Furthermore we have performed a number of studies correlating expression to function. Characterisation of the Na^+ resorptive capacity of this novel human cortical collecting duct cell line has identified HCD cells as a suitable model for future studies which may enable us to gain a greater understanding of the transition from physiological to pathophysiological and may aid our knowledge and discovery of future therapeutic targets.

3.2 Results

3.2.1 Expression of SGK1 in HCD cells

RT-PCR analysis was performed on three different RNA preparations from HCD cells producing PCR products representative of SGK1 mRNA at 699bp (figure 3.1A). Expression was standardized against the housekeeping gene 18SrRNA. To confirm that all three sets of mRNA were appropriately translated, protein expression was determined by western blotting using a specific, polyclonal SGK antibody. Western blot analyses (figure 3.1B) revealed a strong band at ~50 kDa in three different HCD protein preparations.

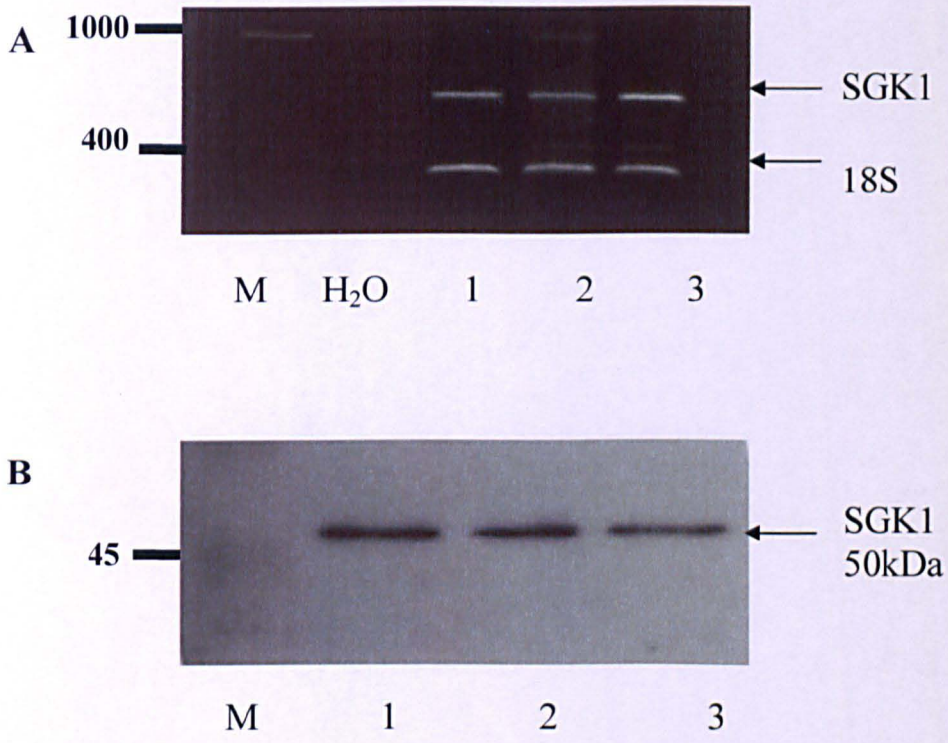

Figure 3.1: Expression of SGK1 mRNA and protein in HCD-cells.
Panel A represents RT-PCR analyses using primers specific for human SGK1. PCR products of 699bp were observed in three different RNA preparations (1, 2 and 3) corresponding to mRNA expression for SGK1. Western blot analyses (panel B) of HCD cell lysates (5µg protein/lane) using an antibody against human SGK confirmed the presence of the SGK1 protein in three different protein preparations (1, 2 and 3). A protein band of approximately 50kDa was detected.

As a control for specificity, SGK1 antibody was pre-incubated at room temperature for 8 hours and then overnight at 4^0C with a 100 fold excess of immunising SGK1 peptide prior to addition of the antibody to the membrane, all other steps in the procedure were identical. Preabsorption of the primary antibody completely abolished the signal upon ECL detection (figure 3.2)

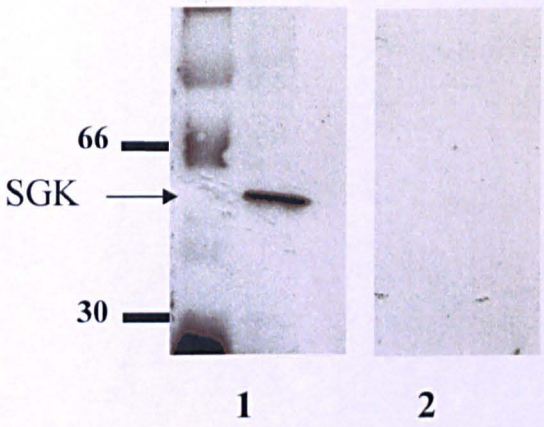

Figure 3.2 Peptide adsorbed antibody abolished SGK1 protein detection by western blotting. A protein band of approximately 50kDa (SGK) was detected in an HCD protein preparation (panel 1), whilst pre-incubation with the peptides abolished any signal upon ECL detection (panel 2).

3.2.2 The localization of SGK1 in HCD cells

The distribution of SGK1 in HCD cells under standard tissue culture conditions was examined by fluorescence immunocytochemistry using the nuclear stain DAPI (blue), the cytokeletal stain phalloidin (red) and an anti-SGK1 antibody (green). The results can be seen in figure 3.3.

In figure 3.3/panel c, SGK1 appears to be localized predominantly to the nucleus with diffuse staining throughout the cytoplasm. The overlay image in panel d illustrates a high degree of co-localization between the nucleus and SGK1.

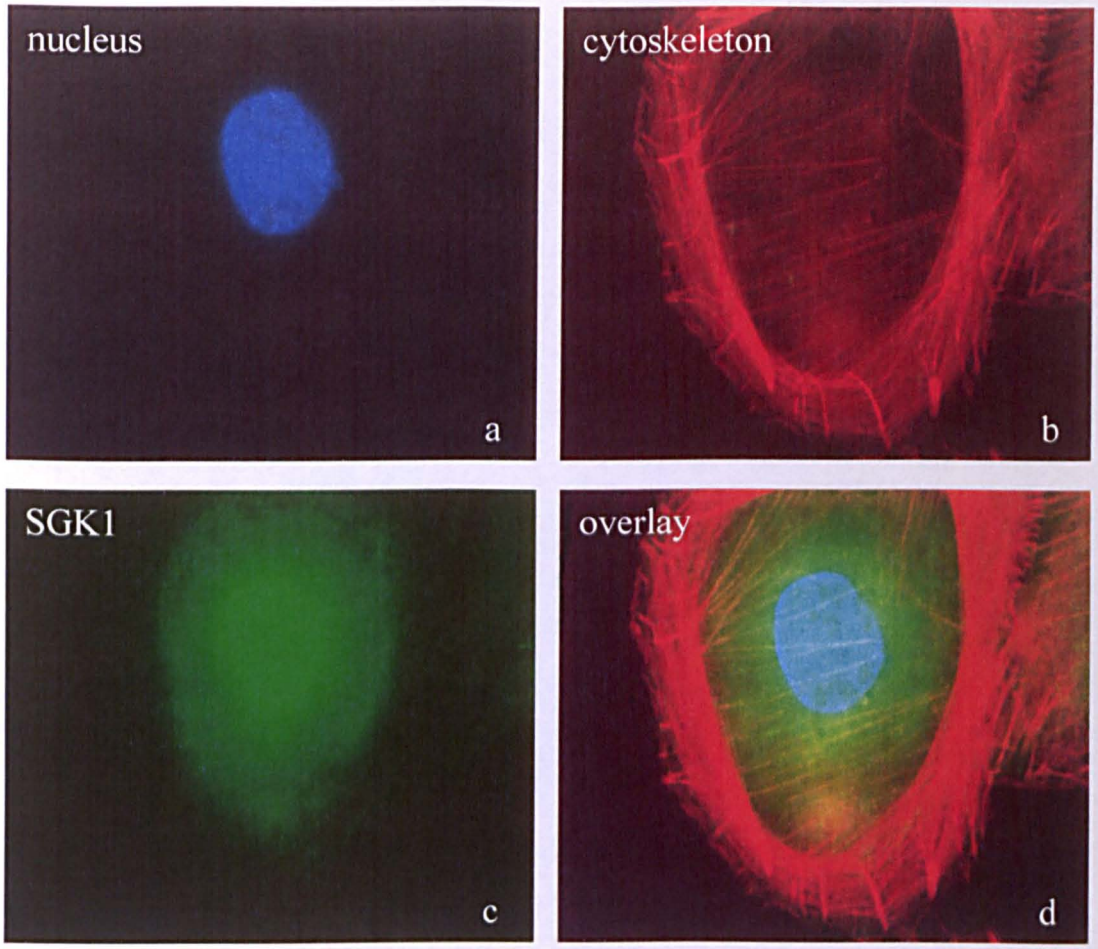

Figure 3.3: Immunocytochemical staining of SGK1 in HCD-cells. Panels a, and b and c show nuclear (DAPI, blue) cytoskeletal (TRITC phaloidin, red) and SGK1 (Alexa-488 green) staining respectively. Panel d depicts an overlay of SGK1 immunolocalization (Alexa-488 green), cytoskeletal staining (TRITC-conjugated phalloidin; red) and nuclear staining (DAPI; blue). SGK1 appears to be predominantly localized to the nucleus with diffuse staining throughout the cytoplasm. An overlay image in panel d shows co-localization of the nuclear stain DAPI and SGK1 in the cell nucleus.

3.2.3 SGK localization is regulated in a stimulus dependent

Recent evidence suggests that the subcellular localization of SGK1 is crucial in SGK1 mediated regulation of cell function (Firestone *et al.*, 2003). Changes in the localization pattern are dependent on both the activating stimulus and tissue specific function of SGK1. (Firestone *et al.*, 2003). Immunocytochemical staining performed

on cells treated with dexamethasone and/or FCS (section 3.4-3.6) confirmed subcellular localization of SGK1 in HCD cells to be dependent upon the stimuli present. Under standard culture conditions, SGK1 appears to be localized to both the nucleus and cytoplasm (figure 3.4). Removal of dexamethasone (5 x 10^{-8}M) from the growth media and addition of 10% FCS restricted SGK1 to the nucleus (figure 3.6). Conversely removal of FCS (2%) from the media induced cytosolic localization of SGK1 (figure 3.5) with no nuclear localization.

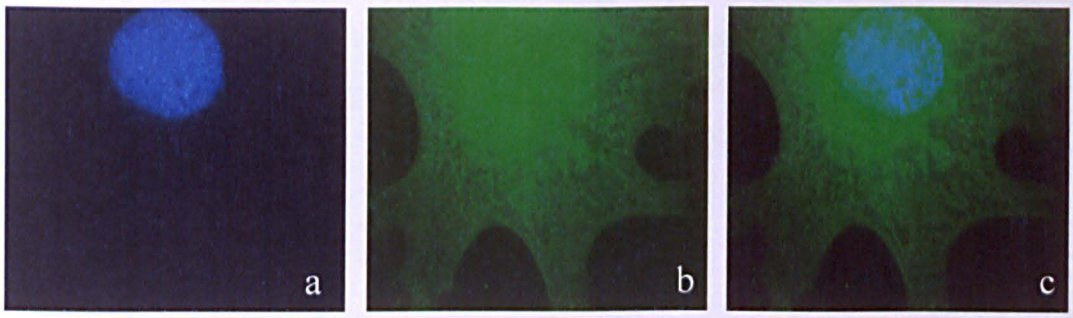

Figure 3.4: Immunocytochemical staining of SGK in HCD-cells following treatment with FCS (2%) and dexamethasone (5 x 10^{-8}M) for 24hrs. Panels a, and b show nuclear (DAPI, blue) and SGK (Alexa-488 green) staining respectively. Figure c depicts an overlay and shows a high degree of co-localization between SGK and the nucleus. SGK protein was detected with a polyclonal antibody and staining was visualised using an Alexa 488 conjugated secondary. SGK (b) appears to be predominantly localized to the nucleus with diffuse staining throughout the cytoplasm.

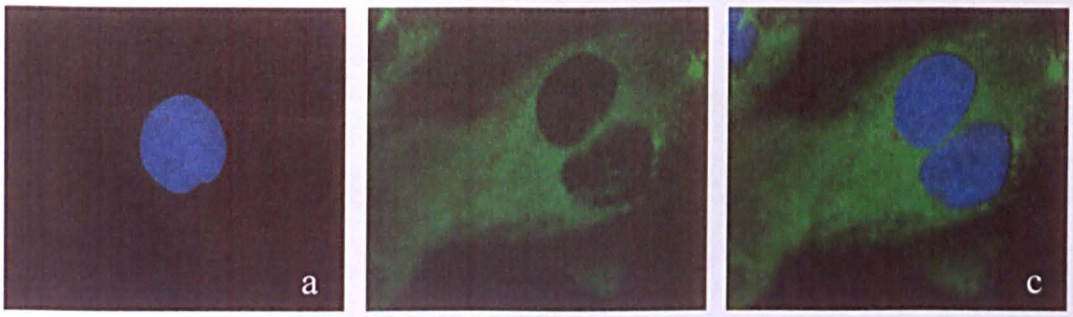

Figure 3.5: Immunocytochemical staining of SGK in HCD-cells following a 24 hr incubation in serum free media, supplemented with Dexamethasone 5 x 10^{-8}M. HCD cells were incubated with DMEM/HAMS F-12 (serum free) supplemented with dexamethasone 5x 10^{-8} M for 24hrs. Panels a and b show nuclear (DAPI, blue) and SGK (Alexa-488 green) staining respectively. Panel c depicts an overlay of SGK immunolocalization (green), and nuclear staining (DAPI; blue). SGK protein was detected with a polyclonal antibody and staining was visualised using an Alexa 488 conjugated secondary. Removal of FCS restricted SGK localisation to the cytosol and minimised nuclear co-localisation (panel c)

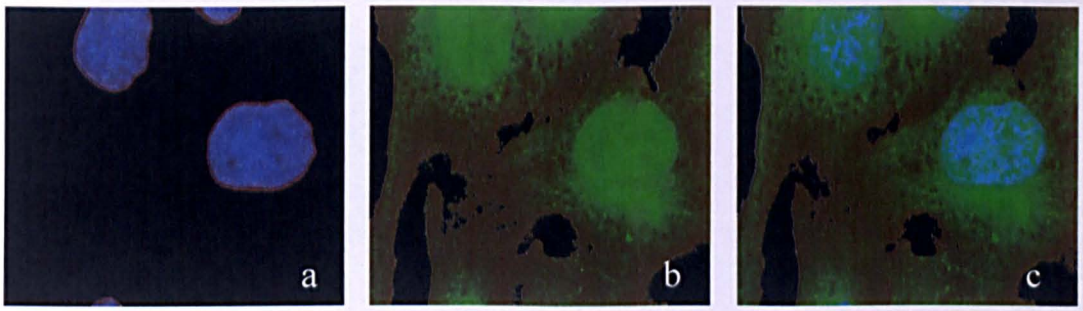

Figure 3.6: Immunocytochemical staining of SGK in HCD-cells following a, 24 hr incubation with 10% FCS. HCD cells were treated DMEM/HAMS F-12 supplemented with 10% FCS for a period of 24hrs. Panels a and b show nuclear (DAPI, blue) and SGK (Alexa-488 green) staining respectively. Panel c depicts an overlay of SGK localization (green), and nuclear staining (DAPI; blue). SGK protein was detected with a polyclonal antibody and staining was visualised using an Alexa 488 conjugated secondary. Addition of FCS and removal of dexamethasone (5 x 10^{-8}M) localized SGK to the nucleus with minimal cytoplasmic staining (panel c).

3.2.4. α-ENaC expression in HCD cells

RT-PCR and western blotting were used to confirm that α-ENaC subunit was expressed at both the mRNA and protein level.

RT-PCR analysis was performed on three different RNA preparations from HCD cells producing PCR products at 601bp (figure 3.7 A). Western blotting was used to confirm that mRNA were appropriately translated. Membranes were probed with an anti- α-ENaC polyclonal antibody and ECL detection revealed a strong band at approximately 97kDa in three different HCD protein preparations (figure 3.7 B)

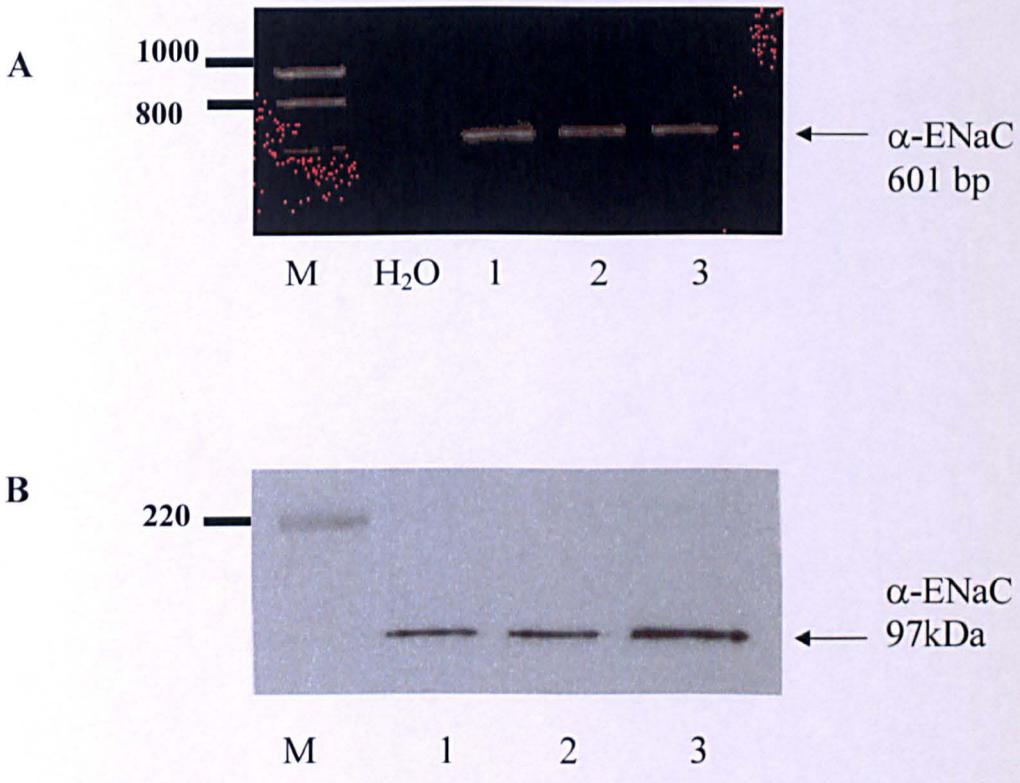

Figure 3.7: Expression of α-ENaC mRNA and protein in HCD-cells.
Panel A represents RT-PCR analyses using primers specific for human α-ENaC. PCR products of 601bp were observed in three RNA preparations (1, 2 and 3) corresponding to mRNA expression for α-ENaC. Western blot analyses of cell HCD cell lysates (panel B, 5μg protein/lane) using an antibody against α-ENaC confirmed the presence of the protein in three protein preparations (1, 2 and 3). A protein band of approximately 97 kDa was detected.

Specificity of the primary antibody was confirmed by blocking α-ENaC antibody with an excess of immunising peptide (100 fold excess) at room temperature for 8 hours and then overnight at 4^0C prior to staining the cells for immunocytochemistry (figure 3.8). Pre-incubation of the primary α-ENaC antibody with the α-ENaC peptide abolished any staining

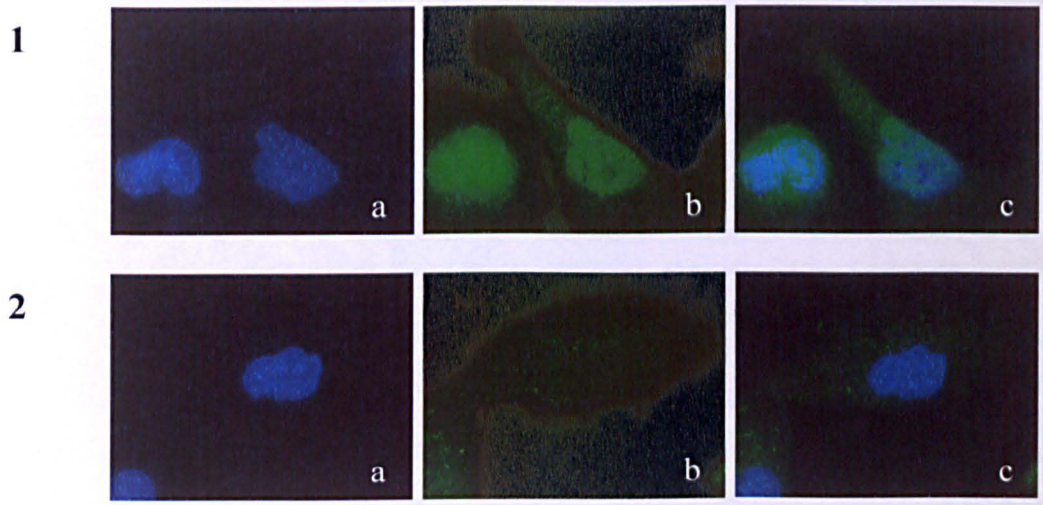

Figure 3.8: Peptide adsorbed antibody abolished the detection of α-ENaC staining by immunocytochemistry. Double staining of HCD cells with an anti- α - ENaC antibody (panel 1.b) and the nuclear stain DAPI (panel 1.a) gave rise an overlay image (panel 1.c) in which co-localization between DAPI and α ENaC was observed in the cell nucleus. Pre-incubation of the α-ENaC antibody and peptide was found to abolish any visible staining when visualized by fluorescence microscopy (panel 2.b) giving rise to an overlay image (panel 2.c) in which only staining of the nucleus was apparent. The faint degree of staining observed in panel b is indicative of background non specific autofluorescence.

3.2.5 Localization of the α-ENaC subunit in HCD cells

The distribution of the α-ENaC subunit in HCD cells under standard culture conditions was examined by fluorescence immunocytochemistry. Cells were stained with an anti-α ENaC polyclonal antibody (figure 3.9 panel c). Panels a, and b show nuclear and cytoskeletal staining respectively whilst panel c, confirms the α-subunit

to be predominantly localized to the cytoplasm. Panel d represents an overlay and shows that there is no co-localization between α-ENaC and the nuclear stain DAPI. The noticable difference in localization of α-ENaC in figure 3.9c as compared to that observed in figure 3.8b is a consequence of a change in culture conditions. Under standard culture conditions α-ENaC appears predominantly cytoplasmic however an overnight period of FCS deprivation prior to treatment results in an, α-ENaC which is retained in the nucleus.

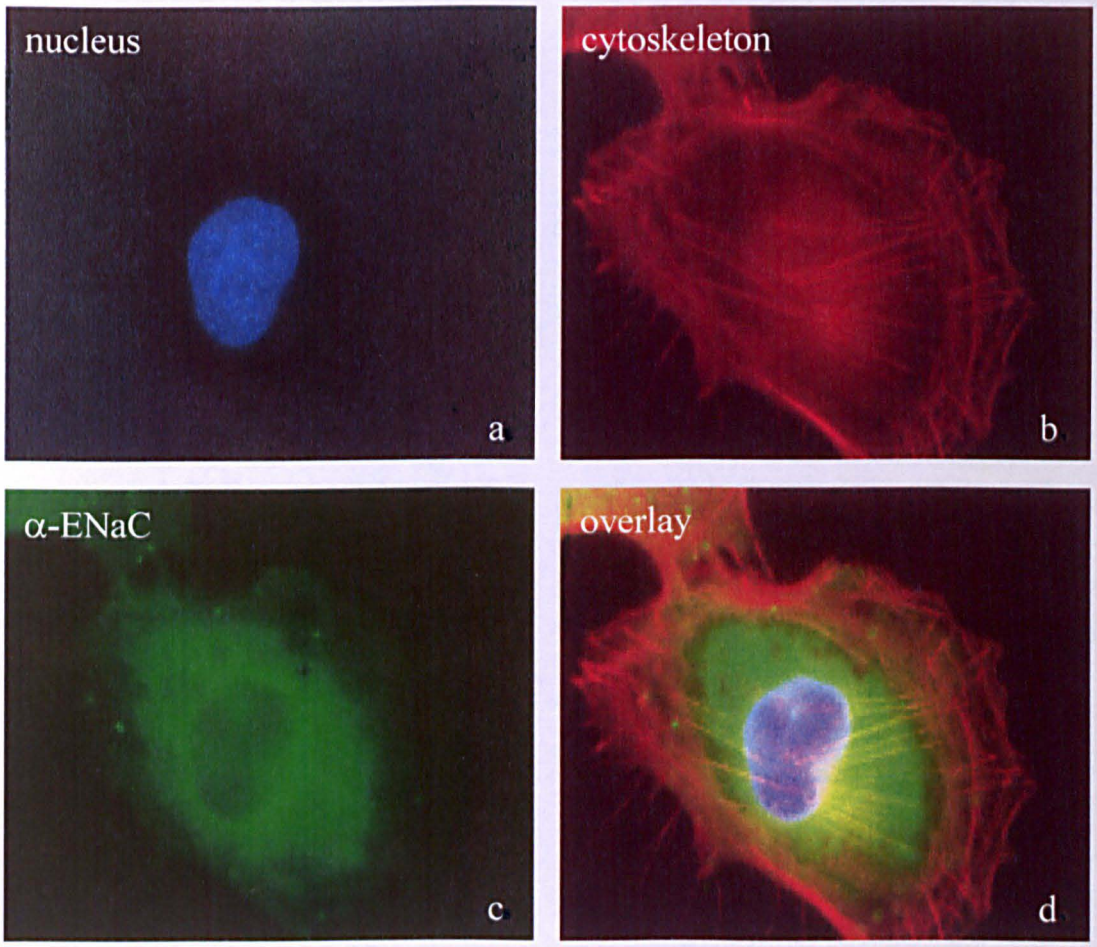

Figure 3.9: Immunocytochemical staining of α-ENaC in HCD cells.
Panels a, and b and c show nuclear (DAPI, blue) cytoskeletal (TRITC phalloidin, red) and α-ENaC (Alexa-488 green) staining respectively. α-ENaC (c) appears to be predominantly localized to the cytoplasm. An overlay image in panel d shows that there is no co-localisation between α-ENaC and the nucleus .

3.2.6 β-ENaC expression in HCD cells

Having confirmed expression of the α subunit, the next stage was to repeat these studies for both the β and γ subunits. To confirm expression of the β-ENaC subunit at the mRNA level; RT-PCR analysis was performed on three different RNA preparations from HCD cells and gave rise to PCR products at 1000bp (figure 3.10). To date, there is no commercially available antibody against β-ENaC that works well in western blotting.

Figure 3.10: Expression of β-ENaC mRNA in HCD-cells.
RT-PCR analyses using primers specific for human β-ENaC detected PCR products of 1000 bp in three RNA preparations (1, 2 and 3) corresponding to mRNA expression for β-ENaC.

3.2.7 Localization of the β-ENaC subunit in HCD cells

Immunocytochemistry assessed the distribution of β-ENaC in HCD cells. Data suggest the localization of the β-ENaC subunit different to that previously observed for the α-ENaC subunit (section 3.2.5). Immunocytochemistry confirmed the β subunit to be predominantly localized to the nucleus with marginal staining in the cytoplasm (figure 3.11c). The slight degree of co-localization observed in panel d reflects an overlap in wavelength emission intensities between the β-ENaC antibody

and the TRITC-conjugated phalloidin, confirmed in previous studies in which phalloidin was omitted from the staining procedure (data not shown).

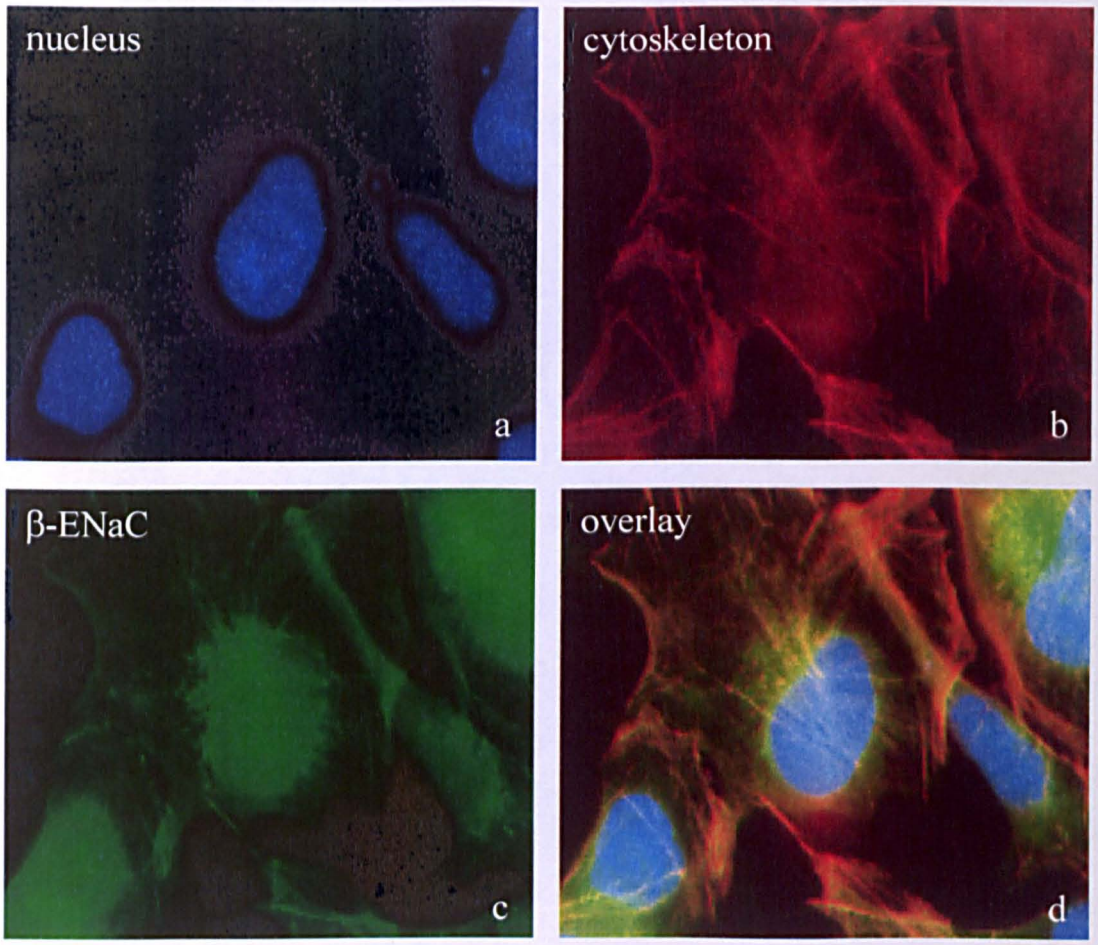

Figure 3.11: Immunocytochemical staining of β-ENaC in HCD cells. Panels a, and b and c show nuclear (DAPI, blue) cytoskeletal (TRITC phalloidin, red) and β-ENaC (Alexa-488 green) staining respectively. β-ENaC (panel C) appears to be predominantly localized to the nucleus. Panel d depicts an overlay and shows co-localization between the nucleus and β-ENaC subunit.

3.2.8 γ-ENaC expression in HCD cells

Expression of the γ subunit at both the mRNA and protein level, were confirmed by RT-PCR and western blotting respectively. Panel A of figure 3.12 illustrates γ-ENaC mRNA expression in 3 different RNA preparations, with PCR products of 696 bp obtained in each preparation. Panel B confirms translation of mRNA into protein giving rise to a doublet at approximately 75kDa representative of γ-ENaC. The nature of the double band is discussed later in section 3.3

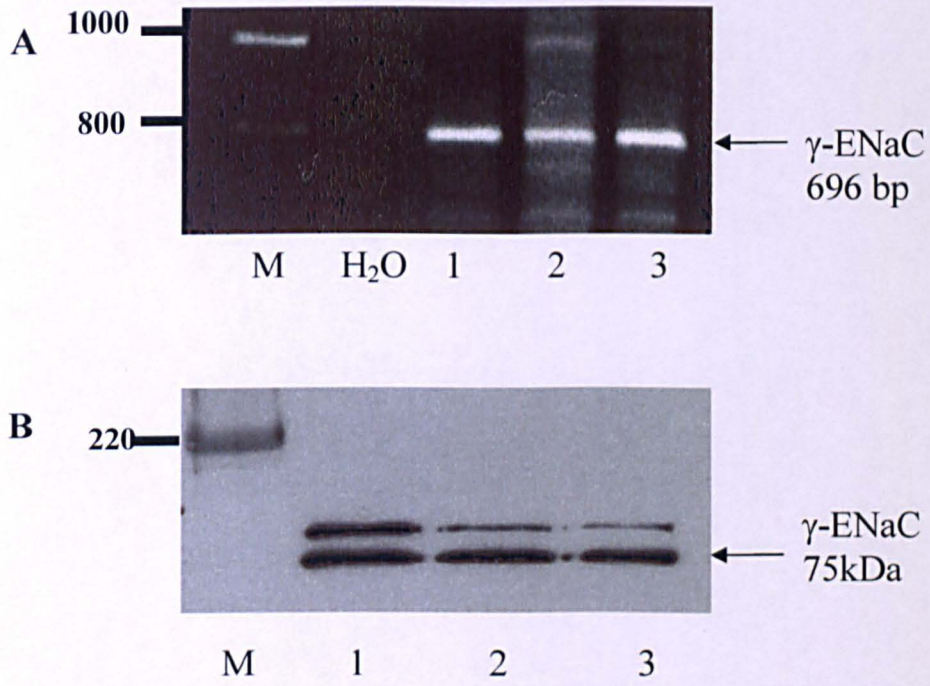

Figure 3.12 Expression of γ- ENaC mRNA and protein in HCD-cells.
Panel A represents RT-PCR analyses using primers specific for human γ-ENaC. PCR products of 696bp were observed in three RNA preparations (1, 2 and 3) corresponding to mRNA expression for the γ-ENaC subunit. Western blot analyses of HCD cell lysates (panel B, 5μg protein/lane) using an antibody against human γ–ENaC confirmed the presence of the protein in three protein preparations (1, 2 and 3). A doublet of approximately 75 kDa was detected.

As a control for specificity, anti-γ-ENaC antibody was pre-incubated at room temperature for 8 hours and then, overnight at 4^0C with a 100 fold excess of immunising γ-ENaC peptide prior to addition of the antibody to the membrane, all other steps in the procedure were identical. Preabsorption of the primary antibody completely abolished the signal upon ECL detection (figure 3.13, panel 2)

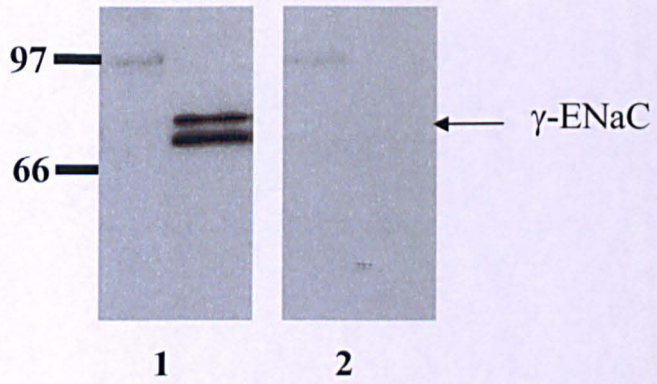

Figure 3.13 Peptide adsorbed antibody abolished γ-ENaC protein expression detection by western blotting. A doublet of approximately 75kDa (γ-ENaC) was detected in two different HCD protein preparations (panel 1), whilst pre-incubation with the peptide abolished any signal upon ECL detection (Panel 2).

3.2.9 The localization of γ-ENaC subunit in HCD cells

Localization of γ-ENaC subunit in HCD cells was assessed by immunocytochemistry and is similar to that observed for the β-ENaC subunit (section 3.2.7). Figure 3.14/panel c clearly shows the γ subunit appears to be predominantly localized to the cell nucleus with diffuse staining throughout the cytoplasm.

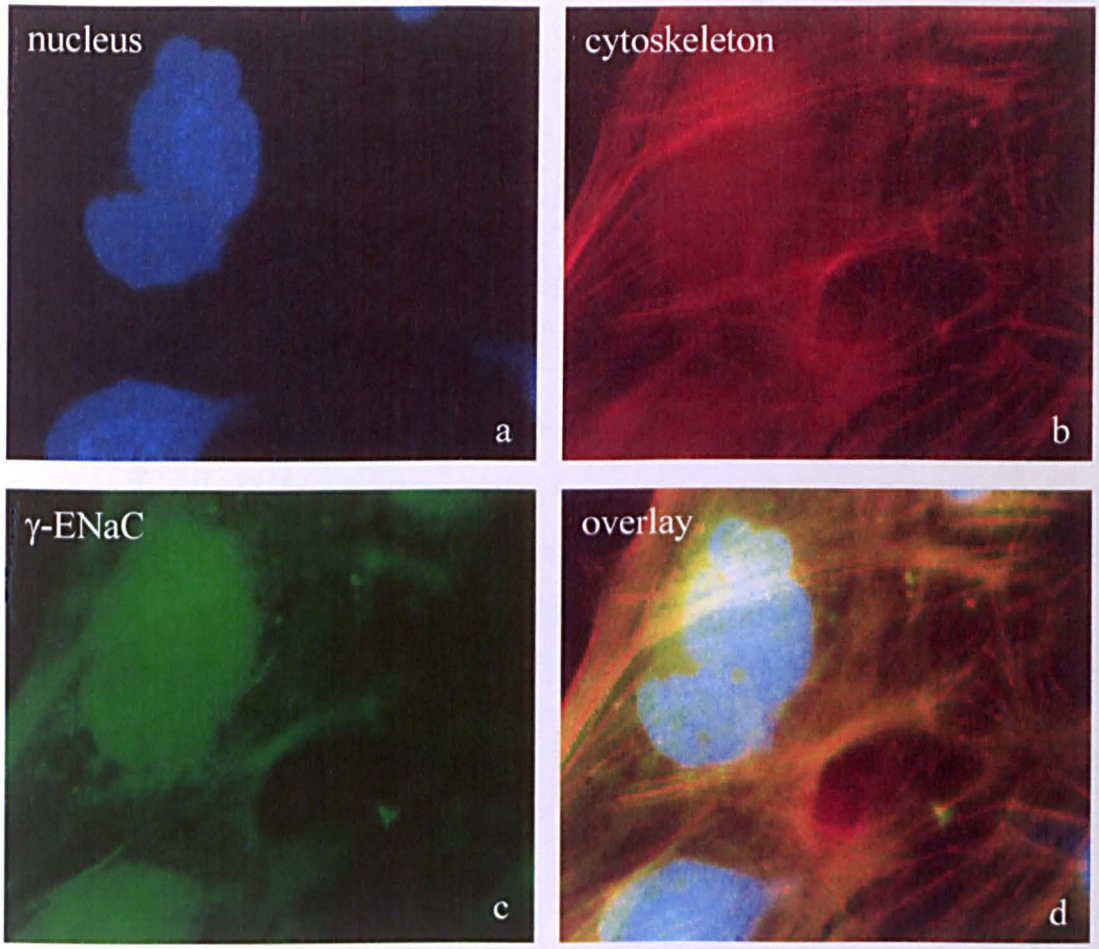

Figure 3.14: Immunocytcochemical staining of γ-ENaC in HCD cells. Panels a, and b and c show nuclear (DAPI, blue) cytoskeletal (TRITC phalloidin, red) and γ-ENaC (Alexa-488 green) staining respectively. γ-ENaC (panel c) appears to be predominantly nuclear. Panel d shows co-localization between the nucleus and γENaC.

3.2.10 Functional expression of ENaC in HCD cells

Transcellular transport of Na^+ mediated by the ENaC is a 2-step transport process, of which ENaC represents the rate-limiting step (Eaton *et al.,* 1995). Those cells expressing the ENaC allow entry of Na^+ into the cell, whilst a Na^+/K^+ ATPase expressed in the basolateral membrane allows for electrogenic extrusion of Na^+ in exchange for K^+. Ouabain and amiloride, antagonists of the Na^+/K^+ ATPase pump and ENaC respectively, will bind to, inhibit and thus prevent influx/efflux of Na^+

into the cell ultimately raising/lowering $[Na^+]_i$ levels respectively. Furthermore, dexamethasone, a synthetic glucocorticoid, has been previously reported to exert stimulatory effects over the ENaC thus raising Na^+ as a consequence of increased entry across the apical membrane.

In order to assess changes in Na^+ transport in HCD cells, single cell microfluorimetry was used to measure changes in cytosolic sodium in response to mediators of ENaC function. Cells were loaded with the sodium fluorophore SBF-1 and the detergent pluronic acid for a period of 90 minutes. Basal readings for $[Na^+]_i$ were taken, prior to and following modulation of the activity of these sodium transporters via commercially available agonists and/or antagonists Cells were pre-incubated for 90 minutes with either one of the following three drugs or a combination of each; ouabain (100μM), dexamethasone ($5x10^{-8}$M) and amiloride (1μM). Incubation with one or more of these compounds gave rise to variable $[Na^+]_i$ levels in HCD cells, the results of which are clearly shown in figure 3.15.

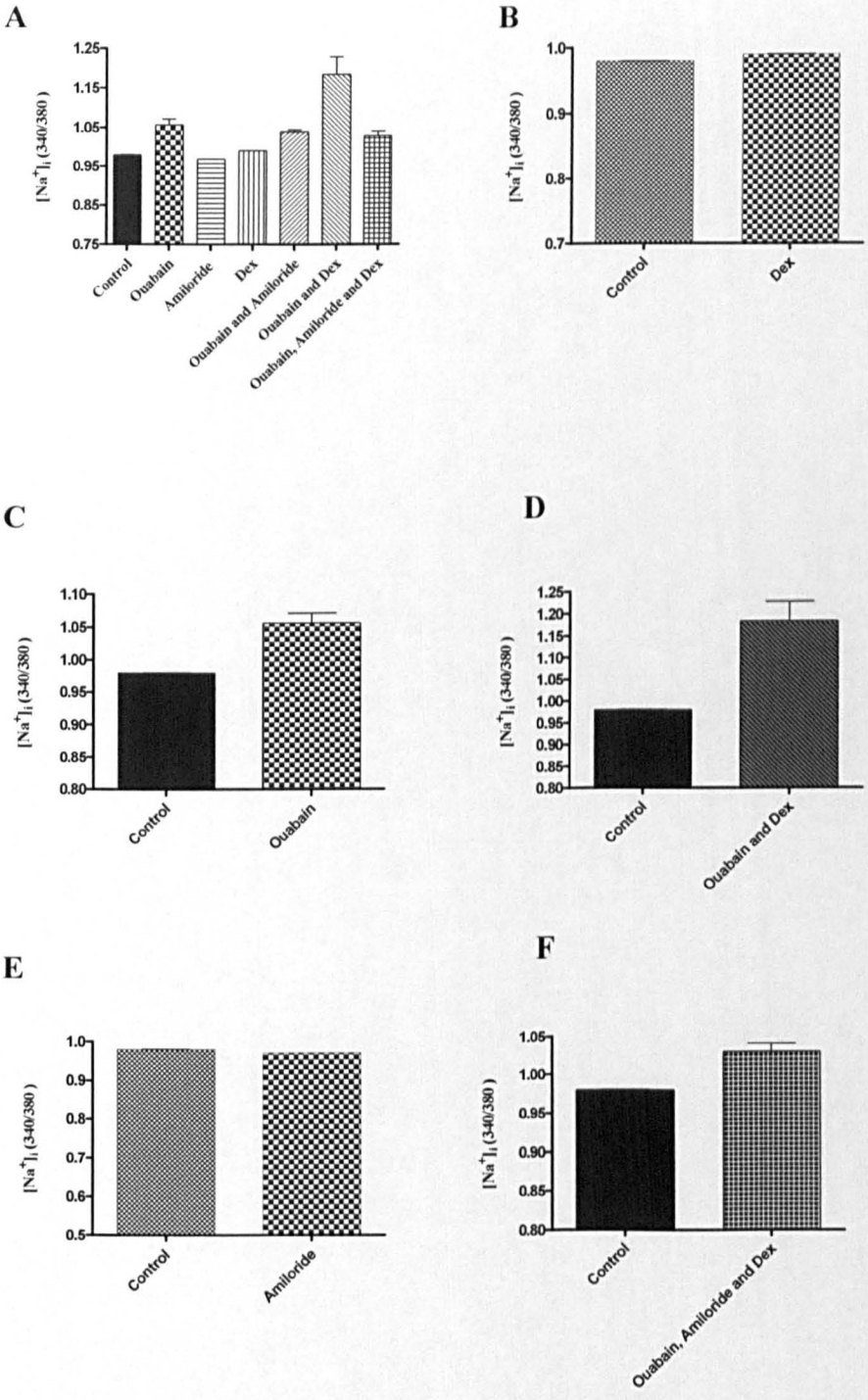

Figure 3.15: Assessing sodium transport in HCD cells. Panel A represents an overview of the results shown in more detail in B-F and illustrates $[Na^+]_i$ in HCD cells under variable conditions and demonstrates that amiloride only marginally inhibits $[Na^+]_i$ levels (E), thus supporting a role for the involvement of ENaC. Both dexamethasone (5 x 10-8M) (B) and ouabain (100μM) (C) increase $[Na^+]_i$ levels, the effects of which are additive (D). However, readings obtained for dexamethasone and ouabain in the presence of amiloride are lower than those compared to dexamethasone and ouabain alone, thus highlighting furthermore the ability of this compound to reduce $[Na^+]_i$ through inhibition of the ENaC. Results represent mean ± SEM. n=6 ** P<0.01, *** P<0.001

Incubation of HCD cells with dexamethasone ($5x10^{-8}M$), would be expected to raise $[Na^+]_i$ levels as a consequence of increased ENaC open probability, an effect mediated by the short term effects of aldosterone in vivo (Alvarez de la Rosa *et al.*, 1999). Whilst dexamethasone ($5 x10^{-8}M$) appeared to only partially increase $[Na^+]_i$ levels through its stimulatory effect on the ENaC (figure 3.15/B) (102 % ± as compared to control 100% ± 0.02%), the Na^+/K^+ ATPase pump inhibitor ouabain (100μM) increased $[Na^+]_i$ levels by 8% (107.8% ± 1.4% n = 6 $P< 0.0001$) (figure 3.15/C). However, the effects of these two drugs together evoked the largest increase in $[Na^+]_i$. Statistical analysis of this microfluorimetric data confirmed that $[Na^+]_i$ levels in HCD cells were found to be approximately 20% higher in those cells which had been treated with both dexamethasone and ouabain (figure 3.15/D) as compared to those cells under control conditions (120% ± 0.16% n = 6 $P< 0.01$).

Contrary to this, incubation with the ENaC antagonist amiloride was found to attenuate $[Na^+]_i$ levels (figure 3.15/E) reducing levels by approximately 8% (91.7% ± 0.02% n=6 $P<0.001$). Whilst incubation with ouabain and dexamethasone increased $[Na^+]_i$ levels, co-incubation of these compounds with amiloride attenuated this induction(105% ± 1.06% n=6 $P<0.01$%) (figure 3.15/F).

3.3 Discussion

The aim of this chapter was to characterise and establish a suitable model for the in vitro study of the biology of Na^+ reabsorption. We have confirmed both SGK1 and ENaC expression in a novel human cortical collecting duct (HCD) cell line, and assessed function in response to a series of commercially available agonists and antagonists of the apically located ENaC and the basolateral Na^+/K^+ ATPase.

RT-PCR and western blot analysis both confirmed SGK1 expression at both the mRNA and protein level respectively, whilst under standard tissue culture conditions, immunocytochemistry localized SGK1 predominantly to the cell nucleus with diffuse cytoplasmic staining. Variability in SGK1 localisation has been demonstrated in numerous cell types (Firestone *et al.*, 2003) and is thought to be dictated by the nature of the stimuli present. The rationale behind this compartmentalisation is explained by the availability and accessibility of this protein to its substrate targets, a mode of cellular control which can be clearly explained by looking more closely at its varied role within the cell. Recently reported to play a key role in intracellular cross talk through which cell surface receptors, nuclear receptors and cellular stress pathways all converge to control a wide variety of cellular processes (Firestone *et al.*, 2003).

Two key stimuli known to alter SGK1 localisation are glucocorticoids and serum, both of which reportedly stimulate the rapid transcription of the SGK1 gene through direct promoter activity (Firestone *et al.*, 2003). Whilst serum stimulation will induce cells to progress through the cell cycle, treatment with glucocorticoids will induce stringent growth arrest. Consequently, the localisation of SGK1 will switch depending upon the requirements of the cell at any given time. In the presence of serum, SGK1 is thought to shuttle between the nucleus and cytoplasm in synchrony with the cell cycle, the transport of which is associated with S and G2/M phase and occurs following its interaction with the nuclear receptor importin-alpha (Firestone *et al.*, 2003), a specific SGK1 interacting protein that associates with SGK1 through nuclear localisation signals in its cargo proteins. This receptor-cargo complex;

through interactions with importin-beta is subsequently transported into the nucleus (Firestone *et al.*, 2003). In contrast, treatment with glucocorticoids, known to induce a G1 cell cycle arrest, was found to induce an SGK1 that becomes localized and retained to the cytoplasmic compartment. In agreement with previous studies my data indicates that compartmentalisation of SGK1 is controlled stringently in a stimulus-dependent manner in my cell line. Coupled with the fact that SGK1 has a short half-life of approximately 20 minutes (McCormick *et al.*, 2005), HCD cells appear well equipped to respond appropriately to extracellular cues, enabling quick retrieval from the system upon removal of the stimulus.

Regulated by SGK1, the epithelial sodium channel expressed in the apical membrane of the principal cells is comprised of three partly homologous subunits, α, β and γ that are inserted into the membrane with a proposed stoichiometry of 2α:1β:1γ. Expression of all three subunits of the ENaC was confirmed in HCD cells at both the mRNA and protein level using RT-PCR and western blot analysis. Lack of availability of a suitable β-ENaC antibody for detection via western blotting meant that we were unable to confirm β-ENaC protein expression via this method. The higher molecular weight band observed on the western blot for γ-ENaC is likely to reflect important issues of ENaC biology (discussed below) and has been cited previously (Knepper *et al.*, 1999, Neilson *et al.*, 2001). Whilst the exact reason for this higher molecular weight band remains to be elucidated, the 72kDa band is thought to correspond to the expected molecular weight based on the open reading frame of the cloned γ ENaC cDNA (Canessa *et al.*, 1994). The higher molecular weight band is thought to represent the glycosylated and inactive form of the subunit since treatment of cells with PNGase, a compound known to induce deglycosylation has been shown to induce a induce a shift in molecular weight from 85kDa to 72kDa in rat kidney cells (Knepper *et al.*,). Deglycosylation by a GPI serine protease; channel activating protease (CAP1) (Rossier *et al.*, 1997) is thought to cleave in the early portion of the extracellular loop, thereby activating the ENaC through increased open state probability (Hess *et al.*, 1998),

Immunocytochemistry of each subunit revealed a localisation pattern different to that reported previously (Harger H *et al.*, 2001). However, consistent with previous findings (Nielson *et al.*, 2001, Loffing J *et al.*, 2000) was a difference in the localisation between the α subunit as compared to both β and γ. α-ENaC appeared to be predominantly perinuclear with some degree of cytoplasmic staining, whilst the β and γ subunits appeared to be confined to the nucleus with diffuse staining throughout the cytoplasm. The physiological significance of the heterogeneity in subcellular localisation remains to be established, but does suggest differences in the regulation of all three subunits of which could be attributed to a number of factors. The α, β and γ subunit are synthesised and glycosylated in the endoplasmic reticulum. Prior to leaving the golgi, they heteromultimerise and traffic together to the cell surface (reviewed in Snyder 2005). However, only the α-subunit is critical to formation of a fully functional Na^+ channel and only expression of the α-subunit is regulated by aldosterone (Masilamani *et al.*, 1999). Increased plasma aldosterone levels have been associated with a marked increase in the abundance of α ENaC protein in kidneys, whilst exerting no effect on β and γ subunit expression. Differences in α-subunit localisation may reflect this level of regulation by aldosterone in conjunction with the requirement of expression for channel formation.

Confirmation of both SGK1 and ENaC expression in the HCD cell line was accompanied by the functional data obtained by SBF-1/AM microfluorimetry. The ability to measure $[Na^+]_i$ levels in this cell line, in conjunction with a wide array of commercially available antagonists and agonists, enabled for pharmacological intervention of both the ENaC and Na^+/K^+ ATPase. The ability to mimic a pathophysiological state may pave way for a clearer understanding of those key signalling elements whose level of regulation is subject to compromise under conditions of osmotic stress.

In conclusion, the results from this chapter have demonstrated that the HCD cell line represents a physiologically appropriate model in which to study ENaC mediated Na^+ reabsorption in the human collecting duct.

Chapter 4

SGK1 and ENaC: a potential role in the progression and development of diabetic nephropathy and renal hypertension

4.1 Introduction

In type 2 diabetes mellitus, insulin insensitivity results in fluctuating levels of hyperglycaemia, and in extreme cases glycosuria. Previous reports have already established the deranged transcriptional regulation of SGK1 under conditions of both hyperglycaemia and diabetic nephropthy (Kumar *et al.*, 1999, Lang *et al.*, 2000). These observations have led to the supposition that SGK1 may function as a potential candidate in the development of hypertension associated with diabetes.

The molecular and cellular events that give rise to both structural and functional complications of diabetic nephropathy include the release of a number of different growth factors and cytokines. Amongst these regulators is Transforming Growth Factor Beta (TGF-β1). With powerful fibrogenic actions resulting from both stimulation of matrix synthesis and inhibition of matrix degradation, TGF-β1 has been demonstrated to play a role in the transcriptional control of SGK1. Hyperglycaemic-induced TGF-β1 formation together with osmotically-driven increases in SGK1 (Bell *et al.*, 2000, Waldegger *et al.*, 1997, Waldegger *et al.*, 2000) provide a link between poorly controlled plasma glucose and the development of excess ENaC-mediated Na^+-resorption that underlies secondary hypertension as seen in some diabetics (reviewed in Marshall *et al.*, 2004).

In addition to these glucose mediated effects on TGF-β1, glucose is also known to acutely increase the concentration of intracellular calcium ($[Ca^{2+}]_i$) in rat proximal tubular cells (Symonian *et al.*, 1998). Whether these, calcium induced changes evoke alterations in both SGK1 and ENaC expression in human cortical collecting duct (HCD) remains to be elucidated. Consequently, whilst there is considerable evidence relating high glucose levels to deranged sodium resorption in the kidney, the

mechanisms by which these elements jointly promote the pathophysiological changes characteristic of diabetic nephropathy requires further clarification.

In the chapter, I have used the previously characterised human cortical collecting duct (HCD) cell line as a model *in vitro* system to assess the effect of high glucose, TGF-β1 and cytosolic Ca^{2+} on SGK1 and ENaC expression. We have correlated these changes to single-cell determination of $[Na^+]_i$ and suggested a potential series of events that may explain how deregulated Na^+ re-uptake may contribute to the pathogenesis of secondary hypertension associated with diabetic nephropathy in type 2 diabetes mellitus.

4.2 Results

4.2.1 Exposure of HCD cells to elevated levels of glucose induces an up-regulation in SGK1 protein expression.

Previous studies (section 3.2.1) confirmed that HCD cells express SGK1 at both the mRNA and protein level. To test for a role of glucose in SGK1 protein expression, HCD cells were incubated for 2 days in a low glucose (5mM) medium for 2 days. After an overnight period of serum starvation cells were then treated with 25 mM glucose for 24 and 48 hours. Cells grown in 25mM glucose exhibited increased SGK1 expression to 185% ± 18.8% of control (5mM) at 24 hours and to 261.8% ± 5.71 of control at 48 hours as confirmed by densitometric analysis (n=3, $P<0.01$, see figure 4.1).

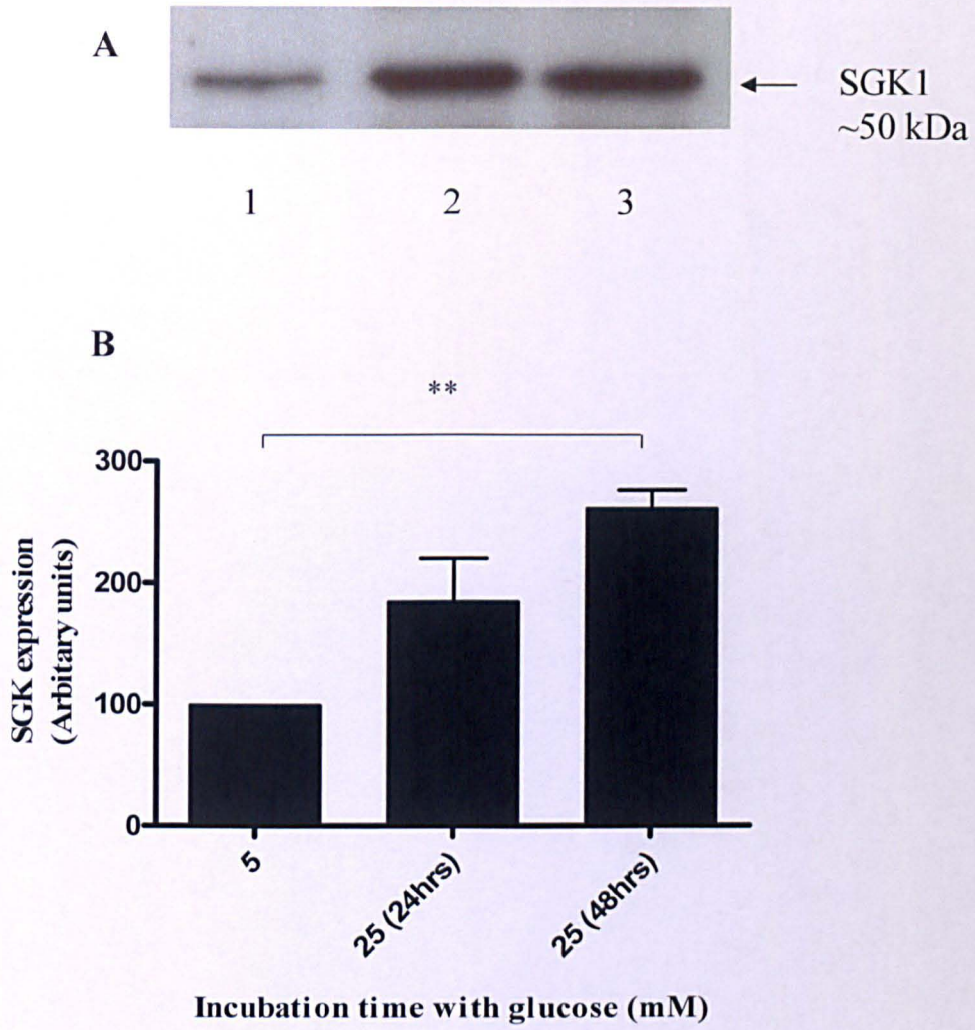

Figure 4.1: Up-regulation of SGK1 protein expression in increased 25mM glucose. HCD-cells were incubated in 5mM or 25mM glucose for 24 and 48hours. (A) Representative western blot analysis using an anti-SGK1 antibody illustrates an upregulation in protein expression at both 24 (lane 2) and 48 hours (lane 3) as compared to control conditions at 5mM (lane 1). (B) Statistical analysis of changes in SGK1 protein expression. Results represent mean ± SEM; n=4; ** $P< 0.01$.

4.2.2 High glucose induced a change in the localization of SGK1

Immunocytochemistry was used to assess if alterations in protein expression correlated with a change in localization. Under control conditions, in which FCS been depleted from the culture media, SGK1, as expected, was found solely in the cytoplasm (figure 4.2 A/2). Exposure to high glucose altered the localization pattern so that SGK1 became predominantly localized to the nucleus after 48 hours incubation in high glucose (figure 4.2 C/2).

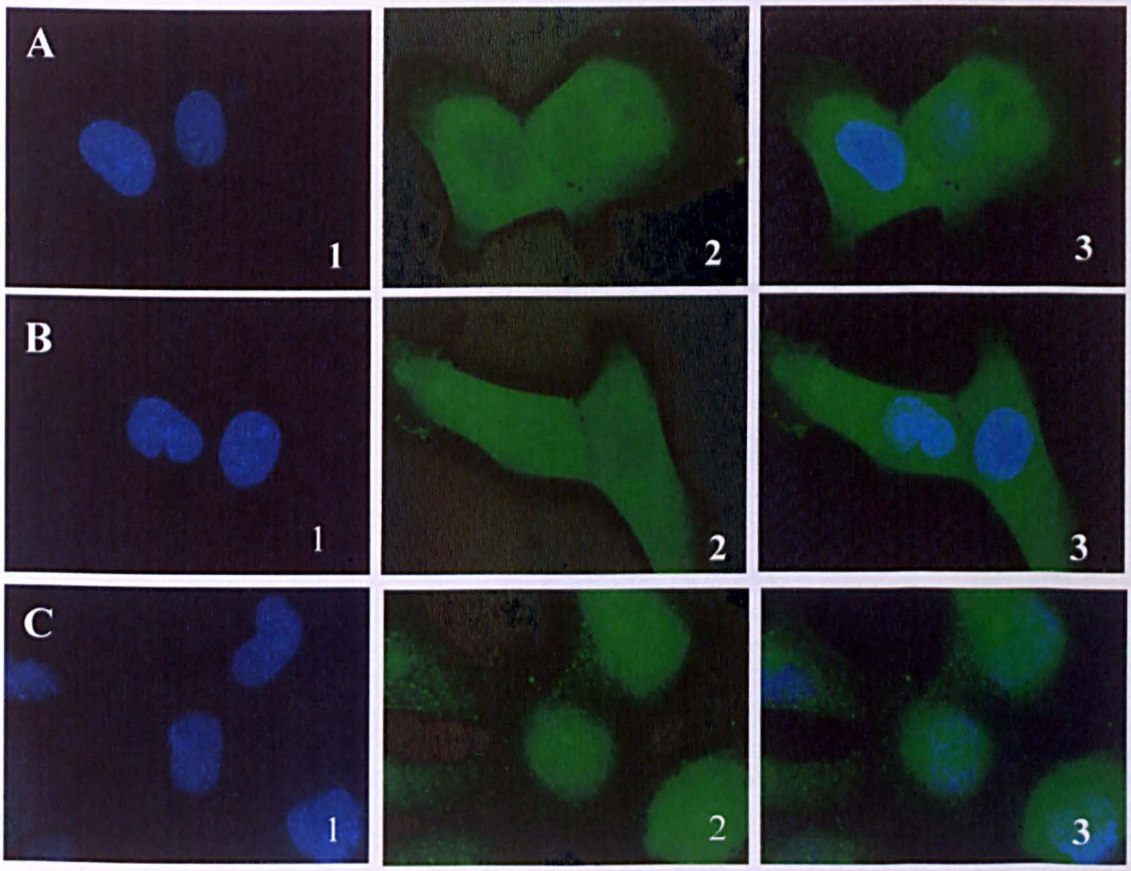

Figure 4.2: Localisation of SGK1 following 25mM glucose treatment. Immunocytochemistry demonstrated that elevated levels of glucose cause a shift in the cellular distribution of SGK1. Under control conditions (row A) and glucose treatment at 24 hours (row B) SGK1 resides solely in the cytoplasm (panel A/2, B/2) whilst following glucose treatment at 48 hours (row C) the localisation of SGK1 becomes predominantly nuclear (panel C/2). An overlay image (panel C/3) shows that at 48 hours co-localisation between SGK1 and the nucleus (stained with DAPI).

4.2.3 Up-regulation of α-ENaC expression in high glucose.

Having confirmed a stimulatory effect of glucose on SGK1 expression, . To test for a role of glucose in α-ENaC protein expression, HCD cells were incubated for 2 days in a low glucose (5mM) medium for 2 days. After an overnight period of serum starvation cells were then treated with 25 mM glucose for 24 and 48 hours. Cells grown under high glucose conditions exhibited increased α-ENaC expression at both 24 and 48 hours. This increase in protein expression amounted to 144.4% ± 7.98% of control (5mM) at 24 hours and 167.4% ± 11.2% of control at 48 hours (n=4,** $P<0.01$, see figure 4.3).

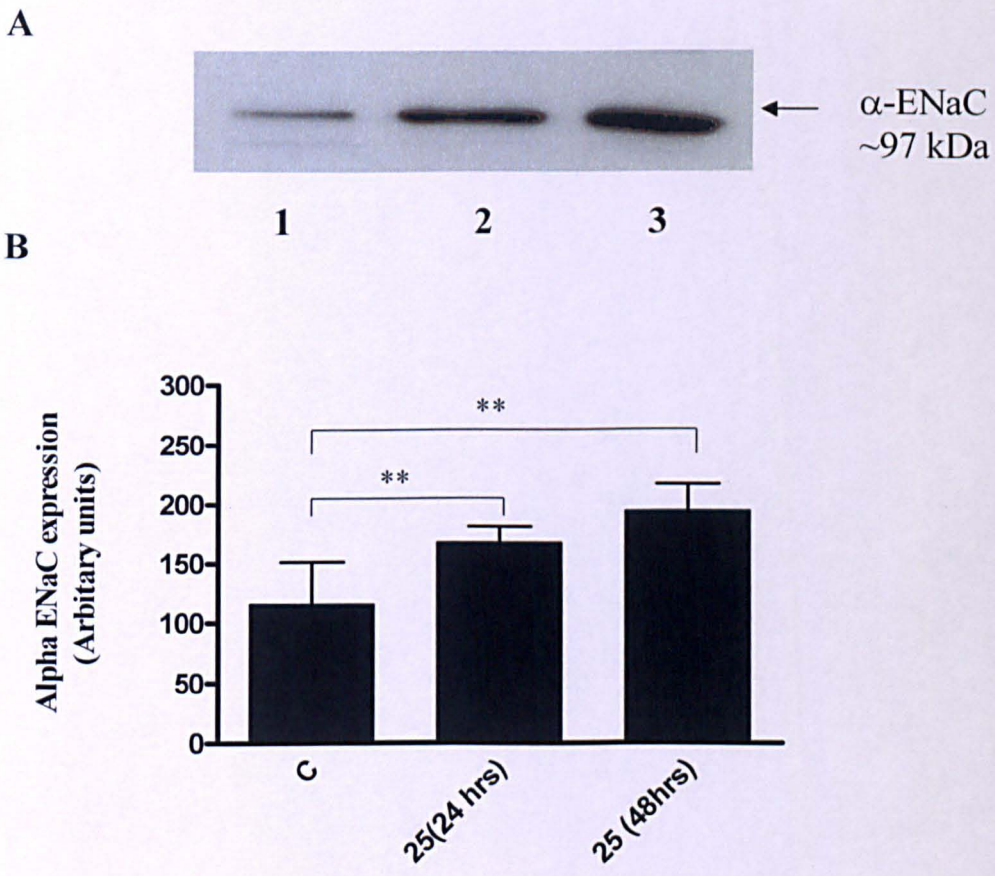

Figure 4.3: Up-regulation of α-ENaC protein expression in response to high glucose. HCD-cells were incubated in 5mM and 25mM glucose for 24 and 48 hours. (A) Representative western blot analysis using an anti-α-ENaC antibody (B) analysis of changes in α-ENaC protein expression. Results represent mean ± SEM; n=4; ** $P< 0.01$.

4.2.4 α-ENaC localisation appears to change following a 48 hour exposure to elevated levels of glucose.

The localisation of α-ENaC was determined to assess any correlation at 24 and 48 hours with the increased protein expression levels observed following exposure to elevated levels of glucose. Under control conditions (5mM), (serum free), α-ENaC was predominantly localized to the cell nucleus (figure 4.4 A/2). However, following a 48 hour incubation period with high glucose (25mM), α-ENaC was distributed between both the nucleus and cytoplasm (figure 4.4 C/2).

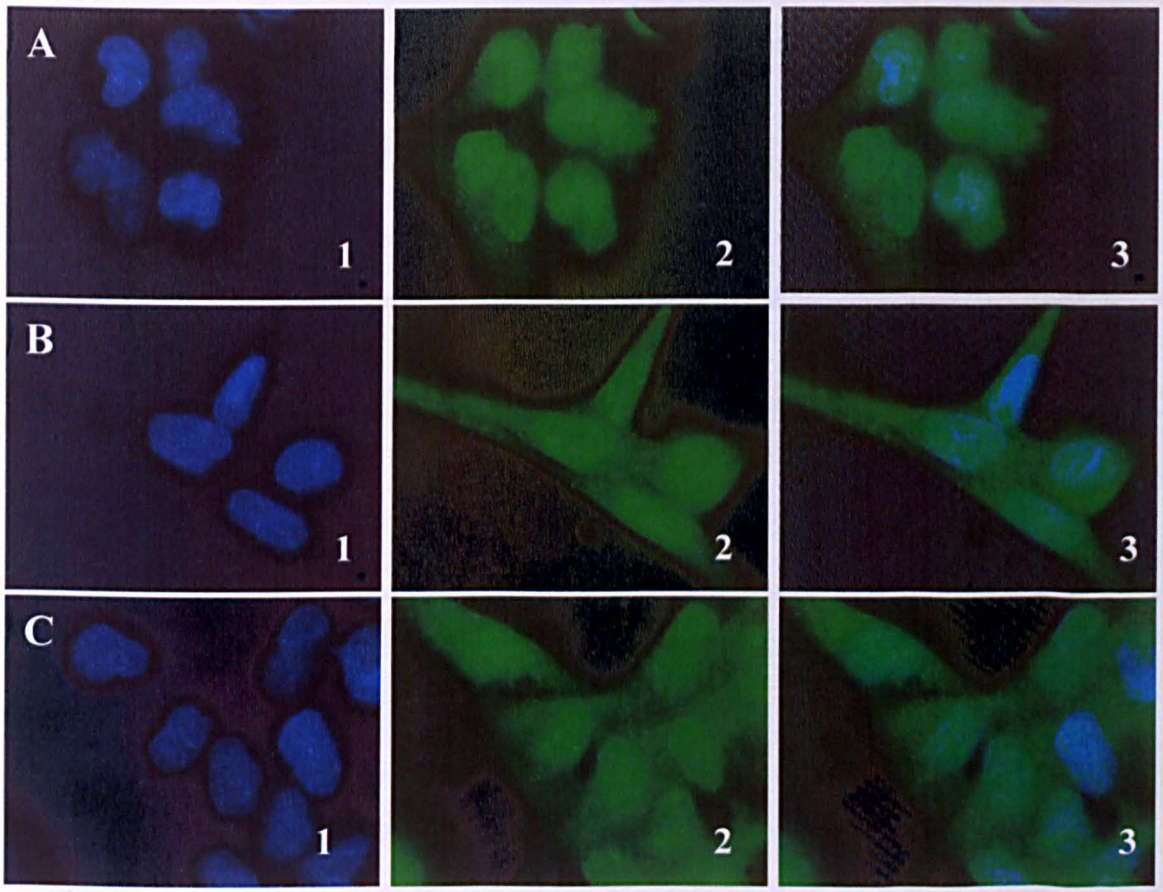

Figure 4.4: Localisation of α-ENaC following 25mM glucose treatment. Immunocytochemistry demonstrated that elevated levels of glucose cause a shift in the localisation of α-ENaC. Under control conditions α-ENaC resides solely in the nucleus (panel A2) whilst following glucose treatment for 48 hours the localization of α-ENaC becomes both nuclear and cytoplasmic (panel C/2). An overlay image (panel C/3) shows co-localization between α-ENaC and the nucleus (stained with DAPI).

4.2.5 Expression of TGF-β1 in HCD cells.

RT-PCR analysis and Western blotting were used to confirm TGF-β1 expression in HCD cells. RT-PCR analysis of several RNA preparations from HCD cells revealed PCR products representative of TGF-β1 mRNA (figure 4.5A). Protein expression was determined by Western blotting (figure 4.5B). Western blot analyses revealed bands at approximately 45Da representative of the non-secreted form of TGF-β1.

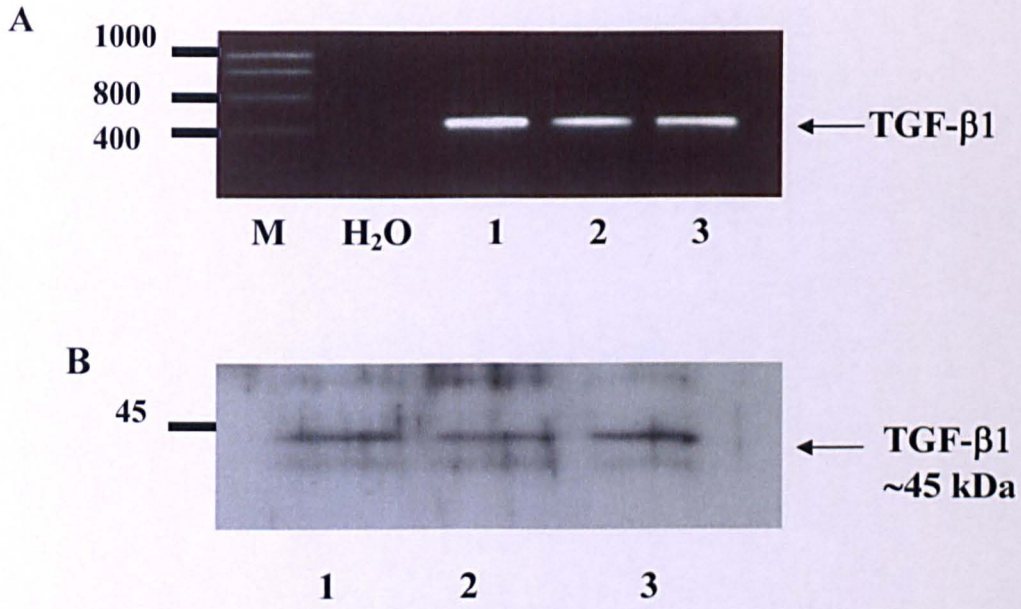

Figure 4.5: Expression of TGF-β1 mRNA and protein in HCD-cells. Panel A represents RT-PCR analyses using primers specific for human TGF-β1. PCR products of 340bp were observed in three RNA preparations (1, 2 and 3) corresponding to mRNA expression for TGF-β1 in HCD cells. Negative controls included water. Western blot analyses of HCD cell lysates (panel B, 5µg protein/lane) using an antibody against human TGF-β1 (panel B, lane 2) confirmed the presence of the protein in 3 different preparations in HCD cells. A protein band of approximately 45kDa was detected.

As a control for specificity we pre-incubated the primary anti-TGF-β1 antibody with a 100 fold excess of the TGF-β1 immunising peptide for 8 hours at room temperature and then overnight at 4^0C prior to addition of the antibody to the membrane, all other

steps in the procedure were identical. Competition of the primary antibody completely abolished the signal upon ECL detection (figure 4.6)

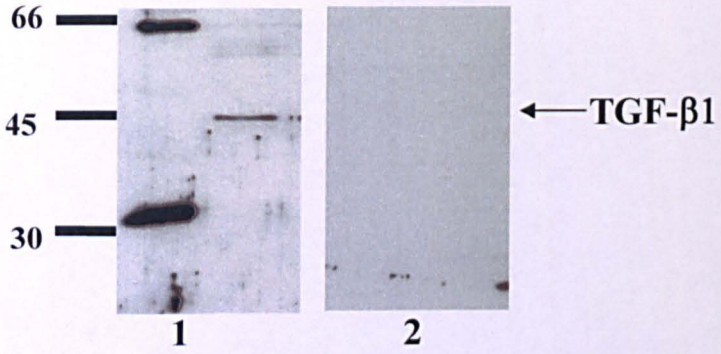

Figure 4.6: Peptide adsorbed antibody abolished TGF-β1 protein expression detection by western blotting. A protein band of approximately 45kDa was detected in an HCD protein preparation (panel 1), whilst pre-incubation with the peptide abolished any signal upon ECL detection (panel 2).

4.2.6 Elevated levels of glucose increase expression levels of the non secreted form of TGF-β1

Previous reports have demonstrated that hyperglycemia is associated with a number of raised signaling intermediates, involving the powerful fibrogenetic cytokine TGF-β1 (Hoffman *et al.,* 1998). Involved in the transcriptional control of SGK1, hyperglycaemic-induced changes in TGF-β1 expression implicate this cytokine as a possible mediator of the deranged transcriptional regulation of SGK1 observed in diabetic nephropathy (Lang *et al.,* 2000).To test for a role of glucose in TGF-β1 protein expression, HCD cells were incubated for 2 days in a low glucose (5mM) medium. After an overnight period of serum starvation cells were then treated with 25 mM glucose for 24 and 48 hours. I observed a significant increase in TGF-β1 (non-secreted form) 187.7% ± 8.4 % at 48 hours as compared to control (100%) (figure 4.7).

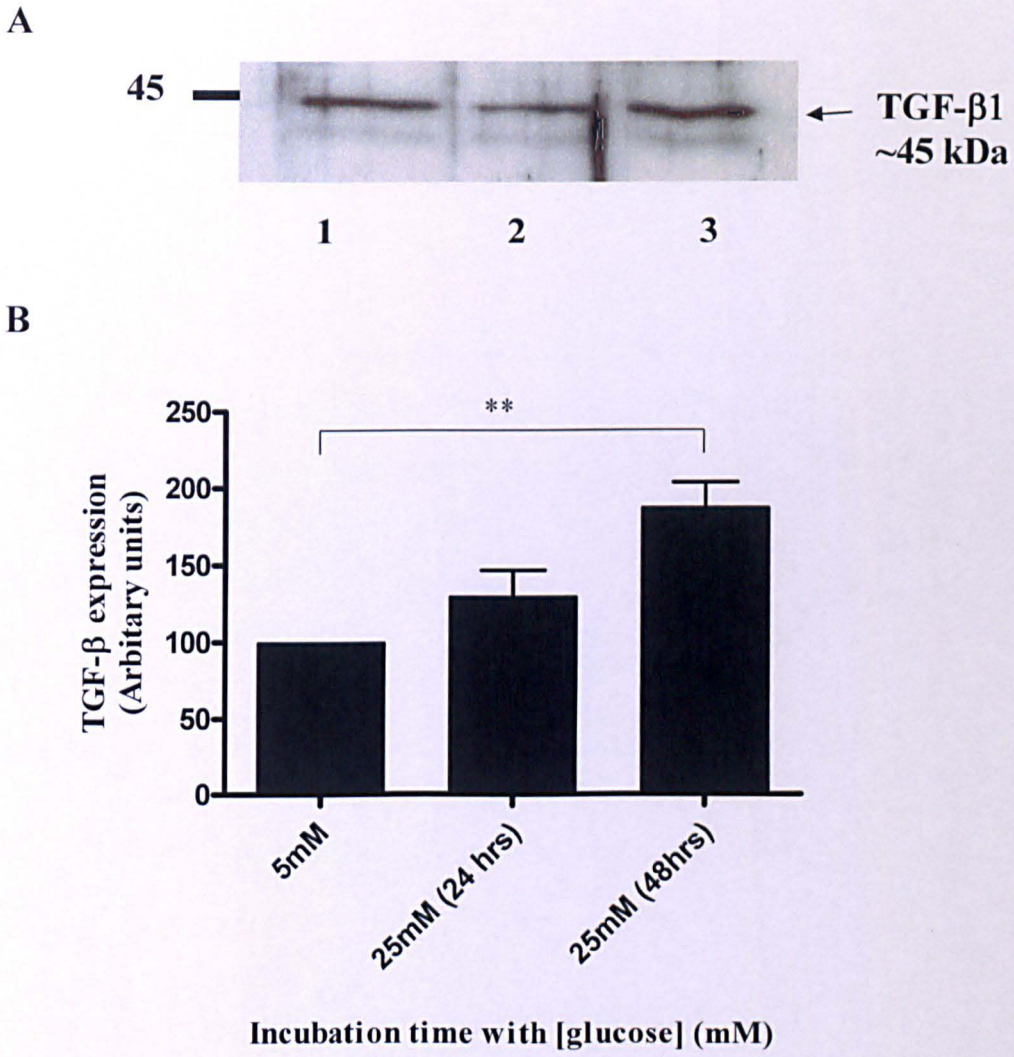

Figure 4.7: Exposure of HCD cells to 25mM glucose induces an upregulation in the non-secreted form of TGF-β1. HCD-cells were incubated in 5mM (lane 1) and 25mM glucose for 24 (lane 2) and 48 hours (lane 3) (A) Representative Western blot analysis using a human anti-TGF-β1 antibody (B) analysis of changes in TGF-β1 protein expression. Results represent mean ± SEM; n=4; ** $P< 0.01$.

4.2.7 TGF-β1 and the calcium ionophore Ionomycin up-regulate SGK1 protein expression levels over a 24 hour time period

Previous reports have suggested that raised $[Ca^{2+}]_i$ and increased circulating levels of the cytokine TGF-β1 play a role in the pathophysiology of hyperglycemia, many studies have attributed the upregulaton of SGK1 observed upon exposure to elevated levels of glucose in various cell types to be linked to TGF-β1 intermediates (Lang *et al.*, 2000).

To assess the effects of TGF-β1 and raised intracellular calcium on the regulation of SGK1 protein expression, cells were incubated for a 24 hour incubation with either TGF-β1 (2ng/ml) or with the Ca^{2+} ionophore ionomycin (1μM). All treatments were performed on cells which had been previously subject to a low glucose treatment (as described in section 4.2.7 to negate any stimulatory effects of high glucose and serum deprived overnight.

Treatment of HCD cells with ionomycin (1μM) was found to significantly increase SGK1 protein expression to 262±6.0% and 263.7±22.8% of control at 6 and 8 hours respectively. Expression levels returned to near basal by 24 hours (figure 4.8 A and B) (n=4 $P<0.001$).

The effect of TGF-β1 was found to be less significant than that observed following application of ionomycin, with SGK1 levels elevated at 8 hours to 128 ± 13.01% as compared to control (figure 4.8 C and D) (n = 4 $P < 0.001$).

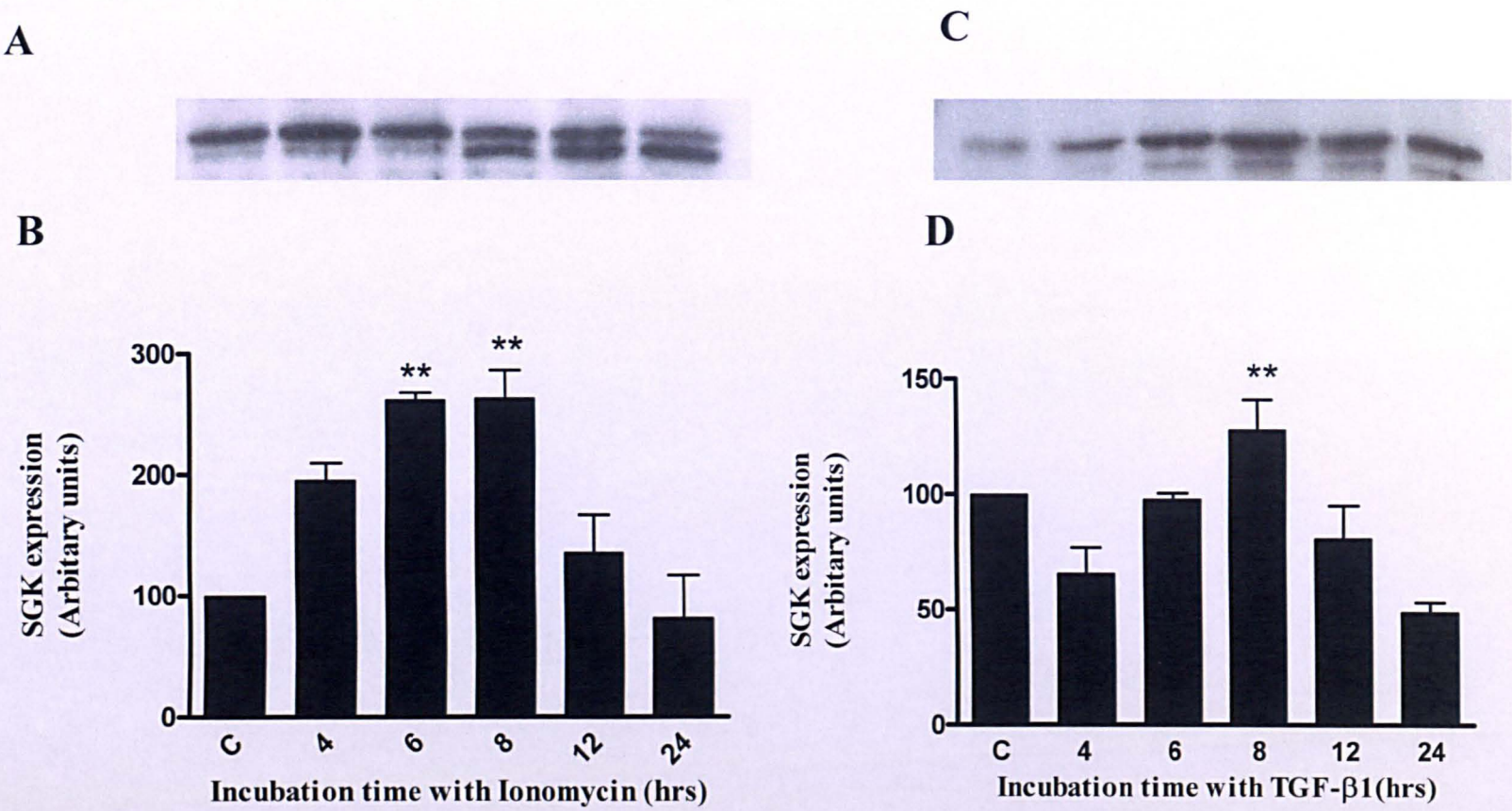

Figure 4.8: Treatment of HCD cells with the calcium ionophore ionomycin and the growth factor TGF-β1 results in increased SGK1 protein expression. HCD cells were incubated with either ionomycin (1μM) or TGF-β1 (2nm) for incubation periods of 4, 6, 8 12 and 24 hours. (A and C respectively). Statistical analysis of changes in SGK1 protein expression (B and D). Results represent mean ± SEM; n=4; ** $P< 0.01$.

4.2.8 Application of TGF-β1 to HCD cells and raised intracellular calcium increased, α-ENaC protein expression.

Treatment of HCD cells with ionomycin (1μM) resulted in increased α-ENaC protein expression levels over a 24 hour incubation period, with expression significantly marked to 175±5.5% of control at 6 hours (n=4 $P<0.001$). Whilst expression was clearly elevated above basal levels at both 4 (135±1%) and 8 hours (136±7.333%) expression was not found to be statistically significant (figure 4.9 A and B).

Administration of TGF-β1 (2ng/ml) over a 24 hour period was also found to increase α-ENaC expression at 6 hours, 159.7 ± 9.8% as compared to control, pointing to a role albeit direct or indirect for both $[Ca^{2+}]_i$ and TGF-β1 in the regulation of SGK1 and α-ENaC protein expression. (figure 4.9 C and D).

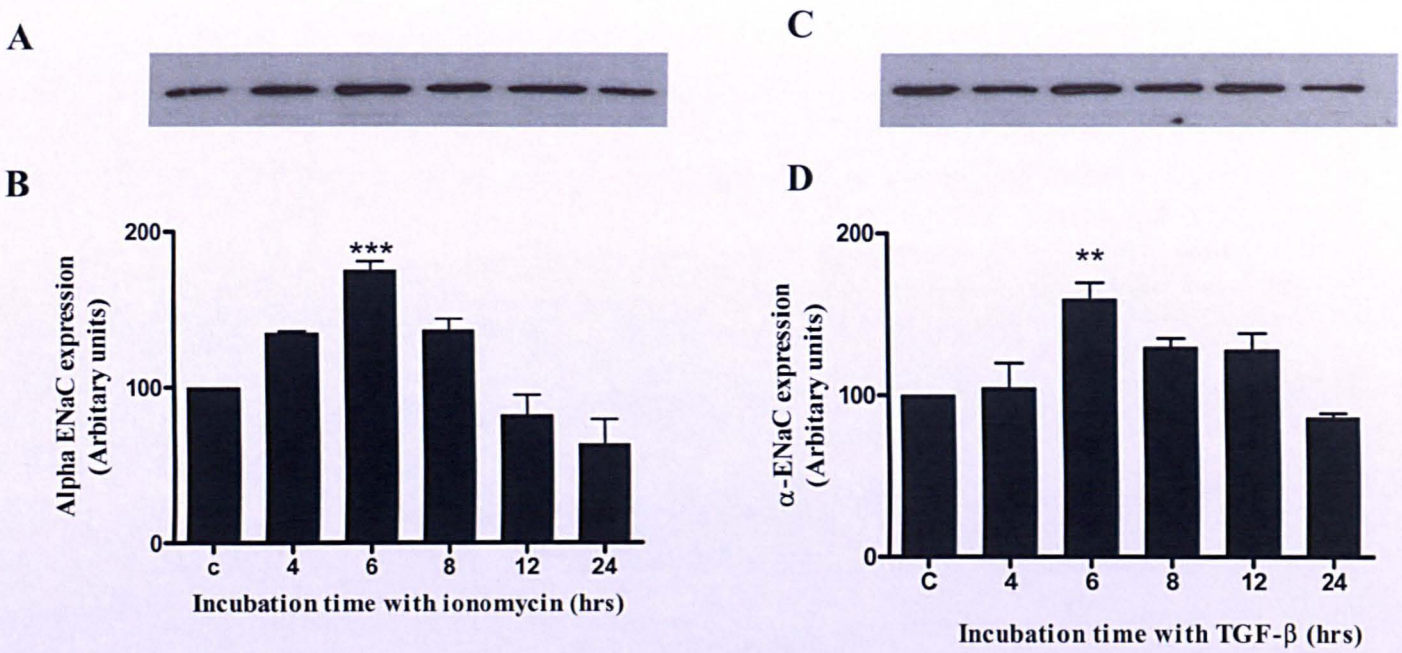

Figure 4.9: Treatment of HCD cells with the calcium ionophore ionomycin and the growth factor TGF-β1 results in increased α-ENaC protein expression.:HCD cells were incubated with either ionomycin (1μM)) or TGF-β1 (2nm) for incubation periods of 4, 6, 8 12 and 24 hours. (A and C respectively). Statistical analysis of changes in α-ENaC expression (B and D). Results represent mean ± SEM n=4; ** $P< 0.01$.

4.2.9 HCD-cells exposed to 25mM glucose exhibit increased $[Na^+]_i$ measured by Na^+ microfluorimetry

To determine if there was any functional correlation between these increased SGK1 and ENaC levels and $[Na^+]_i$ under conditions comparable to hyperglycaemia $[Na^+]_i$ was measured in HCD cells which had been cultured under low and high glucose conditions. Intracellular sodium levels were found to be significantly elevated following 24 (113±1%) and 48 (114±1%) hours exposure to 25mM glucose, as compared to cells cultured in low (5mM) glucose (see figure 4.10). This data taken in conjunction with that described previously suggest that increases in $[Na^+]_i$ expression in response to high glucose after 48 hours may be mediated via the increased expression of both SGK1 and α-ENaC.

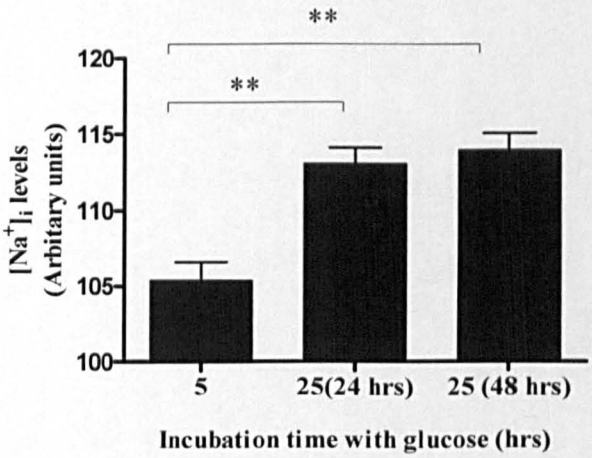

Figure 4.10: HCD cells exposed to elevated levels of glucose exhibit increased intracellular sodium levels. HCD cells were incubated in 5 or 25mM glucose for 24 and 48 hours. Cells were then pre-incubated with the Na^+/K^+ATPAse inhibitor ouabain (100μM). Basal levels of intracellular Na^+ were measured in SBF-1/pluronic loaded HCD cells and variability in $[Na^+]_i$ between glucose treatment was assessed. Results represent mean ± SEM; n=4; ** $P< 0.01$.

4.4 Discussion

Exposure of renal epithelial cells to changes in osmolality necessitates the initiation of cell volume regulatory processes, activation of which serves to restore cell volume preserving both integrity and function. Inability to resolve these changes may have serious repercussions for sodium transport and the development of secondary hypertension associated with renal diseases such as diabetic nephropathy. In the current chapter I have investigated the expression of key signalling elements involved in Na^+ reabsorption under control and high glucose conditions as seen in Type II diabetes.

I have confirmed that incubation with glucose, the Ca^{2+}-ionophore ionomycin and the cytokine TGF-β1 evoked a time-dependent increase in both SGK1 and αENaC protein expression. These molecular changes were correlated to an increase in Na^+-uptake at the single-cell level. These data offer a potential explanation for glucose-evoked Na^+-resorption and the contributory role of SGK1 and ENaCs in development of secondary hypertension, commonly linked to diabetic nephropathy.

Hyperglycaemia has been associated with the generation of elevated cytosolic calcium in a number of diverse cell types from both animal and human models of diabetes (Symonian *et al.*, 1998, Lee *et al.*, 2006, Demerdash *et al.*, 1996). Changes in $[Ca^{2+}]_i$ instigate and mediate a plethora of cell-specific signal-response cascades within cells. Whilst a number of theories concerning the mechanisms by which glucose serves to increase $[Ca^{2+}]_i$ have been proposed in various cell types (Demerdash., 1996, Symonian *et al.*, 1998), the exact nature of these pathways responsible for the effect of hyperglycaemia remain unclear. This link between hyperglycaemia and raised $[Ca^{2+}]_i$ led me to investigate the effect of raised $[Ca^{2+}]_i$ on expression of signaling elements identified in chapter 3. Direct elevation of $[Ca^{2+}]_i$ via ionomycin significantly increased SGK1 protein expression after 6-8hrs, a finding consistent with previous studies in DAN-G pancreatic tumor cells (Klingel *et al.*, 2000). Similarly, glucose-mediated SGK1 transcription in 3T3 mouse fibroblasts is reportedly abolished in the presence of the calcium channel blocker nifedipine (Lang *et al.*, 2000), further confirming a role for increased $[Ca^{2+}]_i$ as a

downstream component of the hyperglycaemic induced increase in SGK1 expression levels reported previously (Lang *et al.*, 2000) and in this chapter.

Once inside the cells, the metabolism of glucose can be ascribed to a number of pathways, all of which are linked intracellulary (Brownlee *et al.*, 2001). In addition to evoking increases in $[Ca^{2+}]_i$, glucose also increases the *de novo* synthesis of diacylglycerol (DAG) eliciting downstream activation of protein kinase C/mitogen activated protein kinase (PKC/MAPK) (Whiteside *et al.*, 2000). Diacylglycerol, a powerful signalling molecule whose formation stems from glycolytic intermediates, is involved in the promotion of those intracellular signalling events relative to the pathogenesis of diabetic nephropathy and mediates its effects through the protein kinase PKC (LeRoith *et al.*, 2004, Brownlee 2000). The application of PKC mimetics to cells accompanied by a subsequent rise in SGK1 transcription has led to the supposition that PKC in conjunction with raised $[Ca^{2+}]_i$ may regulate transcriptional control of SGK1 as downstream components of the hyperglycaemic response.

PKC has emerged as a potential regulator of many aspects of the development and progression of diabetic nephropathy and reportedly plays a key role in TGF-β expression through its actions on the transcription factor complex AP-1 (Weigert *et al.*, 2003). TGF-β1, a multifunctional cytokine known to be increased in type 2 diabetics, reportedly mediates the development of renal hypertrophy and excessive matrix deposition, implicating this cytokine as a key mediator in the development of diabetic nephropathy (Ziyadeh 2000, Sharma *et al.*, 1995, Ricci *et al.*, 2006). Whilst the downstream targets of TGF–β1 remain largely elusive, the cell hypertrophy observed upon TGF-β1 upregulation may be in part be regulated by SGK1 since TGF-β1 reportedly alters SGK1 gene transcription (Lang *et al.*, 2000), an effect believed to be mediated via p38 MAPK (Bell *et al.*, 2000, Waldegger *et al.*, 2000). This further implicates TGF-β1 as a component in renal cell hypertrophy, providing a link between increased SGK1 expression observed following application of PKC mimetics. Observed PKC driven increases in SGK1 expression may therefore be mediated via TGF-β1. This relationship is supported in the current study by the changes in SGK1 expression observed following exogenous application of TGF-β1 ,

an effect known to be reduced in the presence of a TGF-β1 neutralising antibody (Lang *et al.*, 2000). The temporal relationship between Ca^{2+} and TGF-β-evoked increases in SGK1 -expression are consistent with previous reports highlighting a causative link between these key signalling elements.

Whilst it is well established that glucose increases the de-novo synthesis of TGF-β1 (Di Paolo *et al.*, 1996, Hoffman *et al.*, 1998, Yung *et al.*, 2006) TGF-β1 has recently been reported to increases expression of the insulin-independent glucose transporter GLUT 1 (Mogyorosi *et al.*, 1999). The link between GLUT 1 mediated glucose uptake and TGF-β1 may be pivotal to the pathogenesis of diabetic nephropathy, with both TGF-β1 and GLUT1 having demonstrated a mutualistic relationship (Rocco *et al.*, 1992), an effect more pronounced under conditions representative of high glucose. The glucose stimulated TGF-β1 increase of the insulin-independent glucose transporter GLUT1 (Inoki *et al.*,, 1999) in turn leads to enhanced expression of TGF-β1 (Mogyorosi *et al.*, 1999, Brosius *et al.*, 2005) Consequently, GLUT1-mediated increases in TGF-β1 expression will promote and further exacerbate the rate of glucose uptake under conditions of hyperglycaemia, contributing to the pathogenesis of diabetic nephropathy. This feed forward build up of TGF-β1 may provide the link between glucotoxicity and cell dysfunction in diabetic nephropathy, with TGF-β1 mediating glucose-evoked cellular hypertrophy whilst stimulating extracellular matrix biosynthesis, two hallmarks of diabetic renal disease.

Whilst the transient nature of the TGF-β1-evoked response may reflect glucose toxicity associated with exogenous application of high concentrations of the cytokine, perforation of the cell membrane by the Ca^{2+}-ionophore is likely to have multiple non-specific effects that ultimately impair cell function. These effects may offer a potential explanation as to why SGK1 expression appears to respond to changes in Ca^{2+} and TGF-β1 before elevated glucose, even though Ca^{2+} and TGF-β1 are downstream of hyperglycaemia.

SGK1 promotes Na^{+} re-absorption via the epithelial sodium-channel (ENaC). This tetrameric channel resides in the cytoplasm; bound to Nedd 4-2, (Snyder *et al.*, 2002). Phosphorylation of SGK1 via a PI3-K dependent pathway facilitates binding

of Nedd4.2 to SGK1 thereby dissociating the Nedd 4-2/ENaC complex. This dissociation allows for release of the ENaC consequently reducing degradation of the ENaCs, facilitating both translocation and insertion into the cell membrane (Debenoville *et al.,* 2001). This widely accepted association between SGK1 and ENaCs leads me to assume that these glucose-, Ca^{2+}- and TGF-β-evoked changes in αENaC should mimic those already reported for SGK1, an assumption supported by the current study. The net effect of altered ENaC-expression would be an increase in Na^{+}-reabsorption. It seems reasonable therefore to assume that any glucose-evoked increase in α-ENaC expression may result from reduced degradation, as opposed to increased gene transcription. Although at the single-cell level these changes in Na^{+} re-uptake are small, across the epithelium, they represent a potential mechanism to explain as to how hyperglycaemia may lead to the development of secondary hypertension commonly seen in diabetic nephropathy (Marshall *et al.,* 2004).

Chapter 5

TRPV4-evoked alterations in intracellular calcium levels

5.1 Introduction

Prolonged exposure of kidney epithelial cells to changes in both osmolality and fluid shear stress has led to a number of suggestions concerning the mechanisms involved in both detecting and transducing these stimuli. Most cells are thought to be sensitive to both osmotic and mechanical stimulation. Originally linked to mechanosensation in vertebrates the transient receptor potential (TRP) cation channel family is a group of proteins expressed in a wide variety of cell types and are gated by a broad range of ligands (Clapham *et al.*, 1995, Clapham *et al.*, 1995, Vriens *et al.*, 2004). One member, TRPV4, is the mammalian homologue of the OSM-9 gene and was first discovered in nematodes unable to detect and respond to potentially harmful osmotic gradients (Gong *et al.*, 2004). TRPV4 is a Ca^{2+} permeable channel abundantly expressed in the kidney, skin, lung epithelium, vascular endothelium and liver. Originally identified as an osmotically activated channel (Strottmann *et al.*, 2000, Wissenbach *et al.*, 2000, Liedtke *et al.*, 2000) TRPV4 responds to a wide variety of stimuli including mechanical stress, heat, endogenous ligands and synthetic agonists such as 4α-phorbol 12,13-didecanoate (4α-PDD).

A reduction of extracellular osmolarity will induce a degree of cell swelling in most animal cells. Within minutes of exposure to this hypotonic stress, cells will attempt to reduce their cell volume via a regulatory volume decrease (RVD). This hypo-osmotic induced cell swelling has been linked to a rise in cytosolic calcium in various volume-regulating cell types including human bronchial (HBEs) and human embryonic kidney cells (HEKs) (Fernandez-Fernandez *et al.*, 2002, Rohloff *et al.*, 2003, Tinel *et al* 2002). This rise in $[Ca^{2+}]_i$ permits the loss of electrolytes, typically K^+ and Cl^- through Ca^{2+} dependent channels with the subsequent loss of osmotically obliged water, thereby allowing the cell to restore its volume preserving both structure and function.

Since stretch evoked activation of the mechanosensitive channel TRPV4 initiates an increase in $[Ca^{2+}]_i$ and RVD has been shown to be Ca^{2+} dependent (Rothstein *et al.*, 1992, Christensen et *al.*, 1987), the hypotonic activation of TRPV4, with a concomitant rise in $[Ca^{2+}]_i$, (Becker *et al.*, 2005, Nilius *et al.*, 2004) has implicated this Ca^{2+} permeable cation channel as a possible mediator in cellular osmoreception, aiding cell volume recovery via RVD.

In this chapter, single cells within cell clusters were challenged by physical deformation to assess the degree of changes in cytosolic calcium and confirm the nature by which this signal was detected. Data supports the hypothesis that cells of the human collecting duct express functional receptors for detecting mechanical/osmotic stress (TRPV4). I show that TRPV4, like several other TRP channels is modulated by both extra and intracellular Ca^{2+} and in the absence of TRPV4, touch evoked stimulation fails to evoke a rise in $[Ca^{2+}]_i$. Taken together these data suggest that TRPV4 may function as an important mediator in aiding cell volume recovery, serving to detect and respond accordingly to osmotically induced signals by instigating a calcium dependent signal that ultimately restores cell volume.

5.2 Results

5.2.1 Mechanical stimulation of HCD cells evoked a transient increase in $[Ca^{2+}]_i$

Previous studies suggest that increased extracellular osmolarity; initiates a Ca^{2+} dependent cell volume recovery process otherwise known as a regulatory volume decrease (RVD). In the current study touch was used as a surrogate to osmotic stress in order to determine the effect of membrane stretch on $[Ca^{2+}]_i$ levels in HCD cells.

HCD cells were loaded with 2.5 μM of the Ca^{2+} fluorophore Fura-2/AM and subject to mechanical stimulation with a micro-electrode. Physical stimulation of a single HCD cell in culture (Fig 5.1A) evoked an increase in cytosolic calcium. The response was rapid in onset but transient, returning to basal levels even in the continued presence of the stimulus. Propagation of this intercellular Ca^{2+} wave (Figure 5.1B) from the initial point of stimulation through tiers of surrounding cells illustrates co-operativity between these HCD cells and is indicative of a high degree of cell-cell communication.

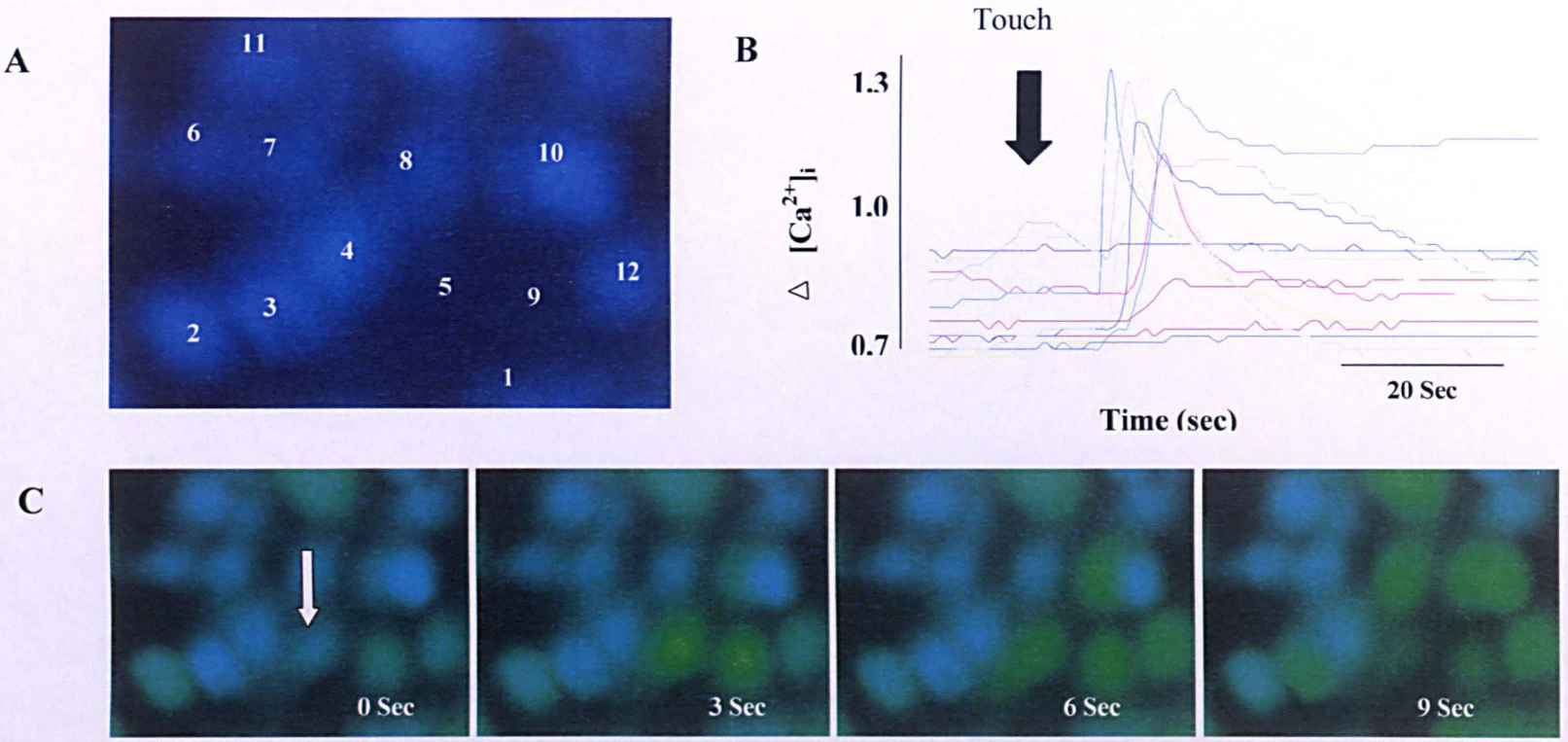

Figure 5.1: Generation of calcium transients in HCD cells upon touch evoked stimulation. HCD cells were loaded with Fura 2 and multiple regions of interest recorded (5.1A). Touch evoked stimulation of an HCD cell within this cluster evoked a transient increase in $[Ca^{2+}]_i$. Panel C demonstrates the rapid spread of a touch-evoked Ca^{2+}-transient between HCD-cells upon physical perturbation. A single cell is mechanically stimulated at '0 sec' at subsequent time-intervals (0-9 sec), the Ca^{2+}-signal propagates away from the point of stimulation into neighboring cells. The generation of calcium transients and the resultant elevation in $[Ca^{2+}]_i$ in each cell is shown in the trace in panel B. Data is represented as estimated change in cytosolic calcium (Δ $[Ca^{2+}]_i$) recorded as a ratio of 340/380 nm excitation.

5.2.2 HCD cells express the mechanoreceptor TRPV4

Having shown that HCD cells respond to touch by increasing $[Ca^{2+}]_i$, initial studies looked to confirm the nature of the receptor responsible for both detection and transduction of this mechanically induced signal. RT-PCR (figure 5.2A) and western blot analysis (figure 5.2B) confirmed expression of the mechanoreceptor TRPV4 at both the mRNA and protein level.

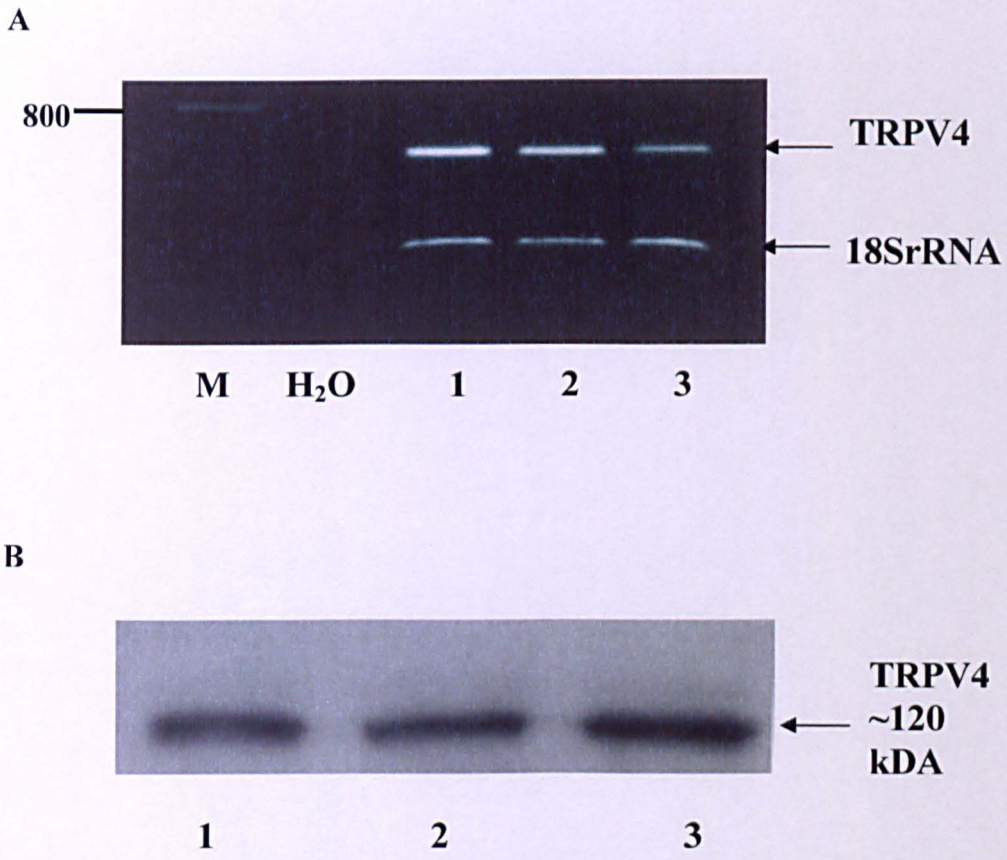

Figure 5.2 Expression of TRPV4 mRNA and protein in HCD-cells.
Panel A represents RT-PCR analyses using primers specific for human TRPV4. PCR products of 618 bp were observed in three different RNA preparations (1, 2 and 3) corresponding to mRNA expression for TRPV4. Western blot analyses of HCD cell lysates (panel B, 5μg protein/lane) using an antibody against human TRPV4 confirmed the presence of the protein in 3 different preparations. A protein band of approximately 120KDa (TRPV4) was detected.

As a control for specificity we pre-incubated the primary anti-TRPV4 antibody with with a 100 fold excess of immunising TRPV4 peptide at room temperature for 8 hours and then overnight at 4°C, all other steps in the procedure were identical. Competition of the primary antibody completely abolished the signal upon ECL detection (figure 5.3).

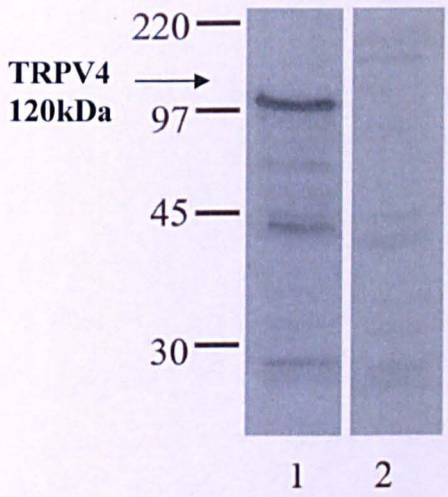

Figure 5.3 Peptide adsorbed antibody abolished TRPV4 protein detection by western blotting. A protein band of approximately 120kDa was detected in an HCD protein preparation (panel 1), whilst pre-incubation with the immunising peptides abolished any signal upon ECL detection (panel 2)

5.2.3 An elevation in cytosolic [Ca^{2+}] in response to touch evoked stimulation involves extracellular Ca^{2+} entry across the plasma membrane

The generation of this mechanosensitive cytosolic $[Ca^{2+}]_i$ response has previously been described in a number of cell types, including airway epithelia (Sanderson *et al.*, 1990), mammary epithelia (Enomoto *et al.*, 1992) and aortic endothelia (Demer *et al.*, 1993) and has been reported to involve both extracellular Ca^{2+} entry/and or Ca^{2+}-release from intracellular stores.

Section 5.2.1 illustrated increased $[Ca^{2+}]_i$, in HCD cells upon touch evoked stimulation. This increase in $[Ca^{2+}]_i$, could occur as a direct result of either release from intracellular stores, an influx of calcium across the plasma membrane or a consequence of both. Consequently, the present study investigated the absolute requirement of extracellular Ca^{2+} on touch-evoked changes in $[Ca^{2+}]_i$.

To examine the role of Ca^{2+}-influx in mediating touch evoked changes in $[Ca^{2+}]_i$, cells were bathed in calcium free media containing the calcium chelator EGTA (1mM) and an individual cell was mechanically stimulated (as described in section 2.8.3). Following stimulation, touch-evoked changes in $[Ca^{2+}]_i$ were still observed under Ca^{2+}-free conditions, and as expected the signal propagated rapidly throughout the cell cluster (Figure 5.4B). Upon removal of extracellular Ca^{2+} the extent of signal propagation was unaltered indicating that in the absence of extracellular calcium these cells are still able to respond to osmotic perturbations. However, the basal-to-peak amplitude of the response was only 35% (Figure 5.4D) of that obtained in the presence of extracellular calcium (Figure 5.4 0.21 ± 0.03 as compared to 0.60 ± 0.12 n = 6 separate experiments for each treatment $P < 0.01$).

My finding that exposure to a calcium free solution did not abolish the rise in $[Ca^{2+}]_i$ following touch evoked stimulation of an HCD cell indicates that an influx of extracellular Ca^{2+} across the plasma membrane is not solely responsible for the generation of this increased $[Ca^{2+}]_i$,. The contribution of intracellular Ca^{2+} stores to the increase in $[Ca^{2+}]_i$ was further assessed by depletion of intracellular calcium stores through inhibition of the Ca -ATPase pump in the endoplasmic reticulum with thapsigargin (1μM) (Thastrup *et al.*, 1990). Prior to touch evoked stimulation, HCD cells were bathed in Ca^{2+} free media following a 60 minute pre-incubation with Thapsigargin. Cells were then subject to touch evoked stimulation and $[Ca^{2+}]_i$ levels recorded..Following the chelation of calcium in the extracellular media and the inhibition of the Ca^{2+}-ATPase with thapsigargin, touch evoked stimulation of HCD cells failed to evoke a rise in $[Ca^{2+}]_i$ (figure 5.4C) thus highlighting the importance of calcium mobilisation from Thapsigargin sensitive stores in generation of this calcium signal. As the figure clearly illustrates, $[Ca^{2+}]_i$ transients were completely negated following both the removal of extracellular calcium from the extracellular media and depletion of intracellular stores.

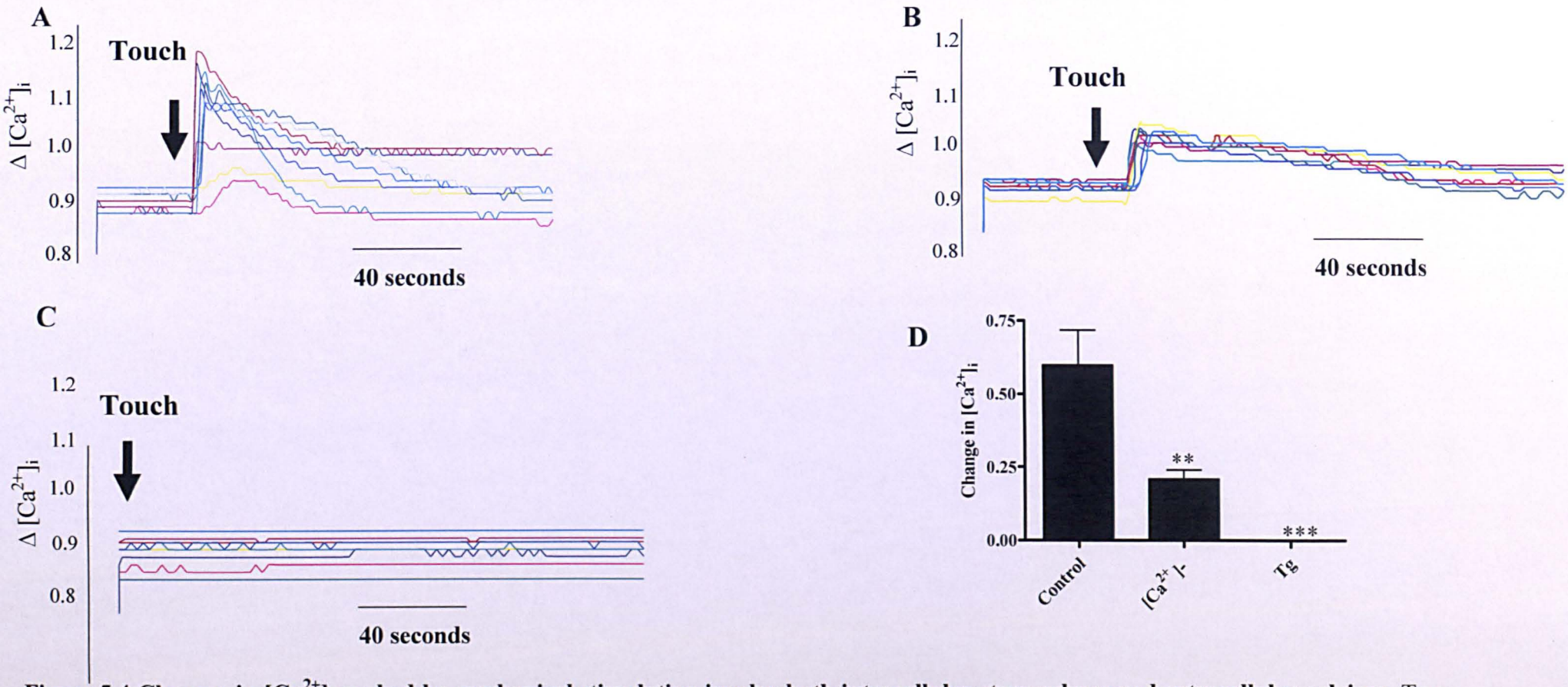

Figure 5.4 Changes in $[Ca^{2+}]_i$ evoked by mechanical stimulation involve both intracellular store release and extracellular calcium. Trace A is representative of control conditions. Trace B illustrates a reduced basal to peak amplitude of the response observed upon stimulation of those cells bathed in a calcium free environment. Trace C represents the response to membrane perturbation upon extracellular Ca^{2+} removal and inhibition of IP_3 sensitive stores. Data is represented as estimated change in cytosolic calcium (change in $[Ca^{2+}]_i$) recorded as a ratio of 340/380nm excitation for fura-2. Statistical analysis (D) (n=3 $^{**}P<0.01$ $^{***}P<0.001$)

5.2.4 Knockdown of TRPV4 expression with siRNA technology

Touch evoked stimulation of HCD cells evoked a transient increase in $[Ca^{2+}]_i$. This rapid response instigates the generation of calcium transients throughout neighbouring cells, a response thought to be crucial in aiding cell volume recovery (Tinel *et al.*, 2002). Responsible for detecting this osmotically induced signal is a stretch/mechanically activated receptor in the cell membrane, upon which, exposure to changes in osmolarity evokes a series of downstream calcium dependent signalling pathways ultimately restoring cell volume thus maintaining blood volume homeostasis. TRPV4, originally identified as a mechanoreceptor yet since, been shown to be receptive and activated upon exposure to hypotonic stress, led to seeking confirmation of expression levels in our collecting duct cell line of this protein. Both RT-PCR and western blot analysis confirmed TRPV4 expression.

The ability of these cells to respond to osmotic perturbation in conjunction with TRPV4 expression, led to the hypothesis that this receptor may be responsible for detection and subsequently transduction of an osmotically induced signal in the collecting duct cells of the kidney. To test this hypothesis; we employed siRNA technology to knock down TRPV4 expression in HCD cells.

The availability of three different siRNAs (invitrogen) led to initial optimisation in determining both the siRNA capable of achieving the greatest knockdown of TRPV4 expression and subsequently the concentration (80μg, 120μg 160μg) at which the transfection procedure appeared to be the most efficient. HCD cells were transfected with individual siRNAs or a combination of all three over a time course of 24, 48, 72 and 96 hours (figure 5.5). Of the three siRNAs transfected into the cell, siRNA 1, appeared to give the greatest knockdown in TRPV4 expression. The percentage knockdown was greatest at both 24 and 48 hours and it was found that variability in the concentration did not affect knockdown efficacy. Thus for future experiments it was decided that cells would be transfected with siRNA 1 (80μg) and for a time period of 24 hours.

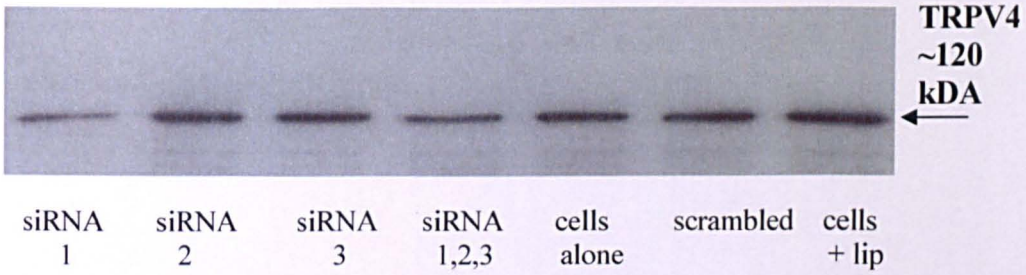

Figure 5.5: Optimisation of TRPV4 knockdown with siRNA. HCD cells were transiently transfected with one of three TRPV4 siRNAs over a period of 24, 48, 72 amd 96 hours. The above blot represents TRPV4 expression post 24 hours transfection. siRNA 1 (lane 1) appeared to give the greatest percentage knockdown of TRPV4 expression as compared to control conditions (lane 5). siRNA 2 (lane 2) and siRNA 3 (lane 3) appeared to exert little effect over the expression of TRPV4, whilst a combination of all three (lane 4) gave a result similar to that observed with siRNA 1. Appropriate controls of cells only (lane 5), cells + scrambled DNA (lane 6) and cells + lipofectamine (lane 7) were performed.

Having determined which siRNA was able to achieve the greatest percentage reduction in TRPV4 expression, HCD cells were then transfected with siRNA 1 (80μg) for 24 hours in preparation for functional analysis via microfluorimatry studies. Cells were seeded onto both 6 well plates and on APES treated coverslips. 24 hours post transfection, cells were harvested for protein analysis and microfluorimetry experiments performed on those cells which had been seeded down on coverslips (see section 5.2.6).

Western blot analysis (figure 5.6A) confirmed that transfection of HCD cells with TRPV4 siRNA1 resulted in approximately a 40 % reduction in TRPV4 expression (figure 5.6B).

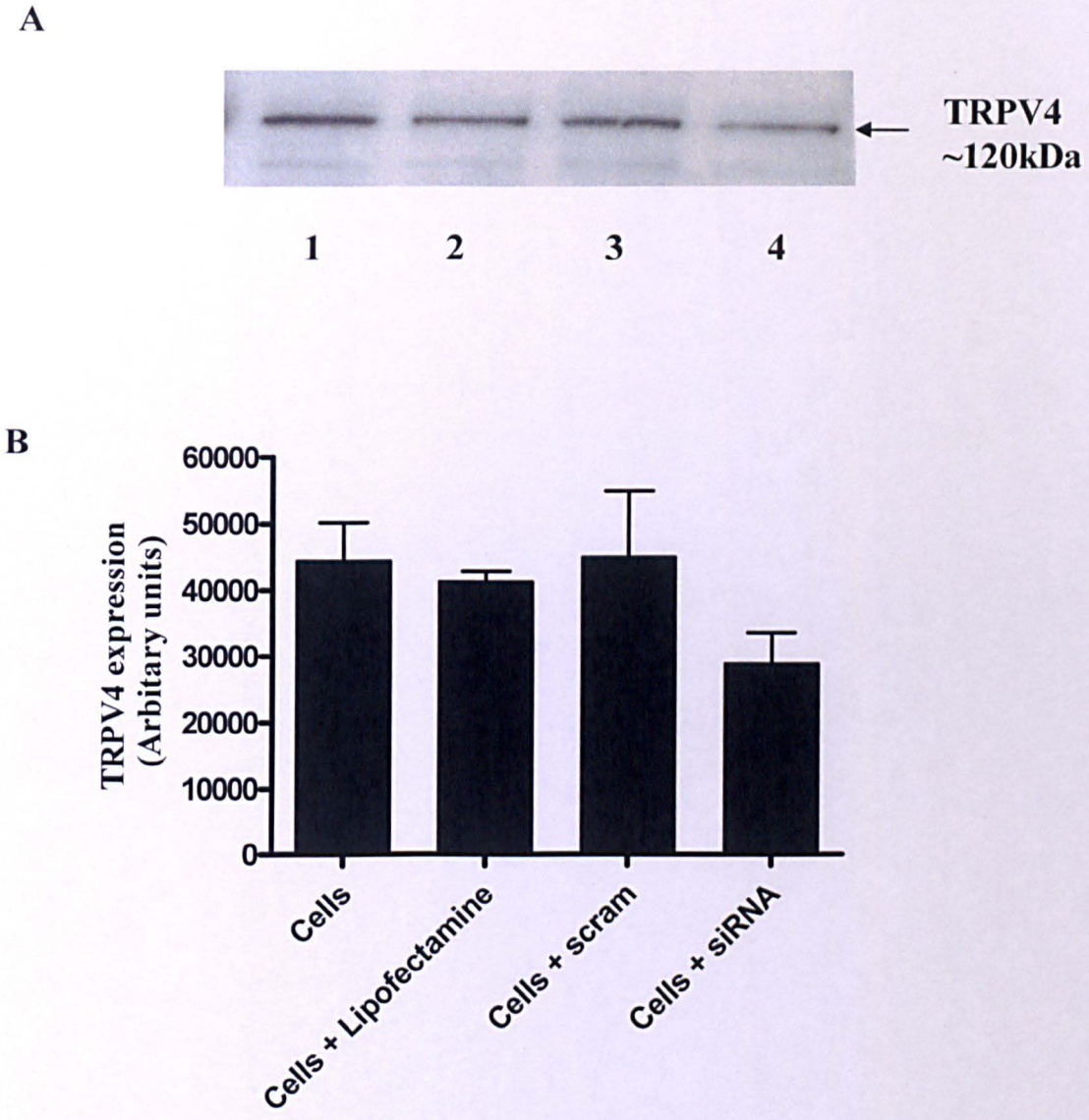

Figure 5.6: siRNA Knock-down of TRPV4 expression in HCD cells. Western blot analyses of HCD cell lysates (5µg protein/lane) using an antibody against human TRPV4 (120kDa) confirmed siRNA knock-down of TRPV4 expression in lane 4, as compared to control cells (lane 1, untransfected cells; lane 2, cells transfected with lipid alone; lane 4, cells transfected with scrambled siRNA). Knock-down reduced TRPV4 expression to approximately 65% of control (cells+ scrambled) (panel B). Results represent mean ± SEM n=4.

5.2.5 TRPV4 knockdown inhibits touch evoked changes in $[Ca^{2+}]_i$

Transiently transfecting cells with siRNA for TRPV4 significantly reduced TRPV4 protein expression in HCD-cells to approximately 65 % of control (figure 5.7) as confirmed by western blot analysis. Studies performed by Dr Dianne Wheelans in which Red Fluorescent Protein and anti-TRPV4 were co-transfected enabling identification of single transfected cells within a cluster of HCD-cells (figure 5.7C and 5.7D; representative of 4 separate experiments). Mechanical stimulation of an individual anti-TRPV4 cell (RFP-tagged cell-2) failed to significantly elevate $[Ca^{2+}]_i$ as previously observed under control conditions. However, mechanical stimulation of a non-transfected cell, cell-1 (figure 5.7B), elicited a rapid increase in $[Ca^{2+}]_i$, (figure 5.7G). Transfection with lipid, RFP alone or scrambled siRNA sequences did not alter responses to touch (Experiments performed by Dr Paul Squires). These data suggest that knock-down of TRPV4 expression inhibits the cells ability to both detect and respond to osmotically induced signals via a Ca^{2+} dependent mechanism.

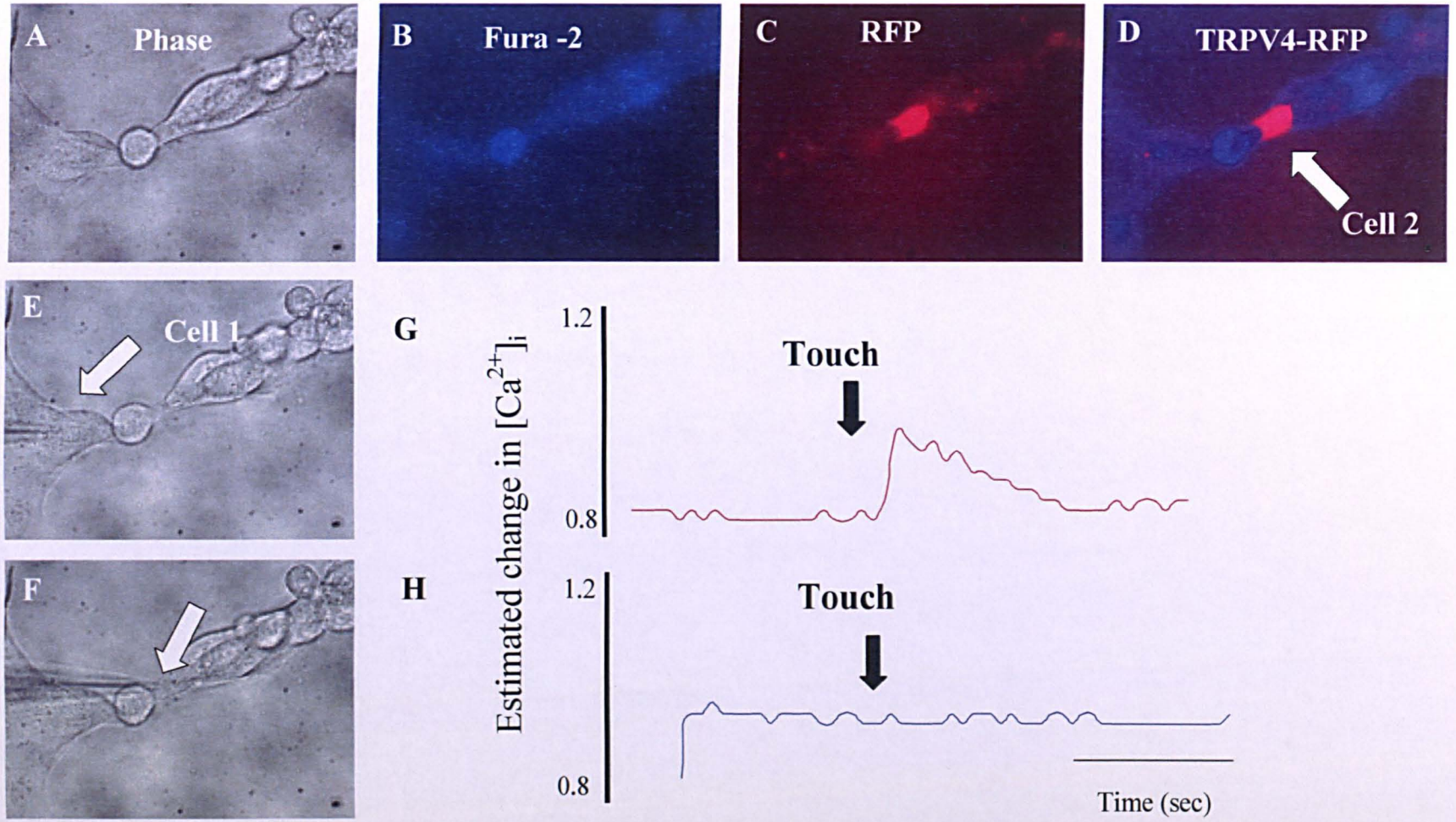

Figure 5.7 Knock-down of TRPV4 expression prevents touch-evoked changes in $[Ca^{2+}]_i$. The cell cluster was visualised either as a phase image (A,) loaded with fura-2 (B), optimised for RFP (C), and as an overlay of fura-2 fluorescence and RFP (D). Mechanical stimulation of a non-transfected cell (cell-1, F) evoked an increase in $[Ca^{2+}]_i$ (trace G). Touch-evoked stimulation failed to significantly elevate $[Ca^{2+}]_i$ in the RFP-tagged cell-2. These experiments were performed by Dr Dianne Wheelans and Dr Paul Squires.

5.3 Discussion

To avoid excessive alterations of cell volume, cells have developed and utilised a number of volume regulatory mechanisms. These mechanisms adjust cell volume by modifying a series of cellular functions, activating either a regulatory volume decrease (RVD) or a regulatory volume increase (RVI) (Montrose-Rafizadeh *et al.,* 1991). The inability to mount an efficient and appropriate RVD or RVI will result in either excessive cell shrinkage or cell swelling. The exposure of renal epithelial cells for example to changes in osmolarity necessitates the need for the initiation of cell volume regulatory processes, activation of which serves to restore cell volume preserving both integrity and function of the nephron.

Expressed in the kidney, the recently cloned transient potential cation channel (TRPV4) is gated by changes in extracellular osmolarity or membrane stretch (Strottman *et al.,* 2000). These mechanosensitive channels have a role in sodium re-absorption and regulate cell volume via a Ca^{2+} dependent mechanism (McCarty *et al.,* 1991, Christensen *et al.,* 1987). The inability to resolve changes in osmolarity or flow could have serious repercussions to sodium transport and may instigate secondary hypertension associated with renal diseases such as diabetic nephropathy. The current chapter examined the effect of touch evoked changes on intracellular calcium in a human collecting duct (HCD) cell line and assessed the contribution of both extra and intracellular calcium in aiding cell volume recovery. I have confirmed that cells of the human collecting duct (HCD) express functional TRPV4 mechanoreceptors, capable of transducing physical stimulation into transient changes in cytosolic calcium $[Ca^{2+}]_i$, a finding consistent with previous data linking membrane stretch in A6 cells to an elevation in $[Ca^{2+}]i$ as part of the regulatory response to a decrease in cell volume (Urbach *et al.,*1999). Touch evoked stimulation of HCD cells evoked a transient increase in $[Ca^{2+}]_i$, that propagated into adjacent cells. Through RNAi technology and single cell imaging, I have shown that transmission of this calcium signal is mediated via gap junctions comprised of the protein connexin 43 (Cx-43) (See chapter 6) (Hills *et al.,* 2006a). This synchronisation of activity is indicative of a high degree of cell-to-cell communication.

To fully understand the mechanisms associated with cell volume recovery it is key to determine how stimulus-response elements e.g. TRPV4; transduce changes in the physical state of the cell into intracellular signals that are able to propagate and regulate the function of the entire epithelium.

A primary function of the kidney is to maintain an osmotic equilibrium during the transition from diuresis to antidiuresis when cells become osmotically challenged. The response of cells to hypo-osmolality is believed to be a two-step process involving detection of increased cell volume via increased membrane stretch, accompanied by alterations in intracellular solute content. The end goal is restoration of cell volume via initiation of a Ca^{2+} dependent regulatory volume decrease (RVD). (Wong *et al.*, 1986, Christensen *et al.*, 1987, Mccarty *et al.*, 1991, Tinel *et al.*, 2002). The degree of cell swelling observed in those cells equipped to regulate their volume is accompanied by the subsequent loss of Cl^- and K^+ via the coordinated activation of Cl^- and K^+ channels (Okada et al., 2001). Associated with this hypo-osmotic response is a rise in $[Ca^{2+}]_i$, shown in many cell types to be the driving force behind increased Ca^{2+} dependent K^+ channel activity (Montroze-Rafizadeh *et al.*, 1991). In conjunction with previous data in which cells from the thick ascending loop of Henle (TALH) and human cervical cancer cells failed to regulate their cell volume in Ca^{2+} free medium (Shen *et al.*, 2001, Tinel *et al.*, 2002), I can hypothesise that Ca^{2+} serves as a key mediator in regulation of this recovery mechanism. Changes in $[Ca^{2+}]_i$ can occur via both Ca^{2+}influx and/or Ca^{2+} mobilisation pathways, both of which have been associated with RVD in various cell types. Certain cell types rely solely on calcium influx alone, a notion further supported by the cell's inability to avoid steep osmotic gradients in the presence of calcium channel blockers nifedipine and verapamil (Wong *et al.*, 1986), whilst contrary to these findings other cell types reportedly require the release of Ca^{2+} from intracellular stores (Terreros *et al.*, 1992). However, depletion of these intracellular stores can also, through store operated calcium entry, induce calcium influx across the plasma membrane resulting in a biphasic Ca^{2+} response in which the early transient phase of store mobilisation is maintained via a sustained phase of Ca^{2+} influx (Tinel H *et al.*, 1994, Tinel H *et al.*, 1997).

The current study provides supporting evidence of a role for TRPV4 in regulating cell volume through a Ca^{2+} dependent mechanism. Since increases in $[Ca^{2+}]_i$ can result from entry of Ca^{2+} from the extracellular space or release of Ca^{2+} from intracellular stores, the present study investigated the absolute requirement of extracellular Ca^{2+} on touch-evoked changes in $[Ca^{2+}]_i$.

In the absence of extracellular calcium the basal-to-peak amplitude of touch-evoked changes in $[Ca^{2+}]_i$ was significantly lower than that evoked by the same stimulus in calcium containing conditions. My finding that exposure to a calcium free solution did not abolish the $[Ca^{2+}]_i$ transient upon membrane perturbation highlighted a role for intracellular calcium stores in generation of this response. Previous studies have suggested that the rise of $[Ca^{2+}]_i$ during cell swelling is a consequence of both TRPV4-mediated Ca^{2+}-influx (Liu *et al.*,, 2006, Strottman *et al.*,2003), and Ca^{2+}-induced Ca^{2+}-release (CICR) from thapsigargin-sensitive intracellular stores, (Urbach *et al.*, 1999). Current data suggest that although Ca^{2+}-influx is not essential in eliciting a rise in $[Ca^{2+}]_i$, Ca^{2+}-entry potentiates the amplitude of the increase in $[Ca^{2+}]_i$, a potential requirement for initiation of a RVD response (Jakab *et al.*, 2002, Okada *et al.*, 2001, Rothstein *et al.*, 1992, Urbach *et al.*, 1999*)*. The reduced $[Ca^{2+}]_i$ response observed in HCD cells in both the absence of extracellular calcium and upon inhibition of the ATPase with thapsigargin, highlights a role both plasma membrane Ca^{2+} entry and the release from intracellular stores. Knockdown of TRPV4 via siRNA prevented the generation of touch-evoked changes in $[Ca^{2+}]_i$ and supports my hypothesis that TRPV4 is essential in transducing osmotic signals into changes in $[Ca^{2+}]$ that stem from both thapsigargin sensitive store release and Ca^{2+} entry across the membrane.

In conclusion, in the current study, I have shown that touch evoked stimulation of TRPV4 channels in HCD cells initiates a rise in cytosolic calcium levels, a consequence of both intracellular store release and $[Ca^{2+}]_i$ influx. Together these are able to instigate an RVD ultimately restoring cell volume. In conditions in which there appears to be a deregulation of cell volume regulatory mechanisms, for example in end stage renal failure, previously associated with Type II diabetes, a reduced capacity for detecting alterations in the surrounding osmotic state accompanied by diminished cell-to-cell communication may further enhance the

damaged status of the cell ultimately contributing to the development of renal disease.

Chapter 6

A role for gap junctions in HCD cell-to-cell communication

6.1 Introduction

Exposure of renal epithelial cells to changes in osmolality initiates cell volume regulatory processes, which restore cell volume, preserving both integrity and function. In Type II diabetic patients presenting with glycosuria, exposure to a hypotonic extracellular milieu will induce cell swelling. Compensatory mechanisms possessed by the cell ensure that cell volume is restored via instigation of a calcium dependent RVD (McCarty *et al.*, 1991). Since the renal tubule is responsible for the regulation and control of cellular solute composition, effective reabsorption across the renal epithelia is a prerequisite for cell volume constancy and therefore requires the collective efforts of cells operating in unison.

In chapter 5 touch evoked stimulation was employed as a surrogate form of osmotic stress and single cells within cell clusters were challenged by physical deformation to assess the degree of change in cytosolic calcium. Touch evoked stimulation was found to induce a transient increase in $[Ca^{2+}]_i$ through the mechanoreceptor TRPV4. However, in the continued presence of the stimulus, a high degree of co-operativity between these cells was illustrated via transmission of the calcium signal away from the original discrete point of contact throughout the cell cluster. This suggests a possible role for gap junctions in mediating transmission. Gap junctions facilitate intercellular communication allowing for the transfer of ions and small molecules such as Ca^{2+} and nucleotides between coupled cells (Goodenough *et al.*, 1996). Cell-to-cell communication of this type ensures the integration of metabolic and physiological activities allowing for adaption of function to match the immediate needs of cells within a cluster (Haefliger *et al.*, 2004). In this chapter I assess the role of Cx-43 mediated gap-junctions in the transfer of touch-evoked Ca^{2+}-waves between HCD cells.

6.2 Results

6.2.1 Expression of connexins in HCD cells.

My former suggestion that propagation of a touch-evoked Ca^{2+} dependent signal is consistent with previously reported high levels of connexin expression in renal epithelia. RT-PCR analysis confirmed expression of Cx-26, Cx-31, Cx-31.1, and Cx-40 at the mRNA level in HCD cells (figure 6.1)

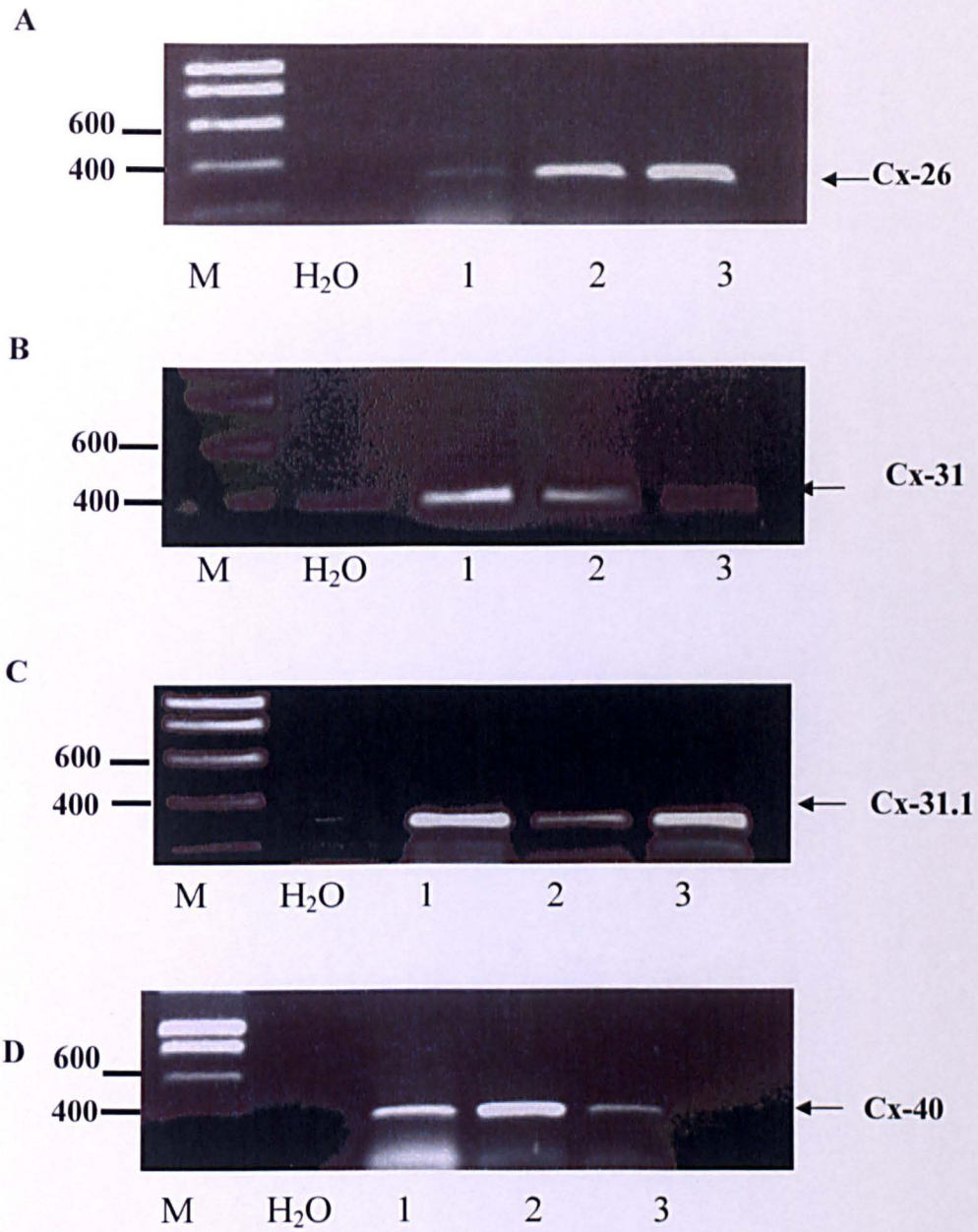

Figure 6.1: RT-PCR analysis of connexins in HCD cells. Panels, A, B, C and D represent RT-PCR analyses using primers specific for human Cx-26, Cx-31, Cx-31.1 and Cx-40 respectively. PCR products were observed in three different RNA preparations (1, 2 and 3) corresponding to mRNA expression for each connexin. A negative control was performed with water.

6.2.2 HCD cells express the gap junction protein Cx-43

Cx-43 has been reported as showing predominant expression levels in the collecting duct (Guo *et al.*, 1998). Studies confirmed the presence of Cx-43 mRNA and protein in HCD cells. RT-PCR analysis of several RNA preparations from HCD cells

revealed PCR products representative of Cx-43 mRNA (figure 6.2A) giving rise to a band at 597bp. Protein expression was determined by Western blotting (figure 6.2B). Western blot analyses revealed a band at approximately 43kDa representative of that expected for Cx-43.

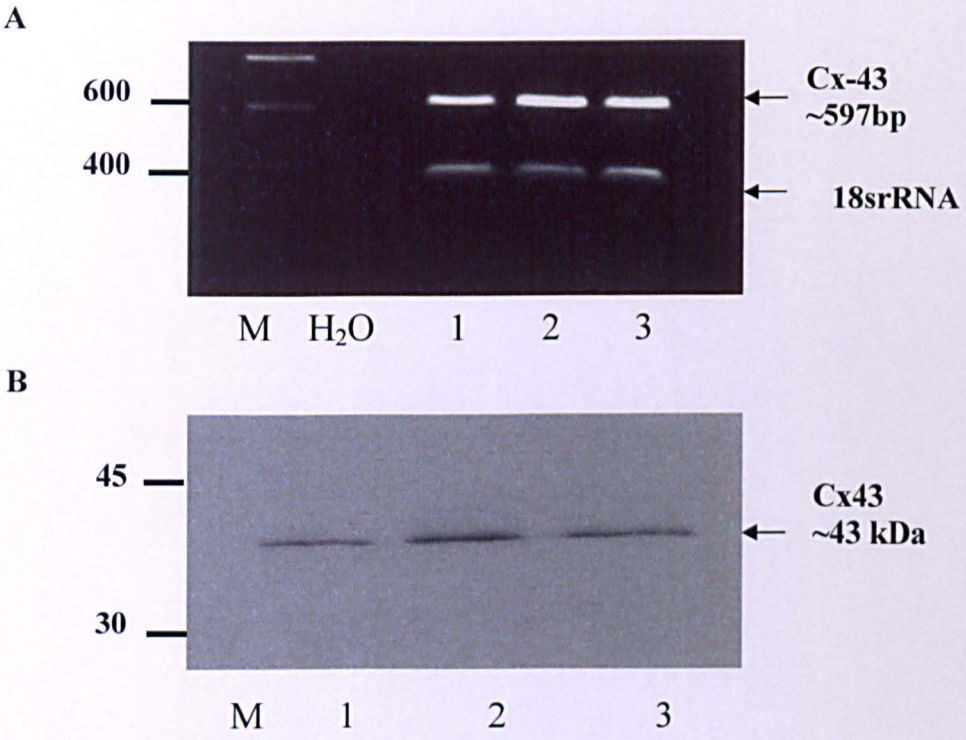

Figure 6.2: Expression of Cx-43 mRNA and protein in HCD-cells. Panel A represents RT-PCR analyses using primers specific for human Cx-43. PCR products were observed in three different RNA preparations (1, 2 and 3) corresponding to mRNA expression for Cx-43. Western blot analyses (panel B) of HCD cell lysates (5µg protein/lane) using an antibody against human Cx-43 confirmed the presence of the Cx-43 protein in three different protein preparations (1, 2 and 3). A protein band of approximately 43kDa was detected.

As a control for specificity I pre-incubated the primary anti-Cx-43 antibody with the Cx-43 immunizing peptide prior to addition of the antibody to the membrane, all other steps in the procedure were identical. Competition of the primary antibody completely abolished the signal upon ECL detection (figure 6.3).

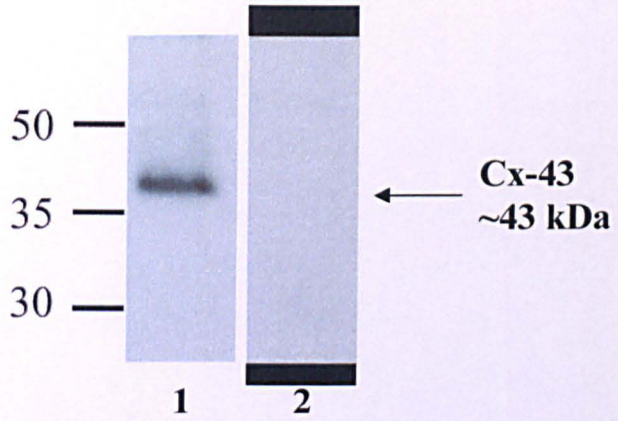

Figure 6.3 Expression of Cx-43 protein in HCD-cells. Western blot analyses of HCD cell lysates (lane 2, 5μg protein/lane) using an antibody against human Cx-43 confirmed the presence of the protein giving rise to a protein band of approximately 43kDa. The control included Cx-43 antibody pre-absorbed with a 100-fold excess of immunising peptide (lane 2).

6.2.3 The localization of Cx-43 in HCD cells

The distribution of Cx-43 in HCD cells was examined by immunocytochemistry (figure 6.4). Immunofluorescence staining with a polyclonal antibody against Cx-43 confirmed that Cx-43 protein expression was localized to the cell membrane with intense perinuclear staining as represented in overlay image (panel c).

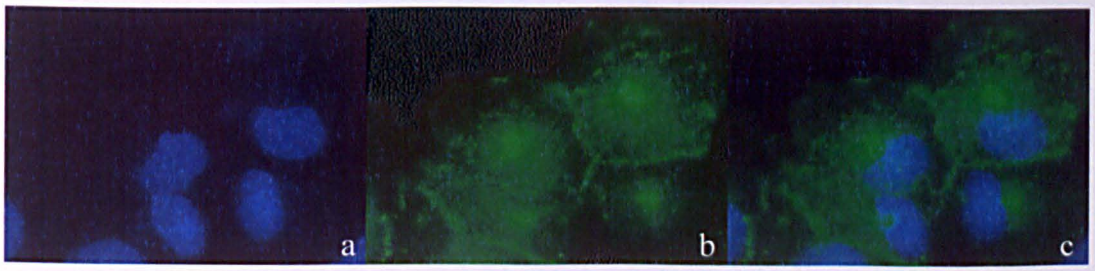

Figure 6.4: Immunocytochemical staining of Cx-43 in HCD-cells. HCD cells were stained with a polyclonal antibody against human Cx-43. Panels A and B show nuclear (DAPI, blue) and Cx-43 (Alexa-488 green) staining respectively. Panel C depicts an overlay of Cx-43 immunolocalization (green) and nuclear staining (blue). Note the intense Cx-43 staining at the cell periphery.

6.2.4 Touch evoked changes in cytosolic calcium in HCD cells.

There are numerous reports that mechanical stimulation of a single cell within a cell cluster results in a propagated increase in $[Ca^{2+}]_i$ that spreads via gap junctions through several tiers of surrounding cells (Sanderson *et al.*, 1994). In chapter 5 touch evoked stimulation was employed as a surrogate form of osmotic stress to determine the effect on $[Ca^{2+}]_i$. Physical stimulation of a single HCD cell evoked an increase in cytosolic calcium (Section 5.2.1). Transmission of this touch evoked $[Ca^{2+}]_i$ signal away from the point of stimulation led to the supposition that gap junctions may play a role in cell-to-cell communication between HCD cells and may therefore mediate transmission of this touch evoked Ca^{2+} signal. Having established that HCD cells exhibit high basal levels of connexin expression (section 6.2.1), function was assessed via Ca^{2+} microfluorimetry. I examined the effect of touch evoked stimulation on the propagation of touch-evoked Ca^{2+}-signals in the presence and absence of the gap junction uncoupler heptanol. As previously observed, touch evoked stimulation under control conditions evoked a transient increase in $[Ca^{2+}]_i$ (figure 6.3 A and B) which propogates throughout the cell cluster. In the presence of the gap junction uncoupler heptanol (1mM) physical stimulation of an individual HCD-cell evoked a transient increase in cytosolic calcium. However, this signal failed to propagate to neighbouring cells (figure 6.3 C and D) supporting our hypothesis that functional gap junctions are a requirement in mediating transmission of this touch evoked Ca^{2+}- signal.

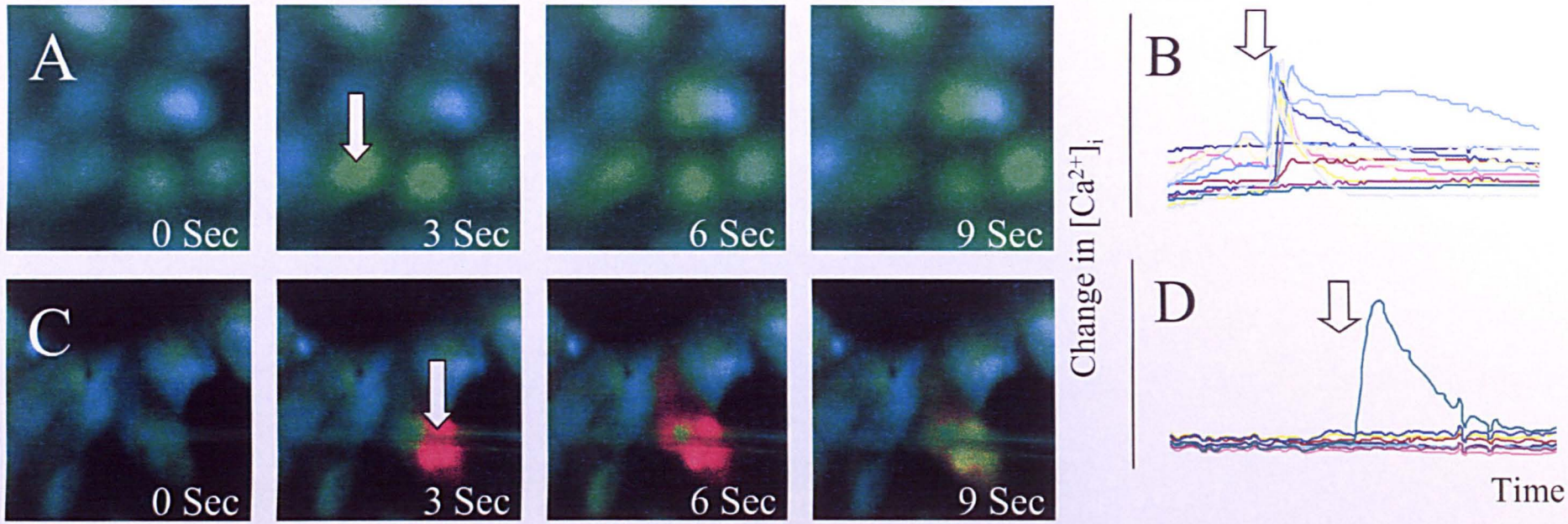

Figure 6.5: Changes in $[Ca^{2+}]_i$ in HCD-cells evoked by mechanical stimulation. Panel A demonstrates the rapid spread of a touch-evoked Ca^{2+}-transient within a 16 cell cluster of HCD-cells. A single cell is mechanically stimulated at 0 seconds. The evoked Ca^{2+}-signal propagates away from the point of stimulation into adjacent cells (3, 6 and 9 seconds). Elevation in $[Ca^{2+}]_i$ in each cell is shown in panel B. Panel C shows data from a similar experiment in a cluster of 8 HCD-cells following application of the gap-junctional uncoupler heptanol. Note that over a similar time-course (0-9 seconds) touch-evoked changes in $[Ca^{2+}]_i$ no longer propagate into adjacent cells. These data are confirmed in panel D, which shows the lack of a Ca^{2+}-response in all cells except that cell directly stimulated by mechanical stress. Data is represented as estimated change in cytosolic calcium (change in $[Ca^{2+}]_i$) recorded as a ratio of 340/380nm excitation for fura-2/AM. Results are representative of 5 separate experiments.

6.2.5 Dye transfer between cells.

To further determine the role of gap-junctions in cell-to-cell communication within my model, Lucifer yellow was injected into an individual HCD-cell and dye spread within the cell cluster was monitored. As seen in figure 6.5 (upper panel), within 3minutes Lucifer yellow had permeated away from the site of injection into coupled cells. Application of the gap-junctional uncoupler heptanol (1mM; lower panel) prevented any dye spread between neighbouring cells. Data representative of 3 separate experiments.

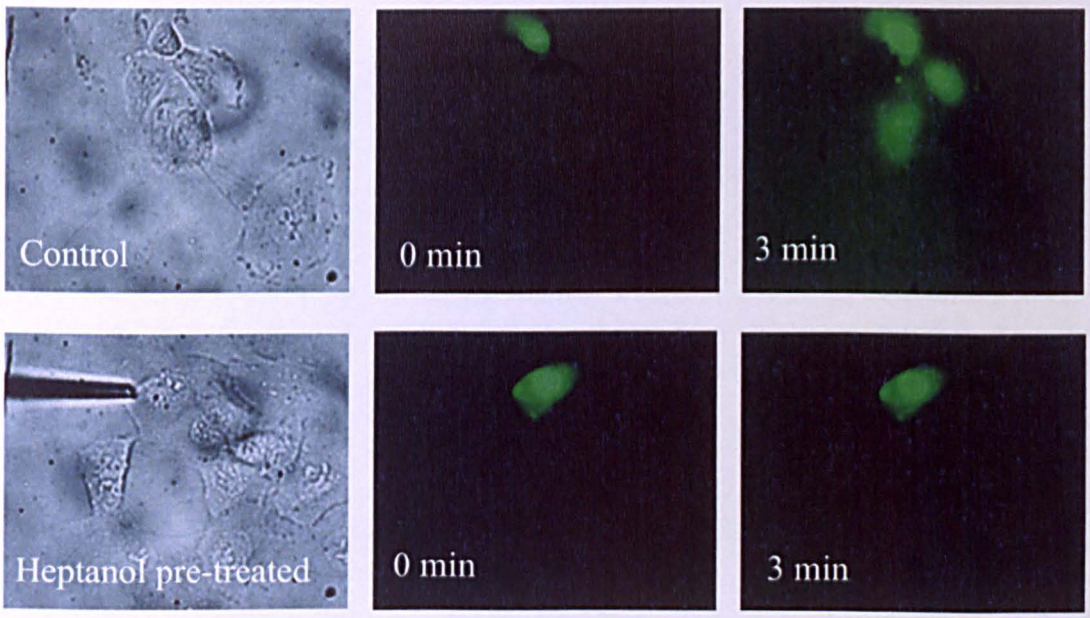

Figure 6.6: Lucifer yellow dye transfer between HCD cells.
The transfer of Lucifer yellow suggests direct cell-to-cell communication between coupled HCD-cells. The monochrome plates illustrate phase images of HCD-cell clusters. The fluorescence (fluorescein) image of the same cell clusters following single-cell injection with Lucifer yellow is shown at 0 minutes (upper and lower panels). The same field of view is recorded 3 minutes after injection of the dye either in the absence (3 minutes, upper panel) or presence (3 minutes, lower panel) of heptanol (1mM). Note: dye spread into neighbouring cells is only seen in the absence of the gap-junctional uncoupler.

6.2.6 Optimisation of siRNA knockdown of Cx-43 in HCD cells

To confirm a role for Cx-43 in mediating signal transmission, RNAi technology was employed. HCD cells were transfected with Cx-43 siRNA (Santa Cruz). Conditions were optimised for both RNA and lipofectamine content and efficiency of Cx-43 knockdown monitored over 24, 48, 72 and 96 hours. To determine transfection efficiency, cells were also transfected with a scrambled RNA conjugated to a fluorescein dye enabling us to visualise and determine percentage DNA uptake into the cell (figure 6.7). Fluorescence microscopy confirmed a transfection rate of approximately 70%.

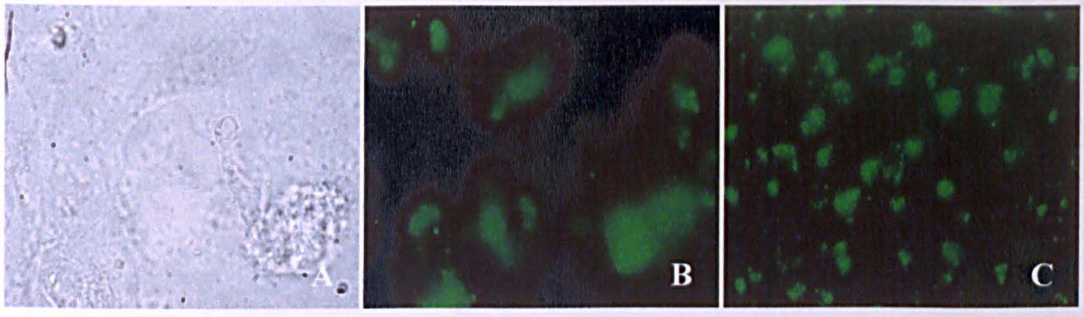

Figure 6.7 Transfection of HCD cells with fluorescein conjugated scrambled siRNA. Cells were transfected with scrambled siRNA conjugated to fluorescein, Panel A represents a phase image of an HCD cell cluster (x100), whilst panel B and panel C represent the positive cells. Transfection visualised at x100 and x20 magnification respectively.

Having optimised for siRNA (80μg) and Lipofectamine (4μl) (see chapter 5), a series of time course studies were devised in which cells were transfected over a 24, 48, 72 and 96 hours. Appropriate controls were set up in which cells were left either untreated or incubated with the transfection reagent alone, to ensure that any gene knockdown was a direct result of RNA inhibition as opposed to an artefact of the transfection procedure. Western blot analysis (figure 6.8) confirmed successful Cx-43 knockdown following siRNA transfection at 24, 48 hrs, 72 and 96 hours. 24 hours post transfection was used for the following experiments.

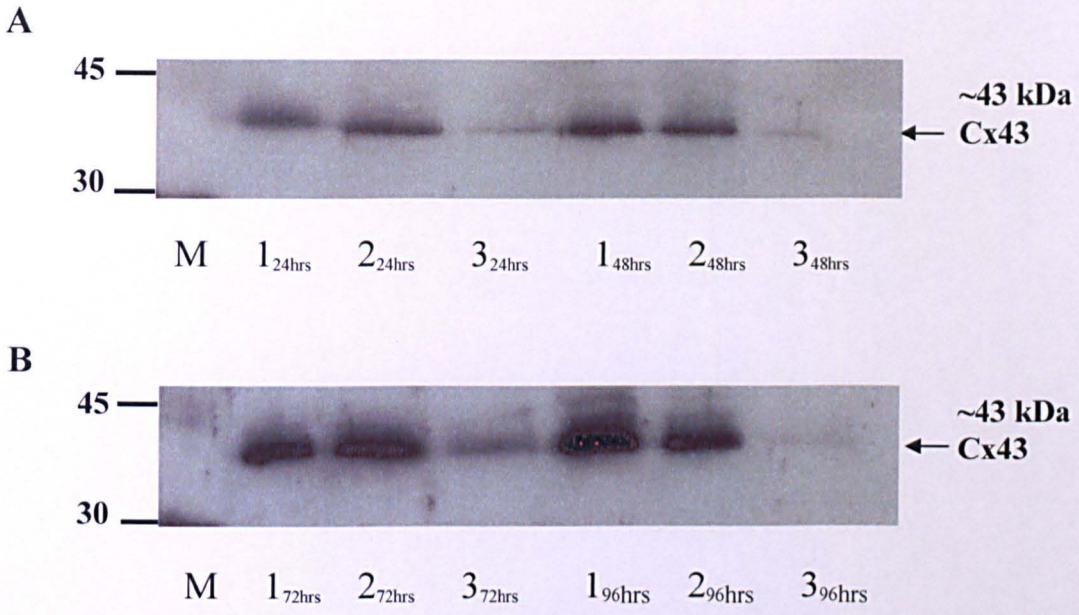

Figure 6.8 siRNA knockdown of Cx-43 in HCD cells. Cells were transfected with Cx-43 siRNA for 24, 48, 72 and 96 hours. Cells were harvested and western blot anaylsis used to determine the level of protein knockdown in my cells. Cx-43 protein expression was successfully knocked down at 24 and 48 hours (panel A lane 3) and 72 and 96 hours (panel B lane 3). Lane 1 is representative of untreated HCD cells. Lane 2 represents cells post-incubation with lipofectamine. Lane 3 represents siRNA transfected cells.

6.2.7 siRNA knockdown of Cx-43 in HCD cells

Cells were transfected with a mix of siRNA (80μg) and lipofectamine (4μl) and left for 24 hours. Controls were set up of untreated cells, cells incubated with transfection reagent alone and cells transfected with scrambled siRNA.

Western blot analyses of HCD cell lysates (figure 6.9A) confirmed siRNA knock-down of Cx-43 expression (lane 3) as compared to cells under control conditions. Densitometric analysis confirmed approximately a 50% reduction in expression as compared to control conditions (cells + scrambled siRNA) (figure 6.9B)

A

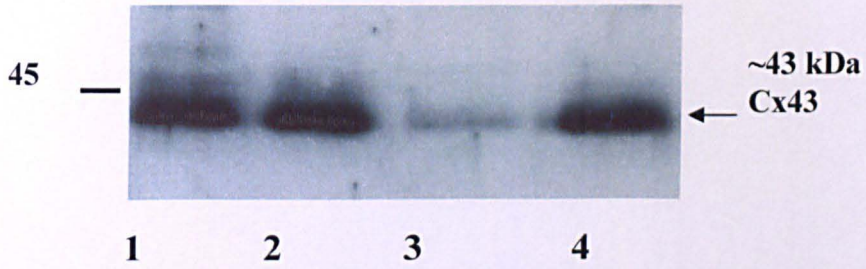

B

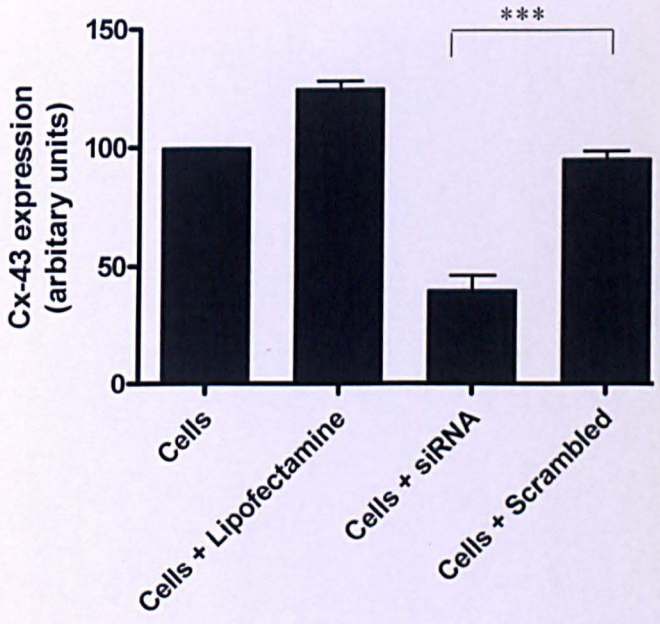

Figure 6.9 Knockdown of Cx-43 expression: In panel A western blot analyses of HCD cell lysates (5μg protein/lane) using an antibody against human Cx-43 (43kDa) confirmed siRNA knock-down of Cx-43 expression in lane 3, as compared to control cells (lane 1, untransfected cells; lane 2, cells transfected with lipid alone; lane 4, cells transfected with scrambled siRNA). Knock-down reduced Cx-43 expression to approximately 50% of control (cells + scrambled) (B). Results represent mean ± SEM; n=3; *** $P< 0.001$.

6.2.8 Cx-43 siRNA knockdown

6.2.8.1 Knock-down of Cx-43 expression prevents cell-to-cell communication

Following optimization of transfection procedure, HCD cells were transfected as described in section 6.2.6 with either control (scrambled) siRNA or Cx-43 siRNA. Cells were then microinjected with membrane impermeant Lucifer yellow. Whilst Lucifer yellow spread from the point of injection throughout the cell cluster with scrambled siRNA, dye transfer was prevented in those cells transfected with Cx-43 siRNA (figure 6.10).

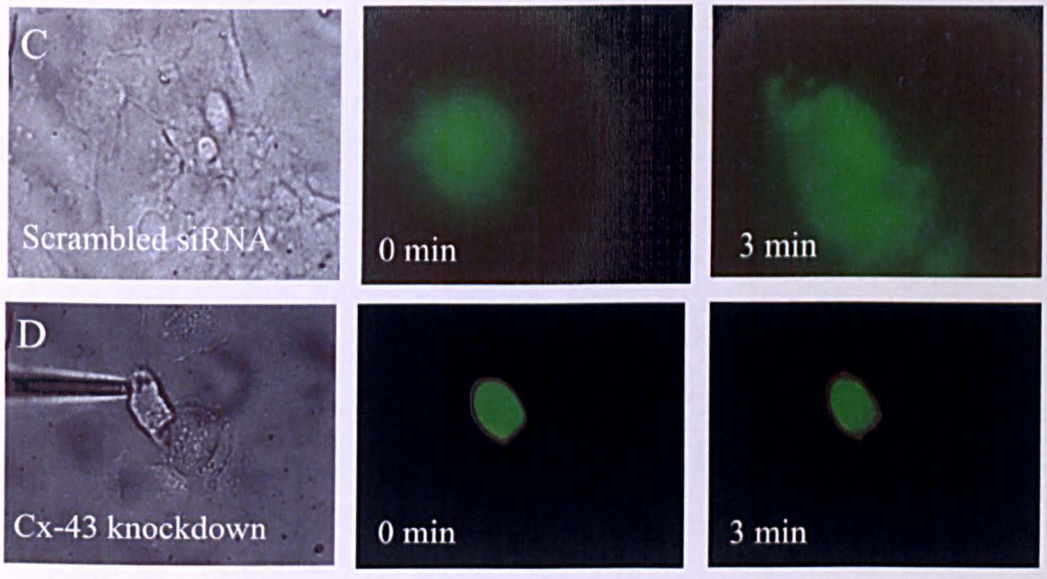

Figure 6.10: Lucifer yellow dye transfer between transfected HCD cells. The transfer of Lucifer yellow suggests direct cell-to-cell communication between coupled HCD-cells. The monochrome plates illustrate phase images of HCD-cell clusters. The fluorescence image of the same cell clusters following single-cell injection with Lucifer yellow is shown at 0 min. The same field of view is recorded three minutes after injection of the dye HCD cells transfected with scrambled siRNA (C), or in Cx-43 knockdown HCD cells (D). Note; dye spread into neighbouring cells is only seen scrambled siRNA cell clusters.

In conjunction with these experiments, mechanical stimulation of an individual cell within a cluster of anti-Cx-43 transfected HCD-cells evoked a transient increase in cytosolic Ca^{2+} that failed to propagate into neighbouring cells (figure 6.11B). A

similar experiment using scrambled DNA (figure 6.11A) failed to negate cell-to-cell communication of Ca^{2+}-signals between coupled HCD-cells.

Two further controls were performed on untreated cells (figure 6.12A) and cells pre-incubated with transfection reagent (figure 6.12B). As expected, touch evoked stimulation evoked a transient increase in intracellular calcium at the discrete point of contact and subsequently propagated throughout adjacent cells in the cluster.

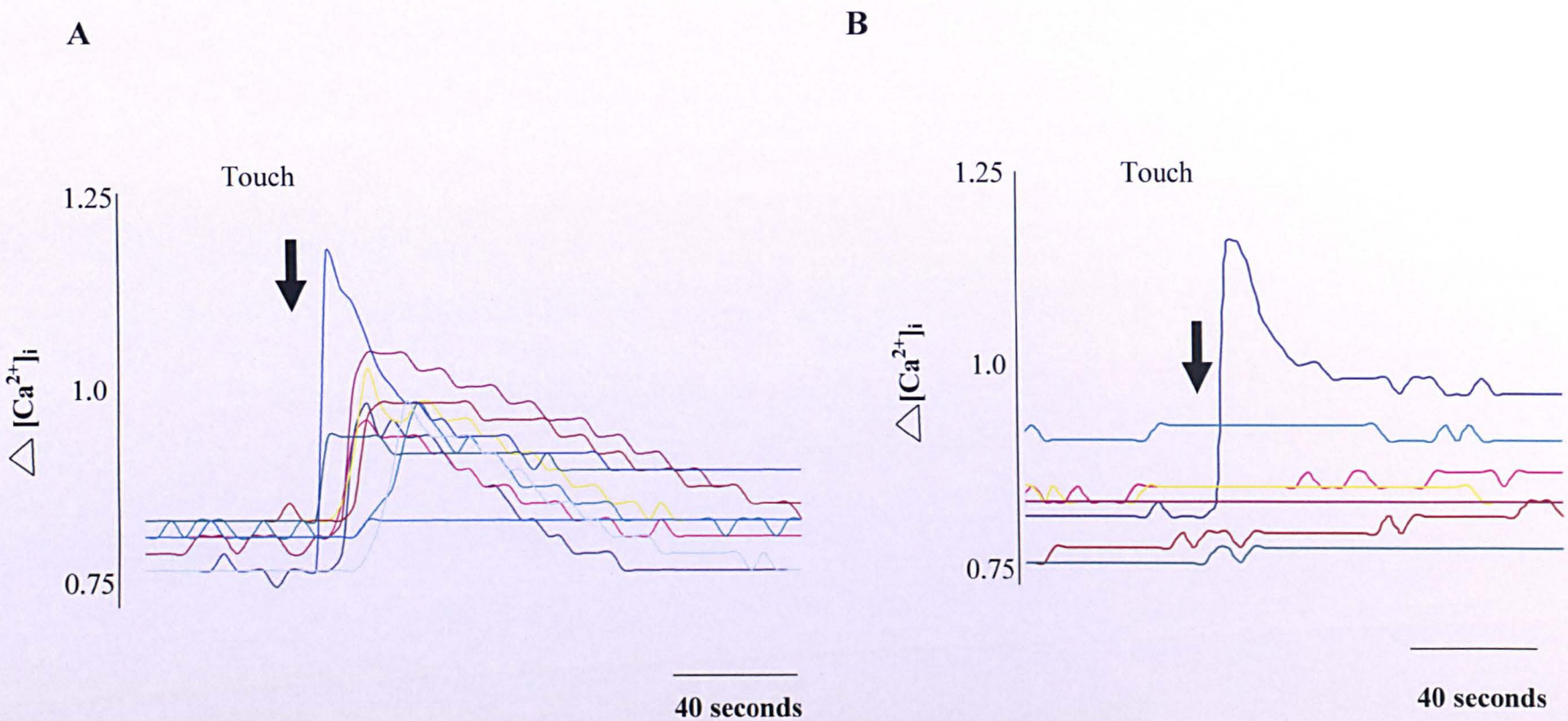

Figure 6.11 Knock-down of Cx-43 expression prevented intercellular communication of touch-evoked changes in $[Ca^{2+}]_i$. Mechanical stimulation of an individual cell transfected with scrambled siRNA evoked a transient increase in cytosolic Ca^{2+} that propagated into neighbouring cells (A). A similar experiment using Cx-43 siRNA (B) evoked a transient increase in cytosolic Ca^{2+}. Failure of this signal to propogate between coupled HCD-cells suggests that knock-down of Cx-43 expression reduces cell-to-cell communication in HCD-cells. NB. ↓ denotes point of mechanical stimulation.

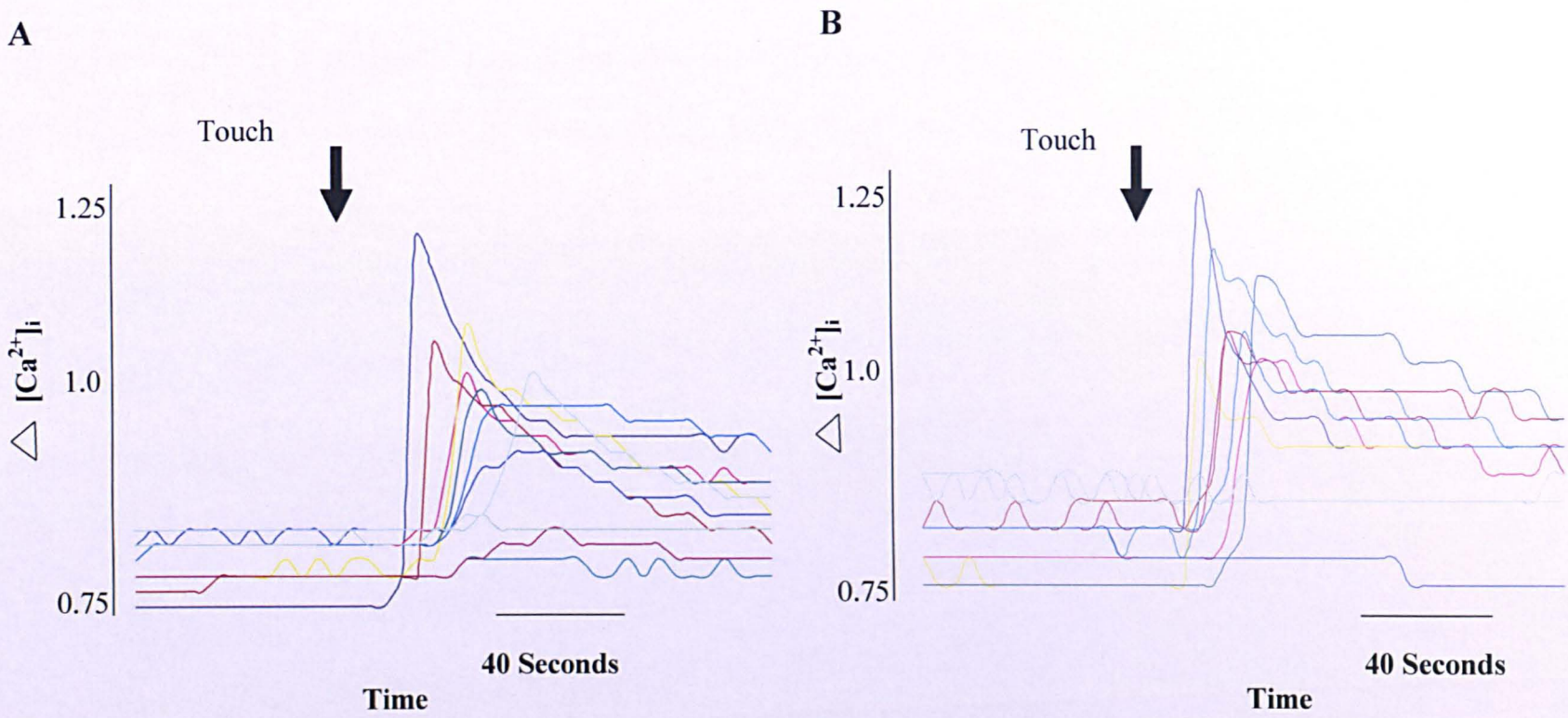

Figure 6.12 Signal transmission upon touch evoked stimulation is unaltered in cells treated with transfection reagent. Mechanical stimulation of an individual cell within a cluster of HCD-cells evoked a transient increase in cytosolic Ca^{2+} that propagated into neighbouring cells (A). Touch evoked stimulation of HCD cells which has been treated with transfection reagent lipofectamine evoked a similar response, confirming that lipofectamine has no effect on Ca^{2+} signalling (B).

6.2.8.2 Knockdown of Cx-43 in HCD cells following co-transfection with anti-Cx-43 siRNA and Red Fluorescent Protein (RFP) using the siLentGene U6 Cassette RNA Interference System.

In a series of supporting experiments performed by Dr Dianne Wheelans, the U6 strike cassette system was employed (Hills *et al.*, 2006a). Co-transfection with red fluorescent protein (RFP) and anti-Cx-43 enabled identification of single transfected cells within a cluster of HCD-cells (figure 6.13). Mechanical stimulation of a non-transfected cell (cell-1, panel A) evoked an increase in $[Ca^{2+}]_i$ that propagated between other, non-transfected, coupled cells (figure 6.13 trace A). The touch-evoked signal failed to significantly elevate $[Ca^{2+}]_i$ in the transfected cell (RFP-tagged cell-2 panel B). However, mechanical stimulation of cell-2 elicited a rapid increase in $[Ca^{2+}]_i$, (figure 6.13 trace B) indicating that Cx-43 knock-down, did not interfere with the cell's ability to respond to touch.

Transfection with scrambled siRNA (figure 6.14) did not alter responses to touch. These data further confirm that knock-down of Cx-43 expression reduced cell-to-cell communication in HCD-cells.

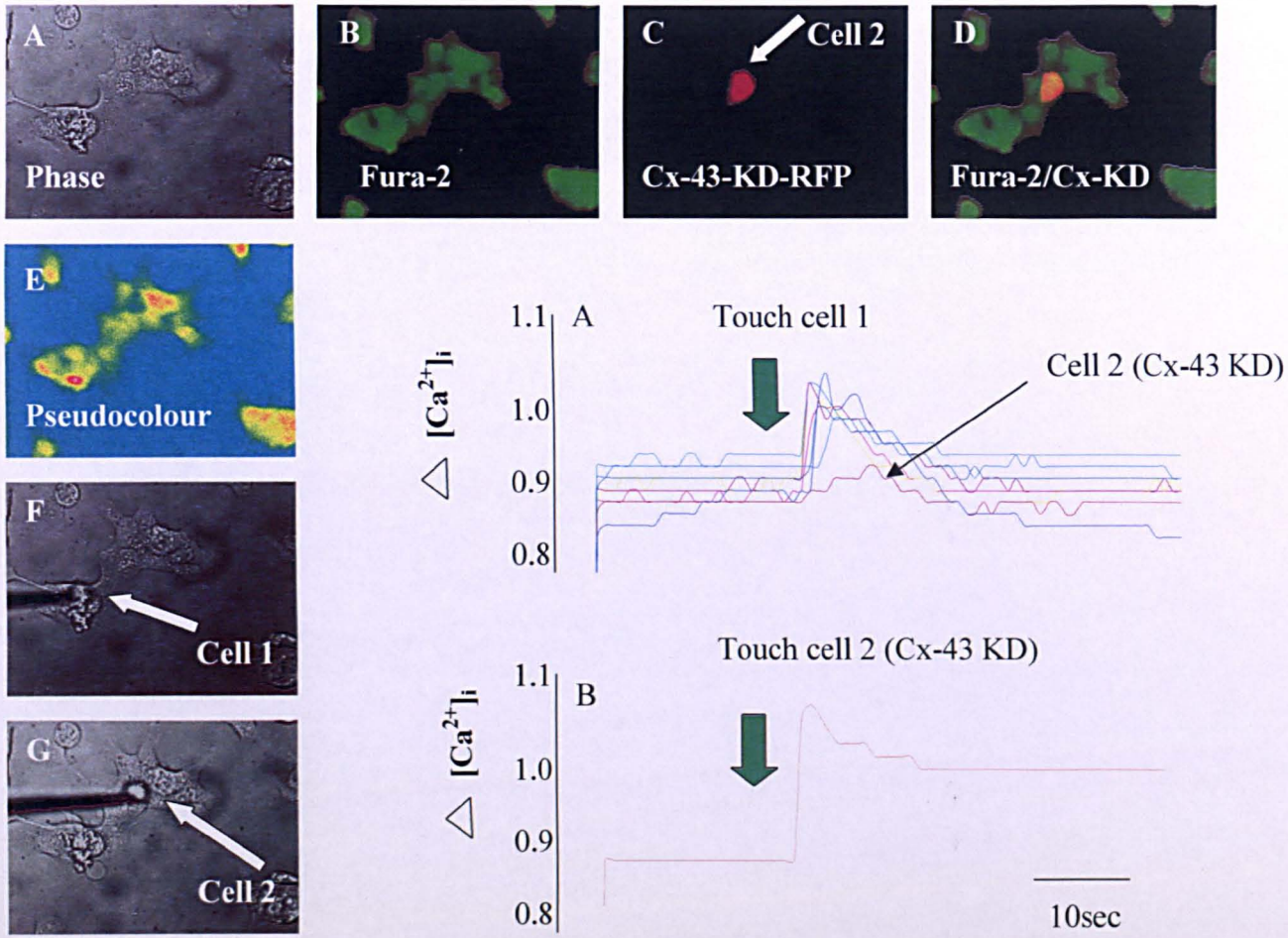

Figure 6.13. Knock-down of Cx-43 expression prevents intercellular communication of touch-evoked changes in $[Ca^{2+}]_i$. The cell cluster was visualised either as a phase image (A,) loaded with fura-2 (B), optimised for RFP (C), and as an overlay of fura-2 fluorescence and RFP (D). Mechanical stimulation of a non-transfected cell (cell-1, F) evoked an increase in $[Ca^{2+}]_i$ that propagated between other, non-transfected, coupled cells (trace A). The touch-evoked signal failed to significantly elevate $[Ca^{2+}]_i$ in the RFP-tagged cell-2. To confirm cell viability the micro-electrode was repositioned to stimulate transfected cell-2 (G). Mechanical stimulation of cell-2 elicited a rapid increase in $[Ca^{2+}]_i$, (trace B). These experiments were performed by Dr Dianne Wheelans and Dr Paul Squires. (Hills *et al.*, 2006a)

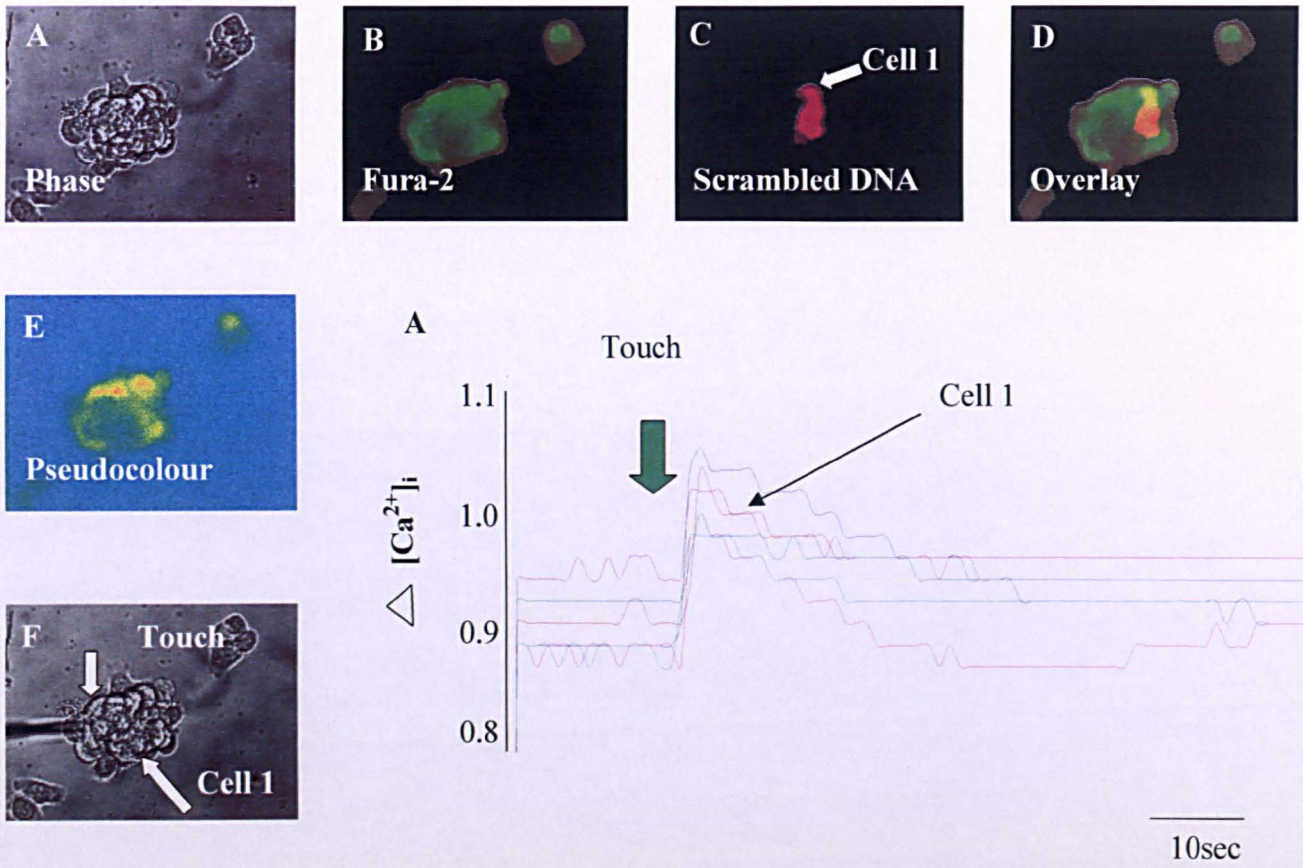

Figure 6.14 Transfection of HCD cells with scambled siRNA fails to negate touch evoked generation of an intracellular calcium signal: The cell cluster was visualised either as a phase image (A,) loaded with fura-2 (B), optimised for RFP (C), and as an overlay of fura-2 fluorescence and RFP (D). Mechanical stimulation of a transfected cell (cell-1, F) evoked an increase in $[Ca^{2+}]_i$ that propagated between other, non-transfected, coupled cells (trace A). These experiments were performed by Dr Dianne Wheelans and Dr Paul Squires (Hills *et al* 2006a).

6.2.9 Cell-to-cell communication in HCD cells is not mediated via paracrine release of ATP

The generation of calcium transients upon mechanical stimulation of the cell membrane has been linked to one of two pathways. Whilst the first pathway involves transmission of a secondary messenger, either Ca^{2+} or Ins (1,4,5) P3 through gap junctions (Enomoto *et al.*, 1992), the second pathway involves the release of ATP into the extracellular medium (Cotrina *et al.*, 1998). Through its paracrine activities ATP is able to act on its corresponding P_2 purinergic receptors expressed on the cell membrane, subsequently eliciting a rise in $[Ca^{2+}]_i$ (Bidet M et al., 2000).

To examine the role of purinergic-receptors in intercellular communication, I repeated the touch evoked calcium studies in the presence/absence of suramin, an established blanket purinoreceptor antagonist. Application of suramin (50μM; a concentration known to block P2 purinergic receptors (Hauge-Evans *et al.*, 2002) failed to negate touch evoked changes in intracellular calcium (figure 6.15) suggesting that cell-to-cell communication was independent of ATP mediated paracrine mechanisms. A bolus of ATP demonstrated the expression of functional purinergic receptors. Transmission of the touch evoked signal in the presence of suramin in conjunction with the siRNA knock down studies would suggest that whilst contributory effects of ATP to signal transmission cannot be dismissed, gap junctions appear to play the predominant role in cell-to-cell communication of those cells in the collecting duct.

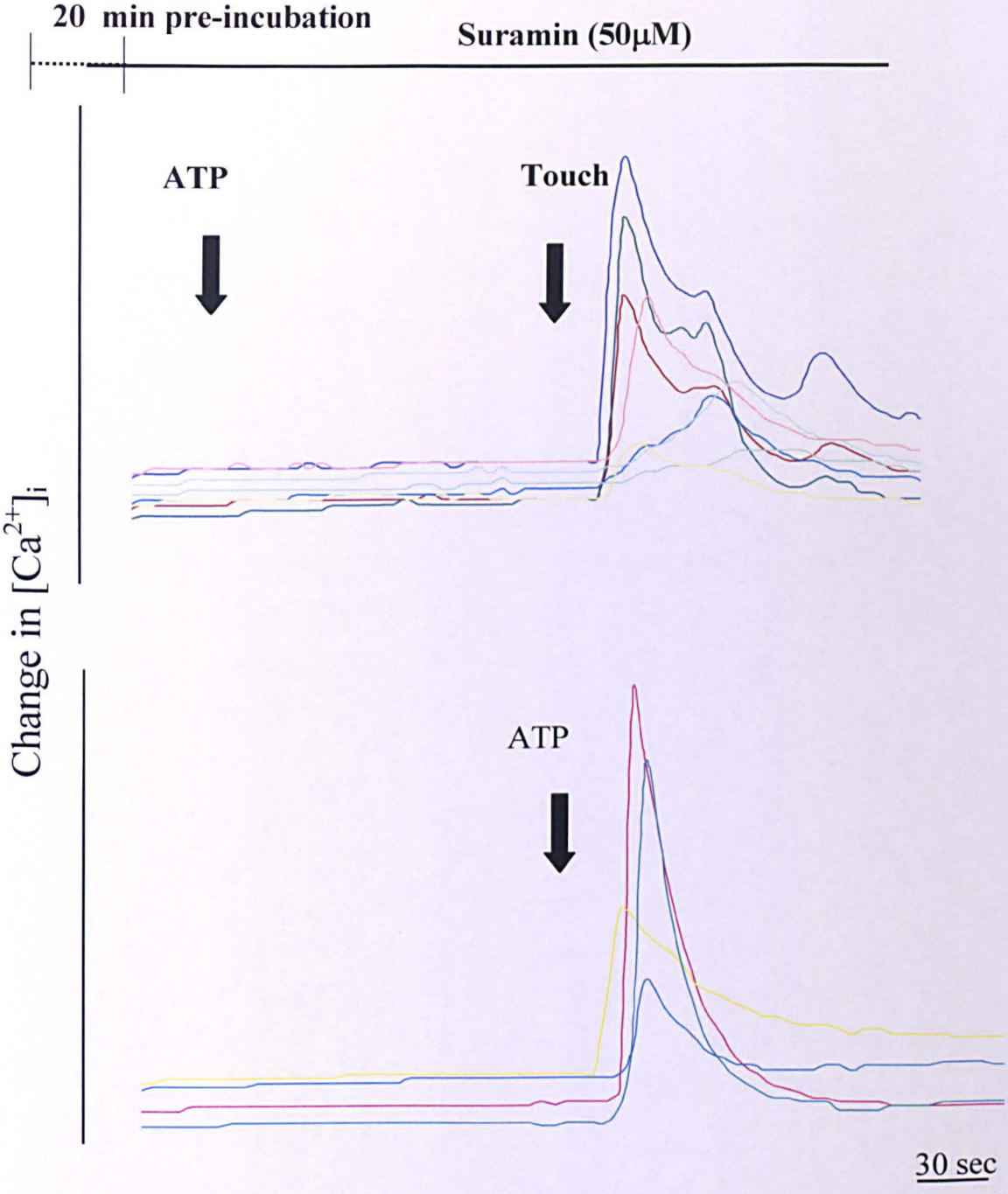

Figure 6.15: Suramin has no effect on touch-evoked changes in $[Ca^{2+}]_i$ in HCD-cells. In the top panel cells were pre-incubated with the P2 purinergic receptor antagonist suramin (50μM) for 20min. Cells were then transferred to the microscope where fresh suramin was applied. ATP (50μM final bath concentration) was applied as a single bolus. There was no discernable change in cytosolic Ca^{2+}. Subsequent touch-evoked changes were obtained in the continued presence of suramin.(n=3). In a separate series of experiments ATP alone (50μM bolus; bottom panel) evoked a rapid, transient increase in $[Ca^{2+}]_i$ (n=3). The data indicate that HCD-cells express functional P2-purinergic receptors, but that these are not responsible for mediating touch-evoked changes in $[Ca^{2+}]_i$.

6.3 Discussion

Intracellular calcium is critical in cell volume regulation and cell-to-cell communication. My results demonstrated that touch evoked stimulation of an HCD cell evoked an increase in intracellular calcium that propagated as an intercellular calcium wave throughout the cluster. These observations suggested a high degree of cell-to-cell communication and implicated a possible role for gap junctions in mediating signal transmission.

In the current chapter the distribution and expression of the gap junction protein Cx-43 was examined. HCD cells express Cx-43 at both the mRNA and protein level. Cx-43 immunoreactivity was localized to both the perinuclear and membrane region of HCD cells. Uuncoupling of gap-junctions, using heptanol, attenuated the transfer of Ca^{2+} signals and Lucifer yellow dye transfer between cells. These data suggest a high degree of organisation between cells of the human collecting duct, which is in part mediated via the direct transfer of information through Cx-43 mediated gap junctions.

Generation of a calcium wave following mechanical stimulation has been reported previously in various cell types including airway epithelia (Sanderson *et al.*, 1990), mammary epithelia (Enomoto *et al.*, 1992), glial cells, (Charles et al., 1993) and aortic endothelia (Demer *et al.*, 1993). Two models have been proposed by which these intercellular calcium waves may be transmitted. Firstly, either inositol triphosphate and/or calcium diffusion between adjacent cells via gap junctions mediated propogation (Sanderson *et al.*, 1990, Boitano *et al.*, 1992). In conjunction with my previous findings (chapter 5), there are numerous reports of mechanical stimulation evoking a rise in $[Ca^{2+}]_i$ as a direct consequence of both Ca^{2+} release from intracellular stores and the influx of extracellular Ca^{2+} through mechanically-activated channels. Propagation of this mechanically induced signal has subsequently been shown by to be mediated via gap junctions (Churchill *et al.*, 1996). The alternative model suggests that a local diffusable synchroniser could mediate co-operativity between cells via a paracrine route. It is well documented that mechanical stress not only elicits a rise in $[Ca^{2+}]_i$ (Sachs *et al.*, 1992) but can also result in the release of ATP. A number of studies have suggested that ATP can be released

through hemichannels into the extracellular space (Cotrina *et al* 1998) and previous reports in isolated basophilic leukaemic cells and hepatocytes have reported propogation of this ATP calcium evoked signal. Unlike the intracellular mode therefore which relies on gap junctions to pass Ca^{2+} and/or Ins (1,4,5) P_3 from cell to cell as a means of communication, the extracellular mode of cell-to-cell communication involves the release of ATP; which subsequently acts as a secondary messenger diffusing to (Hoyle, 1999).

Lucifer yellow and microfluorimetry studies in the presence of the gap junction uncoupler heptanol further support my hypothesis that signal transmission in HCD cells is mediated via gap junctions. Further clarification as to whether a gap junction or P2 receptor mediated pathway contributed to the transmission of calcium waves was assessed by RNAi technology. In HCD cells transfected with anti-Cx-43 siRNA, touch evoked stimulation evoked a transient increase in $[Ca^{2+}]_i$ that failed to propagate and Cx-43 knock down attenuated Lucifer yellow dye transfer suggesting that Cx-43 comprised gap junctions represent the predominant means by which HCD cells communicate. However, since connexins have been shown to be directly involved in controlling the release of ATP (Cotrina *et al.,* 1998), knockdown of Cx-43 expression may negate this response, thus whilst confirming a role for gap junctions in signal transmission they prevent us from a direct assessment of whether signal transmission is a direct result of ATP release from the hemichannels as opposed to direct transfer of signalling intermediates through gap junctions. To further support my data and eliminate a role for ATP and thus the extracellular route as the predominant pathway in enabling transmission of an osmotically induced signal in HCD cells, microfluorimetry was performed on HCD cells in which a bolus of ATP had been administered post pre-incubation with the P2 receptor blocker suramin. As expected, in the presence of suramin, the addition of ATP failed to evoke a calcium response due to P2 receptor inhibition. However, upon touch evoked stimulation in the presence of suramin, the efficacy and velocity of mechanically evoked calcium waves were unaltered, indicating an alternative mechanism by which these cells are able to communicate. The data presented in this chapter suggest that whilst a possible contribution to signal transmission via the paracrine activities of ATP should not be dismissed, gap junctions through an intracellular messenger such as Ca^{2+} or Ins (1,4,5) P_3 appear to form the predominant means by which HCD cells

are able to co-ordinate their activity. Although HCD cells express several members of the connexin family (section 6.2.1), failure of touch evoked stimulation in a Cx-43 siRNA transfected cell to generate a signal which propagates throughout, indicates that these other connexins are unable to compensate in such situations in which Cx-43 may become redundant.

Chapter 7

Glucose-evoked alterations in connexin-43-mediated cell-to-cell communication

7.1 Introduction

Gap junctions play an important role in cell-to-cell communication, allowing for the transfer of both small ions and molecules between adjacent cells. Cell-to-cell coupling allows surrounding cells to lock into a particular frequency of cellular activity, ensuring a simultaneous response across the epithelial layer. The co-ordination of cellular activity via cell-to-cell coupling is a pre-requisite for the maintenance of cell homeostasis. In the kidney, efficient and appropriate re-absorption of sodium within the cortical collecting duct (CCD) depends upon an integrated response of the entire epithelium. If compromised, the consequences are severe, with dramatic repercussions for both cell volume homeostasis and functionality of the nephron. The loss of compensatory mechanisms, there to protect from renal damage may result in overt complications associated with diabetic nephropathy and end stage renal disease (ESRD). Injury or loss in number of visceral epithelial cells of the renal glomeruli (podocytes) as a consequence of glomerulosclerosis or renal disease results in increased Cx-43 expression in rats (Yaoita *et al.*, 2002). This up-regulation of Cx-43 expression is also seen in inflammatory renal disease (Hilliis *et al.*, 1997) and in the kidneys of hypertensive rats (Haefliger *et al.*, 2001). However, compensatory renal growth in mice has been associated with a transient decrease in gap-junction expression and cell-to-cell communication (Li *et al.*, 2002). Cell-to-cell communication within retinal micro-vessels is reduced in streptozotocin-induced diabetic rats (Oku *et al.*; 2001), a situation also observed in vascular cells (Inoguchi *et al.*, 2001) and bovine aortic endothelial cells in response to elevated glucose (Inoguchi *et al.*; 1995, Kuroki *et al.*; 1998). These changes in connexin expression may have important repercussions for macro-vascular dysfunction seen in diabetes such as macroangiopathy, whilst the glucose-dependent down-regulation of Cx-43 protein expression and gap-junctional mediated intercellular communication between bovine retinal pericytes (Li *et al.*, 2003), endothelial cells (Fernandes *et al.*, 2004) and rat retinal epithelial cells

(Gomes *et al.*; 2003) indicates a role in micro-vascular complications such as diabetic retinopathy.

In the current chapter I have assessed the effect of high glucose on both Cx-43 expression and Cx-43 mediated cell-to-cell coupling.

7.2 Results

7.2.1 Up-regulation of Cx-43mRNA and protein expression in response to high glucose.

Previous studies in bovine retinal cells (Fernandes *et al.*, 2004) and rat microvascular endothelial cells (Sato et al 2002) have shown that intercellular communication may be reduced under conditions of high glucose. This reduced level of gap junctional intercellular communication (GJIC) has been linked to decreased levels of Cx-43 expression in various cell types (Inoguchi *et al.*, 2001, Kuroki *et al.*, 1998). In chapter 6 (section 6.2.1), I confirmed that HCD cells express Cx-43 at both the mRNA and protein level. In this chapter I have examined the effect of glucose on Cx-43 expression and function. To test for a role of glucose in Cx-43 expression, HCD cells were incubated in a low glucose (5mM) medium for 2 days. After an overnight period of serum starvation cells were then treated with 25 mM glucose for 24 and 48 hours. RT-PCR analysis demonstrated cells grown in high glucose medium had significantly increased Cx-43 expression at the RNA level at both 24 hours and 48 hours (figure 7.1, 146.2 % ± 8.49 % as compared to 48 hours at 186.8 % ± 7.8%).

Western blot analysis confirmed that cells grown in high glucose medium exhibited increased Cx-43 protein expression at both 24 (175.2 % ± 15.2 %) and 48 hours (234 % ± 12.7 %) of control (5mM) at 48 hours (figure 7.2).

A

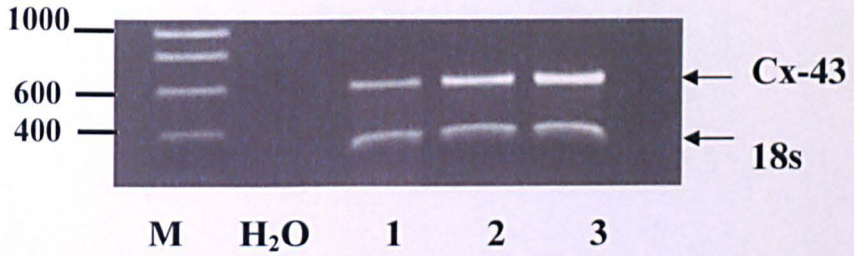

B

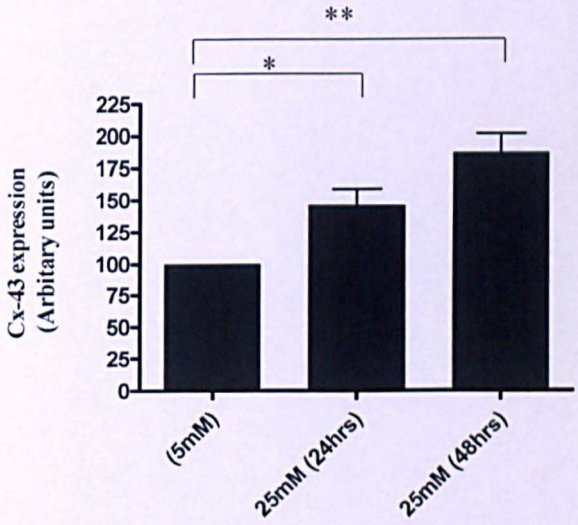

Figure 7.1 Effect of high glucose on Cx-43 mRNA expression. HCD cells were incubated in 5mM (low glucose) or 25mM (high glucose) glucose for periods of 24 and 48 hours. Representative RT-PCR analysis (A) products were obtained at 596bp fom cells which had been treated with high glucose for periods of 24 (lane 2) and 48 hours (lane 3). (B) Statistical analysis confirmed mRNA expression was increased at both 24 and 48 hours. Results represent mean ± SEM; n=3; * $P<0.05$, ** $P< 0.01$.

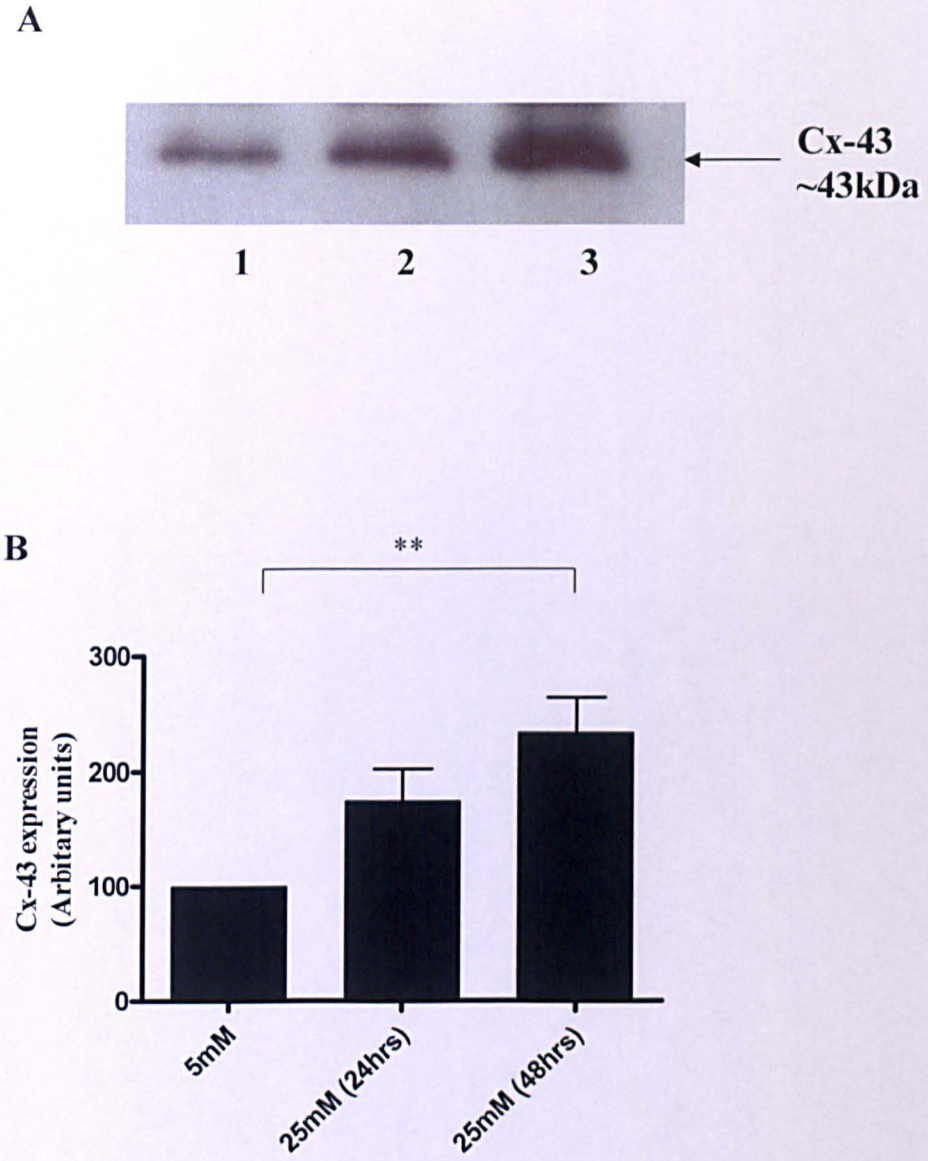

Figure 7.2: Effect of high glucose on Cx-43 protein expression. HCD-cells were incubated in 5mM and 25mM glucose for 24 and 48 hours. (A) Representative western blot analysis using an anti-Cx-43 antibody illustrated an upregulation in protein expression at both 24 (lane 2) and 48 hours (lane 3) as compared to control conditions at 5mM (lane 1). (B) Statistical analysis of changes in Cx-43 protein expression. Results represent mean ± SEM; n=4; ** $P< 0.01$.

To control for glucose induced osmotic alterations, HCD cells were incubated in mannitol (20mM). After 48 hours mannitol was found to increase Cx-43 expression by only 29% of the glucose evoked change seen under identical experimental conditions (figure 7.3).

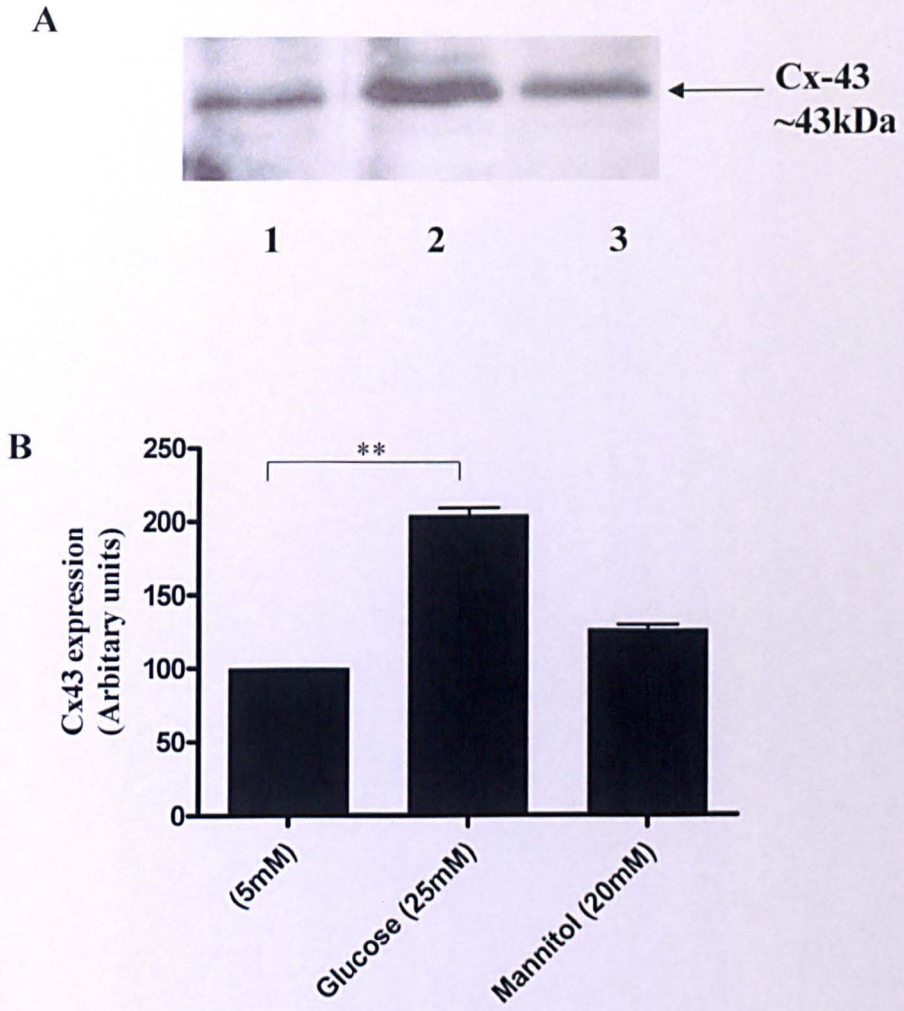

Figure 7.3: Exposure of HCD cells to mannitol (25mM) for 48 hours upregulated Cx-43 protein expression. HCD-cells were incubated under control (5mM) conditions and 25mM glucose and 25mM mannitol for 48hours. (A) Representative Western blot analysis using an anti-Cx-43 antibody illustrates upregulation in protein expression under both high glucose (lane 2) and high mannitol (lane 3) conditions as compared to control conditions at 5mM (lane 1). (B) Analysis of changes in Cx-43 protein expression. Results represent mean ± SEM; n=3; ** $P< 0.01$.

7.2.2 Prolonged exposure to glucose returns Cx-43 expression levels to near basal.

Cells were incubated with a low glucose (5mM) medium for 2 days and then serum starved overnight. They were then incubated in high (25mM) glucose for 8 days. Following an 8 day period of elevated glucose exposure, Cx-43 expression in HCD cells returned to near basal levels (figure 7.4). Restoration of Cx-43 expression may

represent compensatory mechanisms employed by HCD cells to maintain both cell structure and integrity.

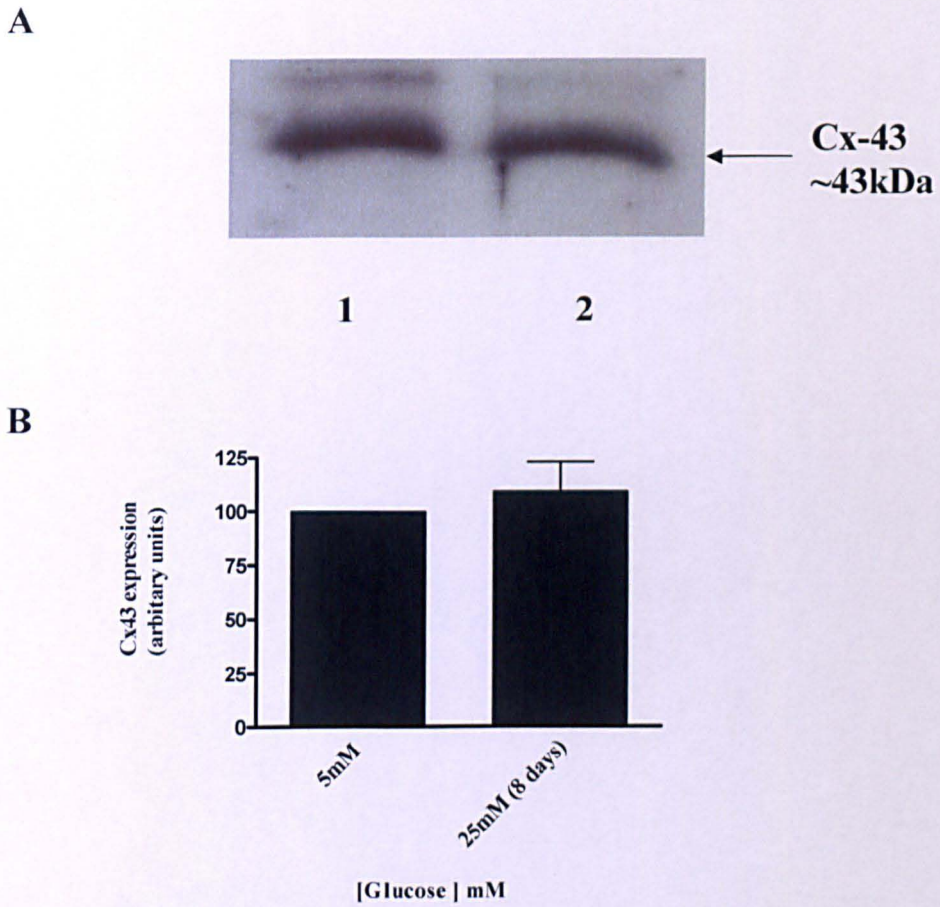

Figure 7.4: Cx-43 protein expression in HCD cells after an 8 day incubation in high glucose. HCD-cells were incubated in 5mM and 25mM glucose for 8 days (A) Representative Western blot analysis using an anti-Cx-43 antibody illustrates no difference in Cx-43 expression under both control (lane 1) and high glucose conditions (lane 2). (B) Statistical analysis of changes in Cx-43 protein expression. Results represent mean ± SEM; n=4 $P>0.05$

7.2.3 Elevated levels of calcium up-regulate Cx-43 expression

Cells were placed in a low glucose (5mM) media for 2 days and then serum starved overnight. The following day cells were treated over a 24 hour time course with the calcium ionophore ionomycin (1μM) for 4, 6, 8, 12 and 24 hours. Ionomycin induced a time-dependent increase in Cx-43 expression and was significantly increased at both 6 (282.7% ± 18.5 %) and 8 (403.7 % ± 25.7 %) hours.

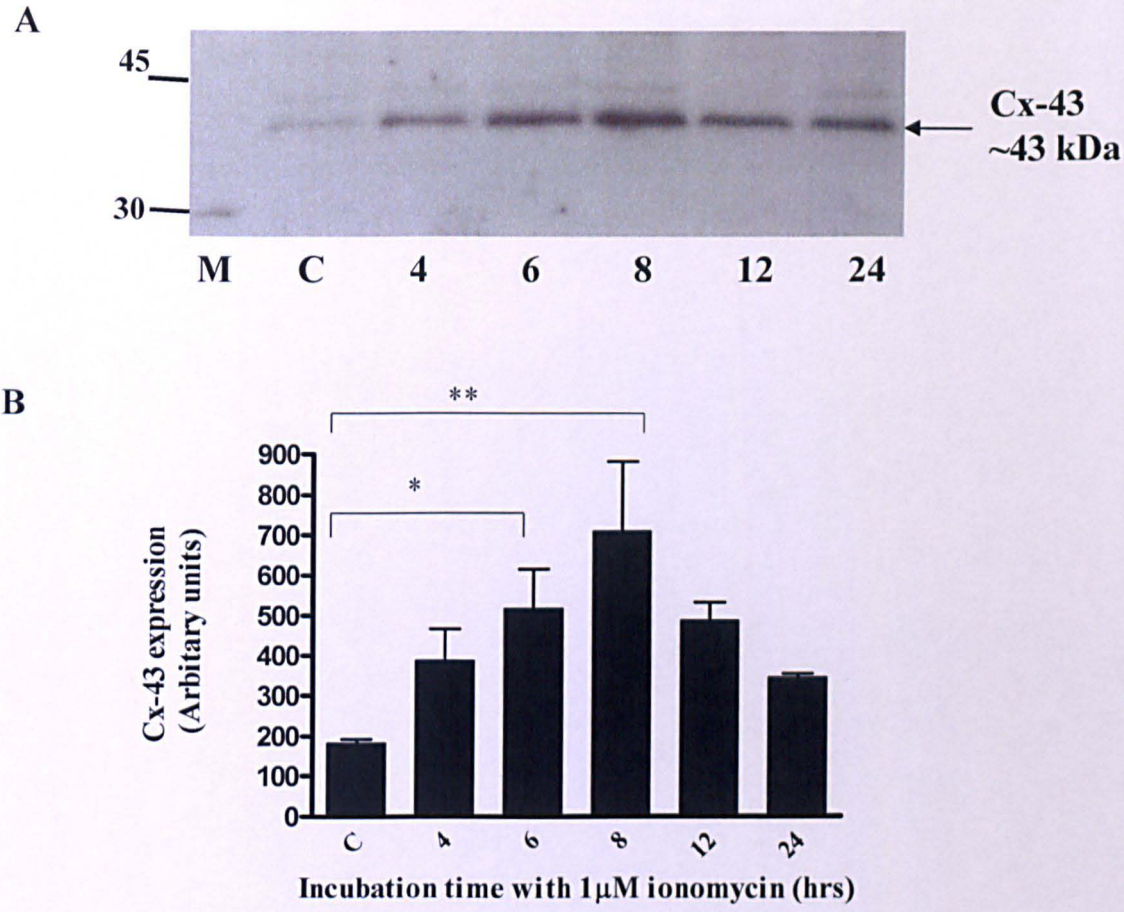

Figure 7.4 Effect of elevated calcium on Cx-43 protein expression in HCD cells. HCD-cells were incubated with ionomycin (1μM) over a 24 hour time period. (A) Representative Western blot analysis using an anti-Cx-43 antibody (B) statistical analysis of changes in Cx-43 protein expression. Results represent mean ± SEM; n=3; * P<0.05, ** *P*< 0.01.

7.2.4 The cytokine TGF-β1 down-regulates Cx-43 expression.

TGF-β1, a cytokine with powerful fibrogenetic effects is key in the development of renal hypertrophy, with glucose induced upregulation of both TGF-β mRNA and protein observed in both diabetic animal models and diabetic nephropathy (Sharma *et al.*, 1995, Rocco *et al.*, 1992). To assess any contribution by TGF-β1 to the glucose mediated upregulation of Cx-43, HCD cells were treated as described previously (7.2.2) and incubated with the cytokine for 4, 6, 8, 12 and 24 hours. Application of TGF-β1 (2ng/ml) to HCD cells exerted a biphasic response. At 4, 6

and 8 hours TGF-β1 inhibited Cx-43 expression, but at 12 and 24 hours Cx-43 expression was increased although none of the changes reached statistical significance. This increase at 12 and 24 hours may represent degradation of the original bolus of TGF-β applied. Incubation of HCD cells with vehicle (V) had no effect over Cx-43 expression.

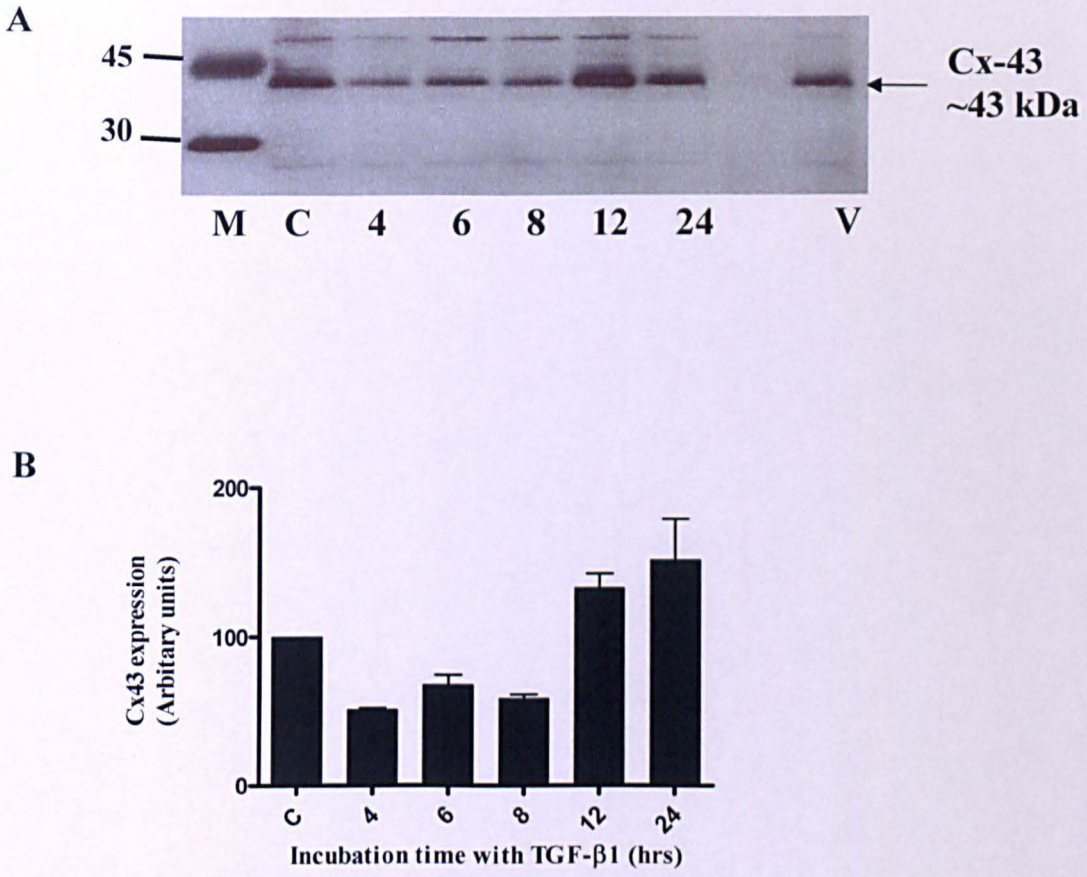

Figure 7.5 The cytokine TGF-β1 (2ng/ml) altered Cx-43 protein expression over a 24 hour time period in HCD cells. Application of TGF-β1 (2ng/ml) induced both a down-regulation and up-regulation in Cx-43 protein expression levels over a 24 hour time period (panel A). Statistical analysis (panel B) of Cx-43 expression. Results represent mean ± SEM; n=3.

7.2.5 Application of the Na^+/K^+ ATPase inhibitor ouabain induces reorganization of the actin cytoskeleton.

Since TGF-β1 has been implicated in reorganisation of the cytoskeleton, an effect which could possibly have implications for gap junction expression and ultimately cell-to-cell communication, I employed the Na^+/K^+ ATPase inhibitor ouabain as a means to induce cell swelling and thus assess the effects that this compound exerted over both cytoskeleton arrangement and ultimately Cx-43 expression. This was done to establish as to whether TGF-β1 may be most likely mediating its effects via a change in cellular architecture due to reorganisation at the cell periphery and ultimately shape changes. HCD cells were incubated with the Na^+/K^+ ATPase pump inhibitor ouabain for periods of 2, 4 and 6 hours. Cells were fixed with PFA and stained with TRITC-conjugated phalloidin to confirm stress induced cytoskeletal reorganisation. Figure 7.6/panel 1b demonstrates cytoskeletal organisation in HCD cells under control conditions and illustrates a dense diffuse network of F-actin filaments spanning the dimension of each cell. These filaments form the so called membrane cytoskeleton which serves to maintain both the shape and integrity of the cell. Following 2, 4 and 6 hour treatment with ouabain, a dramatic reorganisation of the actin cytoskeleton within the cell was observed (figure 7.6 2b, 3b, 4b respectively). Addition of ouabain reorganises these filaments and forms stress fibres to strengthen the cell periphery. This re-organisation became increasingly apparent as the incubation period with ouabain increased. These data highlight a distinct relationship between the cytoskeleton and cell volume recovery.

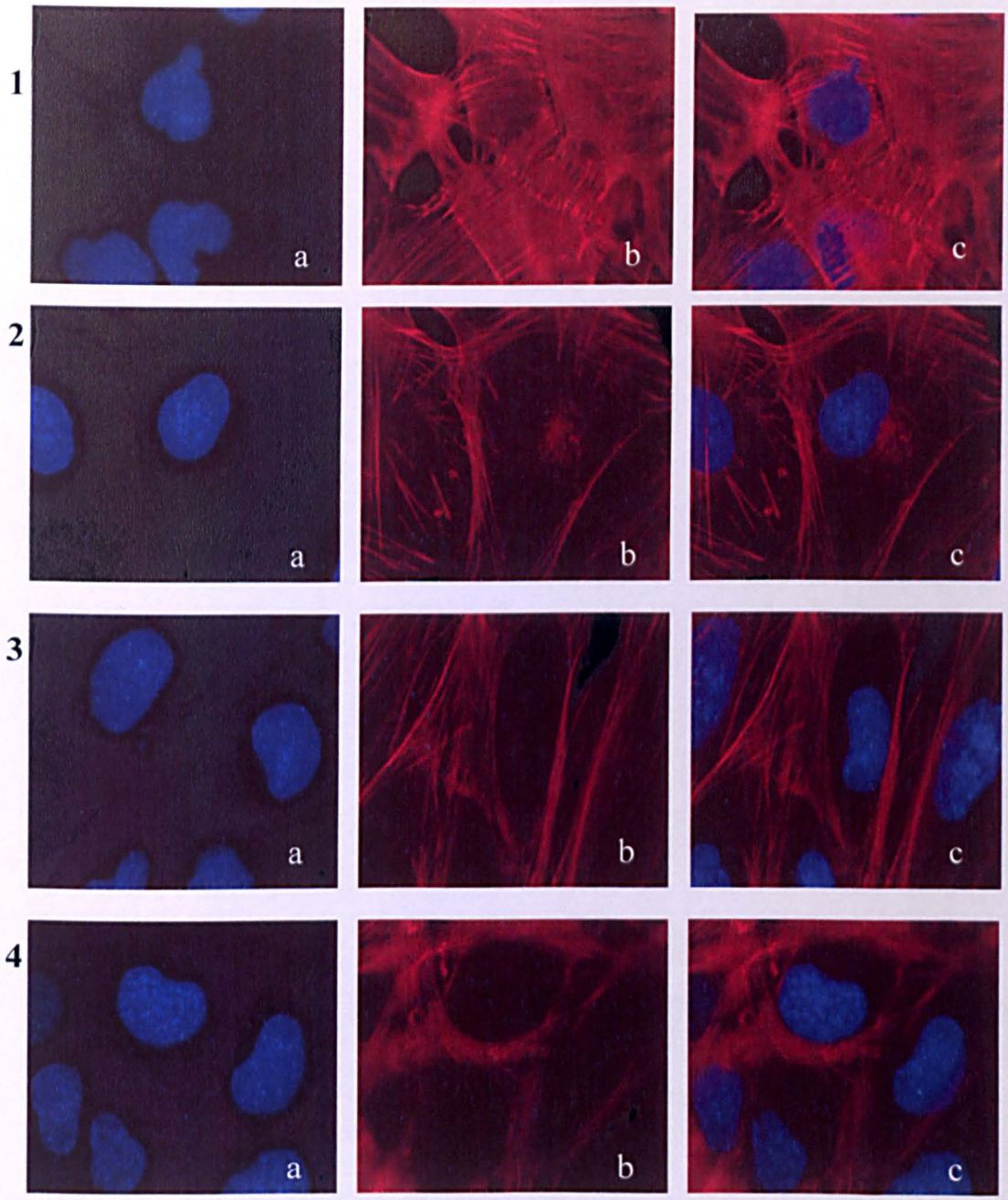

Figure 7.6: Immunocytochemical staining of the cytoskeleton in HCD cells following a 2 4, and 6 hr incubation with ouabain (100μM). HCD cells were treated over a period of 2, (row 2), 4 (row 3) and 6 hrs (row 4) with the Na^+/K^+ ATPase pump inhibitor ouabain and stained with a TRITC phalloidin stain. Row 1 represents those cells under control conditions. Panels a and b show nuclear (DAPI) and cytoskeletal (TRITC phalloidin) staining respectively. Panel c represents an overlay image at each time point and clearly shows a distinct re-organisation of the actin cytoskeleton as the incubation period with ouabain increases.

7.3.6 The Na^+/K^+ ATPase pump inhibitor ouabain downregulated Cx-43 expression

Already proven to induce cytoskeletal rearrangement, most likely to be mediated via an increase in cell volume, the application of ouabain (100μM) was further used to assess if reorganisation of the cytoskeleton could account for TGF-β1 mediated down-regulation of Cx-43. Administration of ouabain down-regulated Cx-43 expression at, 4, 6 and 8 hours (figure 7.7A). Western blot analysis revealed that treatment of HCD cells with Ouabain decreased Cx43 expression (84.4 % ± 16.9%), (36.2% ± 18.1%) (12.6% ± 24.8) at 4 , 6 and 8 hours respectively relative to control (figure 7.7B).

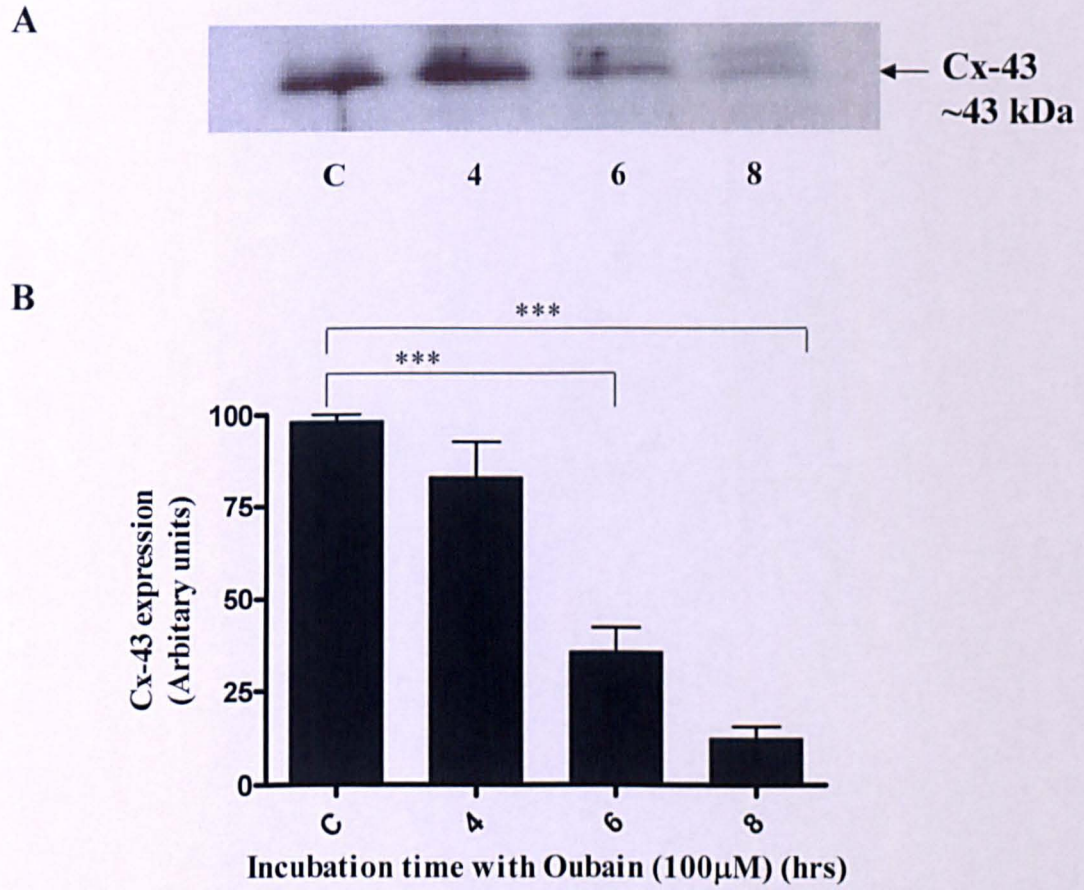

Figure 7.7 Application of ouabain to HCD cells induced a rapid downregulation in Cx-43 protein expression over an 8 hour time period. HCD cells were incubated with the Na^+/K^+ ATPase pump inhibitor ouabain for 2, 4 and 6 hours. Ouabain induced a down-regulation in Cx-43 expression at 2, 4, and 6 hours (panel A). Statistical analysis (panel B) confirmed that reduction in protein expression was significant at 6 and 8 hours. Results represent mean ± SEM; n=3;*** $P< 0.001$.

7.2.7 Acceleration in the velocity of Ca^{2+}-signals between HCD-cells exposed to high glucose.

An association between increased Cx-43 expression in high glucose medium and GJIC activity was assessed by comparing the rate of spread of a mechanically induced calcium signal, in cells cultured under control (5mM) and high glucose (25mM). As previously observed (section 5.1), mechanical stimulation of HCD cells evoked an increase in $[Ca^{2+}]_i$. that propagated between cells within a cluster. The transmission rate of touch-evoked Ca^{2+}-transients between coupled cells was accelerated following exposure to high glucose, providing a functional correlate to increased Cx-43 expression. Propagation was significantly elevated at 48 hours, (321% ± 18.8 %) in cells treated with 25 mM glucose (figure 7.8 and figure 7.9)

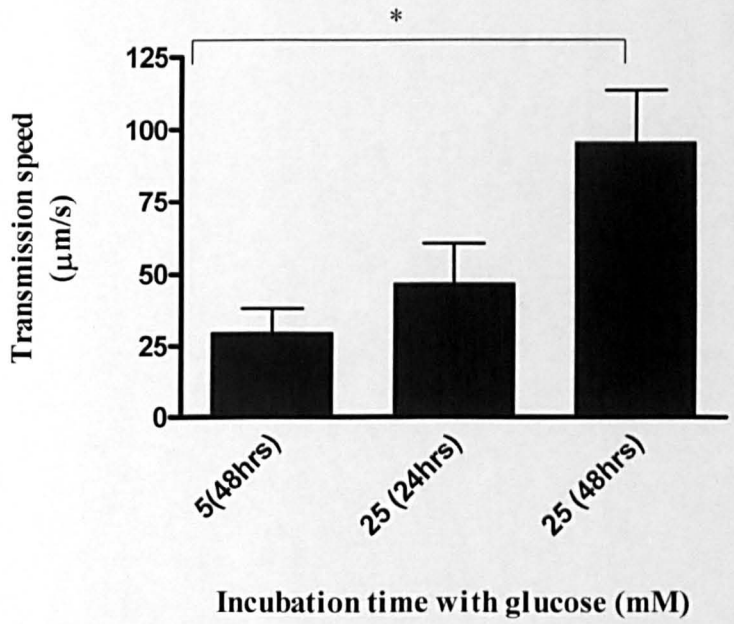

Figure 7.8 Acceleration of touch evoked Ca^{2+} signals between HCD cells by high glucose. HCD cells were incubated in 5 or 25mM glucose for 24 and 48 hours. Cells were then mechanically stimulated and the speed of transmission of the resultant Ca^{2+} transient assessed (µm/s).Results represent mean ± SEM; n=3 *P<0.05.

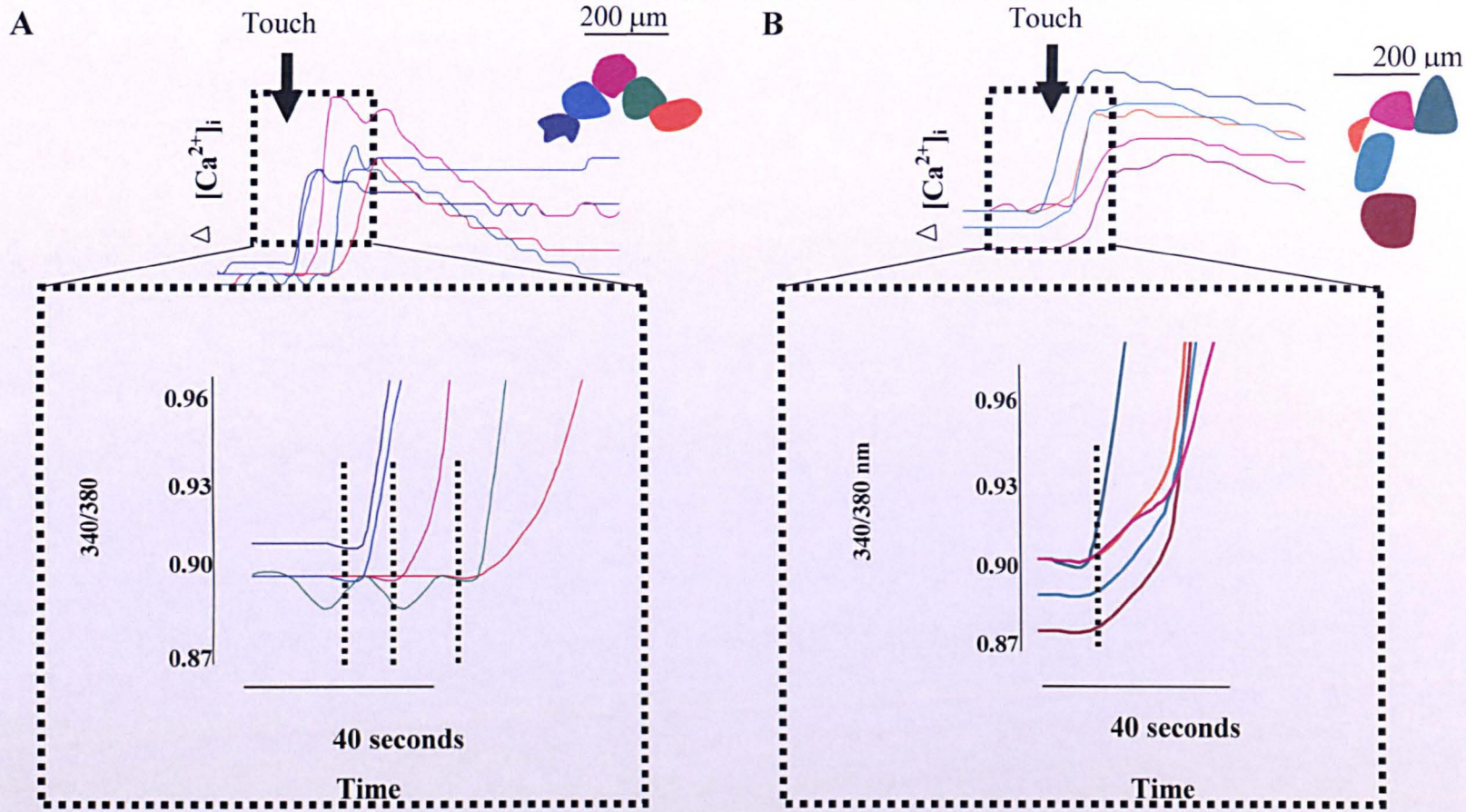

Figure 7.9 Transmission of touch evoked Ca^{2+} transientsare accelerated in high glucose (25mM). The speed of propagating touch evoked Ca^{2+} signals between adjacent cells in HCD clusters was significantly elevated following 48 hours exposure to 25mM glucose (trace B), as compared to cells cultured in low (5mM) glucose (trace A). Trace A clearly shows that in control cells, upon touch evoked stimulation the generation of Ca^{2+} transients in neighbouring cells, indicative of the speed at which this touch evoked signal propagates is far slower than in those cells cultured in high glucose.

7.3 Discussion

Previous studies (chapter 5) have shown that mechanical stimulation of HCD cells evoked a transient increase in $[Ca^{2+}]_i$. Transmission of this calcium signal throughout the cell cluster indicated a high degree of cell-to-cell communication and led to the supposition that gap junctions may mediate transmission of this mechanically evoked signal. In collecting duct epithelium, cell volume regulation is linked to Na^+ absorption and depends upon detection of osmotic and mechanical stresses. A loss of cell-to-cell communication could potentially reduce the ability of renal epithelia to respond appropriately to changes in cell volume and may provide a link between deranged Na^+ reabsorption and the pathophysiological changes associated with some renal diseases such as diabetic nephropathy in which hypertrophy and elevated glucose are characteristic traits. The deregulation of connexin expression is a widespread feature in cell coupling changes associated with various diseases (Hillis *et al.*, 1997, Haefliger *et al.*, 2001). Of these, the variability of connexin expression arising from hyperglycaemia in diabetes has been extensively studied (Li *et al.*, 2003, Malfait *et al.*, 2001, Inoguchi *et al.*, 2001).

In this present chapter I examined the effect of touch on the generation of intracellular calcium signals in HCD cells and investigated the role of Cx-43 mediated gap-junctions in propagating these signals under control and high glucose conditions. Previous reports have demonstrated that exposure to high glucose down regulates intercellular communication by enhancing both phosphorylation and degradation of Cx-43 in several cell types (Sato *et al.*, 2002, Hilliis *et al.*, 1997, Inoguchi *et al.*, 2001), however here I show that increased glucose increased Cx-43 expression. A recent report in which the expression of Cx-43 was studied in glomerular podocytes (Yaoita *et al.*, 2002) subjected to puromycin aminonucleoside (PAN) nephrosis, a model of nephrotic syndrome, demonstrated an increase in Cx-43 expression that correlated with increased GJIC activity, thus raising the possibility that cells throughout the nephron may respond in a different manner to cells of other tissue types e.g. aortic endothelial cells and retinal pigmental epithelial cells, both of which have shown down-regulated levels of both Cx-43 expression and GJIC (Kuroki *et al.*, 1998, Malfait *et al.*, 2001).

Elevated glucose has been shown to decrease gap junctional conductance and disrupt cellular homeostasis in a variety of cell systems (Ngezahayo *et al.*, 1990, Sato *et al.*, 2002). In streptozotocin-induced diabetic rats, dye spread in retinal micro-vessels was reduced in the absence of exogenous insulin (Oku *et al.*, 1990). Similarly, glucose-dependent down regulation of Cx-43 expression and GJIC has been reported in bovine retinal pericytes (Li *et al.*, 2003), endothelial (Fernandes *et al.*, 2004), and epithelial cells (Gomes *et al.*, 2003, Malfait *et al.*, 2001, Inoguchi *et al* 1995, Kuroki *et al.*, 1998) demonstrated that 24hr exposure to high glucose evoked a protein kinase C-dependent decrease in GJIC in bovine aortic endothelial cells, a finding later supported by studies in streptozotocin-induced diabetic rats (Inoguchi *et al.*, 2001). However, the inhibitory effects of hyperglycaemia on Cx-mediated cell-to-cell communication in various micro-vascular and macro-vascular models are not so apparent in other tissues. In a rat osteosarcoma cell line, a 72hr exposure to 25mM glucose had no effect on touch-evoked spread of Ca^{2+}-transients (Gomez *et al.*, 2000), whilst it has been long established that high glucose increased the expression of gap-junctions in pancreatic β-cells (Meda *et al.*, 1990).

In the current study, sub-48hr exposure of HCD-cells to high (25mM) glucose generated a marked increase in Cx-43 protein expression and cell-to-cell transmission velocity for touch-evoked Ca^{2+}-transients. The upregulation of Cx-43 expression was only partially attributable to the osmotic effect of the sugar since similar concentrations of mannitol elicited only a 29% increase in Cx-43 expression under identical experimental conditions. Therefore glucose must work directly via a different signaling pathway to induce Cx-43 expression.

Intercellular communication is dependent upon several different factors and the mere up-regulation of Cx-43 molecules is not necessarily indicative of increased GJIC. Since Cx-43 expression has previously been linked to increased $[Ca^{2+}]_i$ and $[Ca^{2+}]_i$ is known to be elevated under conditions of hyperglycemia, (Symonian *et al.*, 1998) I examined a role for cytosolic calcium in the regulation of Cx-43 expression in our model. In the present study, Cx-43 expression increased in response to elevated cytosolic calcium following ionomycin treatment and although this finding is contrary to that previously reported in osteoblast-like cells in culture, which showed reduced dye spread in the presence of the ionophore A23187 (Schirrmacher *et al.*,

1996), both studies suggest that functional expression of gap-junctions is Ca^{2+}-dependent. Previous studies performed by D'Andrea *et al.,* (2002) demonstrated both increased Cx-43 expression and dye transfer in articular chondrocytes incubated with Interleukin-1 (IL-1). IL-1 evoked a dose dependent increase of $[Ca^{2+}]_i$ which when chelated abolished the increased Cx-43 expression, data which further supports a role for $[Ca^{2+}]_i$ in Cx-43 expression. Up-regulation of Cx-43 expression in cells obtained from human renal biopsies of patients with inflammatory glomerulonephritis paralleled that of the intercellular adhesion molecule (ICAM-1) (Tonon *et al.,* 2002). Cell surface adhesion molecules play vital roles in numerous cellular processes. Some of these include: cell growth, differentiation, embryogenesis, immune cell transmigration and response, and cancer metastasis. There is growing evidence that intercellular adhesion precedes and may even be a prerequisite in enabling the formation of fully functional gap junctions (Jongen *et al.,* 1991, Mege., 1988). The upregulation of both Cx-43 and ICAMs in renal biopsies would support this observation implicating a role for both intercellular adhesion molecules and Cx-43 in tubulointerstitial inflammation (Hillis *et al.,* 1997). The cadherins, a class of calcium dependent adhesion molecules, mediate homotypic cell-cell adhesion and are thought to act in a coordinated fashion with connexins, allowing for gap junction assembly and the subsequent communication between them. Taken in conjunction with previous data and the findings of this chapter, both hyperglycaemia and raised $[Ca^{2+}]_i$ may mediate their effects on Cx-43 through regulation of these intercellular signalling molecules whose subsequent expression allows and enables for the formation of Cx43 comprised gap junctions.

The cytokine TGF-β1 has powerful fibrogenetic effects, and is thought to be involved in the development of renal hypertrophy, with glucose induced upregulation of both TGF-β1 mRNA and protein having been found in diabetic models (Ricci *et al.,* 2006). Studies have confirmed that the most important contributor to the development of nephropathy is hyperglycaemia (Mogyorosi *et al.,* 1999, Marshall *et al.,* 2004), with increased intracellular glucose metabolism promoting the pathological changes characteristic of those observed in diabetic nephropathy. The uptake of glucose into cells is mediated by a series of glucose transporters expressed within the cell membrane (Heilig *et al.,* 1995). Glucose stimulated TGF-β has been

shown to induce upregulation of the insulin-independent glucose transporter GLUT1 (Mogyorosi *et al.*, 1999, Ricci *et al.*, 2006) thus leading to the supposition that TGF-β may provide the link between glucotoxicity and cell dysfunction in diabetic nephropathy.

Application of TGF-β1 inhibited Cx-43 expression. Although eliminating TGF-β as a downstream component of the glucose induced increase in Cx-43 expression, previous reports have highlighted a role for TGF-β in cytoskeleton remodelling and cell-to-cell interactions (Border *et al.*, 1993). Administration of the Na^+/K^+ ATPase pump inhibitor ouabain was found to re-organise the cytoskeleton of HCD cells. These changes probably reflect an attempt by the cell to restore cell volume through initiation of cell volume regulatory mechanisms, therefore preserving membrane rigor and allowing for both cell and blood volume to be restored. Ouabain down-regulated Cx-43 expression comparable to that observed upon application of TGF-β, thus leading to a supposition that the effects of TGF-β may be mediated through the effects induced on the cell's cytoskeleton. Disruption or re-organisation of the architectural framework would inhibit both gap junction expression and assembly. In further support of this hypothesis, the application of TGF-β to proximal tubular cells has been reported to induce both actin microfilament rearrangement and disassembly of tight junctional complexes (Border *et al.*, 1993). This downregulation of Cx-43 expression in HCD cells upon TGF-β application may therefore be an artefact of cytoskeletal reorganisation induced by TGF-β as opposed to a direct effect of this cytokine.

Whilst the application of TGF-β downregulates Cx-43 expression, indicating that this cytokine does not function as a downstream component of the response to high glucose over a 48 hour incubation period, the overall effect of acute high glucose up-regulates Cx-43 expression, most likely mediated via increased $[Ca^{2+}]_i$. Increases in Cx-43 mediated coupling between cells may act to maintain epithelial integrity and prevent immediate and overt renal damage in the short term. Whether this increase in GJIC serves to be of benefit or detriment to the overall functioning of the nephron remains to be elucidated.

Chapter 8
Discussion

Alterations in the resorptive capacity of renal epithelia to sodium can have severe implications for kidney function and may be involved in the development and pathogenesis of secondary hypertension associated with Type II diabetes. To clarify underlying mechanisms that predispose an individual to deranged Na^+ reabsorption and ultimately hypertension, we need to better understand how sodium handling is regulated.

The overarching aim of this thesis was to elucidate mechanisms involved in renal Na^+ handling in a novel cell line of the human cortical collecting duct and to determine potential mechanisms by which these cells identify and transduce osmotically induced signals,that instigate cell volume recovery mechanisms, preserving both structure and function in this distal region of the nephron. In chapter 3, studies confirmed that HCD cells express SGK1 and the α, β and γ subunits of the epithelial sodium channel ENaC. Furthermore, single-cell determination of $[Na^+]_i$ confirmed this cell line as a suitable model for assessing functional changes in Na^+ transport mediated via the ENaC, activity of which is principally regulated by the serum and glucocorticoid-regulated kinase SGK1. SGK1 is known to phosphorylate the neural precursor cell expressed developmentally down-regulated ubiquitin protein ligase Nedd 4.2 (Debonneville *et al.*, 2001, Snyder *et al.*, 2002). SGK1-mediated phosphorylation causes Nedd4.2 to release ENaC to the membrane where it increases Na^+ uptake. Intensive research into diabetic nephropathy and resultant secondary hypertension; has identified SGK1 as a key signalling element whose expression in the kidney is upregulated in both diabetics and models of diabetic nephropathy (Kumar *et* al.,1999). In type II diabetes mellitus, insulin insensitivity results in fluctuating levels of hyperglycaemia and is preceded by glycosuria. Previous reports have already established the deranged transcriptional regulation of SGK1 in response to hyperglycaemia (Lang *et al.*, 2000) and since activation is PI-3 kinase dependent (Park *et al* 1999), this could have severe repercussions for the levels of SGK1 activity in those Type II diabetic patients presenting with hyperinsulinaemia. Consequently I have assessed the effect of glucose on the

expression of these key signalling elements. Consistent with previous findings in mouse fibroblasts (Lang *et al*, 2000), high (25mm) glucose induced a dramatic upregulation in both SGK1 and ENaC protein expression in HCD cells over 48 hours. These data suggest a potential role for deranged transcriptional control of SGK1 in aberrant sodium reabsorption under conditions comparable to hyperglycaemia, a supposition supported by microfluorimetric studies which confirmed that HCD cells cultured in high glucose exhibited increased intracellular sodium levels.

Whilst there is considerable evidence relating high glucose levels to deranged sodium reabsorption in the kidney (Wang *et al.*, 2005, Lang *et al.*, 2000, Kumar *et al.*, 1999), the mechanisms behind this regulation remain to be elucidated and thus require further clarification. As discussed in chapter 1, the metabolism of glucose impinges on a number of cell-specific signal-response cascades within cells. Through increasing *de novo* synthesis of diacylglycerol, hyperglycaemia has been associated with increased PKC and raised $[Ca^{2+}]_i$ levels (LeRoith *et al.*, 2004, Brownlee 2000). Elevated circulating levels of glucose have also been associated with the release of a number of growth factors and cytokines known to be involved in promoting the pathogenesis of diabetic nephropathy, amongst these is the transforming growth factor-β (TGF-β1) (Cohen MP *et al.*, 1998, Di Paolo S *et al.*, 1996, Hoffman BB *et al.*, 1998). PKC, through increased binding of the transcription factor AP-1 to the TGF-β1 promoter, is the most likely mediator in the hyperglycaemic induction of this cytokine (Kim SJ *et al.*, 1990, Weigert C *et al.*, 2003). Treatment of HCD cells with both TGF-β1 and the calcium ionophore ionomycin evoked a time dependent increase in both SGK1 and α-ENaC expression. Whether increased α-ENaC levels represent increased protein translation or a reduction in Nedd4-2 proteasomal mediated degradation remains to be confirmed and forms the basis for future work. Irrespective of the precise mechanism regulating the increase in protein expression these data, are further confirmed by studies in mouse fibroblasts in which the addition of decorin, a TGF-β1 neutralising antibody; and nifedipine, a calcium channel blocker have been used to assess contributory effects of both TGF-β1 and calcium as downstream components of the glucose response (Lang *et al.*, 2000). This stimulatory effect of TGF-β1 on SGK1 expression is thought to be mediated by

increased binding of the Sp1 transcription factor to the SGK1 promoter, controlled upstream by p38 MAPK (Irvine SA *et al.*, 2005). Increased activity of p38MAPK has been shown to be rapidly induced under conditions of both hyperglycaemia and hypertonicity (Igarashi *et al.*, 1999). High glucose can activate p38 MAPK by pathways similar to hyperosmolarity because the addition of 16.5 mM mannitol to 5.5mM glucose also significantly increases p38 MAPK activities (Igarashi *et al.*, 1999). Studies by Waerntges *et al* (2002) on fibrotic lung tissue have demonstrated the effect of TGF-β1 on SGK1 transcription to be blunted in the presence of the p38 kinase inhibitor SB203580 (Waerntges *et al.*, 2002).

Hypo-osmotic polyuria which follows glycosuria as a result of osmotic drag in uncontrolled diabetics; exposes the renal epithelial to increased hypertonicity as the urine flows through the nephron and results in cell shrinkage at the apical side of the membrane. SGK1 has been suggested as a possible mediator of the hyperosmotic response to high glucose, a response mediated by p38 MAPK (Waldegger S *et al* 1997, Waldegger S *et al.*, 2000, Bell *et al.*, 2000). These findings indicate that p38 MAPK can be activated by glucose levels commonly encountered in diabetic patients as well as by extremely high levels of glucose when the effects of osmotic stress are significant. These results indicate that TGF-β1 utilises the same signalling pathway in stimulating SGK1 transcription as p38 MAPK. Hyperglycaemic-induced TGF-β1 formation together with osmotically-driven increases in SGK1 (Waldegger S *et al.*, 1997, Waldegger S *et al.*, 2000, Bell *et al.*, 2000) provide a link between poorly controlled plasma glucose and the development of excess ENaC-mediated Na^+-reabsorption that underlies secondary hypertension as seen in some diabetics (reviewed in Marshall *et al.*, 2004).

In addition to its effects on TGF-β1, glucose is also known to acutely increase the concentration of intracellular calcium ($[Ca^{2+}]_i$) (Symonian M *et al.*, 1998). How raised levels of calcium evoke alterations in both SGK1 and ENaC expression in human cortical collecting duct (HCD) remains to be elucidated. However, since calcium is able to increase PKC activity, it seems feasible that the contribution of calcium to the glucose induced upregulation of both SGK1 and ENaC may stem from its ability to enhance TGF-β1 transcription through increased AP-1 binding. Thus

TGF-β1 is the key player in mediating these hyperglycaemic induced changes in intracellular Na^+ levels through regulating SGK1 and ENaC expression. However, the addition of TGF-β1 neutralising antibodies in hyperglycaemia fails to completely negate the glucose driven increase in SGK1 (Lang *et al* 2000). In conjunction with a further reduction in the response upon blockade of voltage gated calcium channels by nifedipine (Lang *et al,* 2000), it would appear that calcium, albeit through its interaction with TGF-β1, may signal via a separate and unidentified signalling cascade, a hypothesis which forms the basis of future work.

In conclusion, I have used a novel model in vitro system to assess the effect of high glucose, TGF-β1 and cytosolic Ca^{2+} on SGK1 and α-ENaC expression (Hills *et al* 2006b). I have correlated these changes to single-cell determination of $[Na^+]_i$ and suggest that glucose induced upregulation of SGK1 expression and activity, in conjunction with increased α-ENaC expression may represent a critical step in aberrant renal sodium handling seen in Type II diabetes. TGF-β1, Ca^{2+} and p38 MAPK are all known to be up-regulated under conditions of hyperglycaemia. Data presented both in this thesis and in previous studies suggest a critical role for all three signalling molecules in the role and regulation of both SGK1 and α-ENaC. Thus in suggesting a potential series of events to explain glucose-evoked changes in Na^+ re-uptake, it seems likely that DAG, PKC and Ca^{2+}, combine to increase transcription of TGF-β1. Cross talk between the TGF-β1 and MAPK signalling cascades results in the overall activation of p38 MAPK and SGK1 transcription through activation and increased binding of the transcription factor sp1 to the SGK1 promoter (Bell *et al.*, 2000). These increased levels, which we know are accompanied by increase intracellular sodium levels, may have dramatic repercussions for normal kidney function, contributing to the pathogenesis of secondary hypertension associated with diabetic nephropathy in Type II diabetes mellitus.

Whilst the effect of high glucose on SGK1, ENaC and increased intracellular sodium identifies potential mechanisms that are partially, if not completely responsible for regulation of renal sodium handling under those conditions associated with the development of secondary hypertension, it is crucial to remember that diabetic nephropathy is a also linked to both structural and functional disturbances that

damage renal function (Wolf *et al.*, 2003). Understanding how cells of the nephron coordinate their activities to ensure efficient and appropriate absorption, is central to understanding how these structural changes may impinge on normal function under conditions of high glucose.

The obvious question when determining how cells respond to changes in their extracellular environment is to question how these cells detect physiologically appropriate stimuli and instigate a signal which can then propagate to neighbouring cells ensuring minimal damage throughout. Utilising touch as a surrogate form of osmotic stress in conjunction with Ca^{2+} microfluorimetry I have examined how HCD-cells respond and communicate this activity when osmotically challenged. Touch evoked stimulation evoked a calcium-dependent response, which propagated throughout neighbouring cells. The ability to detect and respond to physical deformation at the cell membrane is mediated via the transient receptor potential channel TRPV4 (Gong *et al.*, 2004), a cation permeable channel which is activated upon exposure of the cell to a hypoosmotic environment. Unlike SGK1 which is activated upon cell shrinkage and through its actions on the ENaC and Na^+/K^+ ATPase (Alvarez dela Rosa *et al.*, 2006, Snyder *et al.*, 2002) is able to restore cell volume through Na^+ and water influx, TRPV4 serves as a counterregulatory mechanism. Activated upon cell swelling, TRPV4 mediates Ca^{2+} influx triggering activation of numerous signalling cascades which together aim to restore cell volume through instigation of a RVD. Mechanical stimulation of an HCD cell evoked a transient increase in calcium which subsequently has been shown to be critical in the response of cells to hypoosmolarity allowing for instigation of a RVD (Becker D *et al.*, 2005). Knockdown studies of TRPV4 using siRNA technologies later confirmed that this TRP channel was indeed responsible for detecting membrane stress in HCD cells (see chapter 5). Whilst hyper-osmotic urine will potentially cause epithelial cell shrinkage which will in turn activate SGK1 (Bell *et al.*, 2000), hypoosmotic polyuria will cause an increase in urinary flow rate. This increased flow may be detected by mechanical receptors such as TRPV4 in the epithelial membrane, thereby raising intracellular calcium levels. Whilst under physiological conditions the actions of TRPV4 and SGK1 counteract one another, in a pathophysiological state such as type II diabetes, constitutive activation of both SGK1 and TRPV4 as a result of those factors discussed previously, may serve to further exacerbate the state of cell

swelling through enhanced transcription of our key signalling elements. Subsequently, the rate of Na^+ reabsorption will increase and the ability of the principle cells to regulate blood volume homeostasis may be lost.

Moreover, stimulation of a single cell within a cluster generated a calcium signal that propagated into neighbouring cells, confirming synchronous behaviour indicative of a high degree of cell-to-cell communication. Whilst the contribution of a local paracrine synchroniser could not be ruled out, data suggested direct gap-junction mediated intercellular communication was responsible for co-ordinating activity between cells. Gap junctions represent a well established model by which numerous cell types communicate and exist in multiple isoforms with variable tissue expression. The loss of propagating Ca^{2+} transients between cells which had been pre-treated with heptanol and the heptanol-sensitive spread of the dye between cells, provided initial confirmation that these cells were communicating directly via gap junctions.

Whilst RT-PCR confirmed mRNA expression of several connexins, my studies focussed on the expression and involvement of Cx-43 in GJIC, a protein which has been shown to exhibit high basal expression in the collecting duct (Guo *et al.*, 1998). siRNA and Ca^{2+} microfluorimetric studies confirmed that Cx-43 forms the functional gap junction involved in the transmission of the intercellular Ca^{2+} wave in HCD cells. As with heptanol studies, stimulation of a Fura-2 loaded cell exhibiting knockdown of Cx-43 expression, evoked a transient increase in calcium that failed to propagate into neighbouring cells. Dye spread was also inhibited in those cells lacking functional Cx-43. How the Ca^{2+} wave diffuses across gap junctions remains to be elucidated, but could depend upon diffusion of either Ca^{2+} or InsP3, the latter of which interacts with IP3 receptors to release intracellular Ca^{2+} from the endoplasmic reticulum (ER), generating calcium release from stores. Over the past decade there have been numerous reports of the involvement of Cx-43 in mediating signal transmission in response to mechanical stress (Suadican *et al*, 2000, Fry *et al* 2001). Although some reports have demonstrated that propagation of a Ca^{2+} dependent signal still occurs through Cx-43 comprised junctions, other studies have highlighted a role for both Cx-43 mediated gap junctions and ATP mediated-P2Y receptor activation (Suadicine *et al* 2000). Hemichannel ATP release and the subsequent role

of this nucleotide in regulating calcium signalling (Cotrina et al 1998) initiated a series of studies in which the paracrine release of ATP in generation of touch evoked calcium transients was investigated. Suramin, a P2Y receptor antagonist failed to block touch-evoked propagation of Ca^{2+} transients in HCD cells and further suggested the importance of direct Cx-43 mediated gap junction communication in synchronising activity across monolayer cultures of HCD cells.

Elevated glucose has been shown to decrease connexin expression, gap junctional conductance and disrupt cellular homeostasis in a variety of cell systems. Cx-43 mediated cell-to-cell coupling was examined in HCD cells under high glucose. Contrary to previous findings in glomerular mesangial and retinal endothelial cells (Zhang *et al.*, 2006, Fernandes *et al.*, 2004) acute 48 hour incubation in high glucose increased Cx-43 expression levels in HCD cells. However, chronic incubation reduced Cx-43 expression to near basal after an 8 day period, thus identifying the existence of compensatory mechanisms. In the context of an uncontrolled diabetic presenting with fluctuating periods of hyperglycaemia, Cx-43 expression levels are most likely to vary depending upon the duration and nature of the hyperglycaemic episode and although after 8 days of continuous high glucose, connexin expression returns to near basal, a simple fall and sudden rise in blood glucose levels may; again be enough to trigger this stimulatory response that was observed following acute glucose treatment. Whilst these data conflict with previous reports of downregulatory and inhibitory effects on both expression and gap junction coupling respectively (Li et al 203), increases in Cx-43 functional expression may act to maintain epithelial integrity and prevent immediate and overt renal damage in the short term. Loss of this signal over time however may contribute to the development of renal disease and diabetic nephropathy.

In conclusion, the data presented in this thesis has identified and characterised a novel human collecting duct, confirming these cells a suitable model for the study of sodium reabsorption in principal cells of the cortical collecting duct. Offering advantages over primary tissue of availability and ease of genetic manipulation, I have controlled the extracellular environment to mimic that of conditions associated with hyperglycaemia, e.g. increased glucose, TGF-β1 and intracellular Ca^{2+}, and have subsequently identified key signalling elements involved in the detection of

those changes which we believe are associated with progression from euglycaemia to hyperglycaemia. Regulation of sodium via the ENaC in the collecting duct is critical and must be maintained to prevent excessive reclamation of solutes which will ultimately predispose an individual to the development of secondary hypertension. I have identified how cells of the collecting duct communicate at a synchronous level of activity to maintain the appropriate overall working of the cortical collecting duct thereby contributing to the overall function of the nephron. Molecular and microfluorimetric techniques have been used to assess the effect of pathophysiological conditions on both expression of signalling elements and electrolyte levels within the cell and in doing so has enabled us to construct a proposed pathway by which in type II diabetes deranged regulation of cell volume regulated signalling elements may arise.

Establishing a model of which we can gain a greater understanding into the way in which these mechanisms are controlled will hopefully enable future manipulation and therapeutic modulation of downstream targets whose activity, if we can control, may prevent widespread damage throughout the kidney, thereby preventing and inhibiting those changes associated with the structural and functional disturbances of diabetic nephropathy.

Chapter 9

Future Work

The overarching goal of this thesis was to gain an insight into the mechanisms involved in renal sodium handling in a human cortical collecting duct cell line and establish how these mechanisms may become compromised under conditions of high glucose as associated with type II diabetes. Initial studies characterised this novel cell line and highlighted how cells of the human collecting duct responded in a high glucose environment comparable to that observed in type II diabetes. Although extensive this thesis highlights several areas for further investigation.

In Chapter 3 we confirmed expression of SGK1 and the three principal subunits of the ENaC. However, an important signalling molecule involved in SGK1 mediated regulation of ENaC is Nedd4.2 (Debonneville *et al.*, 2001). Nedd4.2 as previously discussed, is a ubiquitin ligase that resides in the cell bound to the ENaC. Only when SGK1 is rendered active through PI3-K dependent phosphorylation does Nedd4.2 dissociate from ENaC allowing apical insertion (Park *et al.*, 1999). Confirmation of Nedd4.2 expression in response to various treatments would enable further delineation as to whether the increased α-ENaC expression observed in response to high glucose, TGF-β and ionomycin presented in chapter 4 was a consequence of either increased transcription or a reduction in Nedd4.2 mediated proteasomal degradation.

Glucose-evoked upregulation of both SGK1 and α-ENaC at 24 and 48 hours led to a series of experiments in which I identified possible downstream components of the glucose induced response. Application of TGF-β and Ionomycin evoked a time dependent increase in SGK1 and α-ENaC expression. In order to assess the contribution of these agonists would require incubation of HCD cells in a 25mM glucose medium in the presence of a TGF-β neutralising antibody, a calcium channel blocker and lastly both antibody and blocker. If the neutralising antibody negated the glucose response this would suggest that calcium is either a downstream component of the TGF-β pathway or is involved directly in TGF-β transcription. However, if, the antibody failed to negate the response it would seem likely that calcium may be

contributing to the TGF-β response via a separate and unidentified pathway. The upregulation of SGK1 in response to TGF-β co-incides as previously discussed with the work of Lang (Lang *et al.*, 2000). These effects are believed to be mediated via p38 MAPK and have been shown to be blunted in the presence of pharmacological inhibitors of p38 MAPK (Waerntges *et al.*, 2002). Application of p38 MAPK inhibitors in the presence of TGF-β would confirm a role for p38 MAPK in mediating the effects of TGF-β. Leading on from these studies, future work would aim to identify the isoforms involved and potential cross talk between the signalling pathway of TGF-β and the regulation of hSGK expression in response to osmotic stress, both of which have been reported to mediate their effects via p38 MAPK.

In chapter 5 we confirmed that HCD cells express the mechanosensitive TRPV4. TRPV4 has been implicated as a potential osmosensor and thus may have a role in cell volume recovery. Incubation of cells in solutions of variable osmolarity would enable us to determine via western blotting, if this increased activity accompanied by a rise in $[Ca^{2+}]_i$ in response to osmotic stress, is matched by an increase in TRPV4 expression at the cell membrane. Immunocytochemical analysis would highlight any re-distribution of TRPV4 channels at the cell membrane.

Finally, in chapter 6 we confirmed that the touch evoked calcium signal propogates throughout HCD cells via Cx-43 mediated gap junctions. In chapter 7 we assessed the effect of high glucose on increasing both Cx-43 expression and GJIC. Although ionomycin increased Cx-43 expression, TGF-β reduced expression. This may reflect the ability of the cytokine to rearrange cytoskeletal elements (Border *et al.*, 1993). Immunocytochemical studies confirmed that Ouabain, a Na^+/K+ ATPase inhibitor can induce cytoskeletal re-arrangement, an effect most likely mediated via alterations in cell volume. Application of Ouabain to HCD cells was also found to down-regulate Cx-43 expression. Therefore could TGF-β, like Ouabain, play a role in cytoskeletal reorganisation which would undoubtedly have implications for gap junction expression and localization. Future studies would involve confirmation of a role for TGF-β in regulation of the cytoskeleton, paralleled by studies in which cells were exposed to solutions of variable hypo-osmolarity, thereby confirming that the effects of both TGF-β and ouabain were cell volume mediated.

References

Ahmed, S., Diez, J.A., George, CH., and Evans, W.H. (1999). Synthesis and assembly of connexins in vitro into homomeric and heteromeric functional gap junction hemichannels. *Biochem J.* **339,** 247-253.

Alliston, T.N. Maiyar, A.C. Buse P. Firestone, G.L. and Richards JS. (1997). Follicle stimulating hormone-regulated expression of serum/glucocorticoid inducible kinase in rat ovarian granulosa cells: A functional role for the Sp1 family in promoter activity. *Mol Endocrinol.* **11,** 19340-49.

Alvarez de la Rosa, D. Zhang, P. Naray-Fejes-Toth, A. and Canessa C.M. (1999). The serum and glucocorticoid kinase sgk increases the abundance of epithelial sodium channels in the plasma membrane of Xenopus oocytes. *J Biol Chem.* **274,** 37834-37839.

Alvarez de la Rosa, D. Canessa, C.M. Fyfe, G.K. and Zhang P. (2000). Structure and regulation of amiloride sensitive sodium channels. *Annu Rev Physiol.* **62,** 573-594.

Alvarez de la Rosa. D., Gimenez, I., Forbush, B. and Canessa, C. M, (2006). SGK1 activates Na^+/K^+ ATPase in amphibian renal epithelial cells. *Am J Physiol Cell Physiol* **290,** C492-C498.

American Diabetes Association. (2004). Nephropathy in Diabetes. *Diabetes Care.* **27,** 579-583.

Arteaga, C.L., Dugger, T.C. and Hurd, S.D. (1996). The multifunctional role of transforming growth factor (TGF).-beta on mammary epithelial cell biology. *Breast Cancer Res. Treat.* **38,** 49-56.

Atkinson, M.M., Lampe, P.D., Lin, H.H., Kollander, R., Li, X.R. and Kiang, D.T. (1995). Cyclic AMP modifies the cellular distribution of connexin43 and induces a persistent increase in the junctional permeability of mouse mammary tumor cells. *J Cell Sci.* **108,** 3079-3090

Ayo, S.H., Radnik, R., Garoni, J.A., Troyer, D.A. and Kreisberg J.I., (1991). High glucose activates diacylglycerol mass and activates protein kinase C in mesangial cell cultures. *Am J Physiol.* **261,** F571-7.

Bao, X., Altenberg, G.A. and Reuss, L. (2004). Mechanism of regulation of the gap junction protein connexin43 by protein kinase C mediated phoshporylation. *Am J Physiol.* **286,** C647-C654.

Basavappa, S., Pedersen, S.F., Jorgensen N.K., Ellory J.C. and Hoffman, E.K. (1998). Swelling induced arachidonic acid release via the 85 kDa cPLA2 in human neuroblastoma cells. *J Neurophysiol.* **79,** 1441-1449.

Becker, D., Blasé, C., Bereiter-Hahn, J. and Jendrach M (2005). TRPV4 exhibits a functional role in cell volume regulation. *J of Cell Sci.* **118.** 2435-2440.

Bell, L.M., Leong, M.L.L, Kim, B., Wang, E., Park, J., Hemmings, B.A. and Firestone, G.L. (2000).. Hyperosmotic stress stimulates promoter activity and regulates cellular utilisation of the serum and glucocorticoid inducible protein kinase (sgk). by a p38 MAPK-dependent pathway. *J Biol Chem.* **275,** 25262-25272.

Benham, C.D., Gunthorpe, M.J. and Davis, J.B. (2003). TRPV channels as temperature sensors. *Cell calcium.* **33,** 479-487.

Berthoud, V.M., Beyer, E.C., Kurata, W.E., Kanemitsu, M.Y., Loo, L.W.M. Eckhart, W. and Lau, A.F.(1996). Characterisation of the MAP kinase phopshorylation sites on the connexin43 gap junction protein. *J biol Chem.* **271,** 3779-3786.

Beyaert, R. (1996). The p38/RK mitogen activated protein kinase pathway regulates interleukin-6 synthesis in response to tumour necrosis factor. *EMBO J.* **15,** 1914-1923.

Bidet, M., Reniz, G.D., Martial, S., Rubera, I., Tauc, M. and Poujeol P (2000). Extracellular ATP increases $[Ca^{2+}]_i$ in distal tubule cells. Evidence for a P2Y2 purinoreceptor. *Am J Physiol Renal Physiol.* **279,** F92-F101.

Bilato, C. (1995). Intracellular signalling pathways are required for rat vascular smooth muscle and cell migration. *J Clin Invest.* **96,** 1905-1915.

Bittmann, K., Becker, D.L., Cicirata, F. and Parnavelas, J.G. (2002). Connexin expression in homotypic and heterotypic cell coupling in the developing cerebral cortex. *J Comp Neurol.* **443,** 1406-1418.

Bland, R., Walker, EA., Hughes, S.V., Stewart, P.M. and Hewison, M. (1999). Constitutive expression of 25-hydroxyvitamin D_3-1α-hydroxylase in a transformed human proximal tubule cell line: evidence for direct regulation of vitamin D metabolism by calcium. *Endocrinology* **140,** 2027-2034.

Boitano, S., Dirksen, E.R. and Sanderson MJ. (1992).. Intercellular propogation of calcium waves mediated by inositol triphosphate. *Science.* **258,** 292-295.

Border, W.A. Noble, N.A. Yamamoto, T., Harper, J,R. Yamaguchi, Y. Pierschbacher, M.D. and Ruoslahti E (1992). Natural inhibitor of transforming growth factor-β protects against scarring in experimental kidney diseases. *Nature.* **360,** 361-364.

Border, W.A. Noble, N.A (1994). Transforming growth factor beta in tissue fibrosis. *N Engl J Med.* **331,** 1286-92.

Border, W.A. Noble, N.A. and Ketteler M (1995) TGF-β: a cytokine mediator of glomerulosclerosis and a target for therapeutic intervention. *Kidney Int Suppl.* **49,** S59-61.

Brickley, D.R., Mikosz, C.A. Hagan, C.R. Conzen, S.D. (2002). Ubiquitin modification of serum and glucocorticoid induced protein kinase-1 (SGK-1). *J Biol Chem.* **277,** 43064-70.

Brown, D., (2003).. The ins and outs of aquaporin-2-trafficking. *Am J Physiol Renal Phyiol.* **284,** F893-F901.

Brownlee, M. (1995). Advanced protein glycosylation in diabetes and aging. *Annu Rev Med.* **46,** 223-234.

Brownlee, M. (2001). Biochemistry and molecular cell biology of Diabetic complications. *Nature.* **414,** 813-820.

Brosius, F.C. and Heilg, C.W. Glucose transporters in diabetic nephropathy. *Pediatr Nephrol.* **20,** 447-451.

Bruijn, J.A. Roos, A. de Geus, B., and de Heer, E. (1994). Transforming growth factor-beta and the glomerular extracellular matrix in renal pathology. *J Lab Clin Med.* **123,** 34-47.

Bukauskas, F.F., Jordan, K., Bukauskiene, A., Bennett, M.V., Lampe, P.D., Laird, D.W. and Verselis, V.K. (2000). Clustering of connexin 43 enhanced green fluorescent protein gap junction channels and functional coupling in living cells. *Proc Natl Acad Sci.* **97,** 2556-2561.

Burghardt, R.C., Barhoumi, R,. Sewall, T.C. and Bowen, J.A. (1995). Cyclic AMP induces rapid increases in gap junction permeability and changes in the cellular distribution of connexin43. *J Membr Biol* **148,** 243-253.

Butkevich, E., Hulsmann, S., Wenzel, D., Shirao, T., Duden, R. and Majoul I. (2004). Drebrin is a novel connexin-43 binding partner that links Gap junctions to the submembrane cytoskeleton. *Curr Biol.* **14,** 650-658.

Butterworth, M.B., Helman, S.I. and Els., W.J. (2001). cAMP sensitive endocytic trafficking in A6 epithelia. *Am J Physiol* **280,** C752-C762.

Canessa, C.M. Horisberger, J.D. and Rossier, B.C. (1993). Epithelial sodium channel proteins related to neurodegeneration. *Nature.* **361,** 467-470.

Canessa, C.M., Schild, L., Buell, G., Thorens, B., Gautschi, I., Horisberger, J.D. and Rossier, B.C. (1994a). Amiloride sensitive epithelial Na^+ channel is made of three homolgous subunits. *Nature* **367,** 463-467.

Canessa, C.M., Merillat, A.M. and Rossier, B.C. (1994b). Membrane topology of the epithelial sodium channel in intact cells. *Am J Physiol.* **267,** C1682–C1690

Caterina, M.J., Schumacher, M.A., Tominaga, M., Rosen, T.A., Levine, J.D. and Julius, D. (1997). The capsaicin receptor: a heat activated ion channel in the pain pathway *Nature* **389,** 816-824.

Charles, A.C. Naus, C.C.G., Zhu D., Kidder, G.M., Dirksen, E.R. and Sanderson, M.J. (1993). Mechanisms of intercellular calcium signalling in glial cells studied with dantrolene and thapsigargin. *Glia.* **7,** 134-145.

Chen, S., Bhargava, A., Mastroberardino, L., Meijer, O.C. and Wang, J. (1999). Epithelial sodium channel regulated by aldosterone induced protein sgk. *Proc Natl Acad Sci U.S.A.* **96,** 2514-2519.

Chen, S., Hong, S.W., Iglesias-de la Cruz, M.C., Isono, M., Casaretto, A. and Ziyadeh FN. (2001). The key role of the transforming growth factor-beta system in the pathogenesis of diabetic nephropathy. *Ren Fail.* **23,** 471-81.

Chen, S., Jim, B. and Ziyadeh, F.N. (2003). Diabetic nephropathy and transforming growth factor-beta: transforming our view of glomerulosclerosis and fibrosis build-up. *Semin Nephrol.* **23**,(6).532-43.

Chomczynski, P. and Sacchi, N. (1987). Single-step method of RNA isolation by acid guanidinium thiocyanate-phenol-chloroform extraction. *Anal Biochem.* **162,** 156-159.

Christensen, O., (1987). Mediation of cell volume regulation by Ca^{2+} influx through stretch activated channels. *Nature.* **330,** 66-68.

Chung, S.S., EC, Lam. And Chung, S.K. (2003). Contribution of polyol pathway to diabetes induced oxidative stress. *J Am Soc Nephrol.* **14,** S233-236.

Clapham, D.E. (1995). Calcium signalling. *Cell.* **80,** 259-68.

Clapham, D.E. (2003). TRP channels as cellular sensors. *Nature.* **426,** 517-524.

Cohen, M.P., Sharma, K., Guo, J., EWltayeb, BO. and Ziyadeh, FN (1998). The renal TGF-beta system in the db/db mouse model of diabetic nephropathy. *Exp Nephrol.* **6,** 226-233.

Colbert, H.A., Smith, T.L. and Bargmann, C.I (1997). OSM-9. a novel protein with structural similarity to channels. is required for olfaction. mechanosensation and olfactory adaption in caenorhabditis elegans. *J Neurosci.* **17.** 8259-8269.

Cosens, D.J. Manning, A. (1969). Abnormal electroretinogram from a Drosophila mutant. *Nature.* **224,** 285-287.

Cotrina, M.L., Lin, J.H.C., Alives-Rodrigues, A., Liu, S., Li, J., Azmi-Ghadimi Kang, J., Naus, C.G. and Nedergaard M.(1998). Conneixns regulate calcium signalling by controlling ATP release. *Proc Natl Acad Sci USA.* **95,** 15735-15740.

Craven, P.A., DeRubertis, F.R., Protein kinase C is activated in glomeruli from streptozotocin diabetic rats. Possible mediation by glucose. *J Clin Invest.* **83,** 1667-75.

Dasgupta, C., Martinez, A.M., Zuppan, C.W., Shah, M.M., Bailey, L.L. and Fletcher, W.H. (2001). Identification of connexin 43 gap junction mutations in patients with hypoplastic left heart syndrome by denaturing gradient gel electrophoresis. *Mutation Research.* **479,** 173-186.

Debonneville, C., Flores, S.Y., Kamynina, E., Plant P.J., Tauxe, C., Thomas, M.A., Munster, C., Chraibi, A., Pratt, J.H., Horisberger, J.D., Pearce, D., Loffing, J. and Staub O (2001).: Phosphorylation of Nedd4-2 by SGK1 regulates epithelial Na^+ channel cell surface expression. *Embo J.* **20,** 7052-7059.

Demer, L.L., Wortham, C., Dirksen, E.R. and Sanderson, M.J. (1993). Mechanical stimulation induces intercellular calcium signalling in bovine aortic endothelial cells. *Am J Physiol.* **264,** H2094-H2101.

Demerdash, T.M., Seyrek, N., Smogorzewski, M., Marcinkowski, W., Nassermoadelli, S. and Massry, S.G (1996).. Pathways through which glucose induces a rise in $[Ca^{2+}]_i$ of polymorphonuclear leukocytes of rats. *Kidney Int.* **50,** 2032-2040.

Dennler, S., Itoh, S., Vivien, D., Dijke, P., Huet, S. and Gauthier, J. (1998).. Direct binding of smad3 and smad4 to crticial TGF-β inducible elements in the promoter of the human plasminogen activator inhibitor-type 1 gene. *EMBO J.* **17,** 3091-3100.

Diakov, A. and Korbmacher, C. (2004). A novel pathway of epithelial sodium channel activation involves a serum and glucocorticoid inducible kinase consensus motif in the C terminus of the channels α-subunit. J Biol Chem. **279,** 38134-42.

Diez, J.A., Ahmad, S. and Evans, W.H. (1999). Assembly of heteromeric connexons in guinea pig liver en route to the Golgi apparatus. plasma membrane and gap junctions. *Eur J Biochem.* **262,** 142-148.

Dijkink, L., Hartog, A., Van, OS. and Blindels, R.J.M. (2002). The epithelial sodium channel (ENaC). is intracellularly located as a tetramer. *Pflugers Arch-Eur J Physiol.* **444,** 549-555.

Di Paolo, S., Gesualdo, L., Ranieri, E., Grandaliano, G., and Schena FP (1996). High glucose concentration induces overexpression of a transforming growth factor β through the activation of a platelet derived growth factor loop in human mesangial cells. *Am J Pathol* .**149,** 2095-2106.

Duc, C., Farman, N., Canessa, C.M., Bonvalet, J.P and Rossier B.C. (1994). Cell specific expression of epithelial sodium channel α. β and γ subunits in aldosterone responsive epithelia from the rat localisation by in situ hybridisation and immunocytochemistry. *J Cell Biol.* **127,** 1907-1921.

Eaton, D.C et al (1995). Renal sodium channels regulation and single channel properties. *Kidney int.* **48,** 941-949.

Edelstein, D. and Brownlee M (1992). Aminoguanidine ameliorates albuminuria in diabetic hypertensive rats. *Diabetologia.* **35,** 96-97

Elenes, S., Martinez, A.D., Delmar, M., Beyer, E.C. and Moreno, A.P. 2001 Heterotypc docking of Cx43 and Cx45 connexons blocks fast voltage gating of Cx43. *Biophys J.* **81,** 1406-1418.

Embark, H.M., Setiawan, I., Poppendieck, S., Van de Graaf, S.F., Boehmer, C. (2004). Regulation of the epithelial Ca^{2+} channel TRPV5 by the NHE regulating factor NHERF2 and the serum and glucocorticoid inducible kinase isoforms SGK1 and SGK3 expressed in xenopus oocytes. *Cell Physiol Biochem.* **14,** 203-12.

Enomoto, K., Furuya, K., Yamagishi, S. and Maeno, T. (1992). Mechanically induced electrical and intercellular calcium responses in normal and cancerous mammary cells. *Cell Calcium.* **13,** 501-511.

Evans, W.H. and Martin, P.E. (2002). Gap junctions: structure and function. *Mol Membr Biol.* **19,** 121-136.

Farjah, M., Roxas, B.P., Geenan, D.L., Danziger, R.S. (2003). Dietary salt regulates renal SGK1 abundance Relevance to salt sensitivity in the Dahl rat. *Hypertension.* **41,** 874-78.

Fernandes, R., Girao, H. and Pereira P. (2004). High glucose down-regulates intercellular communication in retinal endothelial cells by enhancing degradation of connexin 43 by a proteasome-dependent mechanism. *J Biol Chem.* **279,** 27219-24.

Fernandez-Fernandex, JM., Nobles, M., Currid, A., Vazquez, E. and Valverd, M.A. (2002). Maxi K^+ channel mediates regulatory volume decrease response in a human bronchial epithelial cell line. *Am J Physiol Cell Physiol.* **283,** C1705-C1714.

Firestone, G., Giampaolo, J.R and O'Keeffe B.A. (2003).. Stimulus dependent regulation of serum and glucocorticoid inducible protein kinase (SGK). transcription. subcellular localisation and enzymatic activity. *Cell Physiol Biochem.* **13,** 1-12.

Firsov, D., Schild, L., Gautschi, I., Merillat, A-M., Schneeberger, E. and Rosier, B.C. (1996). Cell surface expression of the epithelial sodium channel and a mutant causing Liddle syndrome: a quantitative approach. *Proc Natl Acad Sci USA.* **93,** 5370-15373.

Firsov, D., Gautschi, I., Merillat, A.M., Rosier, B.C. and Schild, L. (1998). The heterotetrameric architecture of the epithelial sodium channel (ENaC). *EMBO J.* **17,** 344-352.

Flores, S.Y., Loffing-Cueni, D., Kamynina, E., Daidie, D. and Gerbex, C (2005). Aldosterone induced SGK1 expression is accompanied by Nedd4-2 phophorylation

and increased Na^+ transport in cortical collecting duct cells. *J Am Soc Nephrol.* **16,** 2279-97.

Friedrich, B., Feng, Y., Cohen, P., Risler, T. and Vandewalle A (2003). The serine/threonine kinases SGK2 and SGK3 are potent stimulators of the epithelial Na^+ channel α. β. γ ENaC. *Pflugers Arch.* **445,** .601-6.

Fry, T., Evans, J.H. and Sanderson, M.J. (2001).. Propogation of intercellular calcium waves in C6 Glioma cells transfected with Connexins 43 or 32. *Micro Res Tech.* **52,** 289-300.

Fumo, P., Kuncio, GS., Ziyadeh, F.N. (1994). PKC and high glucose stimulate collagen alpha1 (IV). transcriptional activity in a reporter mesangial cell line. *Am J Physiol.* **267,** F632-F638.

Fujimoto, K., Nagafuchi, A., Tsukita, SKA., Ohokuma, A. and Shibata Y (1997). Dynamics of connexins. E-cadherin and α-catenin on cell membranes during gap junction formation. *Journal of cell sciences.* **110,** 311-322.

Gaillard, T.R., Bossetti, B.M., Green, P.A. and Osei K. (1997).. The impact of socioeconomic status on cardiovascular risk factors in African-Americans at high risk for type II diabetes. Implications for syndrome X. *Diabetes Care.* **5,** 745-52.

Gamba, G. (1999). Molecular biology of distal nephron sodium transport mechanisms. *Kidney international.* **56,** 1606-1622.

Gamper, N., Fillon, S., Feng, Y., Friedrich, B. and Lang, P.A. (2002). K^+ channel activation by all three isoforms of serum and glucocorticoid dependent protein kinase SGK. *Pflugers Arch.* **445,** 60-66.

Garcia-Anoveros, J. and Corye, D.P. (1997). The molecules of mechanosensation. *Annu Rev Neurosci.* **20,** 567-594.

Gao, X., Wu, L. and O'Neil, R.G. (2003). Temperature-modulated diversity of TRPV4 channel gating: activation by physical stresses and phorbol ester derivatives through protein kinase C-dependent and -independent pathways. *J Biol Chem.* **278,** 27129-27137.

Garty, H., Benos, D.J. (1988). Characteristics and regulatory mechanisms of the amiloride-blockable Na^+ channel. *Physiol Rev* **68,** 309-373.

Garty, H., Palmer, L.G. (1997). Epithelial sodium channels: function. structure and regulation. *Physiol.Rev.* **77,** 359-396.

Gentry, L.E., Webb, N.R., Lim, G.J., Brunner, A.M., Ranchalis, J.E., Twardzik, D.R., Lioubin, M.N., Marquardt, H. and Purchio, A.F. (1987). Type 1 transforming growth factor β: amplified expression and secretion of mature and precursor polypeptides in chinese hamster ovary cells. *Mol cell Biol.* **7,** 3418-3427.

Gnudi, L., Gruden, G. and Viberti G. Pathogenesis of diabetic nephropathy. (2003).. In: Pickup JC. Williams G eds. *Textbook of diabetes.* 3rd edn. 52.1-53.21 Oxford: Blackwell Science Ltd..

Goldberg, G.S., Lampe, P.D and Nicholson, B.J. (1999). Selective transfer of endogenous metabolites through gap junctions composed of different connexins. *Nat Cell Biol.* **1,** 457-459.

Gong, Z., Son, W., Chung, Y.D., Kim, J., Shin, D.W. and McClung, C.A. (2004).. Two interdependent TRPV channel subunits. inactive and Nanchung. mediate hearing in Drosophila. *J Neurosci.* **24,** 9059-9066.

Goodenough, D.A., Goliger, J.A. and Paul, D.L (1996). Connexins. connexons and intercellular communication. *Annu.Rev.Biochem.* **65,** 475-502.

Gomes, P., Malfait, M., Himpens, B. and Vereecke, J. (2003). Intercellular Ca^{2+}-transient propagation in normal and high glucose solutions in rat retinal epithelial (RPE-J). cells during mechanical stimulation. *Cell Calcium.* **32,** 185-192.

Gomez, P., Vereecke, J. and Himpens, B. (2000). Intra- and intercellular Ca^{2+}-transient propagation in normal and high glucose solutions in ROS cells during mechanical stimulation. *Cell Calcium* **29,** 137-148.

Grenfell, A. Management of nephropathy (1997). In: Pickup JC. Williams G eds. *Textbook of diabetes.* 2nd edn. 54.1-54.19 Oxford: Blackwell Science Ltd.

Gruden, G., Thomas, S.and Burt, D. (1999). Interaction of angiotensin II and mechanical stretch on vascular endothelial growth factor production by human mesangial cells. *J Am Soc Nephrol.* **10.** 730-737.

Grynkiewicz, G., Poenie, M. and Tsien, R.Y. (1985) A new generation of Ca^{2+} indicators with greatly improved fluorescence properties. *J Biol Chem.* **25,** 260 3440-50.

Guler, A.D., Lee, H., Iida, T., Shimizu, I., Tominaga, M. and Caterine, M. (2002). Heat-evoked activation of the ion channel. TRPV4. *J Neurosci.* **22,** 6408-6414.

Guo, R., Liu, L. and Barajas L. (1998). RT-PCR study of the distribution of connexin 43 mRNA in the glomerulus and renal tubular segments. *Am J Physiol.* **275,** 439-47.

Haefliger, J-A., Demotz, S., Braissant, O., Suter, E., Waeber, B., Nicod, P. and Meda P. Connexin 40 and 43 are differentially regulated within the kidneys of rats with renovascular hypertension. *Kidney Int.* **60,** 190-201. 2001.

Han, J., Lee, J.D., Bibbs, L. and Ulevitich RJ (1994). A MAP kinase targeted by endotoxin and hyperosmolarity in mammalian cells. *Science.* **265,** 808-811.

Haneda, M. (1997).. Mitogen activated protein kinase cascade is activated in glomeruli of diabetic rats and glomerular mesangial cells cultured under high glucose conditions. D*iabetes.* **46,** 847-853.

Hansson, J.H., Schild, L., Lu, Y., Wilson, T.A., Gautschi, I., Shimkets, R., Lu, Y., Canessa, C., Iwasaki, T., Rossier, B. and Lifton, R.P. (1995). Hypertension caused by a truncated epithelial sodium channel γ subunit: genetic heterogeneity of Liddle syndrome. *Nat Genet.* **11,** 76-82..

Hansson, J.H., Schild, L., Lu, Y., Wilson, T.A., Gautschi, I., Shimkets, R., Lu, Y., Nelson Williams, C., Rossier, B. and Lifton, R.P. (1995). A de novo missense mutation of the α subunit of the epithelial sodium channel causes hypertension and Liddle syndrome. identifying a proline-rich segment critical for regulation of channel activity. *Proc Natl Acad Sci USA.* **92** 11495-11499.

Harger, H., Kwon, T.H., Vinnikova, A.K., Masilamani, S., Brooks, J., Frokiaer, J., Knepper, M.A., Nielson, S. (2001). Immunocytochemical and immunoclectron microscopic localisation of α–β and γ-ENaC in rat kidney. *Am J Physiol.* **280,** F1093-F1106.

Hauge-Evans, A.C., Squires, P.E., Belin, V.D., Roderigo-Milne, R.D., Persaud S.J. and Jones, P.M (2002). Role of adenine nucleotides in insulin secretion from MIN6 pseudoislets. *Mol. Cell Endocrinology* **191,** 167-176.

Helms, MN., Fejes-Toth, G. and Naray Fejes Toth, A. (2003). Hormone regulated transepithelial Na^+ transport in mammalian CCD cells requires SGK expression. *Am J Physiol.* **284,** F480-87.

Heilig, CW., Concepcion, LA. and Riser, B.L. (1995). Overexpression of glucose transporters in rat mesangial cells cultured in a normal glucose milieu mimics the diabetic phenotype.*J Clin Invest.* **96,** 1802-14.

Heilig, C.W., Kreisberg, J.L., Freytag, S. (2001). Antisense GLUT1 proects mesangial cells from glucose induction of GLUT1 and fibronectin expression. *Am J Renal Physiol.* **280,** F657-F666.

Heldin, C-H., Miyazano, K. and ten Dijke, P. (1997). TGF-β signalling from cell membrane to nucleus through smad proteins. *Nature* **390,** 465-471.

Henke, G., Setiawan., Bohmer, C. and Lange, F. (2002). Activation of the Na^+/K^+ ATPase by the serum and glucocorticoid dependent kinase isoforms. *Kidney Blood Press Res.* **25,** 370-74.

Hilliis, GS., Duthie, L.A., Brown, P.A.J., Simpson, J.G., Macleod, A.M. and Haites, NE.(1997).. Upregulation and co-localization of connexin 43 and cellular adhesion molecules in inflammatory renal disease. *Journal of Pathology.* **182,** 373-379.

Hills, CE., Bland, R., Wheelans, D.C., Bennett, J., Ronco, P.M. and Squires, P.E. (2006a). Glucose-evoked alterations in connexin-43-mediated cell-to-cell communication in human collecting duct: a possible role in diabetic nephropathy. *Am J Physiol Renal Physiol.* **291,** F000-F000.

Hills, C.E., Bland, R., Wheelans, D.C., Bennett, J., Ronco, P.M. and Squires, P.E. (2006b). High glucose upregulates ENaC and SGK1 expression in HCD cells. *Cell Physiol Biochem.***18,** (in press).

Hoenderop, J.G., Nilius, B. and Bindels, R.J. (2005). Calcium absorption across epithelia. *Physiol Rev.* **85,** 373-422.

Hoffman, B.B., Sharma, K., Zhu, Y. and Ziyadeh, F.N. (1998). Transcriptional activation by transforming growth factor β1 in mesangial cell culure by high glucose concentration. *Kidney Int.* **54,** 1107-1116.

Hoyle, C.H. (1999). Neuropeptide families and their receptors: evolutionary perspectives. **848,** 1-25.

Huang, C.L. (2004). The Transient Receptor Potential superfamily of Ion Channels. *J Am Soc Nephrol.* **15,** 1690-1699.

Hudspeth, A.J. (1985). The cellular basis of hearing: the biophysics of hair cells. *Science.* **230,** 745-752.

Hummler, E., Barker, P., Gatzy, J., Beermann, F., Verdumo, C., Schmidt, A., Boucher, R. and Rossier, B.C. (1996).Early death due to defective neonatal lung liquid clearance in α-ENaC deficient mice. *Nat Genet.* **12,** 325-328

Humes, H.D., Nakamura, T., Cieslinski, D.A., Miller, D., Emmons, R.V., Border, W.A. (1993). Role of proteoglycans and cytoskeleton in the effects of TGF-beta 1 on renal proximal tubule cells. *Kidney Int.* **43,** 575-84

Hunter, AW., Jourdan, J., Gourdie, R.G. (2003). Fusion of GFP to the carboxyl terminus of connexin 43 increases gap junction size in HeLa cells. *Cell Adhes Commun.* **10,** 211-214.

Hyytiainen, M., Penttinen, C. and Keski-Oja, J. (2004). Latent TGF-beta binding proteins: extracellular matrix association and roles in TGF-beta activation. *Crit Rev Clin Lab Sci.* **41,** (3).233-64.

Ichimura, T., Yamamura, H., Sasamoto, K., Tominaga, Y. and Taoka, M. (2005). 14-3-3 proteins modulate the expression of epithelial Na^+ channels by phosphorylation dependent interaction with Nedd4-2 ubiquitin ligase. *J Biol Chem.* **280.** 13187-94.

Igarashi, M., Wakasaki, H., Takahara, N., Ishii, H., Jiang, Z.Y., Yamauchi, T., Kuboki, K., Meier, M., Rhodes, J. and King, G.L. (1999). Glucose or diabetes activates p38 mitogen activated protein kinase via different pathways. *J Clin Invest.* **103,** 185-195.

Ingram, A.J. and Scholey, J.W. (1997).. Protooncogene expression and diabetic kidney injury. *Kidney Int* **60** (suppl). S70-6.

Inoki, K., Haneda, M., maeda, S., Koya, D. and Kikkawa, R. (1999). TGF-beta 1 stimulates glucose uptake by enhancing GLUT1 expression in mesangial cells. *Kidney Int.* **55,** 1704-1712.

Inoguchi, T., Ueda, F., Umeda, F., Yamashita, T., and Nawata, H, (1995). Inhibition of intercellular communication via gap junction in cultured aortic endothelial cells by elevated glucose and phorbol ester. *Biochem Biophys Res Comm.* **208,** 492-497.

Inoguchi, T., Yan Yu, H., Imamura, M., Katimoto, M., Kuroki T., Maruyama T., and Nawata, H. (2001). Altered gap junction activity in cardiovascular tissues of diabetes. *Med Electron Microsc.* **34,** 86-91.

Irvine, S.A., Foka, P., Rogers, S.A., Mead, J.R., Ramji, D.P (2005). A critical role for the Sp1 binding sites in the transforming growth factor beta mediated inhibition of lipoprotein lipase gene expression in macrophages. *Nucleic Acids Res.* **33,** 1423-34.

Itani, O.A., Liu, K.Z., Cornish, K.L., Campbell, J.R. and Thomas, C.P. (2002). Glucocorticoids stimulate human sgk1 gene expression by activation of a GRE in its 5' flanking region. *Am J Physiol Endocrinol Metabl.* **283,** E971-79.

Jakab, M., Furst, J., Gschwentner, M., Botta, G., Garavaglia, M.L., Bazzini, C., Rodighiero, S., Meyer, G., Eichmueller, S., Woll, E., Chwatal, S., Ritter, M. and Paulmichl, M. (2002). Mechanisms Sensing and Modulating Signals Arising From Cell Swelling *Cell Physiol Biochem.* **12,** 235-58.

John, S.A., Revel, J.P. (1991). Connexin integrity is maintained by non covalent bonds:intramolecular disulfide bonds link the extracellular domains in rat connexin-43. *Biochem.Biophys.Res.Commun.* **178,** 1312-1318.

Johnson, R.G., Herman, W.S. and Preus, D.M. (1973). Homocellular and heterocellular gap junctions in limulus: a thin section and freeze fracture study. *J Ulstrastruct.res.* **43,** 298-312.

Jongen, W.M.F., Fitzgerald, M. and Asamoto, M. (1991).. Regulation of connexin-43 mediated gap junctional intercellular communication by calcium in mouse epidermal cells is controlled by E-Cadherin. *J Cell Biol.* **114.** 545-556.

Kageyama, S. (1994). Effect of insulin on sodium reabsorption in hypertensive patients. *Am J Hypertens.* **7,** 409-415.

Kanwar, Y.S, Akagi, S., Sun, L., Nayak, B., Xie, P., Wada, J., Chugh, SS., Danesh, F.R. (2005). Cell biology of diabetic kidney disease. *Nephron Exp Nephrol.* **101,** e100-10.

Kellenberger, S. and Schild, L. (2002). The ENaC/Degenerin family of ion channels: a variety of functions for a shared structure. *Physiol Rev.* **3.** 735-67.

Kelsell, D.P., Dunlop, J. and Hodgins, M.B. (2001). Human diseases: clues to cracking the connexin code? *Trends in Cell Biology.* **11.** 2-6.

Kierszenbaum, A.(2002). *Histology and Cell Biology.* 1st edn. Mosby Ltd.

Kingsley, D.M. (1994). The TGF-beta superfamily: new members. new receptors and new genetic tests of function in different organisms. *Genes. Dev.* **2,** 133-46.

Kim, S.J., Angel, P., Lafyatis, R., Hattori, K., Kim, K.Y., Sorn, M.B., Karin, M. and Roberts, A.B. (1990). Autoinduction of transforming growth factor β1 is mediated by the AP-1 complex. *Mol Cell Biol.* **10,** 1492-1497.

Kim, J., Chung, Y.D., Park, D.Y., Choi, S., Shin, D.W. and Soh H (2003). A TRPV family ion channel required for hearing in Drosophila. *Nature.* **424.** 81-84.

Klingel, K., Warntges, S., Bock, J., Wagner, C.A., Sauter, M., Waldegger, S., Kandolf, R. and Lang, F. (2002). Expression of cell volume regulated kinase h-sgk in pancreatic tissue. *Am J Physiol gastrointest Liver Physiol.* **279.** G998-G1002.

Kobayashi, T., Deak, M., Morrice, N., Cohen, P. (1999). Characterisation of the structure and regulation of two novel isoforms of serum and glucocorticoid induced protein kinase. *Biochem J.* **344,** 189-97.

Knepper, M.A. and Inque, T. (1997). Regulation of aquaporin 2-water channel trafficking by vasopressin *Curr Opin Cell Biol* **9.** 560-564.

Kolm-Litty, V., Sauer, U., Nerlich, A., Lehmann, R., Schleicher, E.D. (1998). High glucose induced transforming growth factor β1 production is mediated by the hexosamine pathway in porcine glomerular mesangial cells. *J Clin Invest.* **101.** 160-169.

Kosari, F., Sheng, S., Li, J., Mak, D.O. Foskett, J.K., and Kleyman, T.R. (1998). Subunit stoichiometry of the epithelial sodium channel. *J Biol Chem.* **273,** 13469-13474.

Koya, D., Jirousek, M.R., Lin, Y.W., Ishii, H., Kuboki, K., King, G.L. (1997). Characterisation of protein kinase C beta isoform activation on the gene expression of transforming growth factor β. extracellular matrix components and prostanoids in the gomeruli of diabetic rats. *J Clin Invest.* **100,** 115-126.

Koya, D., Haneda, M. and Nakagawa, H. (2000). Amelioration of accelerated diabetic mesangial expansion by treatment with a PKC beta inhibitor in diabetic db/db mice. a rodent model for type II diabetes. *FASEBJ.* **14.** 439-47.

Krolweski, A.S., Laffel, L.M., Krolewski, M., Quinn, M. and Warram, J.H. (1995). Glycosyltaed haemoglobin and the risk of microalbuminuria in patients with insulin dependent diabetes mellitus. *N Engl J Med.* **332,** 1251-5.

Kruszynska, Y.T. Normal metabolism: the physiology of fuel homeostasis (2003). In: Pickup JC. Williams G eds. *Textbook of diabetes.* 3rd edn. 9.1-9.38Oxford: Blackwell Science Ltd.

Kumar, P. and Clark, M. (2002). Clinical Medicine 5th edn.

Kumar, J.M,. Brooks, D.P,. Olson, B.A. and Laping NJ (1999). SGK. a putative serine/threonine kinase. is differentially expressed in the kidney of diabetic mice and humans. *J Am Soc Nephrol.* **10,** 2488-94.

Kumar, N.M., Gilula, N.M. (1996). The gap junction communication channel. *Cell.* **84,** 381-388.

Kuroki, T., Inoguchi, T., Ueda,. F. and Nawata, H. (1998). High glucose induces alteration of gap junction permeability and phosphorylation of connexin-43 in cultured aortic smooth muscle cells. *Diabetes* **47.** 931-936.

Laing, J.G. and Beyer, E.C. (2000). degradation of gap junctions and connexins. *Current topics in membranes.* **49,** 23-41.

Lampe, P.D., Ngu Yen, B.P., Gil, S., Ususi, M., Olerud, J., Takada, Y. and Carter, W.G., (1998). Cellular interaction of integrin alpha3-beta 1 with laminin 5 promotes gap junctional communication. *Journal of cell biology.* **143,**1735-1747.

Lang, F., Klingel, K., Wagner, C.A., Stegen, C., Warntges, S., Friedrich, B., Lanzendorfer, M., Meizig, J., Moschen, I., Steuer, S., Waldegger, S., Sauter, M., Paulmichl, M., Gerke, V., Risier, T., Gamba, G., Capasso, G., Kandolf, R., Herbert, S.C., Massry, S.G. and Broer, S. (2000). Deranged transcriptional regulation of cell-volume sensitive kinase h-SGK in diabetic nephropathy. *PNAS.* **97** 14.8157-8162.

Lang, F. and Cohen, P. (2001). Regulation and physiological roles of serum and glucocorticoid induced protein kinase isoforms. *Sci STKE.* **RE17.**

Lee, C.T., Lien, Y.H., Lai, L.W., Chen, J.B., Lin, C.R. and Chen, H.C. (2006).. Increased renal calcium and magnesium transporter abundance in streptozotocin-induced diabetes mellitus. *Kidney Int.* **10,** 1786-1791.

Le Roith, D., Taylor, S.I. and Olefsky, J.M. Diabetes mellitus: *A fundamental and clinical text.* ed 3. Philadelphia. Lippincott William and Wilkins. pp1-1540. 2004.

Li, A-F., Sato, T., Haimovici, R., Okamoto, T. and Roy, S. (2003). High glucose alters connexin 43 expression and gap junction intercellular communication activity in retinal pericytes. *Investigative Opthalmology & Visual Science.* **44,** 5376-5382.

Li, G. and Herlyn, M. (2000). Dynamics of intercellular communication during melanoma development. *Molecular Medicine Today.* **6,** 163-169.

Li, H., Liu, T.F., Lazrak, A., Peracchia, C., Goldberg, G.S., Lampe, P.D. and Johnson, R.G. Properties and regulation of gap junction hemichannels in the plasma membranes of cultured cells. *J Cell Biol.* **134,** 1019-1030.

Li, S., Nomata, K., Hayashi, T., Noguchi, M., Kanda, S., and Kanetake H (2002). Transient decrease in gap junction expression during compensatory renal growth in mice. *Urology.* **60,** 726-730.

Liang, X., Peters, K.W., Butterworth, M.B. and Frizzell, R.A. (2006). 14-3-3 isoforms are induced by aldosterone and participate in its regulation of epithelial sodium channels. *J Biol Chem* . **281,**16323-32.

Liberati, N.T., Datto, M.B., Frederick, J.P., Shen, X., Wong, C., Rougier Chapman, E.M., Wang, X-F. (1999). Smads bind directly to the jun family of AP-1 transcription factors. *Proc Natl Acad Sci USA.* **96,** 4844-4849.

Liedtke, W., Chloe, Y., Marti-Renom, M.A., Bell, A.M., Denis, C.S., Sali, A., Hudspeth, A.J., Friedman, J.M. and Heller, S. (2000). Vanilloid receptor-related

osmotically activated channel (VR-OAC).. a candidate vertebrate osmoreceptor. *Cell.* **103,** 525-535.

Lifton, R.P., Wilson, F.H., Choate, K.A. and Geller, D.S. (2002). Salt and blood pressure: new insight from human genetic studies. *Cold spring Harb Symp Quant Biol.* **67,** 445-450.

Lingueglia, E., Voilley, N., Waldmann, R., Lazdunski, M., and Barbry, P (1993). Expression cloning of an epithelial amiloride-sensitive Na^+ channel. *FEBS Lett.* **:318.** 95-99.

Liu, F., Pouponnot, C. and Massague, J. (1997). Dual role of the Smad4/DPC4 tumor suppressor in TGFβ-inducible transcriptional complexes. *Genes Dev.* **11,** 3157-3167.

Liu, T.F., Paulson, A.F., Li, H.Y., Atkinson, M.M., Johnson, R.G. (1997). Inhbitory effects of 12-O-tetradecanoylphorbol-13-acetate on dye leakage from single Novikoff cells and on dye transfer between reaggregated cell pairs. *Methods Find. Exp.Clin.Pharmacol.* **19,** 573-577.

Liu, X., Bandyopadhyay, B., Nakamoto, T., Singh, B., Liedtke, W., Melvin, J.E and Ambudkar, I. (2006). A role for AQP5 in activation of TRPV4 by hypotonicity: concerted involvement of AQP5 and TRPV4 in regulation of cell volume recovery 2006 **281,** 15485-95.

Liu, Y., Gorospe, M., Yang, C. and Holbrookk, N.J. (1995).. Role of mitogen activated protein kinase phosphatase during the cellular response to adriamycin and other chemotherapeutic drugs. *J Biol Chem.* **271,** 30950-30955.

Loffing, J., Pietri, L., Aregger, F., Bloch-Faure, M., Ziegler, U., Meneton, P., Rossier, B.C. and Kaissling, B. (2000) Differential subcellular localization of ENaC subunits in mouse kidney in response to high- and low-Na diets. Am J Physiol Renal Physiol. **279,** F252-8.

Loffing, J,. Flores, S. and Staub, O. (2005). SGK kinases and their role in epithelial transport. *Annu Rev Physiol.* **68,** 16.1-16.3.

Churchill, G.C., Atkinson, M. and Louis, C.F. (1996). Mechanical stimulation initiates cell-to-cell calcium signalling in ovine lens epithelial cells. *J Cell Sci.* **10,** 355-365.

Ma, C. and Chegini, N. (1999). Regulation of matrix metalloproteinases (MMPs). and their tissue inhibitors in human myometrial smooth muscle cells by TGF-beta 1. *Mol Hum Reprod.* **5,** 950-4.

Malfait, M., Gomez, P., van Veen, TAB., Parys, J.B., De Smedt, H., Vereecke, J. and Himpens, B. (2001). Effects of hyperglycaemia and protein kinase C on connexin 43 expression in cultured rat retinal pigment epithelial cells. *J Membrane Biol.* **181.** 31-40.

Mano, I., Driscoll, M. (1999). DEG/ENaC channels a touchy superfamily that watches its salt *BioEssays* **21,** 568-578.

Marshall, S.M. Recent advances in diabetic nephropathy (2004). *Postgrad Med j*:**80,** 624-633.

Martin, P.E.M., Steggles, J., Wilson, C., Ahmad, S, and Evans, W.H. (2000).. Targetting motifs and functional parameters governing the assembly of connexins into gap junctions. *Biochemical journal.* **349.** 281-287.

Martinez, A.D., Hayrapetyan, V., Moreno, AP., Beyer, E.C. (2002).. Connexin43 and connexin45 form heteromeric gap junction channels in which individual component determine permeability and regulation. *Circ Res.* **90.** 1100-1107

Masilamani, S., Kim, G.H., Mitchell, C., Wade, J.B. and Knepper, MA. (1999).. Aldosterone mediated regulation of ENaC alpha. beta and gamma subunit proteins in rat kidney. *J Clin Invest.* **104,** R19-R23.

Mason, R.M., Abdel Wahab, A. (2003). Extracellular matrix metabolism in Diabetic Nephropathy.*J Am Soc Nephrol.* **14,** 1358-1373

Massague, J. (1998). TGF-beta signal transduction. *Annu Rev Biochem.* **67,** 753-91

Mauer, S.M., Steffes, M.W., Ellis, E.N., Sutherland, D.E.R., Brown, D.M. and Goetz, FC: (1984). Structural functionsl relationships in diabetic nephropathy. *J Clin Invest.* **74,** 1143-1155.

McAuliffe, A.V., Brooks, B.A., Fisher, E.J., Molyneaux, L.M., Yue, D.K. (1998). Administration of ascorbic acid and an aldose reductase inhibitor (tolrestat). in diabetes: effect on urinary albumin excretion. *Nephron.* **80,** 277-84.

McCarty, N. and O'Neil, R.G. (1991). Calcium dependent control of volume regulation in renal proximal tubule cells. Swelling activated Ca^{2+} entry and release. *J membrane Biol.* **123,** 149-160.

McCormick, J.A., Bhalla, V., Pao, A.C. and Pearce, D (2005). SGK1: a rapid aldosterone-induced regulator of renal sodium reabsorption. *Physiology* **20.** 134-9.

Meda, P., Denef, J.F., Perrelet, A. and Orci, L. (1980). Nonrandom distribution of gap junctions between pancreatic beta-cells. *Am J Physiol.* **238.** C114-C119.

Mege, R.M., Matsuzaki, F., Gallin, W.J. and Goldberg J.I. Cunningham GM (1988). Construction of epithelioid sheets by transfection of mouse sarcoma cells with cDNAs for chicken adhesion molecules. *Proc Natl Acad Sci USA.* **85.** 7274-7278.

Meyer, T.W., Bennett, P.H. and Nelson, R.G. (1999). Podocyte number predicts long term urinary albumin excretion in Pima Indians with type II diabetes and microalbuminuria. *Diabetologia.* **42.** 1341-4.

Mogensen, C.E., Osterby, R. and Gundersen, H.J. (1979). Early functional and morphological vascular renal consequences of the diabetic state. *Diabetologia.* **17.** 71-6.

Mogyorosi, A. and Ziyadeh, F.N. (1997). Update on pathogenesis. markers and management of diabetic nephropathy. *Curr Opin Nephrol Hypertension* **5**.243-253.

Mogyorosi, A. and Ziyadeh, F.N. (1999). GLUT1 and TGF-beta: the link between hyperglycamia and diabetic nephropathy. *Nephrol Dial transplant.* **14.** 2827-2829.

Montell, C., Jones, K., Hafen, E. and Rubin, G. (1985).Rescue of the Drosophila phototransduction mutation *trp* by germline transformation. *Sciences.* **230.** 1040-1043.

Montell, C. (2005). The TRP superfamily of cation channels. *Sci STKE* **re3**

Montrose-Rafizdeh, C. and Guggino, W.B (1991). Role of intracellular calcium in volume regulation by rabbit medullary thick ascending limb cells. *Am J Physiol.* **260** F402-F409.

Morley, A.R. (1988). Renal vascular disease in Diabetes Mellitus. *Histopathology.* **12.** 343-58.

Morris, R.G. and Schafer, J.A. (2002). cAMP increases density of ENaC subunits in the Apical membrane of MDCK cells in direct proportion to amiloride sensitive Na^+ transport. **120.** 71-85.

Myers, B.D., and Winetz, J.A., Chui, F. and Michaels AS (1982). Mechanisms of proteinuria in diabetic nephropathy: a study of glomerular barrier function. *Kidney Int.* **21** 633-41.

Naray-Fejes-Toth, A., Canessa, C.M., Cleaveland, E.S., Aldrich, G. and Fejes-Toth, G. (1999). sgk is an aldosterone induced kinase in the renal collecting duct. Effects on epithelial Na^+ channels. *J Biol Chem.* **274**:16973-16978.

Naray-Fejes-Toth, A., Helms, M.N., Stokes, J.B. and Fejes-Toth, G. (2004).. Regulation of sodium transport in mammalian collecting duct cells by aldosterone-induced kinase. SGK1: structure/function studies. *Mol Cell Endocrinol.* **217,** 197-202.

Ngezahayo, A., Zeilinger, C., Todt, II., Marten, II. and Kolb, II. Inactivation of expressed and conducting rCx46 hemichannels by phosphorylation. *Pflugers Arch.* **436,** 627-629.

Nilius, B., Vriens, J., Prenen, J., Droogmans, G., and Voets T (2004). TRPV4 calcium entry channel: a paradigm for gating diversity. *Am J Physiol Cell Physiol* **286,** C195-C205.

O'Brodovich, II. (2001). Fetal lung liquid secretion: insights using the tools of inhibitors and genetic knockout experiments. *Am J Respir Cell Mol Biol.* **25.** 8-10.

O'Neil, R.G. and Heller, S. (2005). The mechanosensitive nature of TRPV channels. *Pflugers Arch-Eur J Physiol.* **451.** 193-203.

Okada, Y., Maeno, E., Shimizu, T., Dezaki, K., Wang, J. and Morishima, S. (2001). Receptor mediated control of regulatory volume decrease (RVD). and apoptotic volume decrease (AVD).. *J Physiol* **532,** 3-16.

Oku, H., Kodama, T., Sakagami, K. and Puro, D.G. (2001). Diabetes-induced disruption of gap-junction pathways within the retinal microvasculature. *Investigative Ophthalmology & Visual Science* **42,** 1915-1920.

Osterby, R., Gundersen, H.J., Nyberg, G. and Aurell, M. (1987). Advanced diabetic glomerulopathy: quantitative structural charcaterisation of nonoccluded glomeruli. *Diabetes.* **36,** 612-19.

Owsianik, G., D'hoedt, D., Voets, T., Nilius, B. (2006). Structure-function relationship of the TRP channel superfamily. *Rev Physiol Biochem Pharmacol.* **156,** 61-90.

Pal, J.D., Liu, X., Mackay, D., Shiels, A., Berthoud, V.M., Beyer, E.C. and Ebihara, L. (2000). Connexin 46 mutations linked to congenital cataract show loss of gap junction channel formation. *Am J Physiol.* **279,** C596-C602.

Park, J., Leong, M.L.L., Buse, P., Maiyar, A.C., Firestone, G.L. and Hemmings B.A (1999). Serum and glucocorticoid inducible kinase (SGK). is a target of the PI3-kinase stimulated signalling pathway. *EMBO J.* **18.** 3024-3033.

Parving, H-H., Osterby, R. and Ritz, E. (2000). Diabetic nephropathy; in Brenner BM (ed). The kidney. pp 1731-1773. Philadelphia. Saunders.

Perotti, N., He, R.A., Philips, S.A., Haft, C.R. and Taylor, S.I. (2001). Activation of serum and glucorticoid induced protein kinase (sgk). by cyclic AMP and insulin. *J Biol Chem.* **276,** 9406-12.

Platten, M., Wick, W., and Weller, M. (2001). Malignant glioma biology: role for TGF-beta in growth. mortility angiogenesis and immune escape. Microsc.Res.Tech. **52,** 401-10.

Prie, D., Friedlander, G., Coureau, C., Vandewalle, A., Cassingena, R. and Ronco, P.M. (1995). Role of adenosine on glucagon-induced cAMP in a human cortical collecting duct cell line. *Kidney Int.* **47,**1310-8.

Ramsey, S., Delling, M. and Clapham, D.E. (2006). An introduction to TRP channels. *Annu Rev Physiol.* **68,** 619-47.

Reaven, G.M, (1997). The kidney An unwilling accomplice in syndrome X. *Am J Kidney Dis.* **30,** 928-931.

Reddy, A.S. *Diabetic Nephropathy: Theory and Practice*; East Hanover. College Book Publishers. pp1-5632004

Reeves, W.B. and Andreoli, T.E. (2000). Transforming growth factor β contributes to progressive diabetic nephropathy. *Proc Natl Acad Sci USA.* **97,** 7667-7769.

Reif, M.C., Troutman, S.L. and Schafer, J.A (1986). Sodium transport by rat cortical collecting tubule Effects of vasopressin and deoxycorticosterone. *J Clin Invest.* 77, 1291-1298.

Renard S., Lingueglia, E., Voilley, N., Lazdunski, M. and Barbry, P. (1994). Biochemical analysis of the membrane topology of the amiloride-sensitive Na^+ channel. *J Biol Chem* **269,** 12981–12986.

Ricci, C., Iacobini, C., Oddi, G., Amadio, L., Menini, S., Rastaldi, MP., Frasheri, A., Pricci, F., Pugliese, F. and Pugliese G (2006). Role of TGF-β/Glut1 axis in susceptibility vs resistance to diabetic glomerulopathy in the Milan rat model. *Nephrol Dial Transplant.* **6,** 1514-1524.

Rocco, M.V. Chen, Y., Glodfarb, S. and Ziyadeh, F.N. (1992). Elevated glucose stimulates TGF-β gene expression and bioactivity in proximal tubule. *Kidney Int*: **41,** 107-114.

Rohloff, P., Rodrigue, C.O and Docampo, R. (2003). Regulatory volume decrease in Trypanosoma cruzi involves amino acid efflux and changes in intracellular calcium. *Mol Biochem. Parasitol.* **126,** 219-230.

Rothstein, A. and Mack, E. (1992).. Volume activated calcium uptake: It's role in cell volume regulation of Madin-Darby canine Kidney cells. *Am J Physiol.* **262,** 339-47.

Rotin, D. (2000). Regulation of the epithelial sodium channel (ENaC). by accessory proteins. *Curr Opin Nephrol Hypertens.* **9,** 529-34.

Rumble, J.R., Cooper, M.E. and Soulis, T. (1997). Vascular hypertrophy in experimental diabetes: role of advanced glycation end products. *J Clin Invest.* **99,** 1016-1027.

Saez., J.C., Martinez, A.D., Branes, M.C. and Gonzalez P. (1998). Regulation of gap junctiosn by protein phosphorylation. *Braz J Med Biol Res.* **31,** 593-600.

Sakurai, S., Yonekura, H., Yamamoto, Y., Watanabe, T., Tanaka, N., Li, H., Rahman, A.K., Myint, K.M., Kim, C.H. and Yamamoyo, H. (2003). The AGE-RAGE system and Diabetic nephropathy. *J Am Soc Nephrol.* **14,** S259-S263.

Sanderson, M.J., Charles, A.C and Dirksen, E.R (1990). Mechanical stimulation and intercellular communication increases intracellular Ca^{2+} in epithelial cells *Cell regul* **1,** 585-596.

Sanderson, M.J., Charles, A.C and Dirksen, E.R (1994). Mechanisms and function of intercellular communication increases intracellular Ca^{2+} in epithelial cells. *Mol. Cell. Endocrinology* **98,** 173-187.

Sandow, S.L., Looft-Wilson, R., Doran, B., Grayson, T.H., Segal, S.S. and Hill, C.E. (2003). Expression of homocellular and heterocellular gap junctions in hamster arterioles and feed arteries. *Cardiovasc Res.* **60,** 643-653.

Sato, T., Haimovici, R., Kao, R., Li, A-F. and Roy S (2002). Downregulation of connexin 43 expression by high glucose reduces gap junction activity in microvascular endothelial cells. *Diabetes* **51,** 1565-1571

Schafer, JA. and Hawk, C.T. (1992). Regulation of Na^{+} channels in the cortical collecting duct by AVP and mineralocorticoids. *Kidney int.* **41,** 255-268.

Schena, F.P and Gesualdo, L. (2005). Pathogenetic mechanisms of diabetic nephropathy. *J Am Soc Nephrol* **16,** S30-3.

Schild L., Lu, Y., Gautschi, I., Schneeberger, E., Lifton, R.P. and Rossier, B.C. (1996). Identification of a PY motif in the epithelial Na channel subunits as a target sequence for mutations causing channel activation found in Liddle syndrome. *EMBO J.* **15,** 2381-2387.

Schirrmacher, K., Nonhoff, D., Wiemann, M., Peterson-Grine, E., Brink, PR. and Bingmann, D. (1996). Effects of calcium on gap-junctions between osteoblast-like cells in culture. *Calcif Tissue Int.* **59,** 259-264.

Schmitt, R., Ellison, D.H., Farman, N., Rossier, B.C., Reilly, R.F., Reeves, W.B., Oberbaumer, I., Tapp, R, and Bachmann, S. (1999). Developmental expression of sodium entry pathways in rat nephron. *Am J Physiol Renal Physiol.* **276,** F367-F381.

Schuster, N. and Krieglstein, K. (2002). Mechanisms of TGF-β mediated apoptosis. *Cell Tissue Res.* **307,** 1-14.

Shapiro, L. and Dinarello, C.A. (1995). Osmotic regulation of cytokine synthesis in vitro. *Proc Natl Acad Sci* USA. **92,** 12230-12234.

Sharma, K., Ziyadeh, F.N., Alzahabi, B., McGowan, T.A., Kapoor, S., Kurnik, B.R., Kurnick, P.B. and Weisberg, L.S. (1997). Increased renal production of transforming growth factor-beta 1 in patients with type II diabetes. *Diabetes.* **46,** 854-859.

Sharma, K. and Ziyadeh, F.N. (1994). The emerging role of transforming growth factor beta in kidney diseases. *Am J physiol.* **266,** F829-F842.

Sharma, K. and Ziyadeh, F.N. (1995). Hyperglycaemia and diabetic kidney disease. The case for Transforming growth factor -β as a key mediator. *Diabetes.* **44,** 439-446.

Sheetz, M.J. and King, G.L. (2002). Molecular Understanding of hyperglycamia's adverse effects for diabetic complications: *JAMA.* **288,** 2579-2588.

Shen, M.R., Chou, C.Y., Browning, J.A., Wilkins, R.J. and Ellory, J.C. (2001). Human cervical cancer cells use Ca^{2+} signalling. protein tyrosine phopshorylation and MAP kinase in regulatory volume decrease. *J Physiol.* **537,** 347-362.

Shimkets, R.A., Warnock, D.G., Bositis, C.M., Nelson-Williams, C., Hansson , J.H., Schambelan, M., Gill, J.R.J., Ulick, S., Milora, R.V., Finding, J.W., Canessa, C.M., Rossier, B.C. and Lifton, R.P (1994). Liddle's syndrome: heritable human hypertension caused by mutations in the α subunit of the epithelial sodium channel. *Cell.* **79,** 407-414.

Snyder, P.M., Cheng, C., Prince, L.S., Rogers, J.C. and Welsh, M.J. (1998). Electrophysiological and biochemical evidence that DEG/ENaC cation channels are composed of nine subunits. *J Biol Chem.* **273,** 681-684.

Snyder, P.M. (2002a). The epithelial Na^+ channel: Cell surface insertion and retrieval in Na^+ homeostasis and hypertension. *Endocrine Reviews.* **23,** 258-275

Snyder, P.M., Olsen, D.R. and Thomas, B.C. (2002b). Serum and glucocorticoid regulated kinase modulates Nedd4-2 mediated inhibition of the epithelial Na^+ channel. *J Biol Chem.* **277,** 5-8.

Snyder, P.M. (2005).. Minireview: regulation of epithelial Na^+ channel trafficking Endocrinology **146,** 5079-85.

Staruschenko, A., Adams, A., Booth, R.E. and Stockand JD (2005). Epithelial Na^+ channel subunit stoichiometry. *Biophys J .* **88,** 3966-3975.

Staub, O., Dho, S., Henry, P., Correa, J., Ishikawa, T., McGlade, J., and Rotin, D. (1996). WW domains of Nedd4 bind to the proline-rich PY motifs in the epithelial Na^+ channel deleted in Liddle's syndrome. *Embo J.* **15,** 2371-2380

Stout, C., Charles, A. (2003). Modulation of intercellular calcium signalling in astrocytes by extracellular calcium and magnesium. *Glia.* **43,** 265-73.

Strotmann, R., Harteneck, C., Nunnenmacher, K., Schultz, G. and Plant, T.D. (2000). OTRPC4. a non selective cation channel that confers sensitivity to extracellular osmolarity. *Nat Cell Biol.* **2,** 695-702.

Strotmann, R., Schultz, G. and Plant, T.D. (2003). Ca^{2+} dependent potentiation of the non selective cation channel TRPV4 is mediated by a C terminal calmodulin binding site. *J Biol Chem.* **278,** 26541-26549.

Suzuki, M., Mizuno, A., Kodaira, K. and Imai, M. (2003). Impaired pressure sensation in mice lacking TRPV4. *J Biol Chem* **278,** 22644-22668.

Symonian, M., Smogorzewski, M., Marcinkowski, W., Krol, E., Massry, S.G. (1998). Mechanisms through which high glucose concentration raises $[Ca^{2+}]_i$ in renal proximal tubular cells. *Kidney International* **54,** pp1206-1213.

Szlufcik, K., Missiaen, L., Parys, J.B., Callewaert, G.De. and Smedt, H. (2006). Uncoupled IP3 receptor can function as a Ca2+-leak channel: cell biological and pathological consequences. *Biol Cell.* **98,** 1-14.

Taniguchi, K., Kaya, S., Abe, K. and Mardh S. (2001). The oligomeric nature of Na/K-transport ATPase. *J Biochem* **129,** 335-42.

Thastrup, O., Cullen, P.J., Droback, B.K., Hanley, M.R and Dawson, A.P. (1990). Thapsigargin. a tumour promoter. discharges intracellular Ca2+ by specific inhibition of the endoplasmic reticulum Ca^{2+} ATPase. *Proc Natl Acad Sci* .**87,** 2466-2470.

Tinel, H., Wehner, F. and Sauer, H. (1994). Intracellular Ca^{2+} release and Ca^{2+} influx during regulatory volume decrease in MDCK cells. *Am J Physiol.* **267,** F130-F138.

Tinel, H., Kinne-Saffran, E. and Kinne, R.H. (2002). Ca^{2+} induced Ca^{2+} release participates in cell volume regulation of rabbit TALH cells. *Pflugers Arch.* **443,** 754-761.

Tisher, C.C. (1981). Anatomy of the kidney. In Brenner BM. Rector FC. eds. *The kidney.* 3-75.Philadelphia: Saunders.

Tobin, D., Madsen, D.M., Kahn Kirby, A., Peckol, E., Moulder, G. and Barstead, R. (2002). Combinatorial expression of TRPV channel proteins defines their sensory functions and subcellular localisation in C.elegans neurons. *Neuron.* **35,** 307-318.

Toker, A., Ellis, C.A., Sellers. L. A. and Aitken, A. (1990). Protein kinase C inhibitor proteins. Purification from sheep brain and sequence similarity to lipocortins and 14-3-3 protein. *Eur J Biochem.* **191,** 421–429.

Tominaga, M., caterina, MJ., Malmberg, A.B., Rosen, T.A. and Gilbert, H. (1998). The cloned capsaicin receptor integrates multiple pain producing stimuli. *Science.* **288,** 306-13.

Tomita, K., Pisano, J.J. and Knepper M.A (1985). Control of sodium and potassium transport in the cortical collecting duct of the rat. Effects of bradykinin. vasopressin and deoxycorticosterone. *J Clin Invest.* **76,**132-136.

Tonon, R. and D'Andrea, P. (2002). The functional expression of connexion 43 in articular chondrocytes is increased by interleukin 1β: Evidence for a Ca^{2+} dependent mechanism. *Biorheology* **39,** 153-160

Torok, K., Stauffer, K., and Evans, W.H. (1997). Connexin 32 of gap junctions contains two cytoplasmic calmodulin binding domains. *Biochemical journal.* **326,** 479-483.

Toyofuku, T., Yabuki, M., Otsu, K., Kuzuya, T., Hori, M. and Tada, M. (1998). Intercellular calcium signalling via gap junction in connexin 43 transfected cells. *J Biol Chem.* **273,** 1519-1528.

Urbach, V., Leguen, I., O'Kelly, I. and Harvey, B.J (1999).. Mechanosensitive calcium entry and mobilisation in renal A6 cells. *J Membr Biol.* **168,** 29-37.

US Renal Data System. USRDS (2003). Annual data report: atlas of end-stage renal disease in the United States. Bethesda. MD. National Institute of Health. National Institute of Diabetes and Digestive and Kidney Disease.

Valiuna, V., Gemel, J., Brink, P.R., Beyer, E.C. (2001). Gap junction channels formed by coexpressed connexin40 and connexin43. *Am J Physiol; Heart Circ Physiol.* **281,** 1675-1689.

Van Ibberghen-Schilling, E., Roche, N.S., Flanders, K.C., Sporn, M.B. and Roberts, A.B. (1988).Tranforming growth factor β-1 positively regulates its own expression in normal and transformed cells. *J Biol Chem.* **263,** 7741-7746.

Verselis, V.K., Trexler, E.B., Bukauskas, F.F. (2000). Connexin hemichannels and cell-cell channels: comparison of properties *Braz J Med Biol Res* **33,** 379-389.

Vriens, J., Watanabe, H., Janssens, A., Droogmans, G., Voets, T. and Nilius, B. (2004). Cell swelling. heat and chemical agonists use distinct pathways for the activation of cation channel TRPV4. *Proc Natl Acad Sci USA.* **101.** 396-401.

Waerntges, S., Klingel, K., Weigert, C., Fillon, S., Buck, M., Schleicher, E., Rodemann, H.P., Knabbe, C., Kandolf, R. and Lang, F. (2002). Excessive transcription of the human serum and glucocorticoid dependent kinase hSGK1 in lung fibrosis. *Cell Physiol Biochem.* **12,** 135-42.

Waldegger, S., Barth, P., Raber, G. and Lang, F. (1997). Cloning and characterisation of a putative human serine/threonine protein kinase transcriptionally modified during anisotonic and isotonic alterations of cell volume. *Proc Natl Acad Sci USA.* **94,** 4440-4445.

Waldegger, S., Klingel, K., Barth, P., Sauter, M., Rfer, M.L., Kandolf, R. and Lang, F. (1999). h-sgk serine/threonine protein kinase as a transcriptional target of transforming growth factor beta in human intestine. *Gastroenterology.* **116,** (5). 1081-1088.

Waldegger, S., Gabrysch, S., Barth, P., Fillon, S. and Lang, F. (2000). h-SGK serine/threonine protein kinase as transcriptional target of p38/MAP Kinase pathway in HepG2 human hepatoma cells. *Cell Physiol Biochem.* **10,** 203-208.

Wang, W., Zhou, G., Hu, M., Yao, Z., Tan, T. (1997). Activation of the hematopoietic progenitor kinase-1 (HPK-1). dependent. stress activated c-Jun N-teminal kinase (JNK). pathway by transforming growth factor β (TGF-β). activated kinase (TAK1).. a kinase mediator of TGF β signal transduction. *J Biol chem.* **272,** 22771-22775.

Wang, Q., Zhang, X., Wang, Y., Deng, A., Zhu, Z. and Feng Y (2005). Significance and expression of serum and glucocorticoid-inducible kinase in kidney of mice with diabetic nephropathy. *J Huazhong Univ Sci Technolog Med Sci.* **25,** (2).:170-3.

Watanabe, H., Davis, J.B., Smart, D., Jerman, J.C., Smith, GD., Hayes, P., Vriens, J., Cairns, W., Wissenbach, U. and Prenen, J. (2002). Activation of TRPV4 channels (hVRL-2/mTRP12). by phorbol derivatives. *J Biol Chem.* **277,** 13569-13577.

Watanabe, H., Vriens, J., Janssens, A., Wondergem, R., Droogmans, G. and Nilius B. (2003a). Modulation of TRPV4 gating by intra and extracellular Ca^{2+} .*Cell Calcium.* **33.** 489-495.

Watanabe, H., Vriens, J., Prenen, J., Droogmans, G., Voets, T. and Nilius, B. (2003b). Anandamide and arachidonic acid use epoxyeicosatrienoic acids to activate TRPV4 channels *Nature* **424.** 434-438.

Webster, M.K., Goya, L., G.e Y., Maiyar, A.C. and Firestone, G.L (1993a). Characterisation of sgk. a novel member of the serine/threonine protein kinase gene family which is trancrptionally induced by glucocorticoids and serum. *Mol Cell Biol.* **13,** 2031-2040.

Webster, M.K., Goya, L. and Firestone, G.L. (1993b). Immediate early transcriptional regulation and rapid mRNA turnover of a putative serine/threonine protein kinase. *J Biol Chem.* **268,** 11482-11485.

Weigert, C., Brodbeck, K., Brosius, F.C., Huber, M., Lehmann, R., Friess, U., Facchin-Aulwurm, S., Häring, H.U., Schleicher ED and Heilig CW (2003). Evidence for a novel TGFβ1-independent mechanism of fibronectin production in mesangial cells overexpressing glucose transporters. *Diabetes.* **52,** 527-535.

White, K.E., Bilous, R.W and Marshall, S.M (2002). Podocyte number in normotensive type I diabetic patients with albunminuria. *Diabetes.* **51,** 3083-9.

Whiteside, C.I. and Dlugosz, J.A. (2002). Mesangial cell protein kinase C isozyme activation in diabetic milieu. **282,** F975-F980.

Wissenbach, U., Bodding, M., Freichel, M. and Flockerzi, V. (2000). TRP12 a novel TRP related protein from the kidney. *FEBS Lett.* **485,** 127-134.

Wolf G, Ziyadeh, FN., Zahner, G. Stahl RA (1995). Angiotensin II stimulated expression of transforming growth factor beta in renal proximal tubular cells; attenuation after stable transfection with the c-*mas* oncogene. *Kidney Int.* **48,** 1818-1827.

Wolf, G. and Ritz, B. (2003). Diabetic Nephropathy in Type 2 Diabetes Prevention and Patient management. *J Am Soc Nephrol.* **14,** 1396-1405.

Wong, S.M.E. and Chase, H.S. (1986). Role of intracellular calcium in cellular volume regulation. *Am J Physiology.* **250,** C841-C852.

Wong, F., Schaefer, E.L., Roop, B.C., Lamendola, J.N., Johnson-Seaton, D and Shao, D. (1989). Proper function of the Drosophila *trp* gene product during pupal development is important for normal visual transduction in the adult. *Neuron.* **3,** 81-94.

Xu, H., Zhao, H., Tian, W., Yoshida, K., Roullet, J.B. and Cohen, D.M. (2003). Regulation of a transient receptor potential (TRP). channel by tyrosine phosphorylation. SRC family kinase dependent tyrosine phosphorylation of TRPV4 on TYR-253 mediates its response to hypotonic stress. *J Biol Chem.* **278,** 11520-11527.

Xu, BE., Stippec, S., Chu, P.Y., Lazrak, A. and Li, X.J. (2005). WNK1 activates SGK to regulate the epithelial sodium channel. *Proc Natl Acad Sci USA.* **102,** 10315-20.

Yaoita, E., Yao, J., Yoshida, Y., Morioka, T., Nameta, M., Takata, T., Kamiie, J., Fujinaka, H., Oite, T. and Yamamoto T. (2002). Up-regulation of connexin 43 in glomerular podocytes in response to injury *Am J Pathology* **161,** 1597-1606.

Yamamoto, T., Nakamura, T., Noble, NA., Ruoslahati, E. and Border, W.A. (1993). expression of transforming growth factor beta is elevated in human and experimental diabetic nephropathy. *Proc Natl Acad Sci.* **90,** 1814-8.

Yellowley, C.E., Hancox, J.C. and Donahue, H.J (2002). Effects of cell swelling on intracellular Ca^{2+} and membrane currents in bovine articular chondrocytes. *J Cell Biochem.* **86,** 290-301.

You, H., Jang, Y., You-Ten, A.I., Okada, H. and Liepa, J. (2004). p53 dependent inhibition of FKHRL1 in response to DNA damage through protein kinase. SGK1 *Proc Natl Acad Sci USA.* **101,** 14057-14062.

Yue, J., frey, R. and Mulder, K., (1999). Cross talk between the Smad1 and Ras/Mek signalling pathways for TGF-β. Oncogene **18,** 2033-2037.

Yung, S., Lee, C.Y., Zhang, Q., Lau, S.K., Tsang, R.C. and Chan, T.M. (2006).. Elevated glucose induction of thrombospondin-1 up-regulates fibronectin synthesis in proximal renal tubular epithelial cells through TGF-{beta}1 dependent and TGF-{beta}1 independent pathways. *Nephrol Dial Transplant* **21,** 1504-13.

Zhang, X., Chen, X., Wu, D., Liu, W., Wang, J., Feng, Z., Cai, G., Fu, B., Hong Q. and Du J. (2006). Downregulation of connexin 43 expression by high glucose induces senescence in glomerular mesangial cells. *J Am Soc Nephrol.* **6,** 532-42. .

Zhou, R. and Snyder, P.M (2005). Nedd4-2 phosphorylation induces serum and glucocorticoid regulated kinase (SGK). ubiquitination and degradation. *J Biol Chem.* **280,** 4518-23.

Ziyadeh, F.N. (1993). The extracellular matrix in diabetic nephropathy. *Am J Kidney Dis.* **22,** 736-44.

Ziyadeh, F.N., Sharma, K., Ericksen, M. and Wolf, G. (1994). Stimulation of collagen gene expression and protein synthesis in murine mesangial cells by high glucose is mediated by autocrine activation of transforming growth factor-beta. *J Clin Invest.* **93,** 536-542.

Ziyadeh, F.N., Hoffman, B.B., Han, D.C., Iglesias-de la Cruz, M.C., Hong, S.W., Isono, M., Chen, S., McGowan, T.A. and Sharma, K. (2000). Long term prevention of renal insufficiency. excess matrix gene expression and glomerular mesangial matrix expression by treatment with monoclonal anti-TGFβ antibody in db/db diabetic mice. *Proc Natl Acad Sci USA.* **97,** 8015-8020.

BRITISH LIBRARY

IMAGING SERVICES NORTH

Boston Spa, Wetherby
West Yorkshire, LS23 7BQ
www.bl.uk

The following have been excluded at the request of the university:

Appendix 1

Appendix 2